

Innovative use of recycled materials in reinforced concrete beams

A thesis submitted to The University of Manchester for
the degree of Doctor of Philosophy in the Faculty of
Science and Engineering.

2020

Robert B Ataria

Department of Mechanical, Aerospace and Civil Engineering

Contents

| | |
|---------------------|----|
| List of Figures | 10 |
| List of Tables | 21 |
| Abstract | 25 |
| Declaration | 29 |
| Copyright Statement | 30 |
| Acknowledgements | 31 |
| Publications | 32 |
| Presentations | 33 |
| Awards | 34 |

| | |
|---|-----------|
| <i>Chapter 1</i> | 35 |
| Introduction | 35 |
| 1.1 Background | 35 |
| 1.1.1 Recycled Aggregate from construction and demolition waste (CDW) .. | 35 |
| 1.1.2 Recycling process of recycled aggregate | 37 |
| 1.1.3 Crumb rubber from discarded tyres and rubber recycled aggregate concrete (RRAC) | 38 |
| 1.2 Motivation of research | 40 |
| 1.3 Objectives of research | 41 |
| 1.4 Thesis structure | 42 |
| <i>Chapter 2</i> | 45 |
| Literature Review | 45 |
| 2.1 General Introduction to recycled aggregates and crumb rubber | 46 |
| 2.1.1 Classification of recycled aggregates | 46 |
| 2.1.2 Properties of crumb rubber from waste tyres | 47 |
| 2.2 Workability of recycled aggregate concrete..... | 51 |
| 2.2.1 Moisture state and water absorption of recycled aggregates on workability of recycled concrete | 52 |
| 2.2.2 Workability over time | 55 |
| 2.2.3 Effects of water reducing agents on the workability of recycled aggregate concrete | 57 |
| 2.3 Influence of crumb rubber (CR) concentration and size on the workability of concrete | 58 |
| 2.4 Mechanical properties of recycled concrete | 61 |
| 2.4.1 Compressive strength | 61 |
| 2.4.1.1 Effect of water cement ratio (w/c), RA content and water absorption on the strength of recycled concrete | 62 |
| 2.4.1.2 Effect of admixtures on the strength of recycled aggregate concrete | 64 |

| | |
|--|------------|
| 2.4.1.3 Effect of crumb rubber (CR) on the mechanical properties of concrete | 65 |
| 2.4.2 Splitting tensile strength..... | 67 |
| 2.4.2.1 Splitting tensile strength of recycled aggregate concrete | 67 |
| 2.4.2.2 Splitting tensile strength of crumb rubber concrete | 67 |
| 2.4.3 Elastic modulus and stress strain behaviour | 68 |
| 2.4.4 Methods devised to improve the performance of recycled concrete | 84 |
| 2.4.5 Assessment of improvement methods and limitations. | 88 |
| 2.4.6 Bond Strength..... | 88 |
| 2.5 Durability performance of recycled concrete | 91 |
| 2.5.1 Chlorine permeation | 92 |
| 2.5.2 Drying shrinkage | 94 |
| 2.5.3 Carbonation depth | 97 |
| 2.5.4 Creep strain | 100 |
| 2.6 Flexural behaviour of reinforced recycled concrete beams | 102 |
| 2.6.1 Flexural design of reinforced concrete beams | 106 |
| 2.7 Behaviour of reinforced recycled beams in shear | 108 |
| 2.7.1 Design methods for shear resistance of reinforced concrete beams | 113 |
| 2.7.2 Eurocode 2 method for shear design | 114 |
| 2.7.3 ACI 318 method for shear design | 116 |
| 2.8 Interfacial shear stress between concrete layers | 118 |
| 2.8.1 Methods of checking horizontal shear stress of two-layer interface. | 121 |
| 2.8.1.1 Global force equilibrium from compressive and tensile forces. | 122 |
| 2.8.1.2 Simplified elastic beam behaviour | 123 |
| 2.9 Influence of graphene on concrete mix | 124 |
| 2.10 Summary | 132 |
| <i>Chapter 3.....</i> | <i>133</i> |
| Mechanical properties of recycled concrete | 133 |
| 3.1 Introduction | 133 |
| 3.2 Specification and preparation of constituent materials. | 134 |

| | |
|---|-----|
| 3.3 Concrete mixture | 137 |
| 3.4 Workability of fresh concrete | 139 |
| 3.5 Properties of hardened concrete | 143 |
| 3.5.1 Compressive strength | 143 |
| 3.5.2 Splitting tensile strength..... | 146 |
| 3.5.3 Elastic Modulus..... | 148 |
| 3.5.4 Ultrasonic Pulse Velocity (UPV) | 149 |
| 3.5.5 Stress Strain behaviour..... | 151 |
| 3.6 Bond strength of rebar and recycled concrete | 152 |
| 3.6.1 Materials and mix proportions | 153 |
| 3.6.2 Pull-out test specimen and test set up..... | 153 |
| 3.6.3 Results and discussion..... | 154 |
| 3.6.3.1 Bond strength | 154 |
| 3.7 Interfacial shear strength | 157 |
| 3.7.1 Experimental programme | 158 |
| 3.7.1.1 Materials, mix design and test parameters | 158 |
| 3.7.1.2 Test methods | 159 |
| 3.7.1.3 Interpretation of results (Mohr-Coulomb Criterion) | 162 |
| 3.7.2 Results and discussion..... | 164 |
| 3.7.2.1 Failure mode and differential stiffness..... | 164 |
| 3.7.2.2 Slant shear strength results (interfacial shear strength under a combined normal and shear stress) | 166 |
| 3.7.2.3 Bond split tensile strength..... | 167 |
| 3.7.2.4 Interfacial shear strength without normal stress..... | 169 |
| 3.7.3 Summary and Conclusions..... | 170 |
| 3.8 Effects of graphene on recycled aggregate concrete | 170 |
| 3.8.1 Experimental programme | 171 |
| 3.8.1.1 Materials and concrete mix proportion | 171 |
| 3.8.2 Experimental results | 175 |
| 3.8.2.1: Compressive strength of RRAC with and without graphene solution..... | 175 |

| | |
|--|------------|
| 3.8.2.2: Compressive strength of RAC/NAC with and without graphene solution..... | 176 |
| 3.8.2.3: Tensile strength of RAC/NAC with and without graphene solution | 179 |
| 3.8.2.4: Stress strain curves | 181 |
| 3.8.3 Cost of implication of graphene in a cubic meter of concrete | 183 |
| 3.8.4 Conclusions | 184 |
| <i>Chapter 4</i> | <i>186</i> |
| Experimental study of bending and shear behaviour of two-layer beams..... | 186 |
| 4.1 Introduction | 186 |
| 4.2 Specimen design..... | 187 |
| 4.3 Concrete mix and properties | 189 |
| 4.3.1 Test set up and instrumentation..... | 191 |
| 4.4 Results and discussions | 191 |
| 4.4.1 Crack pattern and failure modes for bending test | 191 |
| 4.4.2 Load-deflection curves | 192 |
| 4.4.3 Crack pattern and failure modes for shear test | 194 |
| 4.4.4 Load deflection plot for shear test..... | 195 |
| 4.5 Summary and Conclusions..... | 197 |
| <i>Chapter 5</i> | <i>198</i> |
| Validation of Numerical Modelling and parametric study | 198 |
| 5.1 Introduction | 198 |
| 5.2 Finite element modelling using ABAQUS..... | 199 |
| 5.3 Material properties and constitutive models | 200 |
| 5.4 Validation of finite element model with published experiment [44] | 202 |
| 5.5 Finite element discretization for this study | 205 |

| | |
|--|------------|
| 5.6 Comparison between ABAQUS numerical simulation results with experimental results | 207 |
| 5.6.1 Load deflection curves at mid-span | 207 |
| 5.6.2 Tensile strain in longitudinal reinforcement | 208 |
| 5.6.2 Crack pattern and failure mode | 210 |
| 5.7 Numerical parametric study results | 211 |
| 5.7.1 Effects of recycled concrete grade on bending performance of two-layer beam | 211 |
| 5.7.2 Concrete shear resistance mechanism: effects of top layer/bottom layer concrete depth ratio and top layer NAC mix on shear capacity of two-layer beams | 214 |
| 5.8 Assessment of design methods | 216 |
| 5.8.1 Bending resistance | 216 |
| 5.8.2 Shear resistance | 217 |
| 5.9 Conclusions | 220 |
| <i>Chapter 6</i> | 222 |
| Practical implications of two-layer beams | 222 |
| 6.1 Introduction | 222 |
| 6.2 Bending reinforcements based on [113] | 223 |
| 6.3 Assessment for additional vertical shear reinforcement | 226 |
| 6.3.1 Vertical shear links for the regular concrete beams | 226 |
| 6.3.2 Vertical shear links for the two-layer beam | 227 |
| 6.4 Assessment for additional horizontal shear links | 229 |
| 6.5 Comparison of shear rebars | 234 |
| 6.6 Conclusion | 236 |
| <i>Chapter 7</i> | 237 |
| Conclusions and recommendation for future research studies .. | 237 |
| 7.1 Summary of research and achievements | 237 |

| | |
|---|------------|
| 7.1.1 General | 237 |
| 7.1.2 Mechanical properties of wet and hardened rubber recycled aggregate concrete | 238 |
| 7.1.3 Influence of graphene on the mechanical properties of recycled aggregate concrete | 239 |
| 7.1.4 Bond strength of recycled concrete and embedded reinforcement bars. | 241 |
| 7.1.5 Interfacial bond strength between two-layers of concrete of different grades. | 241 |
| 7.1.6 Experiments, numerical modelling (ABAQUS), validation, parametric study and design assessment of bending behaviour of two-layer beams. | 242 |
| 7.1.7 Experiments, numerical modelling (ABAQUS), validation, parametric study and design assessment of shear behaviour of two-layer beams..... | 243 |
| 7.1.8 Practical implication of two-layer beams | 244 |
| 7.2 Recommendations for future research..... | 244 |
| <i>Appendix A</i> | 246 |
| Mix design and raw data collated from experiments of recycled and NAC with coefficient of variations..... | 246 |
| <i>Appendix B</i> | 257 |
| Raw data collated from experiments of bond stress slip relationships for all samples. | 257 |
| <i>Appendix C</i> | 260 |
| Raw data collated from experiments of interfacial shear strength tests for all samples. | 260 |
| <i>Appendix D</i> | 262 |

| | |
|--|------------|
| Raw data collated from experiments of graphene recycled concrete for all samples..... | 262 |
| <i>Appendix E.....</i> | <i>269</i> |
| Bending moment and shear capacity calculations of the RC section in Fig4.2 & 4.3 to EC2 and predicted methods. Effects of reinforcement ratio and shear span depth ratio on two-layer beams (ABAQUS). | 269 |
| <i>Appendix F.....</i> | <i>275</i> |
| Detailed calculations of vertical shear links required for beams | 275 |
| References..... | 280 |
| Total word count: 50,952 | |

List of Figures

| | |
|--|----|
| Figure 1.1 (a) Benefits and (b) Lifecycle of recycled aggregate from CDW[15] | 37 |
| Figure 1.2 Recycling processes of recycled aggregates from demolished structure | 38 |
| Figure 1.3 Landfill for waste tyres in Kuwait [24] | 39 |
| Figure 1.4 Detail and sections of the two-layer beam..... | 42 |
| | |
| Figure 2.1 Categories of processed waste tyres of motor vehicles [52]..... | 48 |
| Figure 2.2 Stress-strain curves for tyre rubber with pre-compression tests at strain rate of 1.0 s ⁻¹ (Data extracted from [55]) | 49 |
| Figure 2.3 Stress-strain curves obtained from experimental compression tests[56]..... | 50 |
| Figure 2.4 Stress-strain curves obtained from experimental tensile tests[56]..... | 50 |
| Figure 2.5 Effects of moisture state of recycled aggregates on the workability of concrete over time (Poon et al., 2004). | 54 |
| Figure 2.6 Influence of moisture state and mixing procedure on the workability value of recycled concrete [61] | 55 |
| Figure 2.7 Compaction factor of mixes with different effective w/c ratios and recycled aggregates replacement levels over a period of time from (0-150 minutes) [63] .. | 56 |
| Figure 2.8 Influence of superplasticizers (SP) on the workability of recycled aggregate concrete (data extracted from [11]) | 58 |
| Figure 2.9 Influences of crumb rubber concentration and size on the workability of concrete (data extracted from [37])..... | 59 |
| Figure 2.10: Influence of crumb rubber concentration and size on the workability of concrete (Data extracted from [30])..... | 60 |
| Figure 2.11 Crack pattern of recycled aggregates with attached cement matrix (Kwan et al., 2011). | 61 |

| | |
|--|----|
| Figure 2.12 Relationship between concrete strength and w/c ratio for varying RA content (plotted using data from [47]) | 63 |
| Figure 2.13 Relationship between percentage of replacement and 28-day compressive strength with and without admixtures [11] | 64 |
| Figure 2.14 Influence of crumb rubber size and concentration on the compressive strength of concrete for w/c of 0.48 (data plotted from [37]) | 65 |
| Figure 2.15 Effects of crumb rubber concentration and w/c on the compressive strength of concrete (data extracted from [41]). | 66 |
| Figure 2.16 Splitting tensile strength of RAC and natural aggregate concrete with different w/c and RA concentrations. | 67 |
| Figure 2.17 Influence of crumb rubber concentration and w/c on splitting tensile strength of concrete (data extracted from [41]). | 68 |
| Figure 2.18 Comparisons of modulus of elasticity at 28 days by different researchers between 100% recycled aggregates (RA) and without RA. 1. [11]; 2. [92]; 3.[43]; 4.[93]; 5.[10] | 69 |
| Figure 2.19 Comparison of modulus of elasticity at 28 days by different researchers between 10-20% crumb rubber compared to natural aggregate concrete. 1. [35]2. [30]; 3.[28]4. [25]5. [31] | 70 |
| Figure 2.20 Stress strain curves of recycled aggregate concrete and natural aggregate concrete (Xiao et al., 2005) | 71 |
| Figure 2.21 Stress strain curves for self-compacting rubber concrete (SCCR) at 28 days (Long et al., 2012)..... | 71 |
| Figure 2.22 Mixing procedures for the normal mix (NMA) and the two-stage mixing approach (TSMA) (Tam et al., 2005). | 84 |
| Figure 2.23 Typical splitting failure of a beam end specimen [105] | 89 |
| Figure 2.24 Test load slip curves for; (a) Natural aggregate concrete and deformed rebar; (b) 100% Recycled aggregate concrete and deformed rebars [99] | 90 |

| | |
|---|-----|
| Figure 2.25 Normalized bond strength between 10mm rebars and recycled aggregate concrete of different replacement levels [99, 100]. | 91 |
| Figure 2.26 Comparison of RCPT results from different studies; 1.[108]; 2[109]; 3. [110]..... | 92 |
| Figure 2.27 Rapid chlorine penetration resistance of concrete with crumb rubbers [86] | 94 |
| Figure 2.28 Comparison of drying shrinkage values from different concrete mixes [108] | 95 |
| Figure 2.29 Drying shrinkage of concrete with different recycled aggregate replacement level with and without fly ash (FA)..... | 96 |
| Figure 2.30 Shrinkage behaviour of cement matrix with different crumb rubber content.[112] | 97 |
| Figure 2.31 Carbonation depth of concrete with different RA concentration [9] | 98 |
| Figure 2.32 Carbonation depth with respect to replacement level [83] | 99 |
| Figure 2.33 Carbonation depth of concrete with rubber ash at different replacement levels to sand for w/c of 0.35, 0.45 and 0.55 (data extracted from [42]). | 100 |
| Figure 2.34 Creep strain of concrete with different recycled aggregate replacement levels with and without fly ash (FA) [9] | 101 |
| Figure 2.35 Load- mid-span deflection curves of natural and recycled aggregate concrete beams [14] | 103 |
| Figure 2.36 Comparison of cracks and failure patterns between natural and recycled aggregate concrete beams with 0.28% and 1.46% reinforcement ratio [14] | 103 |
| Figure 2.37 Comparison of experimental/analytical load-deflection curves of all test beams [43]..... | 104 |
| Figure 2.38 Load-deflection plots of reinforced concrete beams with different crumb rubber content [96]..... | 105 |
| Figure 2.39 Singly reinforced rectangular beam section subject to bending [113]..... | 106 |
| Figure 2.40 Crack patterns of recycled aggregate concrete beams in shear compared to | |

| | |
|--|-----|
| natural aggregate concrete beams with the same longitudinal reinforcement ratio [117]..... | 108 |
| Figure 2.41 Load-deflection curves of recycled aggregate concrete beams compared to natural aggregate concrete beams with the same longitudinal reinforcement ratio [117]..... | 109 |
| Figure 2.42 Mid span deflections of the beam with different amounts of shear reinforcement [116]..... | 110 |
| Figure 2.43 Shear capacity of beams with respect to crumb rubber content [122]..... | 111 |
| Figure 2.44 Ratio of experimental to shear strength to that of code predicted methods [122]..... | 112 |
| Figure 2.45 Effect of recycled aggregate replacement ratio to shear load [121]. | 113 |
| Figure 2.46 Internal forces in a cracked beam section with (a) and without (b) web reinforcements [124]..... | 114 |
| Figure 2.47 Variable truss inclination model [113] | 114 |
| Figure 2.48(a) Composite beam section of two layers (b) Horizontal shear stresses of a composite section (c) Horizontal slip due to interface failure (d) Non composite section under bending due to interface failure [126] | 118 |
| Figure 2.49 Shear friction hypothesis [130]..... | 120 |
| Figure 2.50 Inclined shear friction of reinforcement [127]..... | 121 |
| Figure 2.51 Interfacial shear stresses in a simply supported beam under transverse load | 122 |
| Figure 2.52 Horizontal shear stress based on elastic beam behaviour..... | 123 |
| Figure 2.53 Compressive strength of concrete with graphene and graphene oxides compared to reference concrete [46]..... | 126 |
| Figure 2.54 Residual strength with respect to the duration of chemical attack [46]. ... | 126 |
| Figure 2.55 Result of water permeability test for cement matrix [139]. | 127 |

| | |
|--|-----|
| Figure 2.56(a) Stress strain plot of concrete and graphene reinforced concrete (b) strength of concrete over time compared with graphene reinforced concrete. | 128 |
| Figure 2.57 Effect of graphene concentration of the strength and elastic modulus of concrete. | 129 |
| Figure 2.58 Water permeability of graphene reinforced concrete at different concentrations for a 7- day test. | 130 |
| Figure 2.59: Compressive strength of concrete with varying graphene oxide (GO) content at different times of testing [140] | 131 |
| Figure 3.1 Grading of natural aggregates, recycled aggregates and fine sand | 135 |
| Figure 3.2 Crumb rubber (8mm length and 2mm thickness) particles from worn-out tyres | 137 |
| Figure 3.3 Slump measurement [148] | 140 |
| Figure 3.4 Slump of fresh concrete of different mixes. | 140 |
| Figure 3.5 Influence of crumb rubber on the workability of recycled aggregate concrete. | 141 |
| Figure 3.6 Correlation of slump and compressive strength of different mixes. | 142 |
| Figure 3.7 Comparison of compressive strengths of different concrete mixes | 144 |
| Figure 3.8 Influence of crumb rubber content on the compressive strength of recycled aggregate concrete with and without super plasticisers. | 145 |
| Figure 3.9 Comparison of compressive strengths of rubber recycled aggregate concrete with age. | 145 |
| Figure 3.10 Splitting tensile strength of different design mixes | 147 |
| Figure 3.11 Correlation between splitting strength and the percentage of crumb rubber. | 147 |
| Figure 3.12 Elastic modulus of recycled aggregate concrete with and without super plasticiser compared to the natural aggregate concrete mix (NAC) | 148 |

| | |
|---|-----|
| Figure 3.13 Correlation between elastic modulus of recycled aggregate concrete with respect to crumb rubber content..... | 149 |
| Figure 3.14 UPV of natural aggregate concrete mix and recycled aggregate concrete | 150 |
| Figure 3.15 Influence of crumb rubber content on the ultrasonic pulse velocity of recycled aggregate concrete. | 151 |
| Figure 3.16 Compressive stress strain relationships of recycled aggregate concrete with different amounts of rubber particles, all with super plasticiser | 152 |
| Figure 3.17 Cross sectional view of the pull-out specimen | 154 |
| Figure 3.18 Test set up and instrumentation | 154 |
| Figure 3.19 Average bond stress v slip relationships from pull-out tests | 155 |
| Figure 3.20 Comparison of normalized bond strength to concrete shear strength. | 156 |
| Figure 3.21 Slant shear test specimen configuration..... | 160 |
| Figure 3.22 Wooden mould for placing the first layer of concrete | 160 |
| Figure 3.23 Slant shear test set up and instrumentation..... | 161 |
| Figure 3.24 Set up for splitting test..... | 162 |
| Figure 3.25 Failure envelope of both natural aggregate concrete and recycled concrete. | 163 |
| Figure 3.26 Pure shear strength of slant shear test specimens with interfacial failure | 164 |
| Figure 3.27(a) Interfacial and (b) compressive (monolithic behaviour) failure modes of specimens | 165 |
| Figure 3.28 Comparison of interfacial shear strength..... | 167 |
| Figure 3.29 Failure modes of specimens (a) Interfacial failure with partial failure of the substrate (recycled concrete) (b) pure shear failure. | 168 |
| Figure 3.30 Bond strength in tension of test specimen | 168 |
| Figure 3.31 Comparison of interfacial shear strength without a normal stress..... | 169 |
| Figure 3.32 (a) Recycled aggregates (RA2) from crushed brick/concrete | |

| | |
|---|-----|
| (https://www.offertonsandandgravel.co.uk/gravel-aggregate/crushed-brick-concrete-mot) (b) Graphene solution | 172 |
| Figure 3.33(a) Washing set up of recycled aggregates (b) Washed recycled aggregates | 175 |
| Figure 3.34 Comparison of compressive strengths of recycled aggregate concrete with crumb rubber (RRAC) with different concentrations of graphene solution | 176 |
| Figure 3.35 Effects of different graphene concentrations on the compressive strength of natural aggregate concrete | 177 |
| Figure 3.36 Effects of different graphene concentrations on the compressive strength of recycled aggregate concrete | 178 |
| Figure 3.37 Effect of different graphene concentrations on the tensile strength of natural aggregate concrete..... | 180 |
| Figure 3.38 Effect of different graphene concentrations on the tensile strength of recycled aggregate concrete..... | 181 |
| Figure 3.39 Splitting tensile strength and standard deviation of natural aggregate concrete compared to current studies 1[160]; 2[161];3[61];3[162]..... | 181 |
| Figure 3.40 Stress strain curves of natural aggregate concrete with different graphene concentrations | 182 |
| Figure 3.41 Stress strain curves of washed recycled aggregate concrete with different graphene concentrations..... | 183 |
| Figure 4.1 Dimensions of two-layer beam for bending tests | 188 |
| Figure 4.2 Dimensions of two-layer shear test beams | 188 |
| Figure 4.3(a) Recycled aggregates (b) Natural aggregates (c) crumb rubber from worn-out tyres..... | 190 |
| Figure 4.4 Failure modes of beams in bending | 192 |
| Figure 4.5 Load deflection curves of bending test beams..... | 193 |

| | |
|--|-----|
| Figure 4.6 Comparison of experimental load-longitudinal reinforcement bar strain curves of bending test tests | 193 |
| Figure 4.7 Failure modes of shear test beams | 194 |
| Figure 4.8 Load deflection curves for the regular concrete beams and two-layer beams of the shear test. | 195 |
| Figure 5.1 Element types for concrete and steel reinforcement [165] | 200 |
| Figure 5.2 Stress crack opening width curve for cracked concrete [131] | 201 |
| Figure 5.3 Cross section and reinforcement layout of flexural beam test [44] | 203 |
| Figure 5.4 Geometry and Mesh density of the test beam [44] | 203 |
| Figure 5.5 Comparison between load deflection plots at mid span between the experiment of [44] and the author's ABAQUS simulation | 204 |
| Figure 5.6 Comparison of load tensile strain plots for the main reinforcement bar [44]..... | 205 |
| Figure 5.7 Results of mesh sensitivity analysis of regular reinforced concrete beam . | 206 |
| Figure 5.8 Geometry and mesh density of (a) Regular concrete beam (b) Two-layer beam..... | 206 |
| Figure 5.9 Comparison of experimental and numerical load deflection plots for regular concrete beams and two-layer beams in bending..... | 207 |
| Figure 5.10 Comparison of experimental and numerical load-deflection plots, for regular concrete beams and two-layer beams in shear..... | 208 |
| Figure 5.11 Comparison of experimental and numerical simulation results for load-longitudinal tensile steel strain curves for regular concrete beams | 209 |
| Figure 5.12 Comparison of experimental and numerical simulation results for load-longitudinal tensile steel strain curves for two-layer beams | 209 |
| Figure 5.13 Numerical simulation results of crack pattern and failure mode of shear beams | 210 |

| | |
|---|-----|
| Figure 5.14 Numerical simulation results of crack pattern and failure mode of flexural beams | 211 |
| Figure 5.15 Comparison of numerical results of load-deflection at mid-span of two-layer beams of different recycled concrete grades with regular concrete beam ... | 212 |
| Figure 5.16 Comparison of numerical results of strain in longitudinal reinforcement of two-layer beams of different recycled concrete grades with regular concrete beam at mid-span. | 213 |
| Figure 5.17 Concrete stress distribution diagram along beam depth at mid-span. | 213 |
| Figure 5.18 Influence of ratio of top layer thickness to bottom layer thickness on shear resistance of two-layer beam..... | 214 |
| Figure 5.19 Influence of top layer NAC mix on shear resistance of two-layer beam. . | 215 |
| Figure 5.20 Comparison of shear resistance of two-layer beams for different shear span to depth ratios (2.6, 3.4 and 3.9). | 216 |
| Figure 5.21 Ratio of tests or simulation results to predict shear strength of two-layer beams by existing models for a reinforcement ratio of 2.64% and shear span to depth ratio 3.4. | 220 |
| | |
| Figure 6.1 Detailed section of RC Beam (a) Regular concrete beam section (b) two-layer beam section..... | 225 |
| Figure 6.2 Structural detailing of the regular concrete beam..... | 227 |
| Figure 6.3 Structural detailing for the two-layer beam. | 233 |
| | |
| Figure A.1 Compressive stress strain curves of natural aggregate concrete samples .. | 254 |
| Figure A.2 Compressive stress strain curves for recycled aggregate concrete without crumb rubber | 254 |
| Figure A.3 Compressive stress strain curves for recycled aggregate concrete with 5% crumb rubber content (RRACSP 5%)..... | 255 |
| Figure A.4 Compressive stress strain curves for recycled aggregate concrete with 10% | |

| | |
|---|-----|
| crumb rubber content (RRACSP 10%) | 255 |
| Figure A.5 Compressive stress strain curves for recycled aggregate concrete with 15% crumb rubber content (RRACSP 15%) | 256 |
| Figure A.6 Compressive stress strain curves for recycled aggregate concrete with 15% crumb rubber content (RRACSP 20%) | 256 |
| Figure B.1 Average bond stress slip relationship of pull-out test of natural aggregate concrete and rebars for all samples. | 258 |
| Figure B.2 Average bond stress slip relationship of pull-out test of recycled aggregate concrete (RAC) and rebars for all samples. | 258 |
| Figure B.3 Average bond stress slip relationship of pull-out test of recycled aggregate concrete with 5% crumb rubber (RRAC 5%) and rebars for all samples. | 259 |
| Figure B.4 Average bond stress slip relationship of pull-out test of recycled aggregate concrete with 15% crumb rubber (RRAC 15%) and rebars for all samples. | 259 |
| Figure D.1 Compressive stress strain of natural aggregate concrete with 0.01% graphene concentration. | 265 |
| Figure D.2 Compressive stress strain of natural aggregate concrete with 0.02% graphene concentration..... | 265 |
| Figure D.3 Compressive stress strain of natural aggregate concrete with 0.05% graphene concentration..... | 266 |
| Figure D.4 Compressive stress strain of washed recycled aggregate concrete without graphene solution | 266 |
| Figure D.5 Compressive stress strain of washed recycled aggregate concrete with 0.01% graphene concentration | 267 |
| Figure D.6 Compressive stress strain of washed recycled aggregate concrete with 0.02% graphene concentration | 267 |
| Figure D.7 Compressive stress strain of washed recycled aggregate concrete with 0.05% | |

| | |
|--|-----|
| graphene concentration | 268 |
| Figure E.1 Effect of reinforcement ratio on the shear capacity of two-layer beams.... | 274 |
| Figure E.2 Effect of reinforcement ratio on the shear capacity of regular concrete beams | 274 |

List of Tables

| | |
|--|-----|
| Table 1.1 Recovery rate from non-hazardous construction and demolition waste, | 36 |
| Table 2.1 Classification of recycled aggregates [48]. | 46 |
| Table 2.2 Composition of a tyre: Typical components [51] | 47 |
| Table 2.3 Specific gravity and water absorption of crumb rubber particles [54]..... | 48 |
| Table 2.4 Physical properties sea water after immersion in sea water for 42 years [49] | 51 |
| Table 2.5 Properties of natural and recycled aggregates [59] | 52 |
| Table 2.6 Summary of previous research studies on recycled aggregates concrete for 28-day curing compared to natural aggregate concrete..... | 73 |
| Table 2.7 Summary of previous research studies on concrete made with crumb rubber | 77 |
| Table 2.8 Summary of methods devised to improve the mechanical properties of recycled aggregate concrete (RAC) | 85 |
| Table 2.9 Summary of methods to improve the mechanical properties of concrete with crumb rubber | 87 |
| Table 2.10 Ion chloride permeability based on charge passed [111] | 93 |
| Table 3.1 Water absorption rate of natural and recycled aggregates | 135 |
| Table 3.2 Composition of natural and recycled aggregates | 136 |
| Table 3.3 Reference concrete composition | 138 |
| Table 3.4 Experimental programme | 138 |
| Table 3.5 concrete classification based on ultrasonic pulse velocity (Najim and Hall, 2013b, Mohammed et al., 2011) | 150 |
| Table 3.6 Experimental results of the pull-out specimens | 155 |
| Table 3.7 Notation and description of test specimen | 158 |

| | |
|--|-----|
| Table 3.8 Summary of slant shear and splitting tests of all specimens. | 166 |
| Table 3.9 Mix composition of graphene solution | 173 |
| Table 3.10 Reference mix for C40 concrete | 173 |
| Table 3.11 Detailed mix compositions of recycled aggregate concretes with graphene | 173 |
| Table 3.12 Mix composition of graphene solution | 175 |
| Table 4.1 Mix composition of natural aggregate concrete and rubber recycled aggregate concrete with 10% of rubber particles of recycled aggregate weight (RRAC10) per m ³ | 189 |
| Table 4.2 Properties of fresh and hardened concrete for bending and shear tests | 190 |
| Table 4.3 Properties of shear and longitudinal reinforcement for all test beams | 191 |
| Table 4.4 Results of beam tests | 196 |
| Table 5.1 Comparison of bending resistance for all beams to EC2 | 217 |
| Table 5.2 Code methods of the shear strength of beams without stirrups | 218 |
| Table 5.3 Comparison of shear resistance for all test and numerical simulation beams | 218 |
| Table 5.4 Prediction of shear strength of concrete beams with existing equations | 219 |
| Table 6.1 Bar bending schedule for flexural and vertical shear links for the regular concrete beam | 227 |
| Table 6.2 Bar bending schedule for flexural and vertical shear links for the two-layer beam | 229 |
| Table 6.3 Reinforcement schedule for two-layer beam | 234 |
| Table 6.4 Weight of rebars used to resist vertical and horizontal shear for all beams . | 234 |
| Table 6.5 Cost analysis of vertical and horizontal shear links of the two-layer beams compared to the regular concrete beams | 235 |

| | |
|---|-----|
| Table A.1 Sieve analysis of virgin aggregates | 247 |
| Table A.2 Sieve analysis of recycled aggregates (RA1) | 247 |
| Table A.3 Sieve analysis of recycled aggregates (RA2) | 248 |
| Table A.4 Sieve analysis of fine sand | 248 |
| Table A.5 Water absorption test of virgin aggregates | 249 |
| Table A.6 Water absorption test of recycled aggregates (RA1) | 249 |
| Table A.7 Water absorption test of recycled aggregates (RA2) | 250 |
| Table A.8 Mix design of natural aggregate concrete | 250 |
| Table A.9 Compressive strength of 3 samples of different recycled concrete mix without crumb rubber | 251 |
| Table A.10 Compressive strength of 3 samples of different recycled concrete mix with and without crumb rubber | 252 |
| Table A.11 Tensile strength of 3 samples of natural aggregate concrete and recycled aggregate concrete | 252 |
| Table A.12 Tensile strength of 3 samples of different recycled concrete mixes with and without crumb rubber | 252 |
| Table A.13 Ultrasonic pulse velocity (UPV) of recycled and natural aggregate concrete | 253 |
| Table A.14 Ultrasonic pulse velocity (UPV) of recycled concrete with different crumb rubber content | 253 |
| Table C.1 Slant shear test results of 3 samples of all specimens | 261 |
| Table C.2 Splitting shear test results of 3 samples of all specimens | 261 |
| Table C.3 Notation and description of specimen types | 261 |
| Table D.1 Influence of graphene concentration on the strength of recycled concrete with 10% crumb rubber | 263 |

Table D.2 Influence of graphene concentration on the compressive strength of natural aggregate concrete..... 263

Table D.3 Influence of graphene concentration on the tensile strength of natural aggregate concrete..... 263

Table D.4 Influence of graphene concentration on the compressive strength of washed and unwashed recycled aggregate concrete without crumb rubber 264

Table D.5 Influence of graphene concentration on the tensile strength of washed and unwashed recycled aggregate concrete without crumb rubber 264

Table F 1: Cost estimate of the regular concrete beam 279

Abstract

Despite extensive research studies, construction demolition waste (CDW) and worn-out tyres of motor vehicles are still not fully reused and are hence disposed of in ways that are damaging to the environment. . There have been a number of investigations into manufacturing concrete using recycled aggregates from CDW and crumb rubber. However, it has not been possible to make recycled aggregate concrete with the-same performance as standard natural aggregate concrete (NAC) without incurring extra costs. Production of natural coarse aggregates is environmentally damaging and also costly. With surging demand for concrete worldwide, and to respond to the call of sustainable development, it is vital that the enormous quantities of CDW and tyres with high embodied carbon content are used in structural applications without compromising cost and performance. This thesis focuses on two ways of doing so: by finding alternative ways of improving the mechanical properties of recycled aggregate concrete to achieve those of concrete using natural aggregates, and to find new ways of using recycled aggregate concrete where the demand on the mechanical properties of concrete can be easily met by recycled aggregate concrete. Regarding the former, the research investigates the feasibility of adding a tiny amount of graphene (109g) to a cubic metre of recycled aggregate concrete. The 109g of graphene is equivalent to 0.01% (optimized concentration) of the combined weight of cement and sand of the design concrete mix. Regarding the latter, this research considers using recycled aggregate concrete in the tension zone of reinforced concrete beams.

Mechanical property tests have been carried out on recycled aggregate and crumb rubber concrete, with or without graphene. In the first part of this research, comparisons were made between concrete using 10mm size uncrushed quartzite stones (NAC mix, C40), recycled aggregate concrete (RAC) and rubber recycled aggregate concrete mix (RRAC). The slump test results show RAC suffered a 73% reduction in slump value compared to the NAC mix. However, the slump value of RAC was increased by 72% by

introducing an additional amount of water (4.21% of recycled aggregate weight measured from a water absorption test) or by 75% using DARACEM 215 superplasticizers (1% of cement weight). As expected, the compressive and tensile strengths, elastic modulus and ultrasonic pulse velocity of the recycled aggregate concrete were lower than those of the NAC mix, by 14.9%, 14.8% , 4.3% and 7.4% respectively. Introducing crumb rubber (by 5%, 10%, 15% and 20% of recycled aggregate weight) into the recycled aggregate concrete further decreased its workability and mechanical properties with or without superplasticizers. In the interest of workability, this research recommends limiting the weight of rubber to not more than 10% of the recycled aggregate weight. With 5% and 10% rubber, the compressive strengths of RRAC were 32.8% and 47.1% of the NAC mix using uncrushed 10mm quartzite aggregates. Inclusion of rubber crumb seemed to help the ductility of RRAC as observed by the slower rate of stress reduction in the descending branch of the measured stress strain curve.

The second part of the mechanical property investigation explores the feasibility of using graphene to improve the mechanical properties of recycled aggregate concrete and rubber recycled aggregate concrete with 10% of crumb rubber content. Graphene concentrations of 0.01%, 0.02%, 0.05% and 0.1% of the combined weight of cement and sand and of different sizes (5 μ m, 10 μ m and 20 μ m) were incorporated into recycled aggregate concrete and natural aggregate concrete. Except where G5 0.02% was used (graphene size 5 μ m, 0.02% by weight) which resulted in a modest 12.2% increase in compressive strength compared to the recycled aggregate concrete with rubber, including graphene decreased the compressive strength of rubber recycled aggregate concrete. This was attributed to the inability of graphene to enhance the low bonding strength between rubber particles and cement matrix. Due to the excessive amount of dust in the recycled aggregates, adding graphene to recycled aggregate concrete without rubber did not improve the mechanical properties of recycled aggregate concrete. The key to improving the mechanical properties of recycled aggregate concrete is to enhance the bonding at the interface between the cement and aggregates. To do so, the recycled aggregates were washed in further tests. By adding 0.01% (2.2g) of G10 graphene to

the washed recycled aggregate concrete, the compressive and tensile strengths were enhanced by 43.9% and 24.1% respectively to reach values of 39.14MPa and 3.76MPa which are similar to those of C40 NAC with values of 42.MPa and 3.77MPa respectively.

Tests were carried out to obtain the bond strength between rubber recycled aggregate concrete and deformed steel rebar. The bond strength of recycled aggregate concrete without rubber particles was 16.3% higher than that of the NAC. This confirms the results of other investigators and can be attributed to the better interlocking resistance due to the more irregular shapes of recycled aggregates compared to the uncrushed 10mm quartzite stones. Adding crumb rubber particles decreased the rebar pull-out bond strength, due to a lack of resistance of the rubber particles. However, if the rebar bond strength is normalised to the strength of concrete, according to $\tau_{max}/(f_c)^{0.5}$ then incorporating rubber particles would not adversely affect the bond strength of recycled aggregate concrete.

In regular reinforced concrete beams or slabs under bending, the tension strength of concrete is ignored in designs according to EC2, thus providing an opportunity to use recycled aggregate concrete in the tension zone of such members. This would necessitate a two-layer construction in which concrete with natural aggregates is used in the compression zone to provide the required compressive strength. The two layers of concrete are not cast monolithically. It is important that the concrete interface has sufficient shear strength to prevent interfacial shear failure. The slant shear test was used to determine the interfacial shear strength in this work. In this research, two time lags between casting of the two different layers, of 4 and 24 hours, were investigated. The two-layer concrete cast in the 4-hour time interval behaved monolithically while those cast at the 24-hour cast time interval failed at the interface with an interfacial strength of about 1.5MPa for all tests. For the particular types of concrete examined here, it is recommended to cast the two layers of concrete within a time limit of 4 hours in order to reduce the cost of construction by avoiding provisions of extra shear links

that may be necessary for preventing interfacial shear failure between the two layers of concrete.

Experimental, numerical and analytical investigations have been carried out to investigate the feasibility of using concrete made with recycled aggregate and crumb rubber in the tension area of reinforced concrete beams under bending and shear, and to propose design recommendations. In the beams, the top layer ($1/3^{\text{rd}}$) of concrete, mainly in compression, is a higher grade using uncrushed 10mm quartzite stones, and the bottom ($2/3^{\text{rd}}$) layer, in tension, is a lower grade using rubber recycled aggregate concrete. A total of 8 beam tests were conducted, to investigate the effects of changing NAC and recycled concrete strength and, top and bottom layer thickness ratio and shear span to depth ratio. The results confirm that the two-layer beam achieves the same bending resistance as the regular reinforced concrete beam made entirely of the higher grade concrete. The flexural bending resistance of the two layer beam can be calculated in exactly the same way as for the concrete beam made entirely of the higher grade concrete.

In beams without shear reinforcement for investigation of shear resistance, the two-layer beams attained lower shear resistance than the regular concrete beams. This was attributed to the unzipping effect: once the lower strength concrete has failed in shear, it loses its shear resistance and transfers the shear force from the failed lower strength concrete to the natural aggregate concrete in compression. Further FE simulations, using ABAQUS, reveal that the top layer higher grade concrete plays no role in influencing the beam's shear resistance. Therefore, when calculating the shear resistance of concrete of the two-layer beam, the lower concrete grade should be used. However, since the shear force in reinforced concrete beams is mainly resisted by shear links according to EC2, the lower shear resistance of rubber recycled aggregate concrete has very minor implications on beam shear resistance, as demonstrated by representative design cases. Modification of recycled aggregate concrete by adding a small amount of graphene (0.01% of the combined weight of cement and sand) and the proposed two-layer beam construction facilitate the wider adoption of recycled aggregate concrete in structural applications to partially replace natural aggregate concrete (NAC).

Declaration

No portion of the work referred to in the thesis has been submitted in support of an application for another degree or qualification of this or any other university or other institute of learning.

Copyright Statement

- i. The author of this thesis (including any appendices and/or schedules to this thesis) owns certain copyright or related rights in it (the “Copyright”) and s/he has given The University of Manchester certain rights to use such Copyright, including for administrative purposes.
- ii. Copies of this thesis, either in full or in extracts and whether in hard or electronic copy, may be made only in accordance with the Copyright, Designs and Patents Act 1988 (as amended) and regulations issued under it or, where appropriate, in accordance with licensing agreements which the University has from time to time. This page must form part of any such copies made.
- iii. The ownership of certain Copyright, patents, designs, trademarks and other intellectual property (the “Intellectual Property”) and any reproductions of copyright works in the thesis, for example graphs and tables (“Reproductions”), which may be described in this thesis, may not be owned by the author and may be owned by third parties. Such Intellectual Property and Reproductions cannot and must not be made available for use without the prior written permission of the owner(s) of the relevant Intellectual Property and/or Reproductions.
- iv. Further information on the conditions under which disclosure, publication and commercialisation of this thesis, the Copyright and any Intellectual Property and/or Reproductions described in it may take place is available in the University IP Policy (see <http://documents.manchester.ac.uk/DocuInfo.aspx?DocID=24420>), in any relevant Thesis restriction declarations deposited in the University Library, The University Library’s regulations (see <http://www.library.manchester.ac.uk/about/regulations/>) and in The University’s policy on Presentation of Theses.

Acknowledgements

The author wishes to thank his supervisors, Professor Y.C Wang and Paul Nedwell for the supervision, valuable guidance, counsel, continuous support and encouragement throughout the period of this PhD research.

I also wish to express my gratitude to John Mason for the support in the laboratory tests.

Many thanks to Dr Lee Cunningham and Dr P. Mandal for their useful advice in my yearly transfer reports.

Special thanks to all student members of the Structures and Fire group for their care and encouragement.

My appreciation goes to my parents and wife for their moral support and encouragements and to TETFUND for their financial support.

Finally, the author would like to thank GOD for the breath of life and my sound health throughout period of this PhD research work.

Publications

ATARIA, R. B. & WANG, Y. C. 2019. Bending and shear behaviour of two-layer beams with one layer of rubber recycled aggregate concrete in tension. *Structures*, 20, 214-225.

Presentations

- MACE Postgraduate Research Conference 2017, Manchester, UK. (Oral presentation).
- Young Researchers Conference 2018, the Institute of Structural Engineers, London, UK. (Poster presentation)

Panel of Judges

Professor Dennis Lam (University of Bradford), Professor John Forth (University of Leeds), Dr Keerthi Ranasinghe (University of Wales Trinity Saint David), Susan Giahi-Broadbent (Jacobs), Chris Walker (COWI)

Awards

Joint third prize winner in poster presentation category in Young Researchers Conference 2018, the institute of Structural Engineers, London, United Kingdom.

Chapter 1

Introduction

1.1 Background

1.1.1 Recycled Aggregate from construction and demolition waste (CDW)

Recycled aggregates are obtained or produced from the processing of concrete waste generated from the demolition of concrete structures, left-over concrete from mix plants, abandoned precast concrete members, road bed concrete and asphalt pavements etc. Generally, recycled aggregates may be in different forms: glass aggregates, tiles and marble aggregates, concrete aggregates, bricks aggregates. Recycled aggregates are often mixed with tiles, bricks, paper, wood, plastics and several other types of debris that constitute the parent material.

It is estimated that the UK generated 66.2 million tonnes of non-hazardous C&D waste, of which 60.2 million tonnes was recovered. This represents a recovery rate of 91.0% [1] as shown in Table 1.1. The need to reuse the recovered waste in the construction

industry, without compromising cost and performance, is of great concern. The use of recycled materials helps in reducing the need for material extraction which would otherwise result in material depletion and other environmental problems. Despite the environmental benefit associated with the recycling of construction, post-consumer and industrial waste and its ultimate use in construction, research studies have revealed that recycled materials have been under-utilised in construction projects and their acceptance is still low within the construction industry [2].

On the other hand, there is an increasing need for natural aggregates which is about 75% of the concrete weight. It was reported by [4] that up to 20 billion metric tons of natural aggregates are consumed every year around the globe. Construction activities consume about 50% of natural resources, 40% of energy and above all create 50% of waste [5]. Therefore, employing recycled aggregates (RA) as a structural material has many benefits as illustrated in Figure 1.1. How to reuse CDW, especially recycled aggregates, in producing new concrete is an important route towards sustainability in the construction industry.

Table 1.1 Recovery rate from non-hazardous construction and demolition waste, UK and England[1]

| | UK | | | England | | |
|------|------------|----------|---------------|------------|----------|---------------|
| | Generation | Recovery | Recovery rate | Generation | Recovery | Recovery rate |
| | M tonnes | M tonnes | % | M tonnes | M tonnes | % |
| 2010 | 59.2 | 53.1 | 89.7% | 53.6 | 49.4 | 92.2% |
| 2011 | 60.2 | 55.0 | 91.4% | 54.9 | 50.8 | 92.5% |
| 2012 | 55.8 | 50.8 | 91.1% | 50.5 | 46.4 | 92.0% |
| 2013 | 57.1 | 52.0 | 91.2% | 51.7 | 47.6 | 92.0% |
| 2014 | 61.5 | 56.3 | 91.5% | 55.9 | 51.7 | 92.4% |
| 2015 | 63.8 | 58.1 | 91.1% | 57.7 | 53.3 | 92.3% |
| 2016 | 66.2 | 60.2 | 91.0% | 59.6 | 55.0 | 92.1% |

Many researchers have attempted to produce new concrete with recycled aggregates from CDW [6-12]. Many researchers have also studied the performance of reinforced concrete members (beams) made with recycled aggregates from CDW[13, 14].

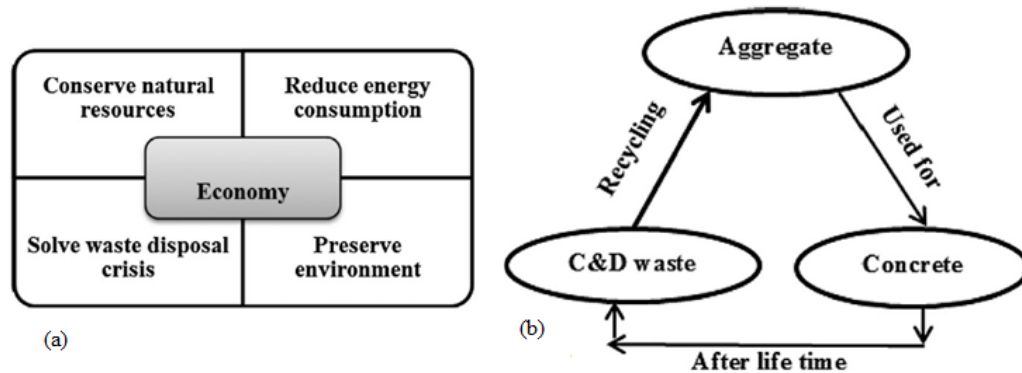


Figure 1.1 (a) Benefits and (b) Lifecycle of recycled aggregate from CDW[15]

1.1.2 Recycling process of recycled aggregate

Recycling is the process of producing new valuable products from used materials. The concept of recycling aggregates is by demolishing/crushing old existing buildings/structures and subjecting the crushed concrete into a process of screening to remove all unwanted debris like reinforcement, plastics, wood etc. as shown in Figure 1.2. Depending on the quality of aggregates to be produced, the process of crushing, sizing, sorting (pre crushing), and removal of contaminants is continuous until the required recycled aggregate is achieved.

Jaw crushers, impact crushers, hammer mill, hand hammer etc. are different types of crushers that can be used in crushing demolished debris/concrete [16]. All the above mentioned crushers affect the physical and mechanical properties of the recycled aggregates produced. The jaw crushers are mainly used to crush oversized concrete into small sizes while the impact crushers are mainly to reduce the amount of attached cement matrix on the recycled aggregates[17, 18]. To achieve the desired grade of recycled aggregates, it is necessary to put them through the process of a primary to a secondary stage of crushing. The type of crushers adopted at each stage depends on the quality of recycled aggregates required with respect to size, amount of fine aggregates, and shape of the recycled aggregates. Some developed countries like the USA, China, Japan, and the Netherlands have devised wet processing techniques along with dry processing techniques (crushing process) to obtain recycled aggregates of better quality, comprising fewer impurities.

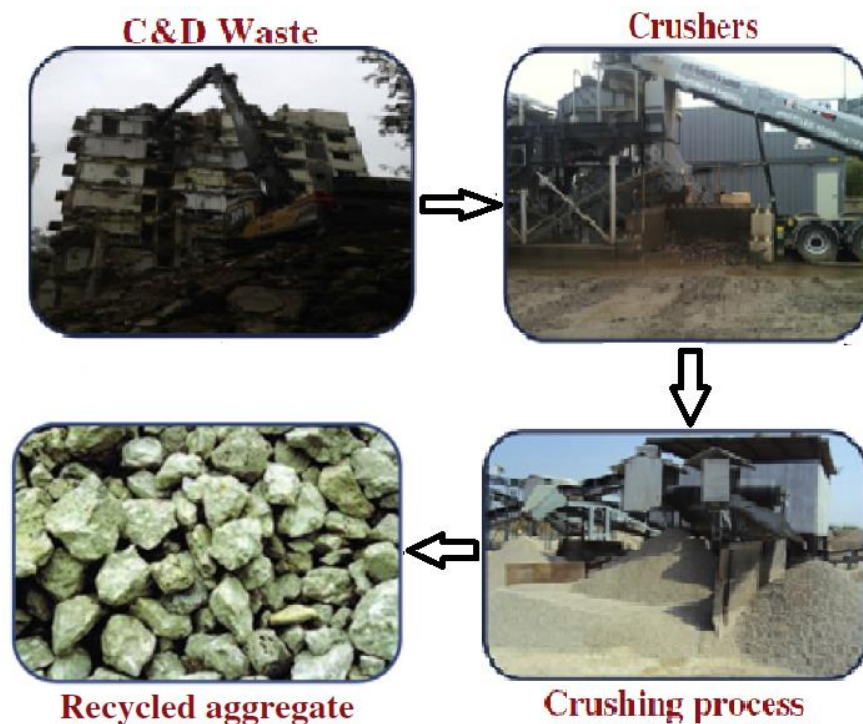


Figure 1.2 Recycling processes of recycled aggregates from demolished structure

Wet processing techniques such as pre-soaking treatment [19], nitric acid dissolution method, the micro waving heating method [20], thermal expansion method, ultrasonic treatment method [21] etc. are mainly used to remove the attached cement matrix from the recycled aggregate.

1.1.3 Crumb rubber from discarded tyres and rubber recycled aggregate concrete (RRAC)

Discarded tyres from vehicles are another major source of solid waste causing serious environmental problems all over the world. The total production of tyres in the EU, which are manufactured in about 90 plants, is estimated at 355 million per year, corresponding to 24% of the total world production [22]. According to European Tyre and Rubber Manufacturers Association (ETRMA), since 1999 more than 24 million

tons of scrap tyres have been recovered both through energy and material recovery, and in 2010 only 4% of the scrap tyre products ended up in landfills. Of the 96% recovered (38% recovery of energy, 40% recycling of materials, 8% reconstruction, and 10% reuse/export). According to the ETRMA report, the annual cost of handling end of life tyres is around 600 million euros [22, 23]. Also stockpiling them in landfills as shown in Figure 1.3 can be a major source of fire outbreak, breeding grounds for mosquitoes and rats and as such are harmful to occupants in the surrounding area.

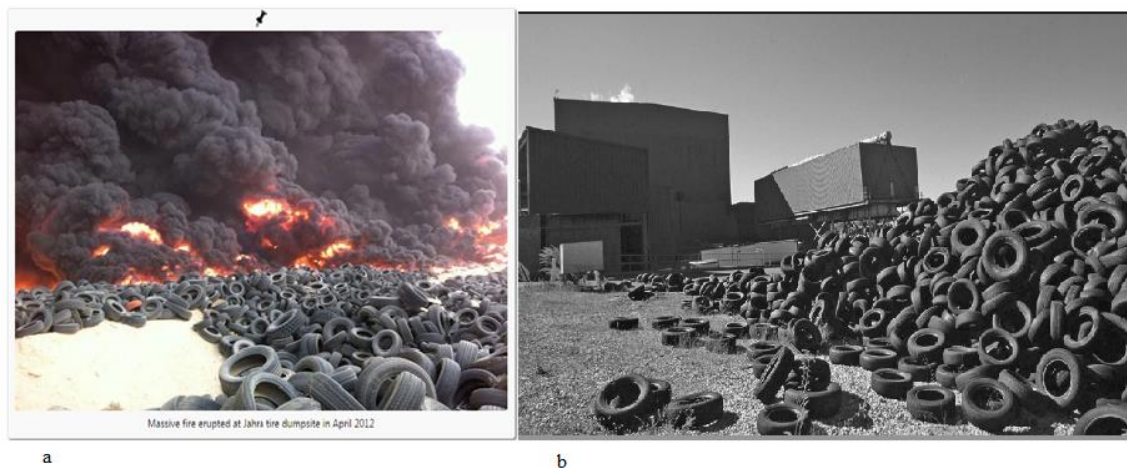


Figure 1.3 Landfill for waste tyres in Kuwait [24]

Due to the aforementioned issues associated with the disposal and recycling of waste tyres, researchers have focused on incorporating rubber particles into concrete mix [25-38]. Their findings have shown lower strength of recycled aggregate concrete incorporating rubber particles. The extent of concrete strength reduction depends on the concentration of crumb rubber in concrete, the treatment process of the crumb rubber prior to use and the use of additives in the design mix.

Considering the above mentioned issues associated with the disposal or reuse of CDW and scrap tyres, a lot of work has been done with regard to incorporating either recycled aggregates or rubber particles into concrete [9, 12, 19, 30, 35, 39-42] but very limited research has been done on concrete containing both recycled aggregates and rubber particles [39]. Rubber Recycled Aggregate concrete (RRAC) is a mixture of cement paste (cement, sand and water), rubber particles (crumb, shred or ash) and recycled

aggregates. This research will investigate the combined effects of crumb rubber and recycled aggregate on the mechanical properties of concrete.

Over the years, researchers have tried to employ recycled aggregate concrete (RAC) in producing structural components but encountered setbacks in terms of lower structural resistance compared to the structural members made of natural aggregate concrete (NAC)[43, 44] due to the reduced material properties of recycled aggregate concrete. As shown in detail in Section 2.2.8, if RRAC with strength lower than NAC is entirely used to make reinforced concrete beams, it will achieve lower resistance and will have higher deflections than beams made with natural aggregate concrete.

In order to enhance the performance of recycled concrete to attain the same strength as the natural aggregate concrete, a number of researchers have carried out investigations to find methods to improve the RRAC mechanical properties, either by adding extra cement or using additives [11, 14]. However, they all incur extra costs in making the structure.

1.2 Motivation of research

There are two potential methods of increasing the use of recycled aggregate concrete: producing recycled aggregate concrete with the same quality as concrete with natural aggregates with low environmental impact, or using recycled aggregate concrete in construction where concrete made of natural aggregates can be replaced by recycled aggregate concrete without loss of performance. This thesis will make new contributions in both aspects.

In terms of improving the mechanical properties of recycled aggregate concrete, with or without rubber particles, section 1.1.2 has mentioned the most common current ones. These techniques are considered time consuming, therefore, expensive, with significant environmental impacts. Therefore, this research will investigate the alternative method of adding a tiny amount of graphene to make recycled aggregate concrete. Previous studies have shown that the addition of graphene to concrete leads to an increase in compressive strength up to 146% and a dramatic decrease in water permeability to

nearly 400% compared to the natural aggregate concrete [45]. Graphene helps improve the weakest component of concrete, the interfacial zone between the cement paste and the aggregates [46] and is considered to have excellent potential to improve the mechanical properties of recycled aggregate concrete. With regards to replacing concrete with natural aggregates by recycled aggregate concrete without loss of structural performance, it is noted that in reinforced concrete beams or slabs, only a small amount of concrete is in compression and the tensile resistance of concrete is ignored. Therefore, if recycled concrete of low strength and stiffness is used in the tension zone of a reinforced concrete beam or slab, to create a two-layer beam as illustrated in Figure 1.4, the structural performance should not suffer. Whilst the effects of low strength RRAC on the bending behaviour of two-layer beams are relatively simple to resolve, this research will conduct some experiments and numerical simulation to validate the idea. The issue of evaluating the vertical shear resistance of two-layer beams requires more extensive investigation to understand the load carrying mechanism. Furthermore, longitudinal interfacial shear failure between the two layers may occur. It will be necessary to obtain longitudinal interfacial shear properties and investigate how they influence the failure mode of two-layer beams.

1.3 Objectives of research

The aims of this research are to explore the potential of adding a tiny amount of graphene to improve the mechanical properties of recycled aggregate concrete, and to test the hypothesis that the two-layer beam has the same or very similar structural performance as the beam made entirely of natural aggregate concrete. The specific research objectives are:

1. To examine the mechanical properties of concrete in the hardened (strength, elastic properties) and wet (workability) states when uncrushed quartzite aggregates of size 10mm are replaced with crumb rubber and recycled aggregates in different proportions with and without graphene.

2. To conduct physical tests and numerical modelling in examining the bending and shear resistances and deflection of reinforced concrete beams using RRAC in the tension area as shown in Figure 1.4.
3. To quantify the additional reinforcement needed to prevent vertical and longitudinal shear failure in practical two-layer beams compared to the regular concrete beam.
4. To conduct physical tests to assess the interfacial shear strength of two-layer beams and ensure monolithic behaviour.
5. To make design and construction recommendations of using RRAC in reinforced concrete beams.

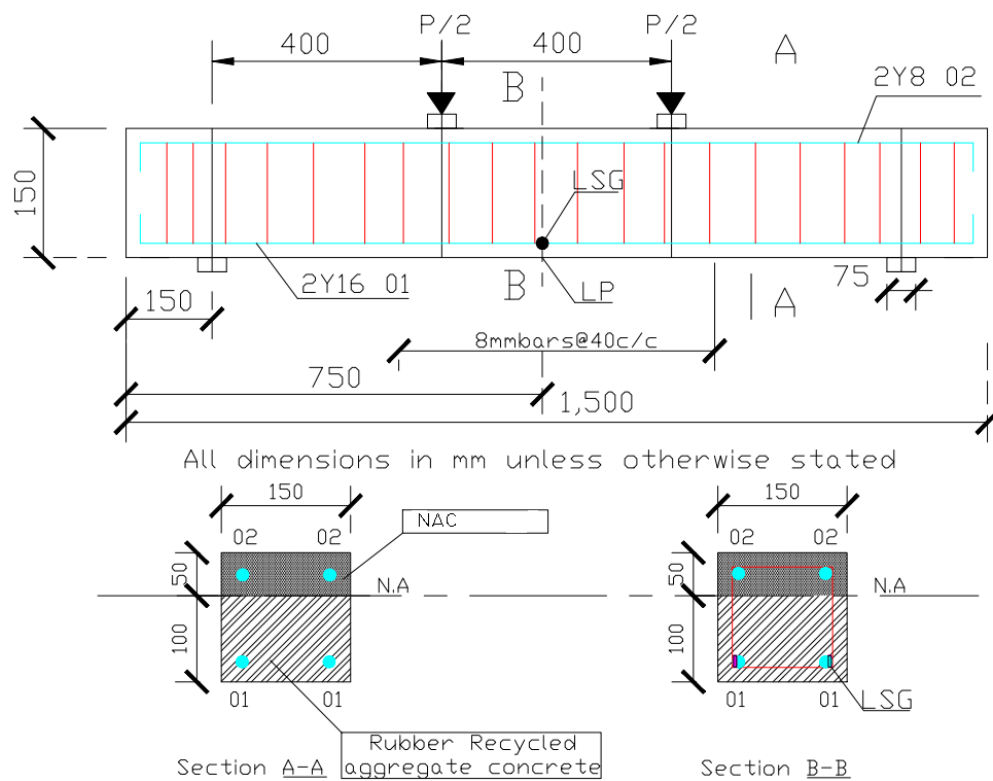


Figure 1.4 Detail and sections of the two-layer beam.

1.4 Thesis structure

This thesis is divided into seven chapters as presented below:

Chapter 1 Introduction

This chapter introduces the background and research objectives of this PhD project.

Chapter 2 Literature Review

This chapter presents a thorough literature review of the mechanical properties (workability, static strength, modulus of elasticity, concrete and rebar bond strength, interfacial bond strength of in layered concrete) of concrete made with either recycled aggregate or RRAC, and performance of structural members made with recycled concrete. The influence of graphene on concrete is also discussed.

Chapter 3 Mechanical properties of rubber recycled aggregate concrete.

This chapter reports the details of an experimental study of making rubber recycled aggregate concretes (RRAC), with and without graphene, and their mechanical properties. It will discuss how to make workable RRAC and their various mechanical properties. The use of graphene to improve recycled aggregate concrete is also investigated in this chapter.

Chapter 4: Experimental study of bending and shear behaviour of two-layer beams.

This chapter presents the observations and results of an experimental programme to investigate the bending and shear behaviour of two-layer beams and a comparison with those of regular concrete beams.

Chapter 5: Numerical modelling of two-layer reinforced concrete beams using RRAC in the tension region. This chapter reports the results of a detailed numerical modelling exercise to broaden the scope of the experiments discussed in Chapter 4. It includes the results of validation, parametric studies to investigate the effects of changing different parameters (NAC and recycled concrete strength, top and bottom layer thickness ratio, reinforcement ratio, shear span depth ratio) on beam behaviour and failure mode.

Chapter 6: Practical implications of two-layer beams

This chapter outlines the cost implications of using two-layer beams in place of regular concrete beams in the construction industry. The extra links required to resist the interfacial shear stress of two-layer beams with respect to cast time intervals (4 and 24 hours) are discussed..

Chapter 7 Conclusions and recommendations for further research

This chapter will provide a detailed summary of this research and the main conclusions and recommendations for further research.

Chapter 2

Literature Review

To tackle the twin challenges of improving properties of recycled aggregate concrete, with or without crumb rubber, and replacing concrete using natural aggregates with recycled aggregate, it is necessary to understand the properties of recycled aggregate concrete with and without crumb rubber, and structural performance of reinforced concrete structures using recycled aggregate concrete. This chapter will present a detailed literature review of these subjects.

For recycled aggregate concrete as a material, this chapter will review its processes and classification, mechanical properties and durability performance. Due to time limits, this research will not deal with how to improve different existing processes of making recycled aggregate concrete. Therefore, adding graphene in concrete, in the context of an alternative method of making recycled aggregate concrete, is covered in a separate section. This is then followed by a review of the structural performance of reinforced concrete structures using recycled aggregate concrete.

2.1 General Introduction to recycled aggregates and crumb rubber

2.1.1 Classification of recycled aggregates

The quality of recycled aggregate concrete is dependent on the quality of the recycled aggregate. Recycled aggregates are classified according to the density, porosity, water absorption, shape and gradation of the aggregates, and their resistance to crushing and abrasion. The residual adhered cement matrix on recycled aggregates affects its density, porosity and the rate of water absorption. The density of recycled aggregates is lower than that of natural aggregates due to the lower density of the attached cement matrix, with a difference of about 6-7% [47]. Porosity and water absorption are related recycled aggregate characteristics also mainly influenced by the adhered cement matrix, with water absorption of recycled aggregates being higher than that of natural aggregates due to the higher porosity of the adhered cement matrix.

The density, porosity, and water absorption of aggregates are the main factors influencing whether the concrete mix can meet its strength and workability requirements. These characteristics are used to classify recycled aggregates into different groups. Table 2.1 summarises the different international grouping methods of recycled aggregates.

Table 2.1 Classification of recycled aggregates [48].

| Country or standard | Recycled aggregate type | Oven-dry density (kg/m ³) | Absorption ratio of aggregate criteria (%) |
|-----------------------------------|-------------------------|---------------------------------------|--|
| Australia (AS1141.6.2) (AS 1996) | Class 1A | $\geq 2,100$ | ≤ 6 |
| | Class 1B | $\geq 1,800$ | ≤ 8 |
| Germany (DIN 4226-100) (DIN 2002) | Type 1 | $\geq 2,000$ | ≤ 10 |
| | Type 2 | $\geq 2,000$ | ≤ 15 |
| | Type 3 | $\geq 1,800$ | ≤ 20 |
| | Type 4 | $\geq 1,500$ | No limit |
| RILEM (1994) | Type 1 | $\geq 1,500$ | ≤ 20 |

| | | | |
|------------------|--------|--------------|-----------|
| | Type 2 | $\geq 2,000$ | ≤ 10 |
| | Type 3 | $\geq 2,500$ | ≤ 3 |
| Spain (EHE 2000) | - | $\geq 2,000$ | ≤ 5 |

Australia (AS 1996): *Class 1A* well graded RA with no more than 0.5 % brick content; *Class 1B* RA blended with no more than 30 % crushed brick.

Germany (DIN 2002): *Type 1* concrete chippings + crusher sand; *Type 2* construction chippings + crusher sand; *Type 3* masonry chippings + crusher sand; *Type 4* mixed chippings + crusher sand.

RILEM (1994): *Type 1* aggregates from masonry rubble, *Type 2* aggregates from concrete rubble; *Type 3* mixture of natural (min 80 %) and recycled (max 20 %) aggregate.

2.1.2 Properties of crumb rubber from waste tyres

Waste tyres have different components as shown in **Error! Not a valid bookmark self-reference**. Tyres are designed to be long lasting and to operate in demanding and abrasive environments. Therefore, they are very difficult to break down naturally [49, 50]. Rubber crumbs are produced from waste tyres by subjecting them to a shredding process: the chipped rubber having a dimension of 25-30mm, crumb rubber with dimensions ranging from 3-10mm and irregular shape, and the ground or ash rubber with less than 1mm in dimension as shown in Figure 2.1. In most cases, crumb rubber made from worn-out tyres contains some contaminants of steel and fibres but fine/grounded grades of crumb rubber are completely free from steel and fibres.

Table 2.2 Composition of a tyre: Typical components [51]

| Ingredients | Passenger Car tyre | Lorry tyre |
|--------------------------------|--------------------|------------|
| Rubber/Elastomers ¹ | 47% | 45% |
| Carbon black ² | 21.50% | 22% |
| Metal | 16.50% | 25% |
| Textile | 5.50% | - |
| Zinc oxide | 1% | 2% |
| Sulphur | 1% | 1% |

| | | |
|--|-------|-----|
| Additives ³ | 7.50% | 5% |
| Carbon-based materials, total ⁴ | 74% | 67% |



ash rubber

• < 1 mm



crumb rubber

• 3-10 mm



chip rubber

• 25-30 mm

Figure 2.1 Categories of processed waste tyres of motor vehicles [52]

The chipped rubber particles are mostly used in replacing coarse mineral aggregates in concrete [31] while the crumb rubber to substitute sand is most often used to replace aggregates of sizes less than 16mm [53]. The ash or grounded rubber is mostly used to replace part of the cement in concrete [35]. The grounded rubber acts as filler material in the concrete because of the size of their tiny particles.

The specific gravities and water absorptions of tyre shreds of different sizes are shown in Table 2.3. The water absorption of different types of tyre shred is almost the same and ranges from 6.7 to 7.1% depending on its size.

Table 2.3 Specific gravity and water absorption of crumb rubber particles [54]

| Tyre size (mm) | Specific gravity | Water adsorption (%) |
|----------------|------------------|----------------------|
| < 50 | 1.10 | 6.70 |
| 50–100 | 1.10 | 6.95 |
| 100–200 | 1.06 | 7.10 |
| 200–300 | 1.10 | 7.00 |

[55] conducted some tests on the compressive properties of tyre rubbers using electromechanical universal test machine. Specimens with 8.10mm height and 17.60mm diameter were cut out from the tyres using the water jet cutting technique and are compressed at strain rate of 1.0 per second. The specimens were pre compressed four

times and the fourth reading was recorded. From the uniaxial compression test, the engineering stress vs. engineering strain curves were obtained, as presented in Figure 2.2.

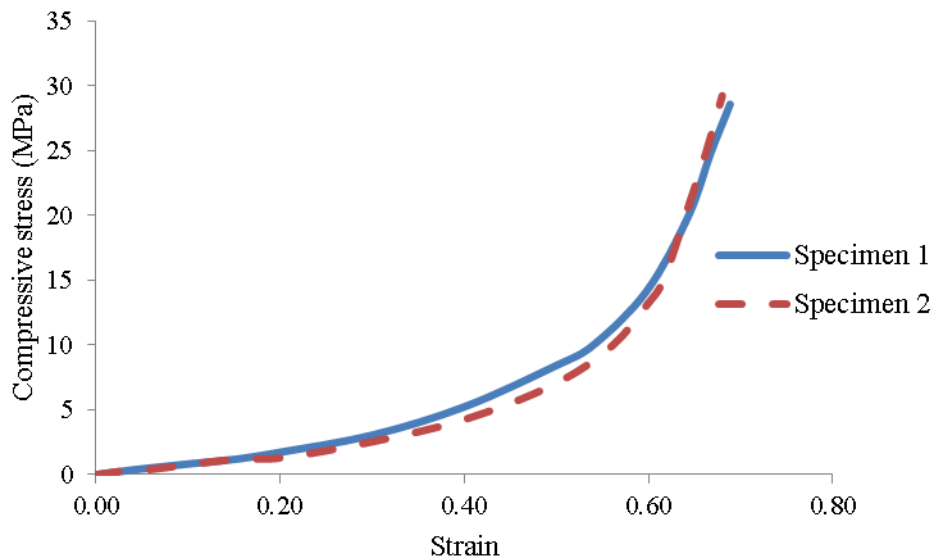


Figure 2.2 Stress-strain curves for tyre rubber with pre-compression tests at strain rate of 1.0 s^{-1} (Data extracted from [55])

[56] also conducted a study on the mechanical properties of tyre rubber coupons. Experimental uniaxial tension and compression tests were carried out on the strength testing machine with the assistance of high-speed camera and special software for strain measurements. The specimens for compression tests were cylindrical coupons with 17.8mm height and a diameter of 35mm. The size of the tensile test specimens is 40mm length and 6mm width. Steel cords of 1.2mm diameter are arranged radially inside tire sidewall, whereas within tread area they are placed circumferentially. The Figure 2.3 and Figure 2.4 presents the stress strain curves for the compressive and tension coupons respectively for different test samples.

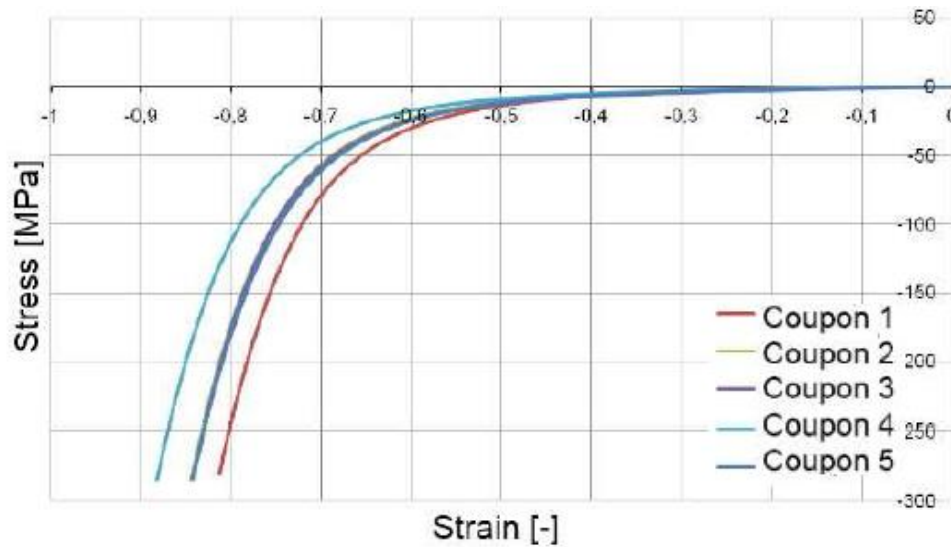


Figure 2.3 Stress-strain curves obtained from experimental compression tests[56]

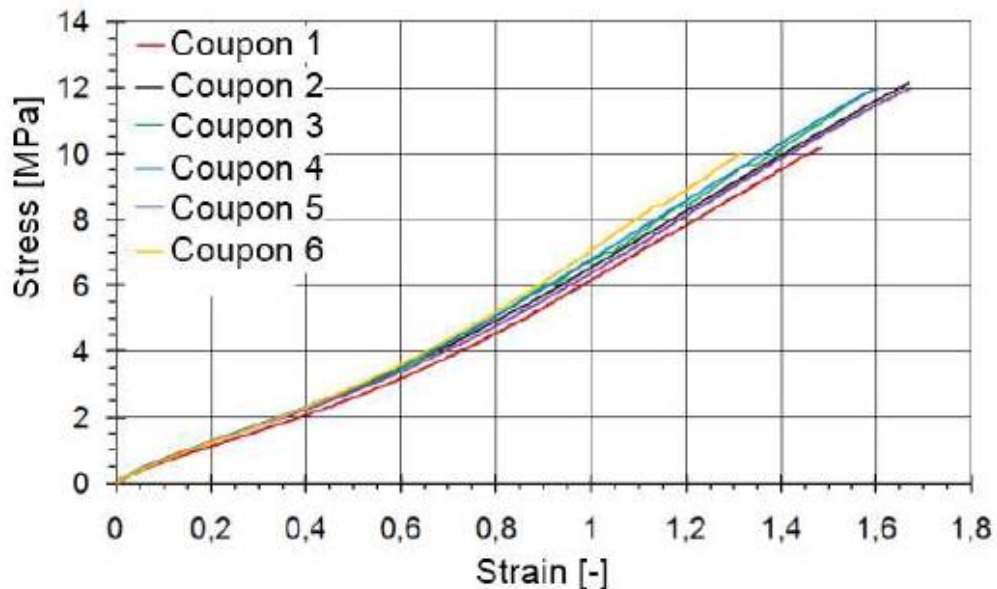


Figure 2.4 Stress-strain curves obtained from experimental tensile tests[56]

It can be observed that compressive stress of tyre rubber for [56] with wire chords is higher than those for [55] without wire chords. Also, the results in Figure 2.2 are more consistent compared to Figure 2.3. This is because, the specimens for Figure 2.2 results were pre compressed up to 4 times before the actual readings were taken. However, this study will be incorporating crumb rubber without steel chords in recycled aggregate concrete.

Tyres are designed to be persistent in abrasive environments in a large temperature span during service. The factors known to affect tyre rubber are oxidation, degradation caused by ultra violet (UV) radiation and heat [57]. In the manufacturing process anti-oxidising agents and stabilisators are often added to the rubber matrix as protection.

[49] carried out a study on the physical condition of vulcanized rubber after immersion in sea water to a depth of 28m for 42 years. The in-situ conditions could be described as slightly alkaline and oxidising. The investigation revealed that there was no serious deterioration of the tyres after immersion in sea water over 42 years and the amount of water absorbed is 4.7%. There was no adverse effect on the properties of the submerged rubber compared to dry rubber of similar formation as shown in Table 2.4. The degradation of tyre rubber under highly alkaline environment for PH >10, over a period of four months was studied. The durability of the tyre rubbers was measured based on mass, swelling, tensile strength and microstructure. There was a minor loss in mass but the swelling, strength and microstructure of the rubber was unaffected by the neutral pH conditions[50].

Table 2.4 Physical properties sea water after immersion in sea water for 42 years [49]

| Test | Inner tube wet | Inner tube dry | New rubber sheet of similar formation |
|--------------------------------|----------------|----------------|---------------------------------------|
| Tensile strength (MPa) | 21 | 22 | 23 |
| Elongation at break (%) | 619% | 593% | 730% |
| Trouser tear strength (N /mm) | 13.7 | 11.5 | 9.5 |

The dry inner tube was achieved in a controlled laboratory condition immediately after removal from sea water.

2.2 Workability of recycled aggregate concrete.

The ease with which concrete can be mixed and cast is vital in work practice. The workability of concrete can be summed up as the amount of internal work required to reach the maximum compaction of the material [58]. Quantitative empirical (e.g. slump)

or quantitative fundamental (e.g., viscosity, fluidity, yield value) methods are used to characterize the behaviour of this internal work and appearance of the fresh mix. The quantitative empirical methods such as slump test and slump flow tests methods provide a single measurement and thus are referred to as one-parameter or single-point tests. The slump test is widely adopted in practice because of its simplicity and sensitivity to changes in small water content.

Several factors affect the workability of recycled aggregate concrete; moisture state of recycled aggregates, quality of recycled aggregates or the rate of water absorption of recycled aggregates, water cement ratio, workability over time and water reducing agents (super plasticisers).

2.2.1 Moisture state and water absorption of recycled aggregates on workability of recycled concrete

[59] conducted a compressive analysis on the effect of the moisture state of recycled aggregates on the workability of concrete over time. The properties of the recycled and natural aggregates are listed in Table 2.5. The recycled aggregates were obtained at the old Kai Tak airport in Hong Kong. They were generated from the demolition activity of different reinforced concrete structures and concrete runway. The cement type for this study was ordinary Portland cement equivalent to ASTM Type I Portland cement.

Table 2.5 Properties of natural and recycled aggregates [59]

| Type | Nominal size (mm) | Density (kg/m ³) | Water absorption (%) | Strength (10% fine value) KN | Porosity (%) |
|--------------------|-------------------|------------------------------|----------------------|------------------------------|--------------|
| Crushed granite | 10 | 2620 | 1.25 | 159 | 1.60 |
| | 20 | 2620 | 1.24 | | |
| Recycled aggregate | 10 | 2330 | 7.56 | 117 | 10.45 |
| | 20 | 2370 | 6.28 | | |

The moisture states considered were oven dry (OD), air dry (AD) and saturated surface dry mix (SSD). All mixes were designed to maintain an equivalent free water cement (w/c) ratio of 0.57. The mixes with 100% OD recycled aggregates exhibited the highest initial slump value in Figure 2.5. This can be better explained by the extra amount of water added to compensate for the recycled aggregates which resulted in higher effective w/c ratio at the time the slump test was conducted. The recycled aggregates at this moment had not absorbed the compensated water. These findings are the same as those of [60]. After 15-30 minutes, all the mixes, regardless of the replacement ratio, showed comparable slump values, indicating that the recycled aggregates had absorbed the compensating water, thereby leaving all the mixes with similar effective w/c ratios. From a practical perspective, using recycled aggregates in its natural state will be preferable because subjecting recycled aggregates to drying or pre-saturation would be time consuming and almost impractical even though these processes may improve the workability of recycled aggregate concrete.

[61] also evaluated the effects of moisture state of recycled aggregates and the mixing procedure on the workability of recycled concrete. The cement type for this study was Type 1 Portland cement comprising of 80% of the total binding material and 20% class C fly ash. The recycled aggregates were sourced from a single stockpile of crushed concrete at O'Hare International Airport. The RA were sieved and recombined to match the gradation of the natural aggregates. The water absorption rate of the natural and recycled aggregates were 1.9% and 5.51% respectively and their specific densities were 2.67 and 2.41 respectively. The use of oven-dry recycled aggregates led to mixes with higher initial slump values when compared to those made with recycled aggregates at a SSD state or water compensated for 80% of their total absorption capacity as shown in Figure 2.6.

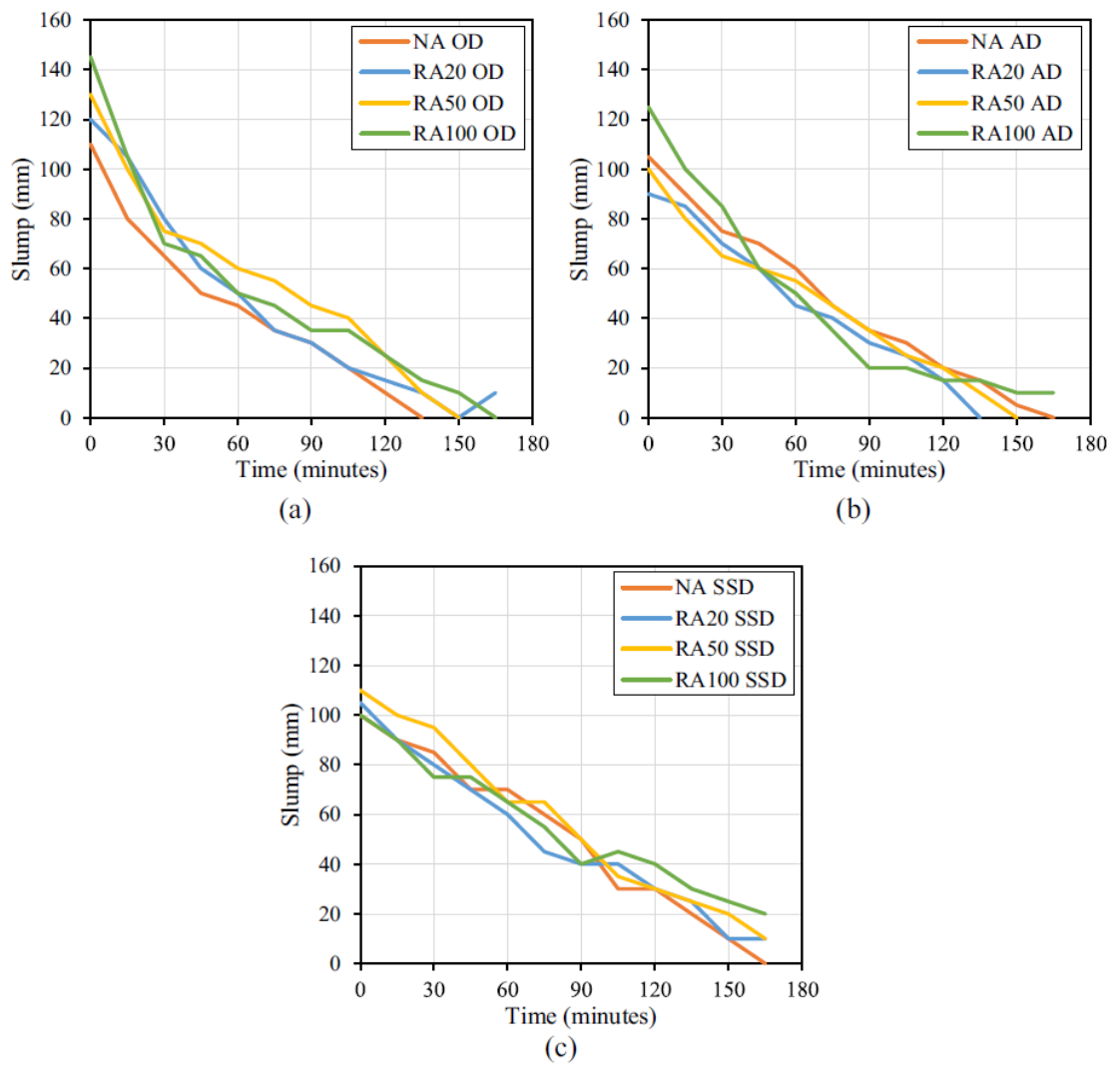


Figure 2.5 Effects of moisture state of recycled aggregates on the workability of concrete over time (Poon et al., 2004).

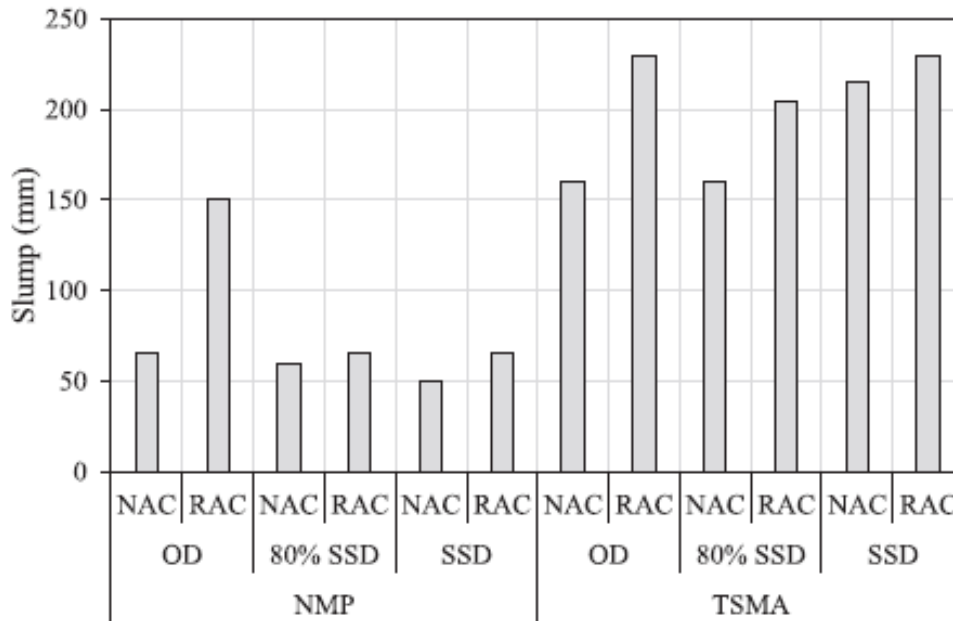


Figure 2.6 Influence of moisture state and mixing procedure on the workability value of recycled concrete [61]

This was attributed to the extra amount of water added during mixing to compensate for the water absorption of the oven dry RA in order to maintain an equivalent effective w/c ratio for all mixes. However, there was not enough time for the oven dry RA to absorb the compensated water during the tests, hence this increased the effective w/c ratio which gave higher slump levels. The two-stage mixing approach (TSMA) as recommended by [62] also enhanced the slump of all mixes compared to the normal mixing procedure (NMP). This increase in slump level was attributed to the fact that the compensated extra water was first mixed with the RA to saturation prior to the addition of any other constituent materials.

2.2.2 Workability over time

It is highly desirable to maintain high workability of concrete mixes for longer periods of time as this enables easy casting and compaction until the concrete sets. It has already been demonstrated by [59] that the moisture state of the RA aggregates affects the workability of the recycled aggregate concrete as shown in Figure 2.5.

[63] carried out a study on the effects of coarse and fine recycled aggregates on the workability of recycled concrete over time, and compared to that of concrete using natural aggregates. The RA was obtained from a demolished structure with unknown constituent materials properties. The recycled aggregates were incorporated into the recycled concrete at saturated surface dry (SSD) moisture state. In order to assess the influence of RA on the retention of workability over time, compaction factor measurements were made at 30 min intervals up to 150 min after mixing. Figure 2.7 shows that the compaction factors of mixes over time made with 100% coarse and 50% fine RCA and with different w/c ratios are higher than those of the NAC mixes (NA) which exhibited a greater loss in terms of compaction factor.

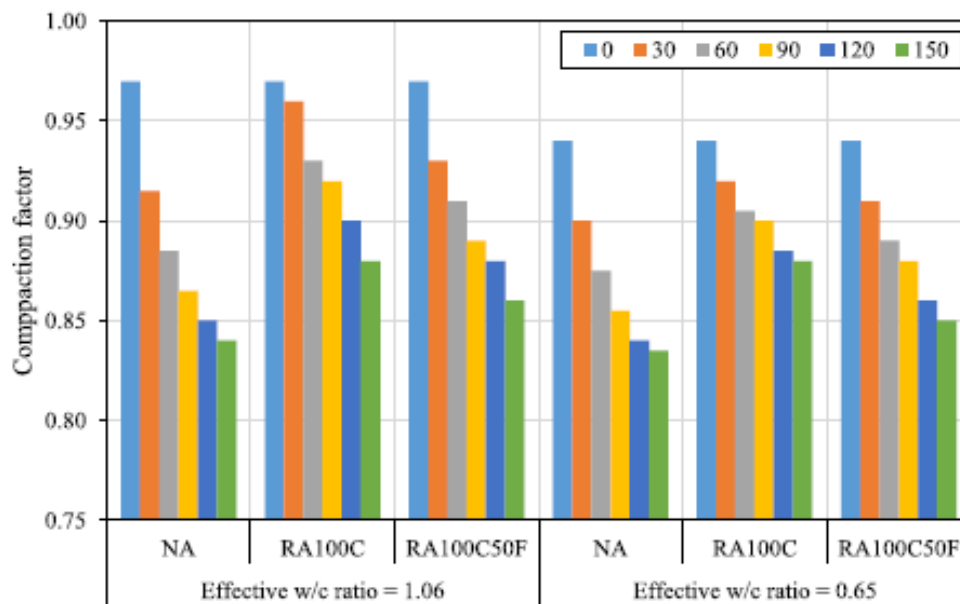


Figure 2.7 Compaction factor of mixes with different effective w/c ratios and recycled aggregates replacement levels over a period of time from (0-150 minutes) [63]

2.2.3 Effects of water reducing agents on the workability of recycled aggregate concrete

The incorporation of admixtures into concrete is done either before or during the mixing process with the aim of retarding or accelerating the setting time for concrete, improving fluidity, air content etc. The use of water reducing agents have gained much attention in the production of recycled aggregate concrete due to their ability to enhance the workability of the mix comprising of RA with irregular shapes and rough surfaces [11, 17].

[11] investigated the use of superplasticizers to improve the workability of recycled aggregate concrete without increasing the total water cement ratio. The amount of superplasticizers was 1% of the cement weight. Three sets of concrete with different replacement ratios (0%, 20%, 50% and 100%) of natural aggregate by coarse recycled concrete aggregate were manufactured for this study and used without admixtures and a high-performance plasticizer. The natural aggregates were extracted from a stone quarry in Zambujal (Sesimbra) ranging between 12mm and 20mm in size. The recycled aggregates were obtained from crushing a 30-day old concrete with jaw crushers to a 4-22.5mm size range. The design w/c for the reference concrete was 0.54 with a slump value of 125mm while that of the recycled concrete with superplasticizers was 0.4. Figure 2.8 shows the influence of using superplasticizer on the workability of the recycled aggregate concrete. The use of superplasticizers (SP) decreased the amount of water required in the mix to satisfy the workability requirement.

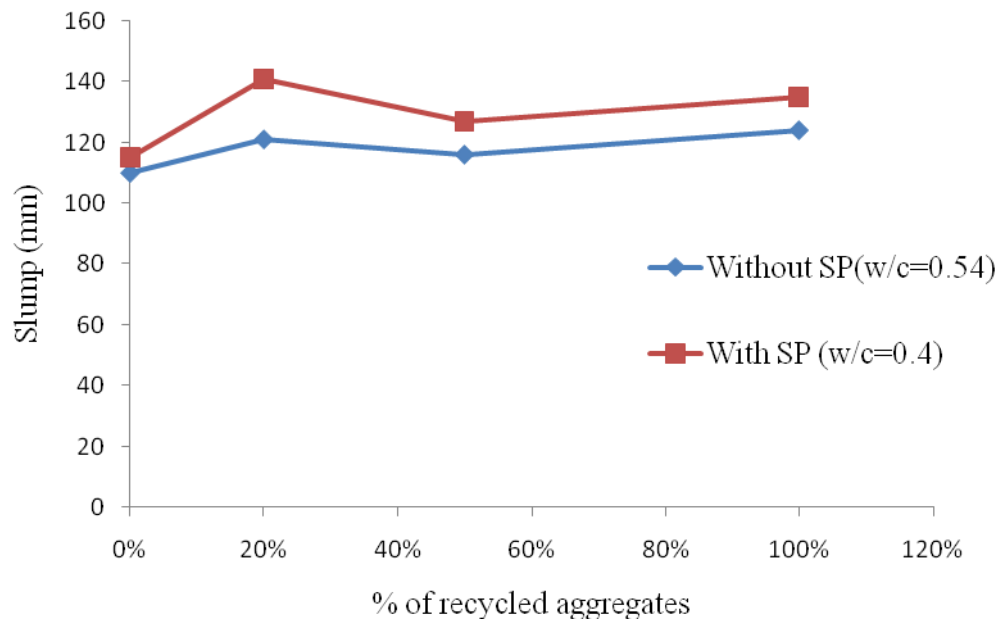


Figure 2.8 Influence of superplasticizers (SP) on the workability of recycled aggregate concrete (data extracted from [11])

2.3 Influence of crumb rubber (CR) concentration and size on the workability of concrete

In the same manner as recycled aggregate, concrete with tyre shreds exhibits low workability. The adverse effect on workability can be minimized by reducing the percentage of rubber replacement [29, 30, 34, 37, 41, 52, 64-66]. Some researchers have shown that the workability of the concrete is better when coarse rubber particles are used in concrete instead of fine rubber particles. This may be attributed to the higher surface area of the fine rubber particles which absorb much more water than coarse rubber particles [67]. However, this view seems to contrast with that of most researchers who observe better workability from using fine rubber particles compared to coarse rubber particles [30, 34, 37, 67].

[37] conducted a study on the effect of crumb rubber size and concentration on the workability of concrete. Coarse aggregates of size 38mm with a specific density of 2.65, Type 1 Portland cement was used for the concrete mix. The w/c of the mix was 0.48.

The rubberized concrete was made by replacing the coarse aggregates with crumb rubber up to 25% in volume. Crumb rubber sizes of 38mm, 25mm, 19mm and 6.4mm were used for this study and were properly cleaned to remove all unwanted materials. Figure 2.9 shows that the workability decreased with the increase in crumb rubber content and size. This may be explained by the fact that tyre chips form an interlocking structure resisting the normal flow of concrete under its own weight; hence these mixes showed less fluidity. [30] also investigated the influence of crumb rubber size (5mm and 15mm) and concentration (12.5%, 25%, 37.5% and 50%) in concrete. The 5mm crumb rubber was used to replace natural sand while the 15mm crumb rubber replaced some coarse aggregates. Type 1 Portland cement and coarse aggregates of 20mm size were used for this study. The specific gravity and water absorption of the crumb rubber were 1.16 and 49.56% respectively while those of natural coarse aggregates were 2.65 and 2.66%. The w/c ratio of all mixes was 0.45. The results are shown in Figure 2.10.

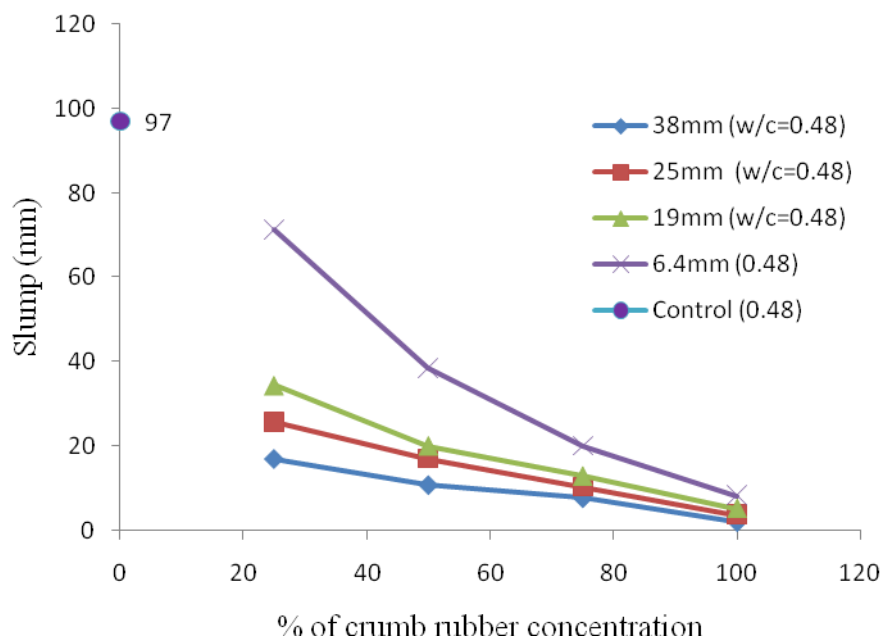


Figure 2.9 Influences of crumb rubber concentration and size on the workability of concrete (data extracted from [37]).

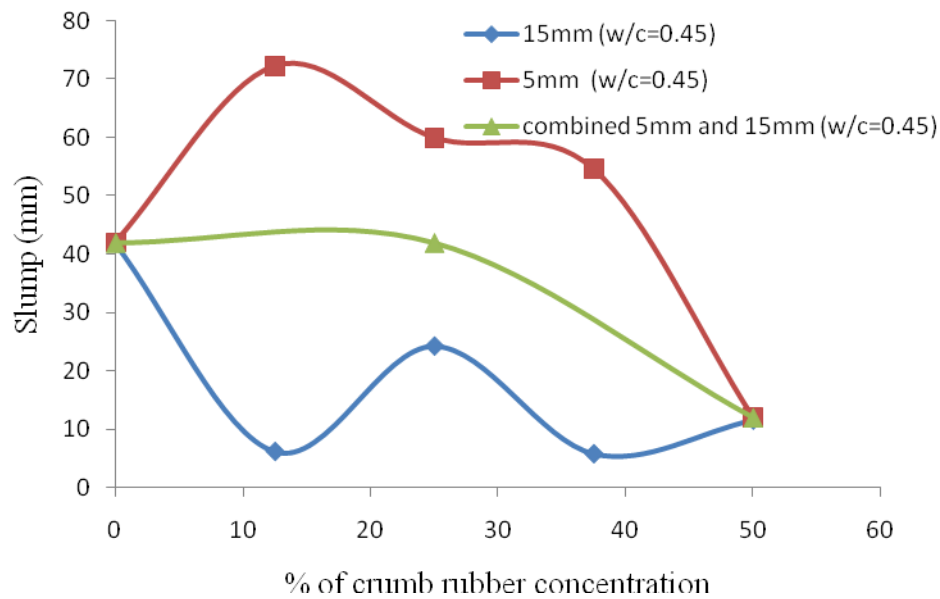


Figure 2.10: Influence of crumb rubber concentration and size on the workability of concrete (Data extracted from [30])

The slump of concrete mix with 5mm is higher than that of the 15mm crumb rubber replacing coarse aggregates. [67] also reported a decrease in workability with crumb rubber concentration regardless of its size. This was attributed to the higher water absorption of the crumb rubber (10.09%) compared to that of the replaced sand (1.37%) at saturated surface dry state. The conflicting views from different researchers as to which particle size of the crumb rubber exhibits better workability may be attributed to the unique properties (surface texture arising from shredding process) of the individual crumb rubber used in the experiments. Generally, the slump of rubberized concrete tends to decrease with an increase in rubber content.

To summarise, recycled aggregate concrete generally has lower workability than natural aggregate concrete. To achieve the same workability as natural aggregate concrete, additional work may be required or superplasticisers should be used. Regarding rubber recycled aggregate concrete, the amount of rubber is an important parameter and the amount of rubber should be limited. This will be further investigated in this research to design rubber recycled aggregate concrete with acceptable workability.

2.4 Mechanical properties of recycled concrete

Recycled aggregate of different qualities (with and without impurities) and quantities are incorporated in concrete, rubber particles of various sizes (tyre shreds, crumb rubber, ash or grounded rubber) can also be used to replace coarse aggregates, sand or cement in concrete. Fly ash, plasticizers and super plasticizers, additional cement have also been used by authors to improve the mechanical properties of modified concrete. The results obtained from these previous studies have been used as a guide by the author in proposing a current design mix considering cost implication, manpower involved and also the environmental impact.

2.4.1 Compressive strength

The strength of recycled aggregate concrete generally decreases [9, 68-72] and the reduction depends on many factors such as the quality of recycled aggregates [73, 74], replacement level in concrete [9, 70], water cement (w/c) ratio [59] etc. The strength reduction may also be due to the amount of attached cement matrix on the recycled aggregates [68, 70, 75] which causes a weak interfacial bond between the attached old cement matrix and the surrounding concrete matrix as shown in Figure 2.11.

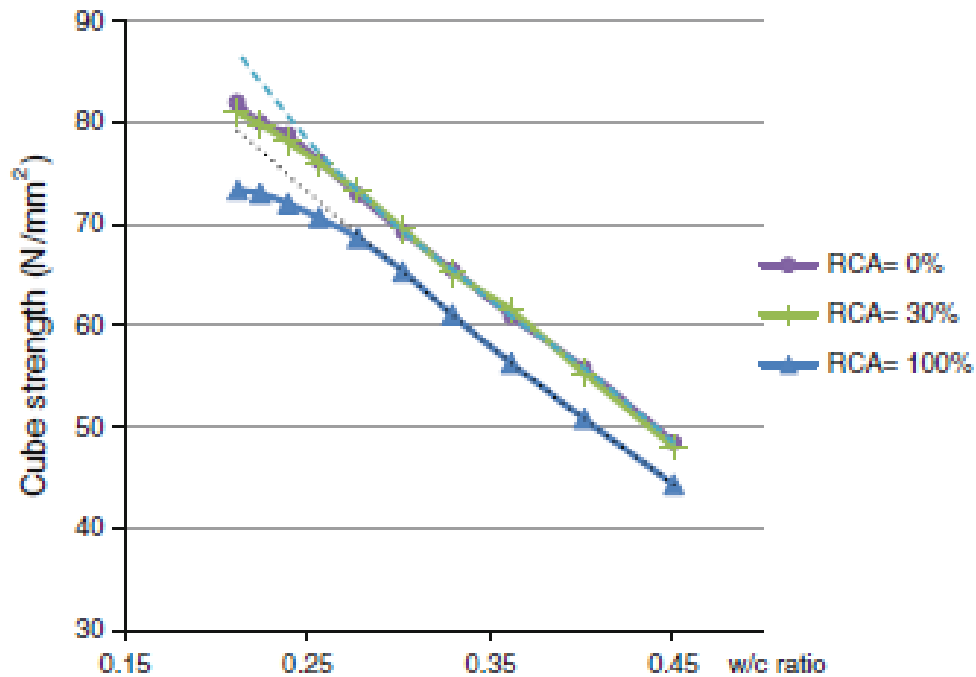


Figure 2.11 Crack pattern of recycled aggregates with attached cement matrix (Kwan et al., 2011).

2.4.1.1 Effect of water cement ratio (w/c), RA content and water absorption on the strength of recycled concrete

The compressive strength of recycled aggregate concrete is affected by the water cement ratio and the percentage of recycled aggregate in concrete. Most researchers have reported that, without changes to the mix involving adjustments to the w/c ratio, up to 25 or 30 % of coarse aggregates can be replaced with recycled aggregates before the compressive strength is significantly compromised.

[47] study has revealed that at 30% RA content, the strength of the recycled aggregate concrete is not affected at the same w/c ratio as the natural aggregate concrete as shown in Figure 2.12. The recycled aggregates for this study are obtained from condemned precast concrete and are graded into fractions of 20-10mm and 10-15mm size with water absorption of 4.9% and 5.2% respectively. The data for 30 % RAC follows that of natural aggregate concrete for almost every w/c ratio tested, while the 100 % RAC data lie at compressive strength values below that of natural aggregate concrete (NAC) or 30 % RAC by about 5 N/mm². [12, 18] also revealed that 20-25% of recycled aggregate in concrete with same w/c does not affect its compressive strength as shown in Table 2.6. However, this entirely depends on the quality of the recycled aggregates used. Table 2.6 shows that RA made from demolished precast structural elements or laboratory concrete waste exhibits the same performance as the NAC with less than 30% replacement [11, 40], if the recycled aggregates were carefully sorted by removing all unwanted impurities prior to use. [18] demonstrated that it was also possible to adjust the w/c ratio of recycled aggregate concrete to maintain the same compressive strength as that of the natural aggregate concrete for RA replacement levels greater than 25% as shown in Table 2.6. The w/c ratios for the NAC and the recycled concrete with 25% of RA were kept constant at 0.55 while those for the 50% and 100% RA replacements were adjusted (lowered) to 0.52 and 0.5 respectively (therefore using more cement).



RCA- Recycled coarse aggregates

Figure 2.12 Relationship between concrete strength and w/c ratio for varying RA content (plotted using data from [47])

In general, as shown in Table 2.6, the compressive strength of concrete decreases with an increase in the recycled aggregate content for the same water cement (w/c) ratio. This is attributed to the weak interfacial zone between the recycled aggregate and the old attached cement matrix. It should be noted that the recycled concrete has two interfacial zones (ITZ); one formed between the original aggregate and the old cement matrix and the other between the recycled aggregate surrounded by the old cement matrix and the new cement matrix. When pre-soaked RA is used, the high water content inside the particles may bleed during casting whereby the water inside the RA particles moves towards the cement matrix, creating a region with an increased w/c ratio and high porosity. The bleeding process can weaken the bond between the recycled aggregate and the new cement matrix, leading to a lower strength of the recycled aggregate concrete. Therefore, cleaning recycled aggregates by removing the adhered old cement matrix can increase the strength of recycled aggregate concrete.

2.4.1.2 Effect of admixtures on the strength of recycled aggregate concrete

The w/c ratio has an important influence on the quality of concrete for construction. A lower w/c ratio leads to higher strength and durability, but may make the mix harder to cast, but these difficulties can be resolved by using water-reducing agents such as super plasticizers. The extra water added to recycled aggregate concrete to compensate for the high water absorption of the RA for workability requirements affects strength negatively. [11] reported that the compressive strength of recycled aggregate concrete was enhanced by incorporating plasticizers (C-P) and super plasticizers (C-SP) respectively in the mix as shown in Figure 2.13. The w/c ratio for the recycled aggregate concrete mixes without SP (C) is 0.54 while that of C-P and C-SP is 0.5 and 0.45 respectively. All mixes meet the required workability the help of the super plasticizers regardless of the reduced w/c ratio for C-P and CP-SP. [14] and [76] also maintain the compressive strength of the recycled aggregate concrete to that of the natural aggregate concrete when 3 and 12 percent of cement content is added respectively as presented in Table 2.6. The increase in the amount of cement reduces the w/c ratio of the mix, hence increasing the strength of the recycled concrete.

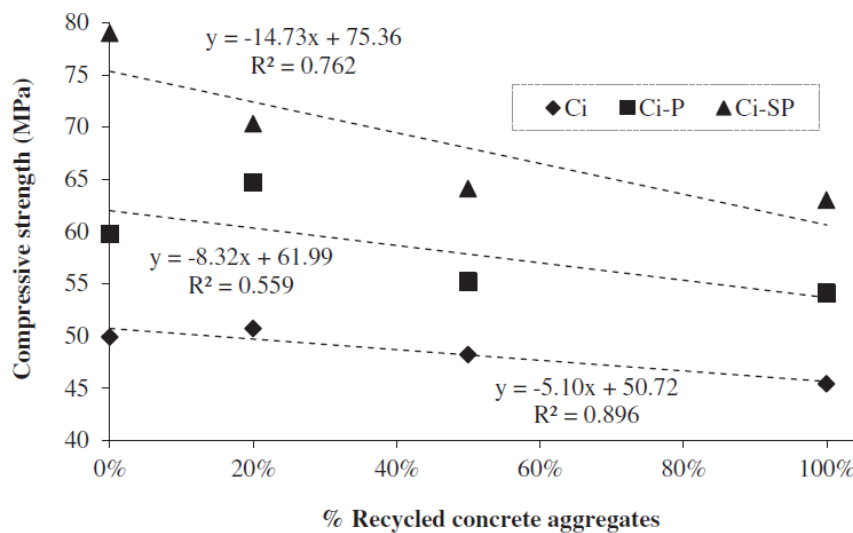


Figure 2.13 Relationship between percentage of replacement and 28-day compressive strength with and without admixtures [11]

2.4.1.3 Effect of crumb rubber (CR) on the mechanical properties of concrete

The use of crumb rubber in concrete of different w/c ratios has been reported to reduce its compressive and tensile strengths. A collection of the support data is presented in Table 2.7 from different researchers. This is attributed to the lower strength of rubber particles used to replace fine and coarse mineral aggregates which have a much higher strength. Rubber particles are also reported to result in weaker bonds with the cement matrix [24, 26, 29-31, 33-35, 37, 38, 42, 64, 65, 77-83]. However, most researchers have indicated that rubberized concrete can still maintain the same mechanical properties as the natural aggregate concrete mix if not more than 5% in volume is used in replacing natural aggregates in the concrete [35, 84] as shown in Table 2.7. It was also reported by [30, 37, 67] that rubber particles with small sizes gave higher strength than coarse rubber particles as shown in Figure 2.14 and Table 2.7. This was attributed to the formation of larger air voids in concrete when coarse crumb rubber particles were used [41]. Also, as shown in Figure 2.15, replacing natural aggregates by 6.2mm crumb rubber particles caused greater reductions in compressive strength of concrete than when rubber particles were used to replace sand for different w/c ratios.

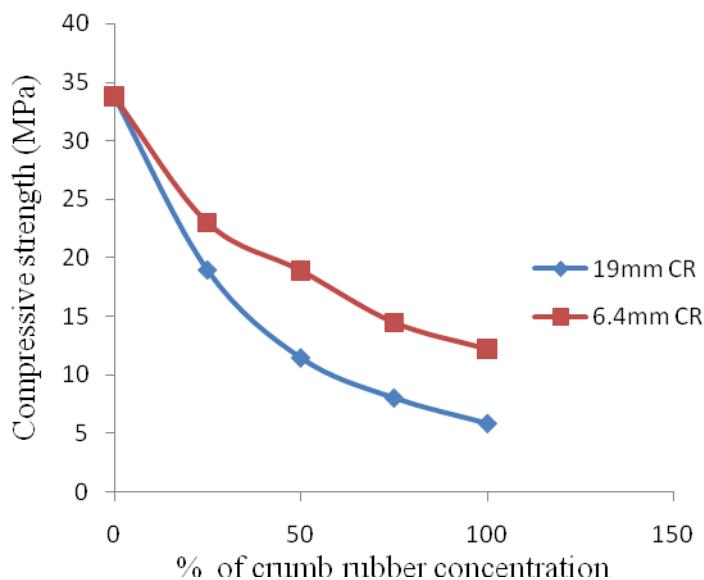


Figure 2.14 Influence of crumb rubber size and concentration on the compressive strength of concrete for w/c of 0.48 (data plotted from [37])

This may be explained by the relative increase in specific surface area with coarse aggregate (CA) replacement and the relative increase in number of rubber particles in comparison with the sand replacement.

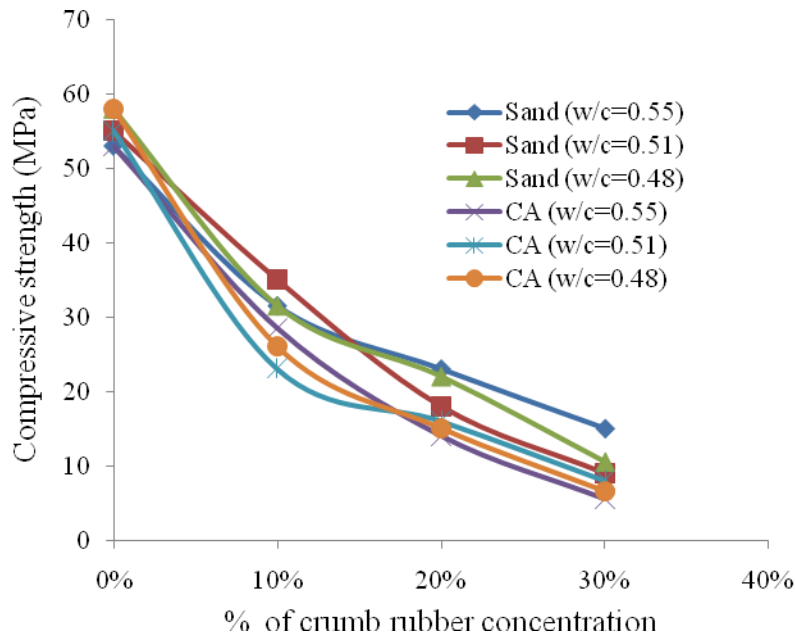


Figure 2.15 Effects of crumb rubber concentration and w/c on the compressive strength of concrete (data extracted from [41]).

To enhance the mechanical properties of rubberized concrete, [85-87] suggested the use of silica fume. The ultrafine silica fume is believed to create a good bonding between the rubber particles and the surrounding cement matrix. [88] carried out pre-treatment of the rubber particles by soaking them in sodium hydroxide NaOH solution before incorporating them into concrete. It was observed that the strength of the rubberized concrete was enhanced compared to the one without pre-treatment. This was attributed to the fact that the NaOH solution dislodges the zinc stearate on the rubber surface, thus enhancing the bonding between the rubber powder and the concrete substrate. [66] also pre-soaked rubber particles in water before it was used in concrete and a 22% increase in strength compared to using untreated rubber particles was discovered. A good distribution of rubber particles was also observed in concrete when pre-soaked in water.

2.4.2 Splitting tensile strength

2.4.2.1 Splitting tensile strength of recycled aggregate concrete

The splitting tensile strength of recycled aggregate concrete decreases with an increase in the proportion of recycled aggregates due to the existing attached cement matrix on the recycled aggregates; however, the extent of reduction is less than that observed in compressive strength [11, 13, 71, 89]. Figure 2.16 presents some of the results of the splitting tensile strength of recycled aggregate concrete in Table 2.6 with different w/c and equivalent aggregate size of 20mm. While the residual adhered cement matrix creates a weakened spot under compression, a limited quantity can help load transfer under tension. Obviously, an excessive amount of attached cement matrix reduces the tensile strength as well as the compressive strength, as demonstrated by using 100% recycled aggregates.

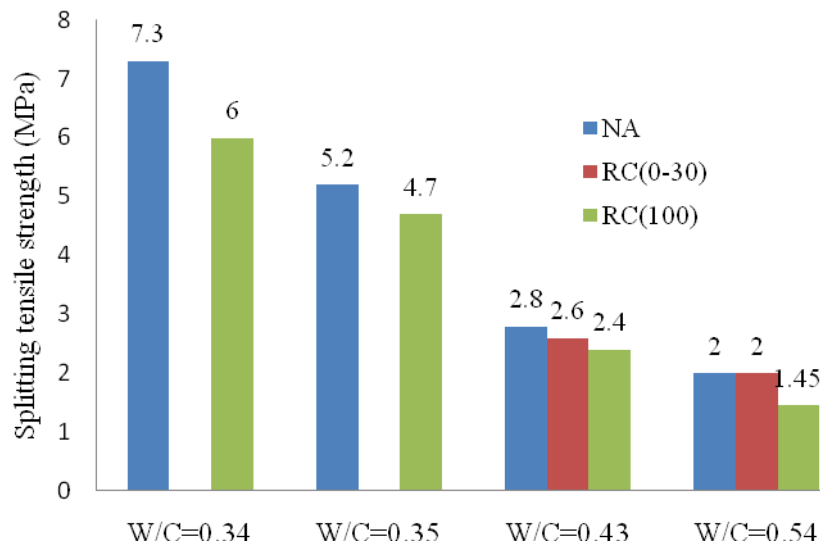


Figure 2.16 Splitting tensile strength of RAC and natural aggregate concrete with different w/c and RA concentrations.

2.4.2.2 Splitting tensile strength of crumb rubber concrete

The splitting tensile strength of concrete decreases with an increase in crumb rubber concentration regardless of the w/c ratio and crumb rubber size as presented in Table

2.7. However, the reduction in splitting tensile strength of rubberized concrete is less than that observed for compressive strength [29, 80, 84]. This is because the tensile strength of rubber relative to the tensile strength of concrete is greater than the relative compressive strength. In fact, some studies report a comparative performance in tensile strength when less than 10% of crumb rubber is used to replace sand or coarse aggregate (CA) in concrete [41, 80]. However, literature results can be inconsistent. For example, Figure 2.17 shows the same splitting tensile strength of rubberized concrete with 10% crumb rubber of 6.2mm size for a w/c ratio of 0.55. However, for w/c ratios of 0.48 and 0.51, a decrease of 46% was observed. This was explained as a result of the low quality cement matrix used rather than as a result of using crumb rubber.

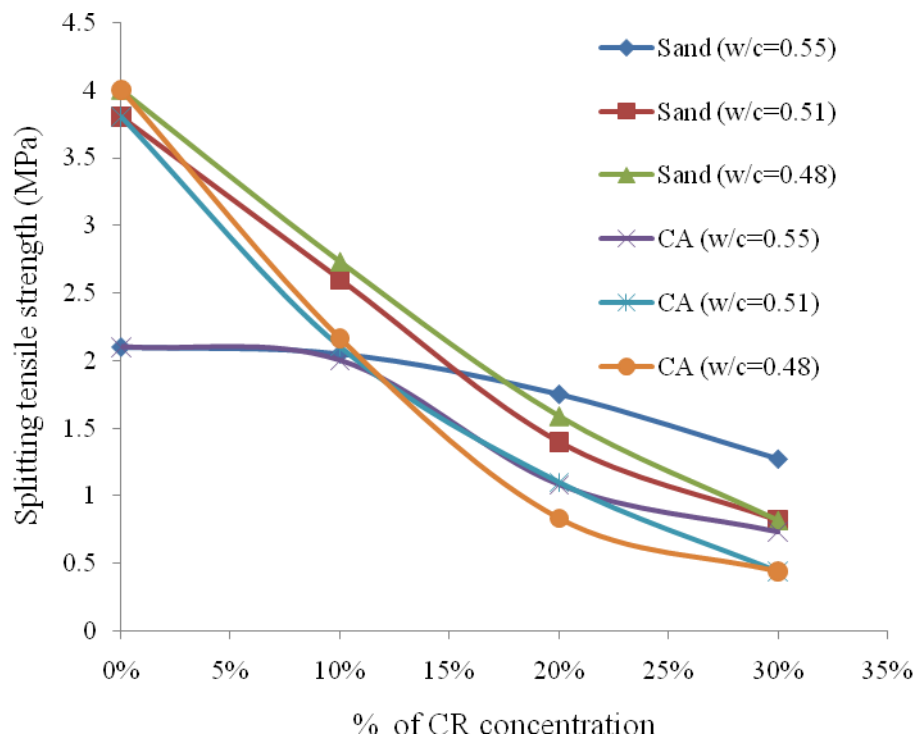


Figure 2.17 Influence of crumb rubber concentration and w/c on splitting tensile strength of concrete (data extracted from [41]).

2.4.3 Elastic modulus and stress strain behaviour

The modulus of elasticity of concrete is affected by several parameters, such as the porosity of aggregates and matrix, transition zones of the aggregates and matrix, quality

of aggregates etc. Researchers have shown that the elastic modulus of concrete made with recycled aggregates of all types, as presented in Table 2.6, decreases as the amount of recycled aggregates increases [7, 10, 11, 13, 14, 43, 68, 90-93]. This behaviour is attributed to the poor quality of the recycled aggregates arising from cracks generated during the recycling process, porosity [92] and the poor interfacial zone of the old attached cement matrix on the aggregates and of the new cement matrix. Figure 2.18 shows the variations of elastic modulus of 100% recycled aggregates in concrete compared with when natural aggregates are used by different researchers. The results show up to a 33% reduction in elastic modulus of concrete made with 100% recycled aggregates [10, 11, 43, 92, 93]. Similar trends were observed in Figure 2.19 for concrete made with crumb rubber [25, 29, 31, 35, 41, 82] and was attributed to the low stiffness of the crumb rubber used for replacing sand or coarse natural aggregates in concrete.

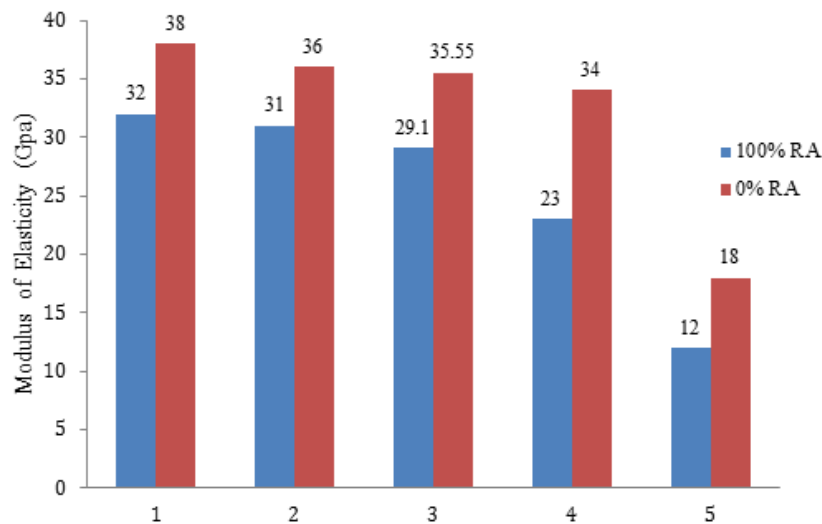


Figure 2.18 Comparisons of modulus of elasticity at 28 days by different researchers between 100% recycled aggregates (RA) and without RA.1. [11]; 2. [92]; 3.[43]; 4.[93]; 5.[10]

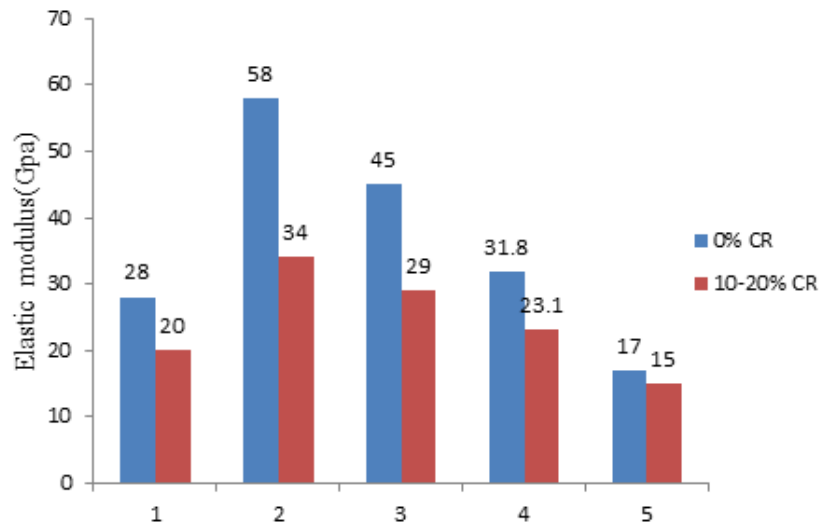
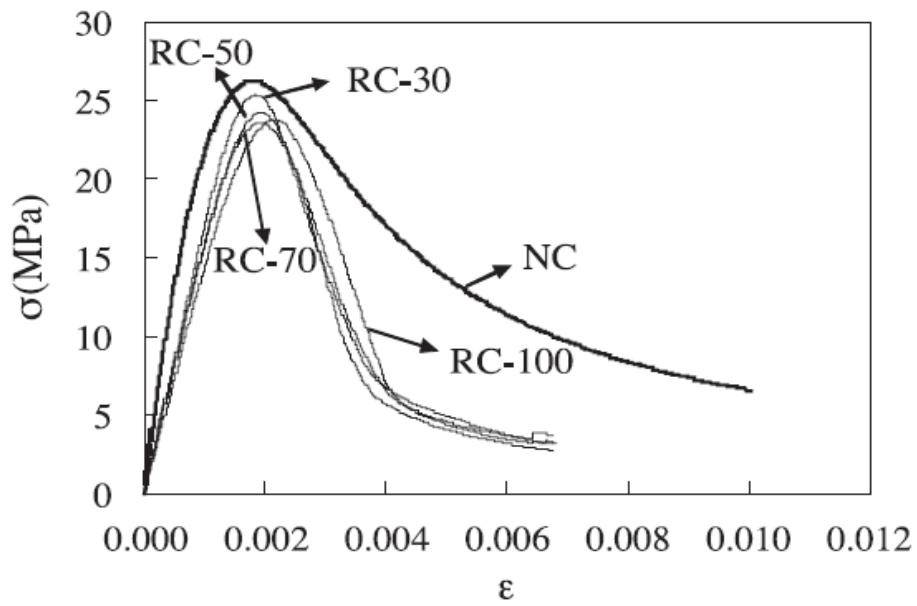


Figure 2.19 Comparison of modulus of elasticity at 28 days by different researchers between 10-20% crumb rubber compared to natural aggregate concrete. 1. [35]2. [30]; 3.[28]4. [25]5. [31]

Figure 2.20 shows similar stress-strain curves for recycled aggregate and natural aggregate concretes with recycled aggregate concrete exhibiting higher strains at the same stress due to lower elastic modulus [94]. Using recycled aggregate concrete tends to make the concrete more brittle as indicated by the more rapid reduction in stress after reaching the peak value. The stiffness, strength and ductility of recycled aggregate concrete with and without crumb rubber has been improved by adding steel fibres [95, 96].

On the other hand, the stress-strain curves in Figure 2.21 indicate that rubberized concrete exhibits better ductility compared to natural aggregate concrete [30, 33, 64, 78, 84]. This is attributed to the high deformability of the crumb rubber compared to the replaced natural aggregates.



NC*- Natural aggregate concrete; RC*- Recycled concrete

Figure 2.20 Stress strain curves of recycled aggregate concrete and natural aggregate concrete (Xiao et al., 2005)

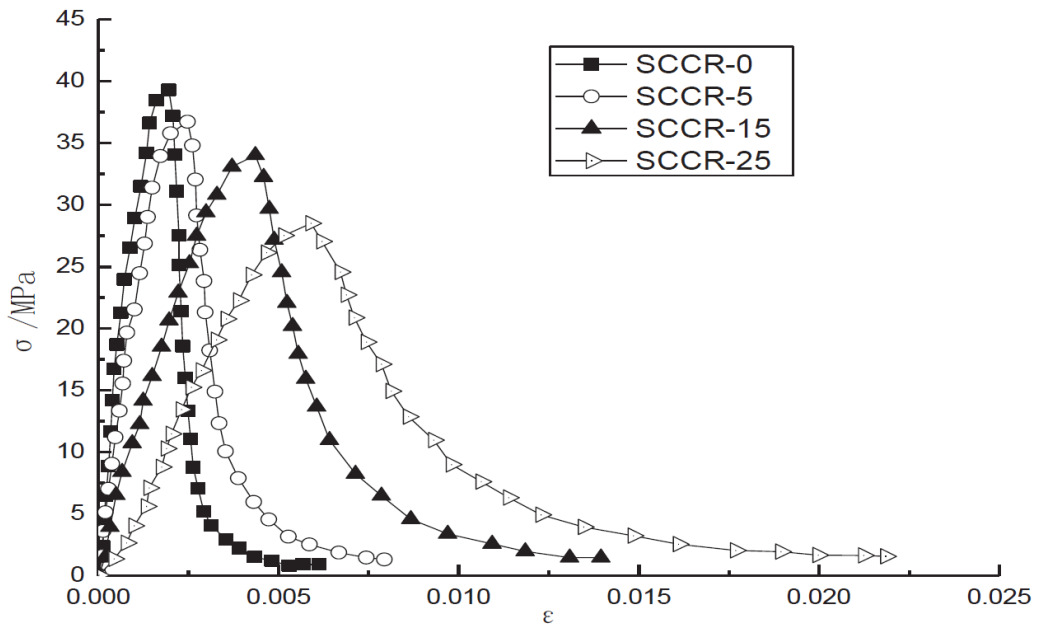


Figure 2.21 Stress strain curves for self-compacting rubber concrete (SCCR) at 28 days (Long et al., 2012)

In summary, the results in Table 2.6 and Table 2.7 show a reduced performance when recycled aggregates and crumb rubber are used to replace natural aggregates in concrete. This reduction in performance is more pronounced in concrete made using rubber particles. The strength reduction in concrete made with 100% recycled aggregate concrete can be up to 33% and as high as 91% when 100% crumb rubber is used. This large reduction in concrete mechanical properties using recycled aggregates and crumb rubber is a major setback when such concretes are used in the construction industry, where strength is a major concern. In contrast, if placing such concretes in structural members where the contribution of concrete to structural performance is minimal, as in the tension zone, then the large reduction in mechanical properties of recycled or rubberised concrete may cease to be an issue.

Table 2.6 Summary of previous research studies on recycled aggregates concrete for 28-day curing compared to natural aggregate concrete.

| Source (s) | Replacement ratio | RA source/ properties | Natural aggregates type | Water abs of RA (NA) (%) | Free w/c | RA moist state | Comp strength (NAC) MPa | f_{fs} (NAC) Mpa | f_{ct} (NAC) Mpa | E_c (NAC) GPa |
|-------------|-------------------|---|-------------------------------------|--------------------------|----------|---------------------|-------------------------|--------------------|--------------------|-----------------|
| [97] | 100% of CRA | 15 years old demolished concrete | dolomite quarries of 20mm size | 3.92 (0.201) | 0.43 | SSD | 43 (50) | 4.92(5.23) | 2.33(2.67) | 23.57(31.22) |
| | 50% of CRA | Size:20mm; unwashed | | | 0.43 | | 45 (50) | 4.42(5.23) | 2.05(2.67) | 21.54(31.22) |
| | 25% of CRA | | | | 0.43 | | 46.5(50) | 4.17 (5.23) | 2.03(2.67) | 20.35(31.22) |
| | 100% of CRA | | | | 0.54 | | 25.5(31) | | 1.45(2.00) | |
| [40] | 80% of CRA | demolished precast structural elements and are of 5-20mm size | Crushed limestone of 5-20mm size | 5.3 (2.4) | 0.54 | SSD | 25 (31) | - | 1.65(2.00) | - |
| | 60% of CRA | | | | | | 25.5(31) | | 1.90 (2.00) | 2.00(2.00) |
| | 20% of CRA | | | | | | 33(31) | | | |
| [11] | 100% of CRA | 30 days old crushed concrete blocks of 4-25mm size | Stone quarry of 12 and 20mm size | 7.34 (1.25) | 0.54 | Air dried condition | 46(50) | | 9.00(11.00) | 32(38) |
| | 50% of CRA | | | | | | 48(50) | - | 8.00(11.00) | 36(38) |
| | 20% of CRA | | | | | | 52(50) | | 8.50(11.00) | 37(38) |
| [7] | 100% of CRA | Demolished building of size 4-8mm and 8-32mm | Crushed basalt aggregates of 8-32mm | 4.3 (0.6) | 0.5 | Pre-soaked for | 34.1(35.8) | | 2.41(2.25) | 25.2(28.1) |

| | | | | | | | | | |
|------|--------------|---|--|--------------|------|-----------------------------------|--------------|------------|------------|
| [9] | 100% of CRA | Recycling facility in Hong Kong of 10mm size | Crushed granite of 20mm size | 3.52 (1.11) | 0.55 | 24hours Air dried condition | 38.1(48.6) | | |
| | 50% of CRA | | | | 0.55 | | 42.5 (48.6) | | |
| | 20% of CRA | | | | 0.55 | | 45.3 (48.6) | | |
| [12] | 100% of CRA | Crushed concrete blocks of 4-20mm size | The NA type is unknown of 4- 16mm size | 6.93 (1.53) | 0.6 | Air dried condition | 40.86(42.02) | 4.8(4.71) | 25.1(27.3) |
| | 50% of CRA | | | | 0.6 | | 42.51(42.02) | 4.68(4.71) | 25.9(27.3) |
| | 20% of CRA | | | | 0.6 | | 42.86(42.02) | 4.65(4.71) | 26.2(27.3) |
| [92] | 100% of CRA | Laboratory concrete waste of 25mm maximum size | Natural limestones of 25mm size | 6.1 (1.3) | 0.43 | Air dried condition | 51.2(51) | 2.4(2.8) | 31(36) |
| | 50% of CRA | | | | 0.43 | | 51.3(51) | 2.8(2.8) | 35.5(36) |
| | 20% of CRA | | | | 0.43 | | 48.8(51) | 2.6(2.8) | 35(36) |
| [10] | 100% of CRA | Commercial recycling plan of size 5-20mm. | Natural gravel of maximum size 20mm | 5.3 (0.61) | 0.58 | SSD | 45(38) | 4.9(5.0) | 12.5(19) |
| | 50% of CRA | | | | 0.61 | | 40(38) | 4.6(5.0) | 15(19) |
| | 30% of CRA | | | | 0.66 | | 32(38) | 5.1(5.0) | 14(19) |
| | 100% of CRA1 | | | | 0.67 | SSD | 18.0(18.1) | 3.7(3.9) | 23.4(27.1) |
| | 100% of CRA2 | | | | 0.67 | | 15.0(18.1) | 3.2(3.9) | 22.6(27.1) |

| | | | | | | | | | |
|--------------------------------------|--------------|--|--|------------|------|------------------------------|------------|----------|------------|
| [93] | 100% of CRA1 | Crushing of 2 years | Natural granitic | RA1 3.9 | 0.35 | | 36.4(37.5) | 5.3(5.2) | 28.8(33.1) |
| | 100% of CRA2 | old concrete of | crushed stones | RA2 3.8 | 0.35 | | 35.7(37.5) | 4.7(5.2) | 28.3(33.1) |
| | 100% of CRA1 | varyingfc to 6- | of 6-30mm size | (0.5) | 0.34 | | 44.4(48.4) | 6.0(7.3) | 34.2(39.9) |
| | 100% of CRA2 | 30mm aggregate | | | 0.34 | | 43.8(48.4) | 5.8(7.3) | 32.7(39.9) |
| size. RA1 is 55MPa and RA2 IS 30MPa. | | | | | | | | | |
| [18] | 0% of CRA | Unknown source of size 4-25mm | Unknown aggregate type with size ranging from 4-25mm | - | 0.55 | Pre-wetted and not saturated | 29 | 2.49 | 32.56 |
| | 25% of CRA | | | | 0.55 | | 28 | 2.97 | 31.3 |
| | 50% of CRA | | | | 0.52 | | 29 | 2.7 | 28.59 |
| | 100% of CRA | | | | 0.5 | | 28 | 2.72 | 27.76 |
| [94] | 100% of CRA | waste concrete from airport runway in Shanghai, China of size 6-20mm | Natural gravel of size 6-20mm | 9.25 (0.4) | 0.43 | Pre-soaked prior to use | 26.7(35.9) | | 17(27) |
| | 70% of CRA | | | | 0.43 | | 30.3(35.9) | | 16(27) |
| | 50% of CRA | | | | 0.43 | | 29.6(35.9) | | 16(27) |
| | 30% of CRA | | | | 0.43 | | 34.1(35.9) | | 15(27) |
| [98] | 100% of CRA | RA crushed from 14MPa concrete cubes to size 4-32mm | Natural gravel of 4-32mm | - | 0.57 | Pre-soaked prior to use | 14(20) | 1.6(2.2) | |
| | 70% of CRA | | | | 0.57 | | 16.5(20) | 1.7(2.2) | |
| | 50% of CRA | | | | 0.57 | | 17.8(20) | 1.7(2.2) | |
| | 30% of CRA | | | | 0.57 | | 18.2(20) | 2.0(2.2) | |

| | | | | | | | | | | |
|-------|--|---|--|-----------|------------------------------|-------------------------|---|----------|----------|------------|
| [69] | 64% of CRA | RA obtained from 15years old concrete of 36MPa strength. RA size is 16-25mm | Natural gravel of size 16-25mm | 7.0 (1.2) | 0.48 | Air dried condition | 45.6(41.3) | 4.9(6.4) | 3.0(3.8) | 24.9(31.4) |
| | 37% of CRA | | | | 0.48 | | 44.7(41.3) | 4.8(6.4) | 4.1(3.8) | 26.9(31.4) |
| | 27% of CRA | | | | 0.48 | | 51.4(41.3) | 5.8(6.4) | 3.2(3.8) | 30.3(31.4) |
| [14] | 0% of CRA | RA obtained from old demolished bridge crushed to size 8-31.5mm | Natural river gravel of size 8-31.5mm | 3.8 (0.5) | 0.52 | Oven dried condition | 43.7 | | 3.1 | 26.6 |
| | 50% of CRA | | | | 0.52 | | 44.2 | | 2.7 | 26.2 |
| | 100% of CRA | | | | 0.51 | | 42.5 | | 3.2 | 25.4 |
| [99] | 0% of CRA 50% of CRA 100% of C | RA was obtained by processing waste concrete at shanghai. 12mm size | Crushed stones of 12mm size | 9.25(04) | 0.43 0.43 0.43 | Pre-soaked prior to use | 43.52 39.27 34.63 | | | |
| [100] | 0% of CRA 25% of CRA 50% of CRA 75% of CRA 100% of CRA | RA were obtained from laboratory concrete waste and crushed to 12.5mm size | Crushed stone of unknown type and of 12.5 mmm size | 6(0.98) | 0.54 0.54 0.54 0.54 | SSD | 36.91 28.88 24.04 26.16 24.71 | | | |

Table 2.7 Summary of previous research studies on concrete made with crumb rubber

| Author (s) | Replacement ratio | CR Size (mm) | CA or sand replaced with CR | Free w/c | Density for CR(NAC) kg/m ³ | Comp strength for CR (NAC) MPa | F _{fs} for CR (NAC) MPa | F _{ct} for CR (NAC) MPa | E _c for CR(NAC) MPa |
|------------|--|--------------|--------------------------------------|----------|---------------------------------------|--------------------------------|----------------------------------|----------------------------------|--------------------------------|
| [101] | 30% of FR for sand 20% of FR for sand | 4 | Dried natural river sand of size 4mm | 0.5 | 1710(2150) 1610(2150) | 16(38) 8(38) | 1.8(3) 0.9(3) | | 12.45(20.2) 8.25(20.2) |
| [27] | 5% of CR for CA | 12.5 | CA of unknown type with 8-16mm size | 0.41 | | 29(40) | 5.2(6.1) | | |
| [35] | 5% of CR for CA | 20 | Crushed | 0.5 | | 33(32) | 5.4(5.4) | 2(3) | 24(28) |
| | 7.5% of CR for CA | 20 | siliceous | 0.5 | | 30(32) | 3.8(5.4) | 1.7(3) | 22(28) |
| | 10% of CR for CA | 20 | coarse | 0.5 | | 25(32) | 3.4(5.4) | 1.6(3) | 20(28) |
| | 5% of GR for cement | 600μm | aggregates | 0.5 | | 30(32) | 4.9(5.4) | 2.6(3) | 24(28) |
| | 7.5% of GR for cement | 600μm | of size | 0.5 | | 27(32) | 4.8(5.4) | 2.3(3) | 22(28) |
| | 10% of GR for cement | 600μm | 25mm | 0.5 | | 20(32) | 3.9(5.4) | 1.7(3) | 18(28) |

| | | | | | | | | |
|-------|-------------------|------|-------------|------|------------|--------------|-----------|------------|
| [102] | 1% of FR for sand | 0.25 | | 0.39 | 2448(2497) | 97(112.3) | 5(5.4) | 55.6(56.1) |
| | 2% of FR for sand | 0.25 | | 0.39 | 2416(2497) | 92.7(112.3) | 4.7(5.0) | 51.8(56.1) |
| | 3% of FR for sand | 0.25 | River sand | 0.39 | 2398(2497) | 86(112.3) | 4.3(5.0) | 43.9(56.1) |
| | 1% of FR for sand | 0.42 | of size 1- | 0.39 | 2448(2497) | 102(112.3) | 5(5.4) | 47.4(56.1) |
| | 2% of FR for sand | 0.42 | 4mm and | 0.39 | 2416(2497) | 99.2(112.3) | 4.8(5.4) | 45.5(56.1) |
| | 3% of FR for sand | 0.42 | Crushed | 0.39 | 2398(2497) | 95.8(112.3) | 4.7(5.4) | 41.9(56.1) |
| | 1% of FR for sand | 1 | granite | 0.39 | 2448(2497) | 103.5(112.3) | 5.2(5.4) | 45.1(56.1) |
| | 2% of FR for sand | 1 | stone of | 0.39 | 2416(2497) | 89(112.3) | 5.0(5.4) | 48.5(56.1) |
| | 3% of FR for sand | 1 | size 5- | 0.39 | 2398(2497) | 86.7(112.3) | 4.9(5.4) | 45.4(56.1) |
| | | | 30mm | | | | | |
| [41] | 10% CR for sand | 6.2 | | 0.55 | 2345(2372) | 31.5(53) | 2.05(2.1) | 30(45) |
| | 20% CR for sand | 6.2 | | 0.55 | 2187(2372) | 23(53) | 1.75(2.1) | 28(45) |
| | 30% CR for sand | 6.2 | | 0.55 | 2080(2372) | 15(53) | 1.27(2.1) | 21(45) |
| | 50% CR for sand | 6.2 | Hope | 0.55 | 1813(2372) | 2.5(53) | 0.19(2.1) | 18(45) |
| | 10% CR for CA | 6.2 | valley grit | 0.55 | 2259(2372) | 28.5(53) | 2(2.1) | 29(45) |
| | 20% CR for CA | 6.2 | sand of | 0.55 | 2041(2372) | 14(53) | 1.08(2.1) | 22(45) |
| | 30% CR for CA | 6.2 | size 1- | 0.55 | 1926(2372) | 5.5(53) | 0.73(2.1) | 18(45) |
| | 50% CR for CA | 6.2 | 3mm and | 0.55 | 1492(2372) | 1.4(53) | 0.13(2.1) | 10(45) |
| | 10% CR for sand | 6.2 | Hope | 0.51 | 2284(2381) | 35(55) | 2.6(3.8) | 29.5(45.5) |
| | 20% CR for sand | 6.2 | valley | 0.51 | 2170(2381) | 18(55) | 1.4(3.8) | 27.5(45.5) |
| | 30% CR for sand | 6.2 | rounded | 0.51 | 2070(2381) | 9(55) | 0.82(3.8) | 14(45.5) |
| | 50% CR for sand | 6.2 | gravel of | 0.51 | - | - | - | - |
| | 10% CR for CA | 6.2 | size 10mm | 0.51 | 2217(2381) | 23(55) | 2.1(3.8) | 28(45.5) |
| | 20% CR for CA | 6.2 | | 0.51 | 2065(2381) | 16(55) | 1.1(3.8) | 24.5(45.5) |
| | 30% CR for CA | 6.2 | | 0.51 | 1907(2381) | 8(55) | 0.44(3.8) | 20.5(45.5) |

| | | | | | | | | |
|------|-----------------|------|--|------|--|------------|------------|------------|
| | 50% CR for CA | 6.2 | | 0.51 | - | - | - | - |
| | 10% CR for sand | 6.2 | | 0.48 | 2283(2390) | 31.5(58) | 2.73(4.0) | 37(47) |
| | 20% CR for sand | 6.2 | | 0.48 | 2158(2390) | 22(58) | 1.59(4.0) | 34(47) |
| | 30% CR for sand | 6.2 | | 0.48 | 2014(2390) | 10.5(58) | 0.82(4.0) | 28(47) |
| | 50% CR for sand | 6.2 | | 0.48 | - | - | - | - |
| | 10% CR for CA | 6.2 | | 0.48 | 2228(2390) | 26(58) | 2.16(4.0) | 23(47) |
| | 20% CR for CA | 6.2 | | 0.48 | 1995(2390) | 15(58) | 0.83(4.0) | 15(47) |
| | 30% CR for CA | 6.2 | | 0.48 | 1905(2390) | 6.5(58) | 0.4(4.0) | 21.5(47) |
| | 50% CR for CA | 6.2 | | 0.48 | - | - | - | - |
| [26] | 25% CR for CA | | | | | 19.6(31.9) | 3.5(3.8) | |
| | 50% CR for CA | 12.7 | | 0.5 | - | 13.8(31.9) | 3.1(3.8) | |
| | 75% CR for CA | | | | | 9.9(31.6) | 2.8(3.8) | |
| | 100% CR for CA | | | | | 7.5(31.6) | 2.4(3.8) | |
| | | | | | Crushed stone coarse aggregates of size 19mm and natural sand of size 4.76mm | | | |
| [80] | 5% CR for sand | | | 0.35 | | 46(64) | 4.1(6.49) | 3.68(3.48) |
| | 10% CR for sand | 0-1 | | 0.35 | | 34(64) | 3.15(6.49) | 3.08(3.48) |
| | 20% CR for sand | | | 0.35 | 4mm natural sand from kvesai | 14(64) | 2.15(6.49) | 1.83(3.48) |
| | 30% CR for sand | | | 0.35 | | 10(64) | 1.81(6.49) | 1.7(3.48) |
| | 5% CR for sand | | | 0.35 | quarry and 4-16mm | 48(64) | 5.1(6.49) | 3.51(3.48) |
| | 10% CR for sand | 1--2 | | 0.35 | | 40(64) | 4.65(6.49) | 3.74(3.48) |
| | 20% CR for sand | | | 0.35 | | 22(64) | 3.6(6.49) | 3.08(3.48) |

| | | | | | | | | | |
|------|--|--------|---|------|------------|------------|------------|------------|------------|
| | | | CA from kvesai quarry | 0.35 | | 11(64) | 2.62(6.49) | 1.77(3.48) | |
| | | | | 0.35 | | 51(64) | 5.34(6.49) | 3.68(3.48) | |
| | | 2--3 | | 0.35 | | 47(64) | 4.95(6.49) | 3.02(3.48) | |
| | | | | 0.35 | | 23(64) | 3.94(6.49) | 2.54(3.48) | |
| | | | | 0.35 | | - | - | - | |
| [84] | | | Crushed stones of unknown size | 0.52 | 2355(2415) | 17(18.8) | 5.07(5.28) | | |
| | | - | | 0.52 | 2335(2415) | 15.5(18.8) | 4.8(5.28) | | |
| | | | | 0.52 | 2252(2415) | 15(18.8) | 4.55(5.28) | | |
| [29] | | | Yishu river sand | | | | | | |
| | | | of | 0.45 | 2420(2495) | 36.9(38.6) | | 2.78(2.95) | 33.8(36.4) |
| | | | maximum | 0.45 | 2355(2495) | 35.4(38.6) | | 2.66(2.95) | 30.1(36.4) |
| | | - | size 5mm | 0.45 | 2280(2495) | 31.8(38.6) | | 2.45(2.95) | 27.5(36.4) |
| | | | and | 0.45 | 2205(2495) | 29.9(38.6) | | 2.23(2.95) | 24.2(36.4) |
| | | | limestone | 0.45 | 2110(2495) | 27.6(38.6) | | 2.01(2.95) | 20.6(36.4) |
| | | | CA of size 8-10mm | | | | | | |
| [88] | | | | 0.42 | | 34.4(38.4) | 4.2(4.7) | | 31.2(35.8) |
| | | | Natural sand of unknown size and gravels of | 0.42 | | 18.2(38.4) | 3.3(4.7) | | 29.2(35.8) |
| | | Powder | | 0.42 | | 12(38.4) | 2.2(4.7) | | 19.7(35.8) |
| | | | | 0.42 | | 8(38.4) | 2.1(4.7) | | 15.2(35.8) |
| | | 0.1-5 | | 0.42 | | 33(38.4) | 4.2(4.7) | | 33.4(35.8) |

| | | | | | | | |
|------|--|------|-----------------|------|--------------|----------|------------|
| | | | size 5-25mm. | 0.42 | 22.6(38.4) | 3.4(4.7) | 30.4(35.8) |
| | | | | 0.42 | 13.2(38.4) | 2.8(4.7) | 21(35.8) |
| | | | | 0.42 | 10.7(38.4) | 2.5(4.7) | 19.1(35.8) |
| | | | | 0.42 | 33.3(38.4) | 4.1(4.7) | 34.2(35.8) |
| | | 2--8 | | 0.42 | 18.7(38.4) | 3.6(4.7) | 30.3(35.8) |
| | | | | 0.42 | 14.1(38.4) | 3.2(4.7) | 25.2(35.8) |
| | | | | 0.42 | 11.5(38.4) | 2.4(4.7) | 19.2(35.8) |
| [37] | | | | | | | |
| | | | Crushed | 0.48 | 18.96(33.79) | | 2.14(3.44) |
| | | 19.1 | stone | 0.48 | 11.46(33.79) | | 1.48(3.44) |
| | | | aggregates | 0.48 | 8.04(33.79) | | 1.16(3.44) |
| | | | of size19-38mm | 0.48 | 5.86(33.79) | | 0.83(3.44) |
| | | | | 0.48 | 23(33.79) | | 2.81(3.44) |
| | | | | 0.48 | 18.9(33.79) | | 2.36(3.44) |
| | | | | 0.48 | 14.47(33.79) | | 2.01(3.44) |
| | | 6.4 | | 0.48 | 12.19(33.79) | | 1.63(3.44) |
| | | | | | 40.4 | | |
| | | | | | 37.6 | | |
| | | | | | 34.8 | | |
| | | | | | 24.3 | | |
| [86] | | 2.3 | Fine sand | 0.47 | 38.7 | | |
| | | | of size 0.8-6mm | | 36.1 | | |
| | | | | | 25.5 | | |
| | | | | | 52.1 | | |

| | | | | | |
|------|-----------------|-----------|----------------------|------|-------|
| | 5% CRPS | | | | 45.9 |
| | 10% CRPS | | | | 34.9 |
| | 15% CRPS | | | | |
| | 0% for CA | | 11- | | |
| | 5% for CA | | 25.4mm | 0.43 | 50 |
| [83] | 10% for CA | 11.8 | crashed | 0.44 | 42 |
| | 15% for CA | | Limestone aggregates | 0.46 | 37 |
| | | | | 0.48 | 28 |
| | 0% GR for sand | | | 0.35 | 59.25 |
| | 5% GR for sand | | | 0.35 | 57.25 |
| | 10% GR for sand | | | 0.35 | 56.75 |
| | 15% GR for sand | | Crushed | 0.35 | 55 |
| | 20% GR for sand | 2 to 3mm | gravel of | 0.35 | 42.5 |
| | 0% GR for sand | width and | 12.6mm | 0.45 | 50.25 |
| [42] | 5% GR for sand | 20mm | size. water | 0.45 | 48.75 |
| | 10% GR for sand | length | absorption | 0.45 | 48.5 |
| | 15% GR for sand | | of 0.5% | 0.45 | 45.25 |
| | 20% GR for sand | | | 0.45 | 45 |
| | 0% GR for sand | | | 0.55 | 33.5 |
| | 5% GR for sand | | | 0.55 | 34.25 |

| | | |
|-----------------|------|-------|
| 10% GR for sand | 0.55 | 34.25 |
| 15% GR for sand | 0.55 | 35 |
| 20% GR for sand | 0.55 | 35.25 |

*Water abs (NA) - Water absorption of recycled aggregate (RA). The value in brackets represents that of natural aggregates (NA); * f_{fs} (NAC) - Flexural strength of recycled aggregate concrete. The value in brackets represents that of natural aggregate concrete; * f_{ct} (NAC) – Splitting tensile strength of recycled aggregate concrete. The value in brackets represents that of natural aggregate concrete; * E_c (NAC) - Elastic modulus of recycled aggregate concrete. The value in brackets represents that of the NAC; *CRA- Coarse recycled aggregates; CA-Coarse aggregates; CRPS-Pre-coated crumb rubber modified with silica fumes.

CR- Crumb rubber used for replacing natural coarse aggregate, FR- fine rubber particles for replacing natural sand, GR- grounded rubber used for replacing cement in concrete.

2.4.4 Methods devised to improve the performance of recycled concrete

Due to the above aforementioned issues exhibited by recycled aggregate and rubberized concretes, many researchers have taken up the challenge to devise methods to enhance the performance of the recycled concrete. Some of these techniques are summarized in Table 2.8 and Table 2.9 respectively. The methods include the addition of extra amounts of cement, use of super plasticizers, incorporation of fly ash, silica fume [7, 9, 11, 14]. [103] went a step further and proposed a two-stage mixing approach (TSMA) which involved splitting the mixing into two stages contrary to the normal mixing approach. In this approach, sand, recycled aggregates, cement and half of the water was first mixed for 150 seconds; the other half of the water was added and mixing was continued for another 120 seconds as shown in Figure 2.22.

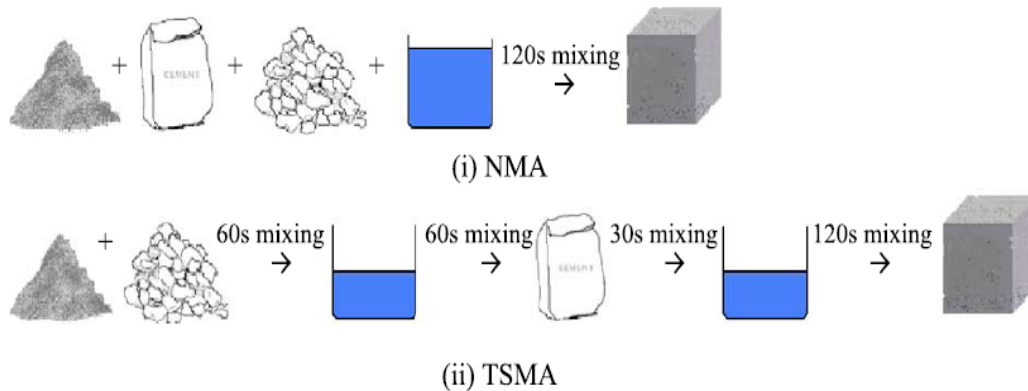


Figure 2.22 Mixing procedures for the normal mix (NMA) and the two-stage mixing approach (TSMA) (Tam et al., 2005).

The results in Table 2.8 show a 21.19% increase in strength compared to the normal mixing approach. [19] also adopted a method of pre-soaking recycled aggregates in

hydrochloric acid and sulphuric acid solution, and the results recorded (water absorption, strength) were better than the ones without pre-soaking as presented in Table 2.8. The two-stage mixing approach was also modified by adding cement (TSMAC) and silica fume plus cement (TSMASC) at the pre-mix stage [62]. The compressive strength of the TSMASC was enhanced by up to 6% more than the normal mixing approach (NMA) shown in Table 2.8.

Silica fume and blast furnace ash were added to concrete made with crumb rubber to enhance performance as shown in Table 2.9. About a 9-37% of strength increase was recorded when 10% silica fume was incorporated into the rubberized concrete [85]. Also [28] carried out research on pre-coating of the crumb rubber, washing of the crumb rubber, soaking it in sodium hydroxide solution (NaOH) before incorporating it into concrete. The crumb rubbers was pre-coated with cement, cement matrix, washed with water, soaked in sodium hydroxide solution (NaOH) prior to use. The results from the research shown in Table 2.9 indicate a higher performance (29% strength increase) for crumb rubber pre-coated with cement matrix than untreated rubber particles. This same scenario occurs for all other treatment methods as shown in Table 2.9 but better performance is found in cement matrix pre-coated crumb rubber because of the bond enhancement between the crumb rubber and the cement matrix.

Table 2.8 Summary of methods devised to improve the mechanical properties of recycled aggregate concrete (RAC)

| Source | Proposed Methodology | Outcome |
|--------|---|---|
| [14] | Addition of extra 3% of cement to the design mix | Target strength was achieved. Performance under bending is identical to NAC mix |
| [11] | Addition of 1% plasticizers and super plasticizers of cement weight | Target strength was achieved with both admixtures. The use of super plasticizers increased strength up to 32% Plasticizers also enhanced strength by 19%. |

| Source | Proposed Methodology | Outcome |
|--------|---|---|
| | weight | The use of fly ash meets durability requirements of RAC by reducing drying shrinkage, water absorption, creep effect, chlorine ion penetration. |
| [17] | Use of super plasticizers measured with respect to cement weight | Enhances the compressive and splitting tensile strength of the RAC. Higher water reducing agent results in higher strength and better workability. |
| [7] | Incorporation of 5-10% of silica fume of cement weight | Compressive and tensile splitting strength of the RAC were enhanced and suitable for structural application for 30% replacement ratio. |
| [103] | Two-stage mixing approach | The 28 day comprehensive strength was enhanced using two-stage mixing approach. 21.19% strength increase for 25% replacement ratio. Enhances the interfacial transition zone of the RA by filling its cracks and pores |
| [19] | Pre-soaking treatment methods in H ₂ SO ₄ and HCL acid solution | Reduces the water absorption of RAC. The compressive and flexural strength, modulus of elasticity were increased after pre-soaking in H ₂ SO ₄ , HCL solution. The alkalinity of the RA, Chlorine and sulphate contents were not adversely affected. |
| [62] | Diversifying two-stage mixing approach by adding silica fume at the pre-mix stage(TSMA _S)and also adding cement and silica fume in the pre-mix stage(TSMA _{SC}) | Both the TSMA _S and TSMA _{SC} enhance the compressive strength of the RAC by filling up the cracks and pores of the RA. However the strength increase observed in TSMA _{SC} is higher than that of TSMA _{SC} and NMA with 5.7% and 6% respectively. |

RA-Recycled aggregate; RAC- Recycled aggregate concrete; TSMA_S- Two-stage mixing approach with addition of silica fume at the pre-mix stage; TSMA_{SC}- Two-stage mixing approach with the addition of silica fume and cement at the pre-mix stage; HCL- Hydrochloric acid; H₂SO₄- Sulphuric acid

Table 2.9 Summary of methods to improve the mechanical properties of concrete with crumb rubber

| Source | Proposed methodology | Outcome |
|--------|--|---|
| [85] | Addition of 10% silica fume and 3% super plasticizers by cement weight | Enhances the compressive strength more than the mix Without super plasticizers and silica fume. Reduces the chlorine ion penetration. The super plasticizers were used to meet workability requirement |
| [28] | Cement matrix pre-coated rubber aggregates | Enhances compressive strength up to 29% compared to untreated rubber particles. Enhances bonding of the interfacial transition zone between the rubber particles and cement paste. |
| | Cement paste pre-coated rubber aggregates | Enhances strength up to 14% more than the untreated rubber particles Reduces the crack mouth opening displacement under bending better than other pre-treatment methods. Enhances interfacial bonding of the rubber and cement matrix |
| | water washed rubber aggregates | Strength up to 4.5% higher than untreated rubber particles. |
| | NaOH pre-treated rubber aggregate | Compressive strength up to 3% higher than the untreated rubber particles. |
| [81] | Incorporation of 20-40% blast furnace slag to cement weight | Enhances the compressive strength of the rubberized concrete compared to the one without blast furnace slag . 17% strength increase for 40% blast furnace slag to cement weight Improved abrasion resistance. Increase the energy absorption capacity. |
| [66] | Water pre-soaking method | Strength higher by 22% at 7days and by 11% at 28 days than the untreated rubber particles Enhances better distribution of rubber particles in concrete. 2% less entrapped air in the mixture. |

2.4.5 Assessment of improvement methods and limitations.

Holistically, the measures taken to improve the mechanical performance of concrete made with recycled aggregates and crumb rubber were quite impressive but little consideration was given to cost and feasibility of adopting these methods in the construction industry. For instance, the addition of extra cement, silica fume, super plasticizers [7, 11, 14] to meet the mix strength requirement incurs more cost to the design concrete. Pre-soaking of recycled aggregates in hydrochloric and sulphuric acid [19], pre-soaking of crumb rubber in sodium hydroxide [28] solution requires extra manpower and cost. The pre-treatment of crumb rubber with cement matrix and cement yields better results [28] but will be very expensive considering the extra amount of cement and sand (50% of cement weight) required to get the work done. Also the pre-coating procedure is time-consuming since it requires 28 days' curing of the coated crumb rubber prior to use. This will automatically increase the manpower and will also require advanced technical know-how. The two-stage mixing approach (TSMA) proposed by [103] requires extra time (150 seconds) to get the concrete mix done compared to the normal mix approach (NMA). This research will explore an alternative method: by adding a tiny amount of graphene to recycled aggregate concrete. A detailed review of the effects of graphene in concrete will be presented in Section 2.9.

2.4.6 Bond Strength

Adequate bonding of steel reinforcement and concrete is a basic requirement of reinforced concrete application. Bond behaviour is affected by concrete type (low strength or normal aggregate concrete), rebar geometry (plain or deformed), concrete cover, loading conditions and construction details. Pull-out failure usually occurs when there is sufficient confinement or cover to the reinforcement by shearing of the concrete surrounding the reinforcing bars. On the other hand, splitting failure shown in Figure 2.23 occur when there is insufficient concrete cover by generating tensile stresses around the reinforcing bars. Splitting failure often occurs with deformed bars than with

plain bars under the same loading condition because of the rough surface of deformed bars [104].

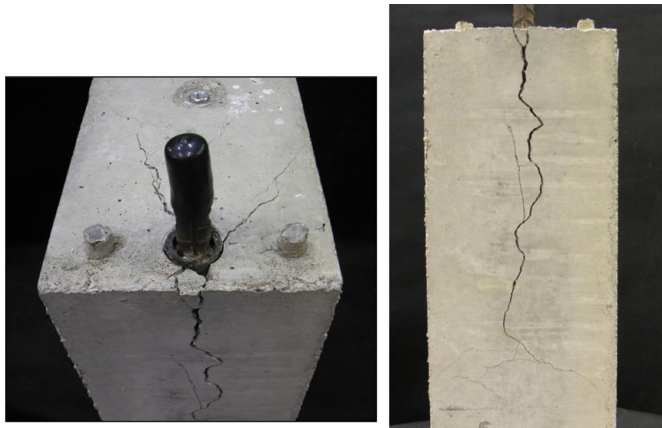


Figure 2.23 Typical splitting failure of a beam end specimen [105]

The results of all existing research studies suggest that using recycled aggregates in concrete does not lead to reduction in the bond strength between recycled aggregate concrete and reinforcement regardless of the effects of recycled aggregates on other mechanical properties. For example, as shown in Figure 2.24, the load slip curves are similar in terms of micro slip, internal cracking, pull-out, descending and residual stages for both concrete types. In fact, at the same concrete compressive strength, the bond strength for recycled aggregate concrete is observed to be higher compared to natural aggregate concrete [99, 106], due to the more irregular shapes of recycled aggregates compared to natural aggregates, thereby providing better bond between cement matrix and aggregates. The details of the recycled aggregate and natural aggregate type, compressive strength of the recycled aggregate and natural aggregate concrete used for the tests in Figure 2.24 are summarized in Table 2.6.

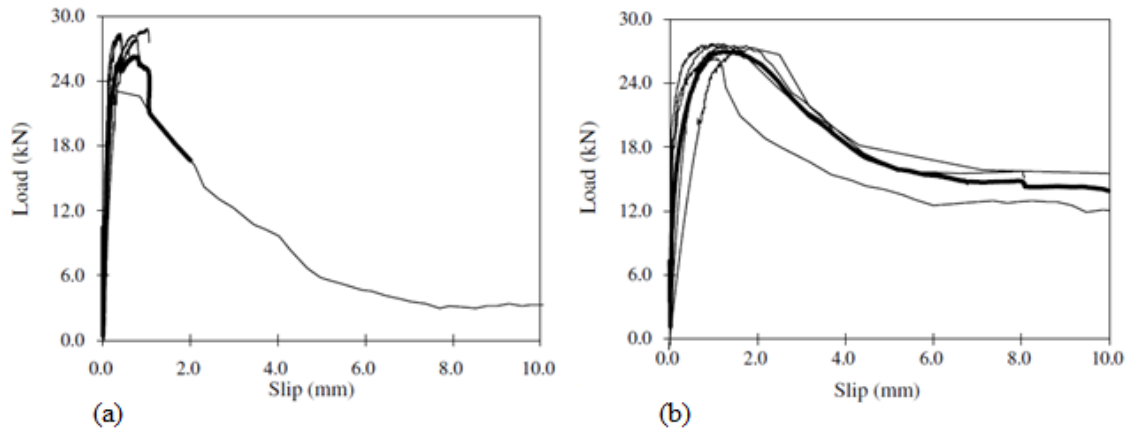


Figure 2.24 Test load slip curves for; (a) Natural aggregate concrete and deformed rebar; (b) 100% Recycled aggregate concrete and deformed rebars [99]

[100] also conducted some pull out tests on 8 and 10 mm diameter deformed steel bars embedded in recycled aggregate (RA) concrete of 0, 25, 50, 75 and 100 % replacement level. The bond strength of the 8mm ribbed bar and the recycled aggregate at 0, 25, 50, 75 and 100 % replacement level is 23.34, 13.94, 21.14, 16.94 and 22.71MPa respectively and for the 10mm ribbed bar is 17.98, 19.26, 17.27, 17.59 and 18.32MPa. Details of the natural and recycled aggregates type, compressive strength of concrete type are presented in Table 2.6.

In fact, if the bond strength is normalized to the compressive strength of concrete, as a ratio of bond strength to the square root of compressive strength, using recycled aggregate concrete would give higher values as shown in Figure 2.25 [99, 100]. In summary, using recycled aggregate concrete would not be an issue for bond strength. Therefore, the same anchorage length for deformed reinforcement bars as in concrete using natural aggregates can be used in recycled aggregate concrete [99, 100]

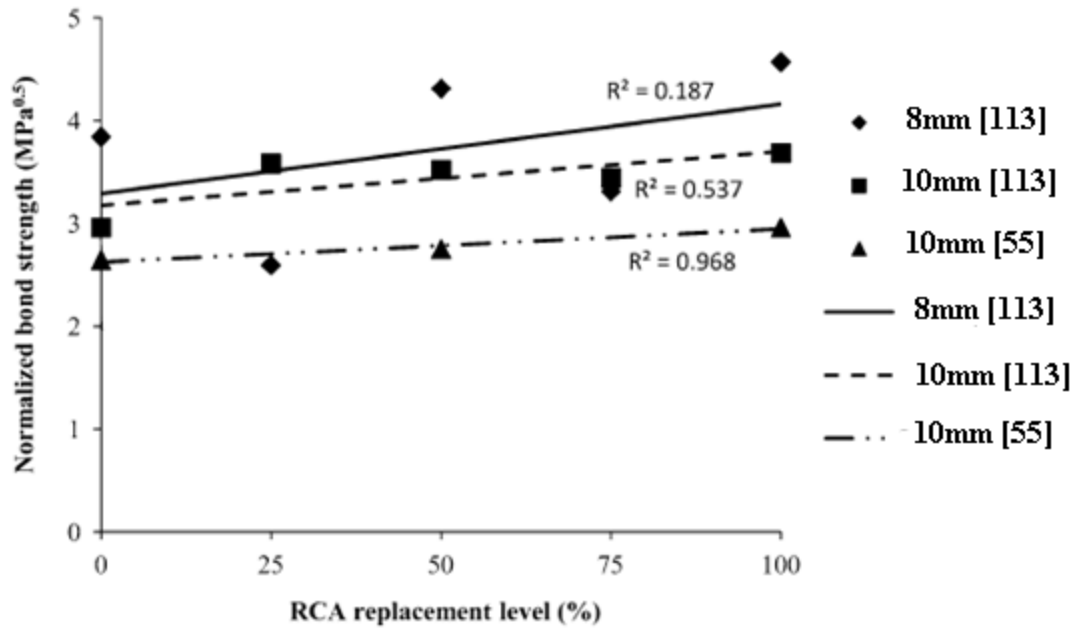


Figure 2.25 Normalized bond strength between 10mm rebars and recycled aggregate concrete of different replacement levels [99, 100].

However, there is little information about the bond strength for reinforcing bars in rubber recycled aggregate concrete and this will be investigated in this research.

2.5 Durability performance of recycled concrete

For regular reinforced concrete structures using recycled aggregate concrete, durability is a particular concern [9, 69, 107, 108] because recycled aggregates in their natural crushed state have higher porosity and permeability than natural aggregates, and are therefore more susceptible to corrosion of the reinforcement. Durability performance requirements include porosity, creep and shrinkage, freeze and thaw, chloride penetration, water absorption and a large number of research studies have investigated these different performance requirements. A number of methods of enhancing the durability of recycled aggregate concrete have been investigated. This section provides a review of the existing studies of durability of recycled aggregate concrete and an assessment of the different methods of improvement.

2.5.1 Chlorine permeation

A number of researchers have conducted rapid chloride penetration tests (RCPT) on recycled aggregate concrete and their results are compared in Figure 2.26. In these tests, the recycled aggregates were not processed after crushing. The RCPT values range from 1,800 to 8,000 Coulombs and tend to increase with decreasing compressive strength. According to the criteria in Table 2.10, most of the RCPT values are classified between low to medium ion permeability except for the case of [109] which has a low compressive strength for 100% RA replacement level.

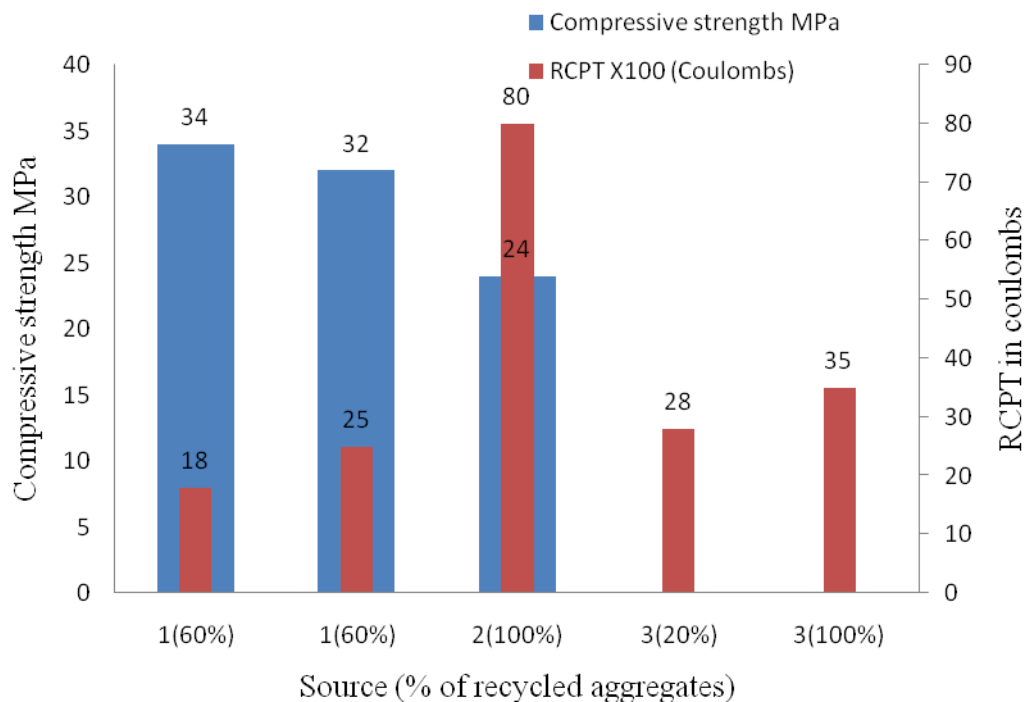


Figure 2.26 Comparison of RCPT results from different studies; 1.[108]; 2.[109]; 3. [110]

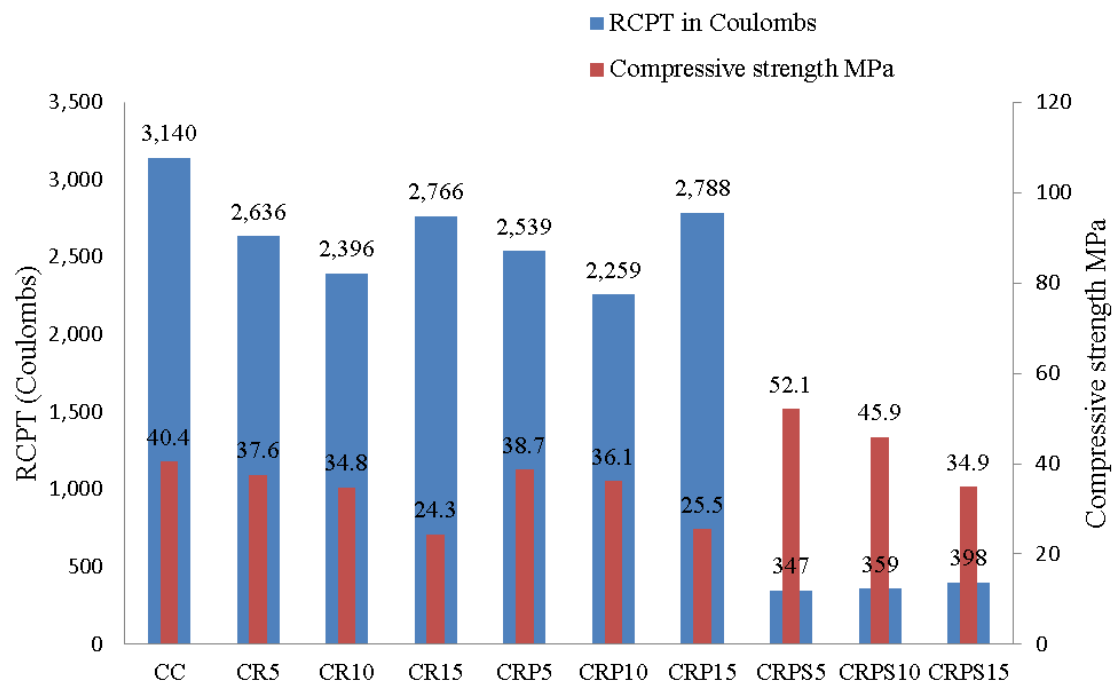
The results of [108] achieved chloride ion penetration results of 1,800-2,500 Coulombs, within the range of low to medium according to Table 2.10. The water cement ratio was 0.45. The low chloride permeability results may be due to the use of recycled aggregates after processing them by removing the adhered cement matrix.

Table 2.10 Ion chloride permeability based on charge passed [111]

| Charge Passed (Coulombs) | Chloride Ion Permeability |
|---------------------------------|----------------------------------|
| > 4,000 | High |
| 2000- 4000 | Moderate |
| 1000-2000 | Low |
| 100-1000 | Very Low |
| < 100 | Negligible |

[110] noted that the Two-Stage Mixing Approach (TSMA) process could be used to achieve RCPT values in the moderate range between 2800 to 3500 C for 20% and 100% replacement respectively by adopting a water cement ratio of 0.45 as shown in Figure 2.26.

A study was also conducted to improve the chlorine permeation of concrete with 5%, 10% and 15% of crumb rubber for fine aggregates substitution [86]. Details of the concrete mix are shown in Table 2.7. The techniques were considered; pre coating crumb rubbers with limestone powder and the use of 15% silica fumes as partial replacement to cement. At 5% and 10% of crumb rubber in concrete, the charge transmitted in the rubberized mixtures was lower than that of the NAC samples as shown in Figure 2.27 and is attributed to the surface insulation property of the crumb rubber. While the quantities of charge transmitted in the mixtures containing as-received crumb rubber without treatment and coated crumb rubber were similar, the charge transmission in the mixtures containing silica fume was significantly reduced as shown in Figure 2.27. This was attributed to the dense microstructure of the specimens as a result of the filler effect of the silica fume fine particles and the additional pozzolanic hydration products. The concrete made with pre coated crumb rubbers and 15% of silica fume as partial replacement to cement has a very low chlorine ion permeability based on the recommendations given in Table 2.10.



*CC-Natural aggregate concrete; *CR5,CR10 and CR15-Crumb rubber concrete with 5,10 and 15% replacement level; *CRP5,CRP10 and CRP15- Concrete with pre coated crumb rubber of 5,10 and 15% replacement level; CRPS5, CRPS10 and CRPS15- Pre coated crumb rubber at 5, 10 and 15% replacement level with 15% silica fume as partial replacement to cement.

Figure 2.27 Rapid chlorine penetration resistance of concrete with crumb rubbers [86]

2.5.2 Drying shrinkage

There is a direct relationship between the drying shrinkage of aggregate and its absorption capacity. The lower the drying shrinkage is, the better the concrete durability performance. The results in Figure 2.28 revealed that RAC 1-3 with higher compressive strength exhibits lower dry shrinkage compared to RAC 4-6 of lower compressive strength. Hence, the study concluded that concrete with a relatively higher compressive strength exhibits lower drying shrinkage compared to low-strength concrete.

The dry shrinkage of recycled aggregate concrete was improved by the addition of 35% in weight of fly ash (FA) as a partial replacement of cement or in addition to cement as shown in Figure 2.29. The dry shrinkage of concrete increased with an increase in RA replacement. The existing attached cement matrix on the recycled aggregates combined

with the new cement paste, increases the volume of paste, hence increasing the drying shrinkage of the resulting concrete. In summary, the use of fly ash, either as a replacement for or an addition to concrete, reduces the drying shrinkage values and was attributed to the dilution effects of fly ash particles. It is also worth noting that the reduction in drying shrinkage is more pronounced by the addition of fly ash than when it is used to replace cement. This is due to the fact that the addition of FA decreases the water cement ratio of the concrete mix from 0.55 to 0.42 indicating that a decrease in w/c reduces the drying shrinkage of concrete.

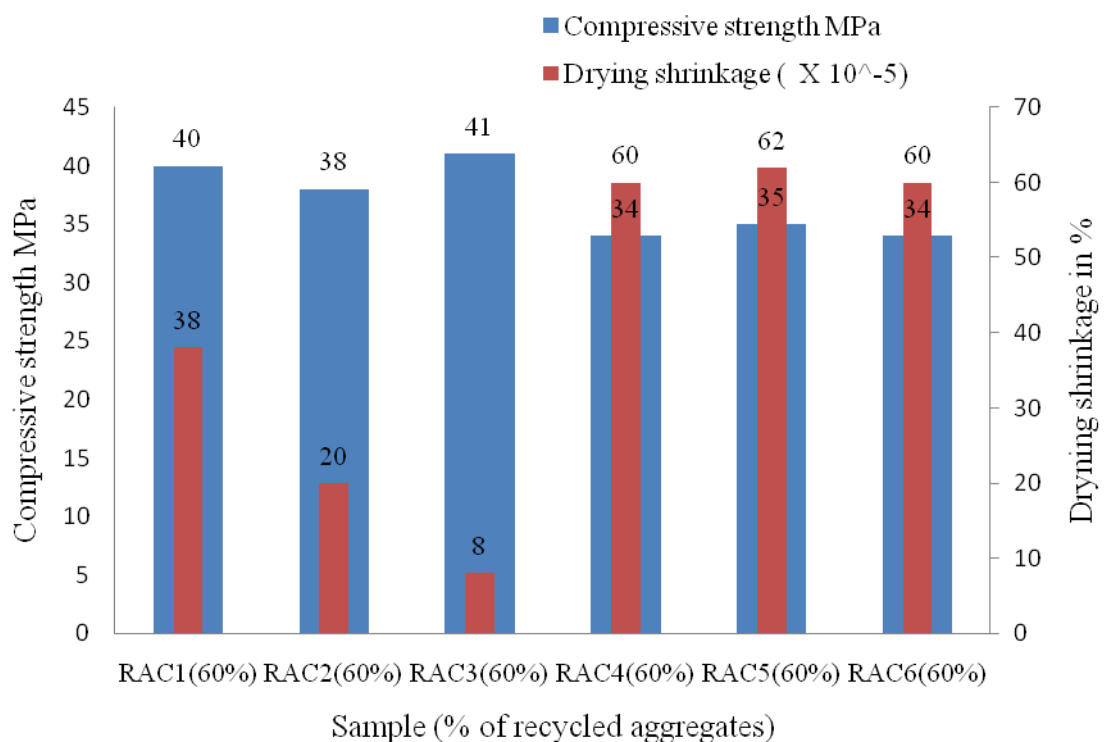


Figure 2.28 Comparison of drying shrinkage values from different concrete mixes [108]

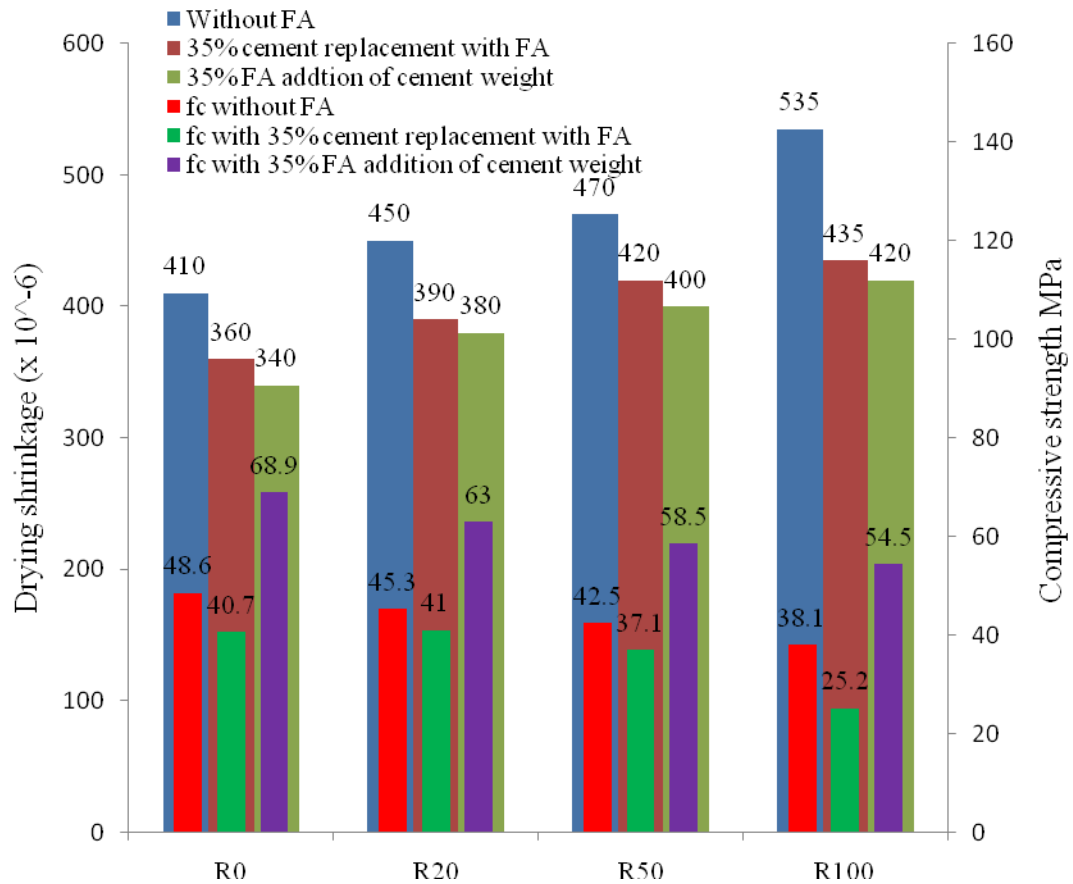


Figure 2.29 Drying shrinkage of concrete with different recycled aggregate replacement level with and without fly ash (FA)

A study was also conducted in the attempt to improve the drying shrinkage of rubberized cement matrix by treating crumb rubbers with NaOH solution [112]. The following cement matrix mixes were considered; the fine aggregate of the cement matrix was replaced with 0% (M0), 15% as received rubber (M-AS-15). Also the cement matrix of 15% (M-OH-15) and 25% (M-OH-25) NaOH-treated rubber by volume of the total fine aggregate was considered. The shrinkage of cement matrix samples increased with an increase in the concentration of crumb rubbers as shown in Figure 2.30. The increased shrinkage deformation of rubberized cement matrix was due to the reduced internal restraint of the structure. The average length change of treated samples M-OH-15 was 0.003% less than that of untreated samples M-AS-15. This can be explained by the enhanced adhesion between rubber particles and cement matrix due to NaOH surface treatment which in turn increases the internal restraint in treated

rubberized samples. In general, all samples have less than 0.03% length changes at 28 days, as shown in Figure 2.30, which indicates less shrinkage damage potential for cement concrete.

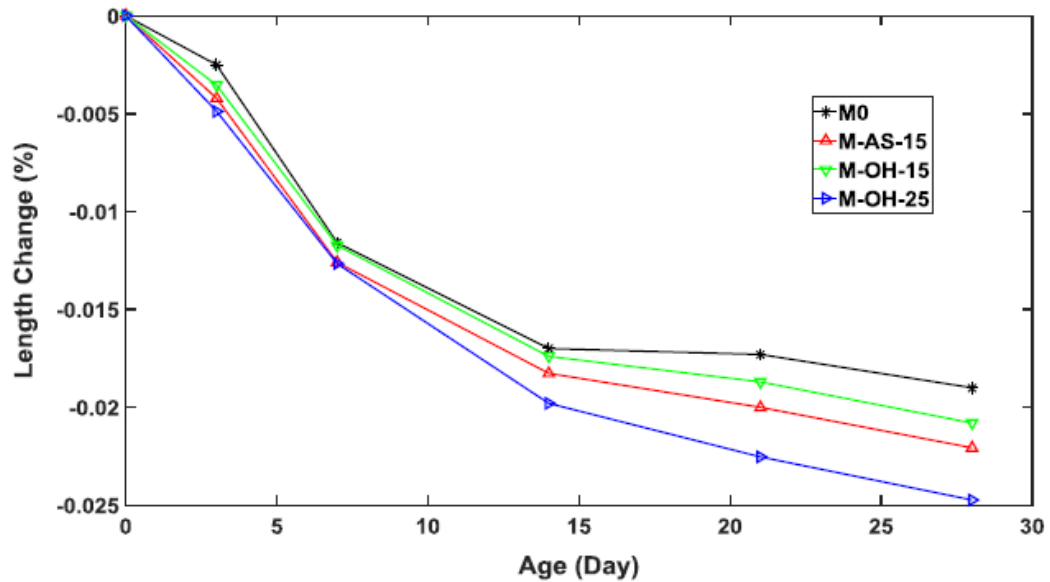


Figure 2.30 Shrinkage behaviour of cement matrix with different crumb rubber content.[112]

2.5.3 Carbonation depth

The carbonation depth of recycled aggregate concrete was improved by the addition of 35% in weight of fly ash (FA) as a partial replacement of cement or in addition to cement as shown in Figure 2.31. It can be observed that the carbonation depth of concrete increased with the increase in recycled aggregate content. However, the use of fly ash as a partial replacement of cement and an addition to cement decreased the carbonation depth of the concrete at different replacement levels.

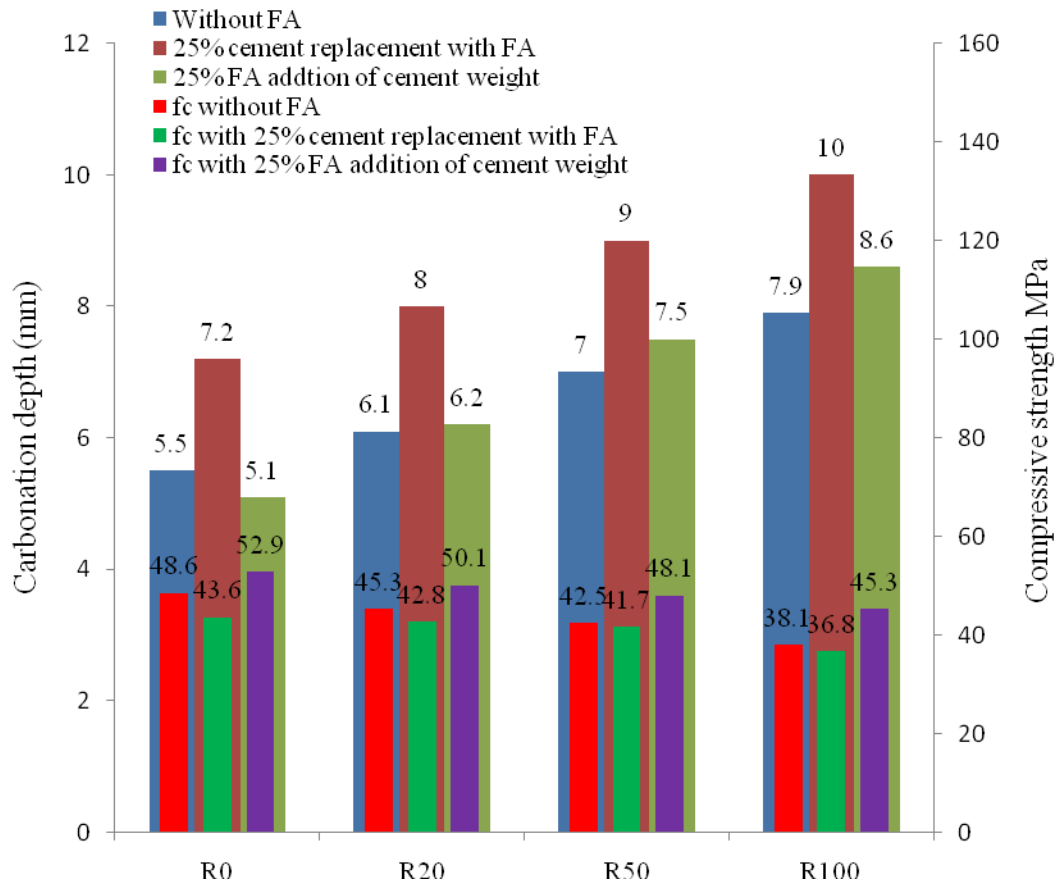


Figure 2.31 Carbonation depth of concrete with different RA concentration [9]

[83] conducted a durability study on concrete made with crumb rubber particles at replacement levels. Concrete mixes were produced in which 5%, 10% and 15% of the volume of natural aggregate (NA) were replaced by aggregate derived from used tyres. Details of the mechanical properties of concrete mixes are presented in Table 2.7. The carbonation depth increases with an increase in the replacement level of the natural aggregates with the crumb rubber as shown in Figure 2.32. The increase in carbonation depth was attributed to the higher water content of crumb rubber concrete, needed to maintain the workability in all the mixes, and to the greater void volume between crumb rubber and the cement matrix. The 28-day carbonation depth increased by 56% when 15% of the coarse natural aggregate was replaced with crumb rubbers.

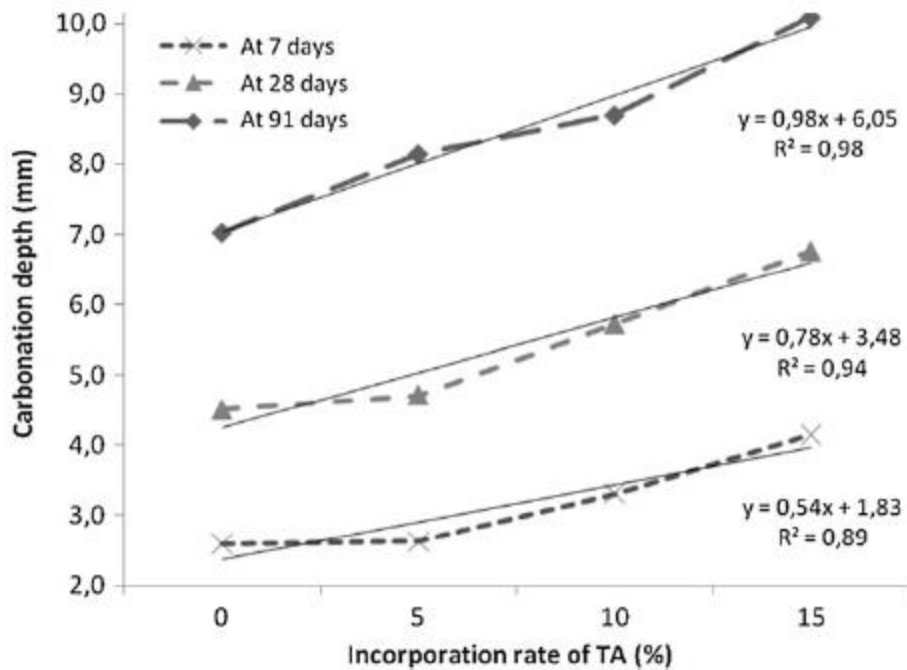


Figure 2.32 Carbonation depth with respect to replacement level [83]

[42] also conducted a durability test on rubberized concrete by replacing 5%, 10%, 15% and 20% of fine sand with crumb rubber ash for a water cement ratio of 0.35, 0.45 and 0.55. Details of the concrete mixes are presented in Table 2.7. It was observed that the carbonation depth for any replacement level increases for all selected w/c ratio as shown in Figure 2.33. The carbonation depth of 4.7 mm has been observed for 0.35 w/c ratio and 7.9 for 0.55 w/c ratio at 25% replacement level. The incorporation of crumb rubber fibres decreases the density of the concrete mix, hence decreasing the carbonation depth. It can also be noted from Figure 2.33 that the carbonation depth observed in the most adverse conditions (w/c ratio 0.55, replacement level 25%) is less than 15mm which is equivalent to the minimum cover required for any Reinforced Cement Concrete (RCC) members.

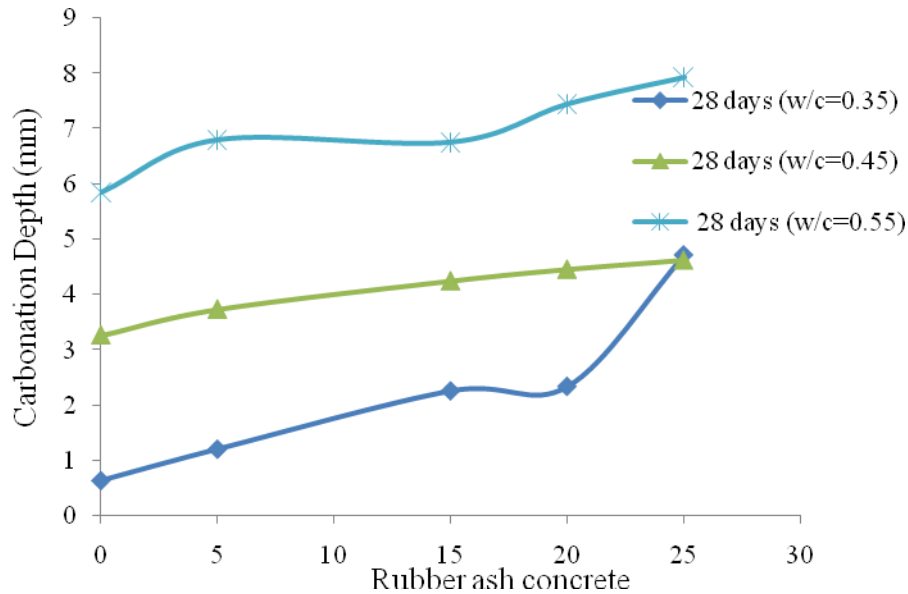


Figure 2.33 Carbonation depth of concrete with rubber ash at different replacement levels to sand for w/c of 0.35, 0.45 and 0.55 (data extracted from [42]).

2.5.4 Creep strain

The creep strain of recycled aggregate concrete was improved to that of the natural aggregate concrete by adding 35% in weight of fly ash (FA) as a partial replacement of cement or the addition of FA to cement as shown in Figure 2.34. It was observed that the deformation of the concrete specimens increased with an increase in the recycled aggregate content. This was attributed to the increased volume of cement matrix in the recycled aggregate concrete compared to that in the natural aggregate concrete. The creep strain of concrete with partial replacement of cement with FA was higher than that of the concrete addition of FA to cement. This might be due to the use of fly ash as the addition of cement decreased the W/B ratio and resulted in an increased compressive strength as shown in Figure 2.34.

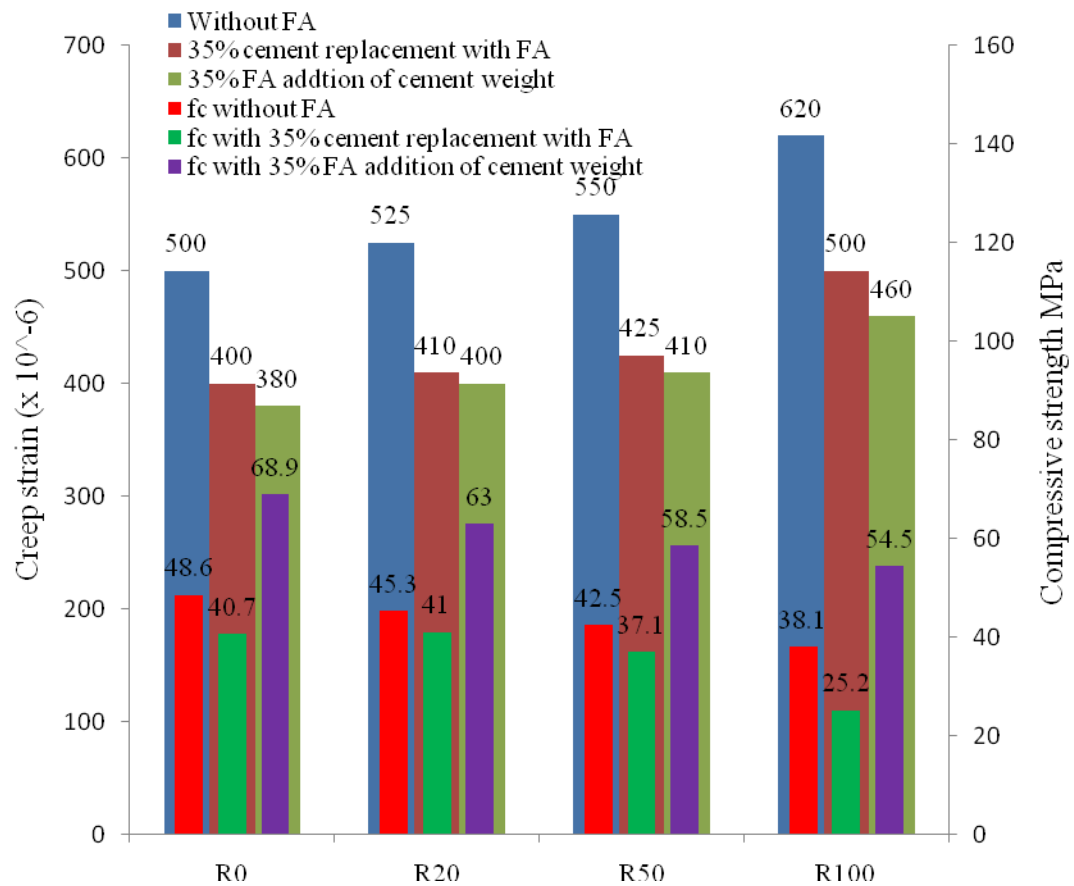


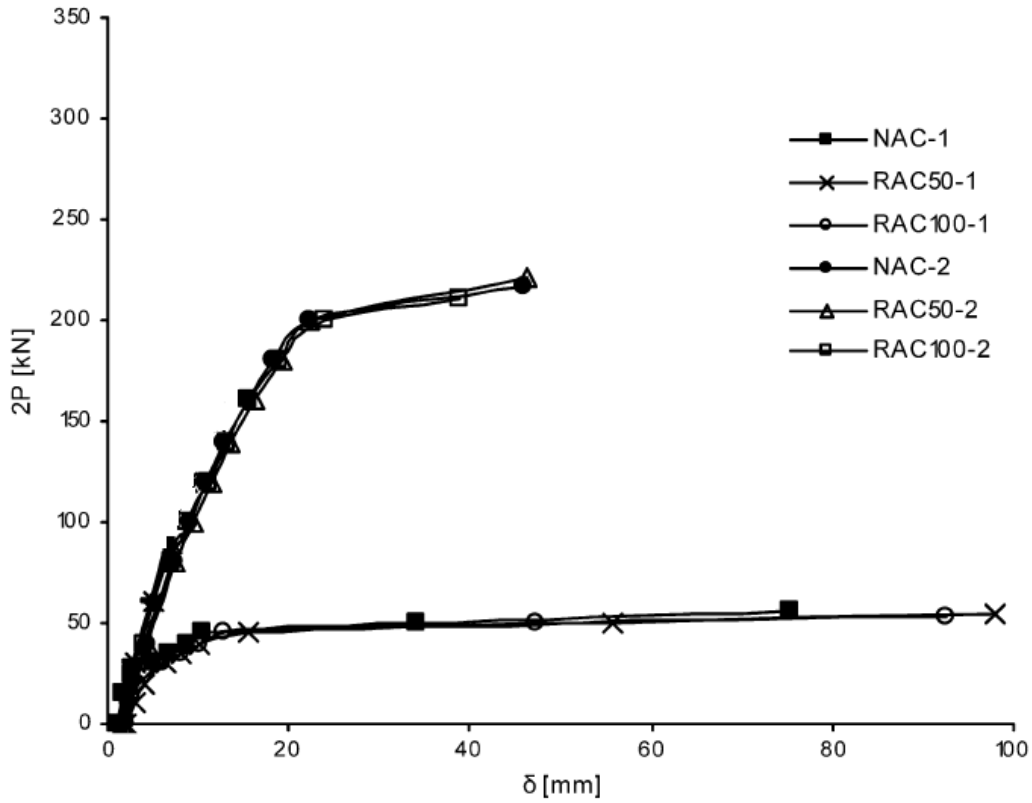
Figure 2.34 Creep strain of concrete with different recycled aggregate replacement levels with and without fly ash (FA) [9]

In summary, the durability of concrete made with recycled materials (crumb rubber and recycled aggregates) is worse than that of concrete made with natural aggregates. However, the use of fly ash as a partial replacement for, or as an addition to cement improves the durability performance of recycled concrete to that of the natural aggregate concrete. The durability performance for concrete made with crumb rubbers and recycled aggregates needs to be thoroughly investigated, through experiments to determine the exposure conditions under which recycled concrete can be used. Adding a tiny amount of graphene to recycled concrete has the potential to improve the durability of recycled concrete because graphene flakes can form a tortuous route to reduce the transportation of matters to corrode the reinforcement. Although durability is an important issue for reinforced concrete, a lack of time prevents this subject from being explored in detail in this research. This study will focus on the mechanical

properties of recycled concrete and the structural performance of recycled concrete structures.

2.6 Flexural behaviour of reinforced recycled concrete beams

Compared with extensive research studies on mechanical properties in the wet (workability) and hardened state (compressive and tensile strength) of recycled concrete, there are few studies on the performance of structural members made with recycled aggregate concrete or rubberized concrete. [14] carried out 9 tests to compare the bending behaviour of reinforced concrete beams using natural aggregate concrete and recycled aggregate concrete for different longitudinal reinforcement ratios (0.28% and 1.46%). The reinforced concrete beams are of 3m length with a cross section of 300mm depth and a width of 200mm. The quality of the recycled aggregates was very good and the recycled aggregates were free from any form of impurities (bricks, glass, tiles etc). An extra amount of cement (3%) was added to the case of 100% replacement of natural aggregates by recycled aggregates. The 28-day compressive strengths of the natural aggregate concrete, concrete with 50% of recycled aggregate replacement, and concrete with 100% recycled aggregates, were almost identical, being 43.7MPa, 44.2Mpa and 42.5Mpa respectively. Figure 2.35 shows their recorded load-deflection curves of the beams with different concretes. Because the mechanical properties of the different concretes were almost identical, it is not surprising that the beam behaviours were the same. However, due to the more brittle nature of recycled aggregate concrete, the beams using recycled aggregate concrete suffered more extensive damage at failure, as shown in Figure 2.36.



NAC*-1: Natural aggregate concrete; RAC50*-1: 50% Recycled aggregate concrete; RAC100*-1: 100% Recycled aggregate concrete for 0.28% reinforcement ratios while NAC*-2, RAC50*-2: 50% and RAC100*-3: 100% is for a reinforcement ratio of 1.46%

Figure 2.35 Load- mid-span deflection curves of natural and recycled aggregate concrete beams [14]

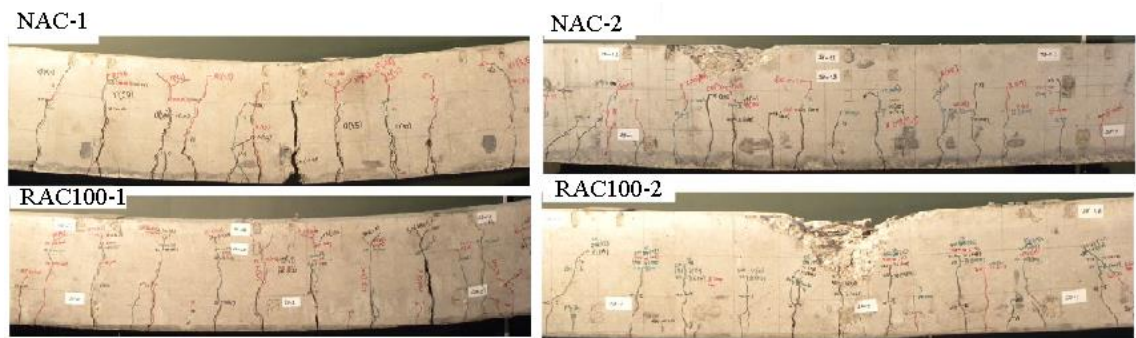
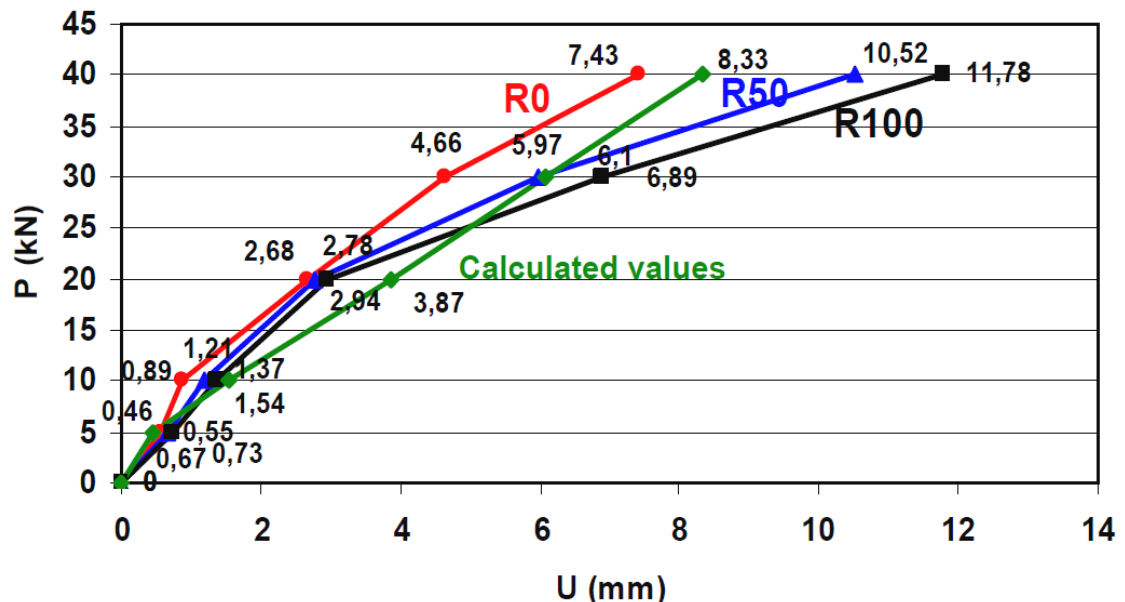


Figure 2.36 Comparison of cracks and failure patterns between natural and recycled aggregate concrete beams with 0.28% and 1.46% reinforcement ratio [14]

[43] also tested three beams of 3m length with a cross section of 150mm width and 250mm depth. The beams were reinforced with ribbed reinforcement 3R ϕ 12 in the

lower zone, $2R\emptyset 10\text{mm}$ in the upper zone and with stirrups. The beams were made of natural aggregate concrete (R0), recycled aggregate concrete with 50% and 100% recycled aggregates. The recycled aggregates were obtained from laboratory concrete cubes and precast columns of unknown strength. They were of high quality and free of impurities. The compressive strength of the natural aggregate concrete (R0), 50% recycled aggregates concrete (R50) and 100% recycled aggregates concrete (R100) were 44.2, 47.6 and 48.1 respectively. Figure 2.37 plots their recorded load-deflection curves which indicate that the recycled aggregate concrete beams exhibited the same deflection at the elastic stage. Again, because the recycled aggregate concrete was made to have the same strength as the natural aggregate concrete (R0), all beams attained the same bending resistance irrespective of the amount of recycled aggregates.

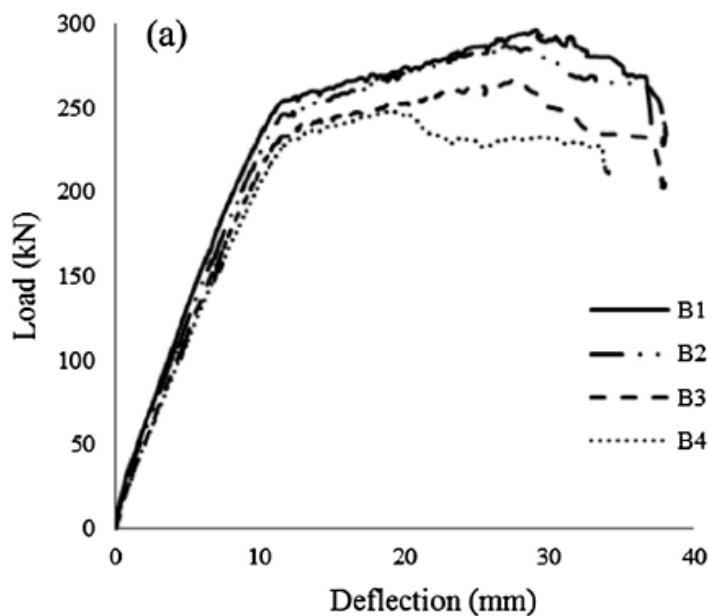


*R0, R50 and R100- Concrete made with 0%, 50% and 100% of recycled aggregate.*the calculated values were for R0.

Figure 2.37 Comparison of experimental/analytical load-deflection curves of all test beams [43]

If recycled aggregate concrete has lower mechanical properties than concrete with natural aggregates and replaces concrete with natural aggregates entirely, the flexural

behaviour of the structure would degrade, as expected. [96] conducted experiments on twelve self-consolidated and vibrated reinforced rubberized concrete beams in bending. Crumb rubbers at different concentrations (0%, 5%, 15% and 25%) were used to replace the sand in volume. The compressive strength of concrete with 0%, 5%, 15% and 25% of crumb rubbers is 65.61MPa, 58.44MPa, 48.35MPa and 38.35MPa respectively. All test beams had an identical cross-sectional area of 250 mm by 250 mm, with a total length of 2440 mm, an effective span and depth of 2040 mm, and 197.5 mm. The longitudinal tension reinforcement ratio was kept constant at 2.03%, which consisted of two 25-mm diameter steel bars having a clear concrete cover of 40 mm. The shear span-to-depth ratio for all beams is 3.44. The shear reinforcement consisted of 10- diameter closed stirrups spaced at 155 mm, with a constant clear cover of 30 mm. Figure 2.38 shows some deteriorations in the flexural behaviour of the beams using recycled aggregate concrete (increased deflections, reduced peak loads).



Note: B1*-Natural aggregate concrete, B2*-concrete with 5% crumb rubber, B3*-concrete with 15% crumb rubber, B4*- Concrete with 25% crumb rubber.

Figure 2.38 Load-deflection plots of reinforced concrete beams with different crumb rubber content [96].

In summary, if a reinforced concrete beam is made entirely of recycled concrete comprised of either recycled aggregates or crumb rubber, its structural performance

(deflections, load carrying capacity) will suffer loss compared to a beam made with natural aggregate concrete due to its lower strength. If the recycled concrete beams are required to achieve the same load carrying capacity as the natural aggregate concrete beams, then the recycled concrete should have the same strength as the natural aggregate concrete by adding different admixtures or increasing cement content, which would incur additional costs.

2.6.1 Flexural design of reinforced concrete beams

In unconfined reinforced concrete beams, failure of the compressive concrete is usually brittle and so the design of reinforced concrete beams is based on tension control (under reinforced) according to Eurocode 2[113]. The basic assumptions made in reinforced concrete design are: perfect bond between reinforcement and concrete, plain section remaining plane, and ignoring the tensile strength of concrete. Figure 2.39 indicates a reinforced concrete section and the associated strain and stress distributions at the maximum bending resistance of the cross-section.

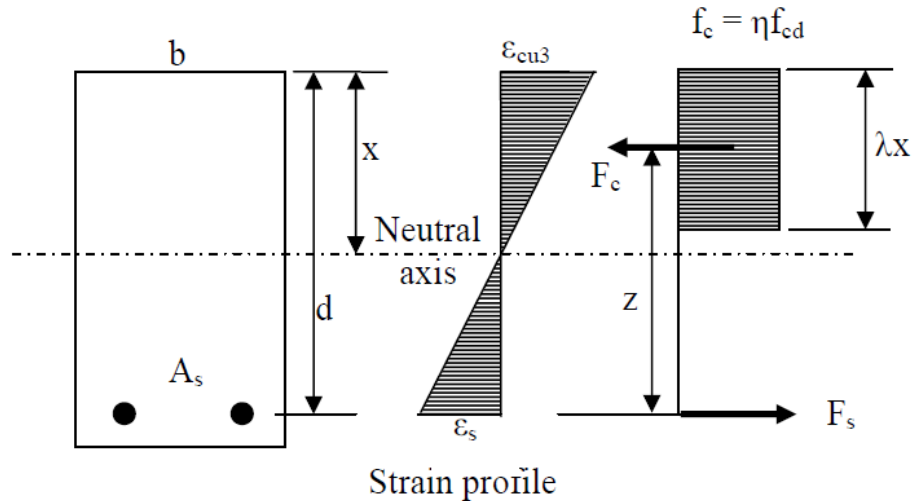


Figure 2.39 Singly reinforced rectangular beam section subject to bending [113]

For equilibrium purposes, the forces acting on the section must balance.

$$F_c = F_s \dots\dots\dots 2.1$$

Where ; $F_c = \lambda X b f_c$ and $F_s = A_s f_s$

F_c = force in concrete under compression ; F_s = Force in steel

λ = the equivalent stress block height.

The value of the equivalent rectangular stress block λ is taken as 0.85 which shows good agreement with beam test data [114, 115]

X = Neutral axis from the compressive face of the section

η = a factor that defines the effective strength of concrete, to be obtained from;

$$\eta \alpha_{cc} f_{ck} \lambda X b / \gamma_c = A_s f_s / \gamma_s \dots\dots\dots 2.2$$

where;

α_{cc} = coefficient that takes account of the long term effect of concrete strength

γ_c and γ_s are safety factor of steel and concrete respectively.

A_s = Area of steel

2.7 Behaviour of reinforced recycled beams in shear

Researchers [116-123] have studied the behaviour of recycled concrete beams either from recycled aggregates or crumb rubber under shear.[117] carried out tests on 12 full scale beams made with recycled aggregate and natural aggregate concrete respectively, comprising different longitudinal reinforcement ratios (1.27%, 2.03% and 2.71%). All beams tested had a rectangular cross section with a width of 300 mm, a height of 460 mm, a length of 4300 mm, and shear span-to-depth ratios of 3.0. The maximum nominal size of both the natural and recycled aggregates is 25mm but the type and source of aggregates are unknown. The water cement ratio of the natural aggregate and recycled aggregate concrete is kept constant at 0.4. The compressive strength of the natural aggregate concrete and recycled aggregate concrete were 37.2MPa and 30MPa respectively while the splitting tensile strengths were 3.48MPa and 2.55MPa. The observed crack patterns of recycled aggregate and natural aggregate concrete beams were identical as shown in Figure 2.40 with the same reinforcement ratio.

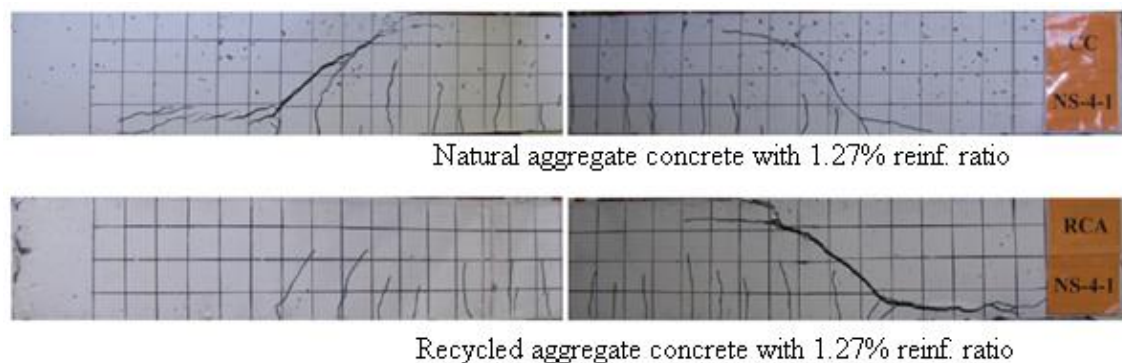
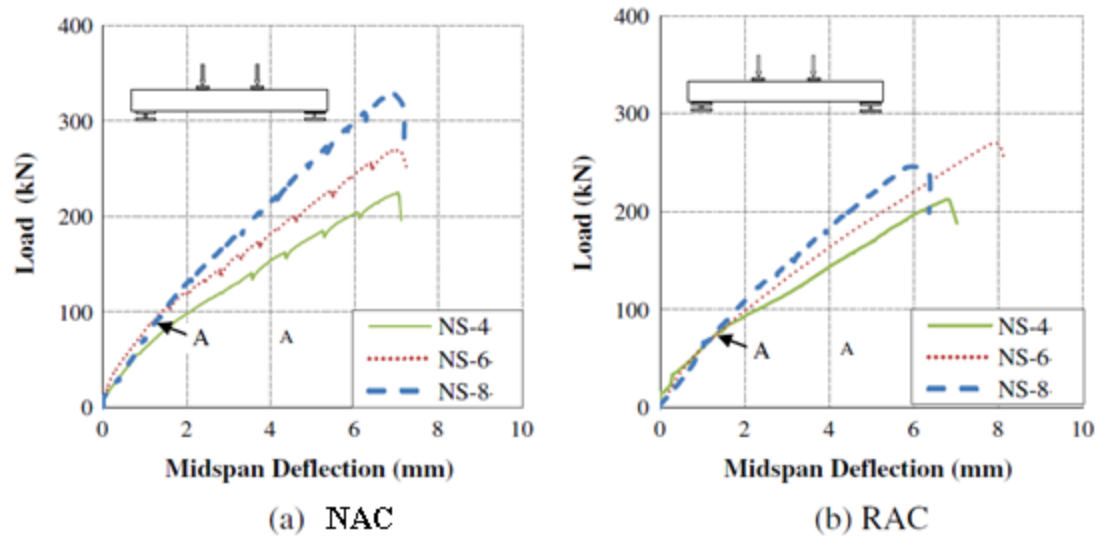


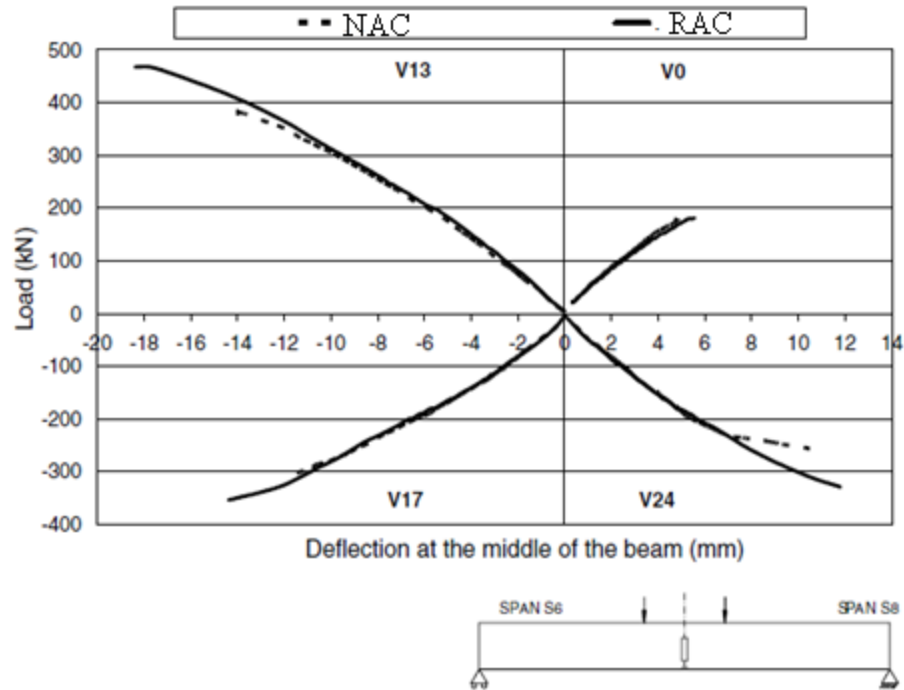
Figure 2.40 Crack patterns of recycled aggregate concrete beams in shear compared to natural aggregate concrete beams with the same longitudinal reinforcement ratio [117]



NS-4, NS-6 and NS-8 are reinforcement ratios 1.27%, 2.03% and 2.715 respectively.

Figure 2.41 Load-deflection curves of recycled aggregate concrete beams compared to natural aggregate concrete beams with the same longitudinal reinforcement ratio [117]

For beams with 2.71% and 1.27% reinforcement ratio, the recycled aggregate concrete (RAC) beams had shear capacities of 24.2% and 4.4% lower than those of the natural aggregate concrete beams respectively, due to the lower strengths of the RAC compared to the natural aggregate concrete as shown in Figure 2.41. In contrast, when RAC has the same strength as the natural aggregate concrete, as in the tests of [116], the beams with RAC would behave almost identically as the NAC beams in shear, as shown in the results in Figure 2.42. The compressive strengths of natural aggregate concrete (NAC) and recycled aggregate concrete (RAC) for test series V0 were 40.2MPa and 39.56MPa, 37.66MPa and 40.6MPa respectively for test series V13, 39.08MPa and 41.49MPa for test series V17 and 39.16MPa and 39.23MPa respectively for test series V24. The beams are rectangular cross sections with 350 mm (depth) by 200 mm (width) and were tested with a shear span-to-depth of 3.3. The reinforcement ratios in the transverse direction for V0, V13, V17 and V24 are 0%, 0.22%, 0.17% and 0.12% respectively. Figure 2.42 reveals nearly the same shear resistances for both the RAC beams and the NAC beams without shear reinforcement.

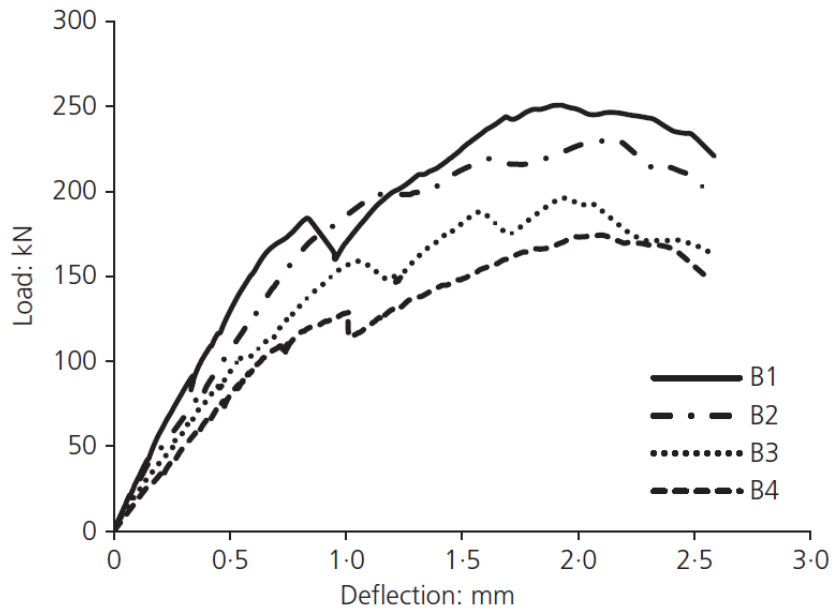


*V0- No web reinforcement; *V13- 0.22% Web reinforcement ratio at 130mm/c; *V17- 0.17% Web reinforcement ratio at 170mm/c; *V24- 0.12% Web reinforcement ratio at 120mm/c

Figure 2.42 Mid span deflections of the beam with different amounts of shear reinforcement [116]

[122] investigates the shear capacity of concrete made with crumb rubber ranging from 0 to 25%. The natural aggregate used for this study is 10mm crushed stone with a water absorption rate of 1%. In this study, the fine aggregate was partially replaced by crumb rubber aggregate, which had a maximum size of 4.75 mm, a specific gravity of 0.95 and negligible water absorption. The water cement ratio for all concrete mixes was kept constant at 0.4; however, polycarboxylate super plasticizers were used to meet workability requirements. The compressive strength of natural aggregate concrete (B1) was 65.6MPa and crumb rubber concrete B2, B3B4 for 5%, 15% and 25% of crumb rubber concentration was 58.6MPa, 48.6MPa and 38.4MPa respectively. The beams had a length of 1120mm with a cross sectional dimension of 250mm by 250mm for constant reinforcement ratio of 0.02%. The shear span-to-depth ratio was kept constant at 2.2 for all beams. All beams were designed to fail in shear by omitting shear links along the

shear span length. It was observed that the beams with crumb rubber reduce stiffness from the load deflection plot in Figure 2.43.



Note: B1*-natural aggregate concrete, B2*-concrete with 5% crumb rubber, B3*-concrete with 15% crumb rubber, B4*- Concrete with 25% crumb rubber.

Figure 2.43 Shear capacity of beams with respect to crumb rubber content [122]

The shear strength of the beams decreases as the percentage of crumb rubber increases as shown in Figure 2.43. Increasing the percentage of crumb rubber from 0 to 25% reduces the shear load to 30%. This behaviour was attributed to the low concrete strength within the shear region, thereby allowing diagonal cracks to develop at relatively lower loads which eventually lead to failure. The ratio of the experimental to code methods ranges from 1.10 to 1.39 with a mean and standard deviation of 1.25 and 0.10 respectively as shown in Figure 2.44.

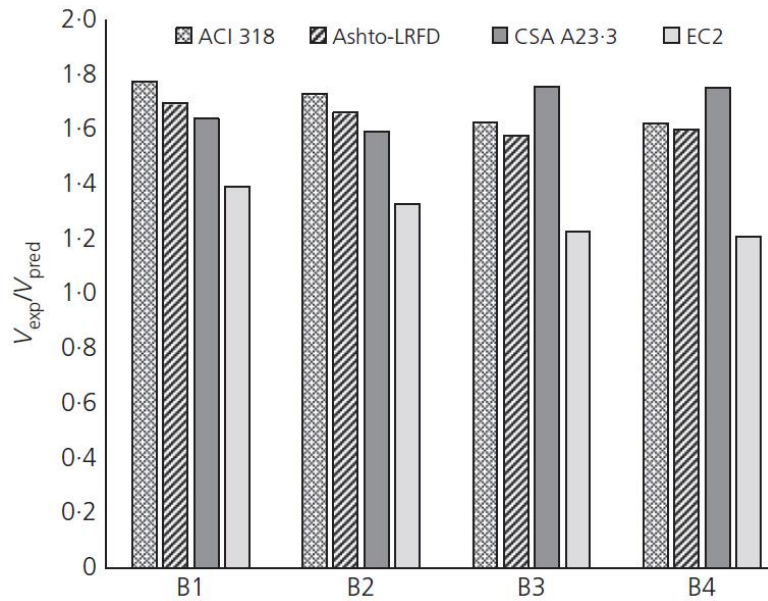


Figure 2.44 Ratio of experimental to shear strength to that of code predicted methods [122].

[121] conducted push-off tests to ascertain the shear transfer mechanism in recycled aggregate concrete beams across cracks compared to that in natural aggregate concrete beams. The maximum nominal size of both the recycled and natural aggregate is 26.5mm with water absorption rates of 5.6% and 0.6% respectively. The natural aggregates are crushed stones of an unknown type and the source of the RA was also not reported. The effects of recycled coarse aggregate (RCA) replacement ratio and the concrete strength on the shear transfer performance were carefully investigated for different replacement levels (30%, 50%, 70% and 100%). The experimental results and data analysis show that the shear transfer mechanism and process across cracks in RAC is largely the same as that in natural aggregate concrete (NAC). Figure 2.45 shows a variation in the ultimate shear loads with replacement ratios of 30%, 50%, 70% and 100% with a similar concrete strength ($f_c \approx 20$ MPa). It can be observed that the ultimate shear load of RAC is nearly the same as that of NAC for replacement ratios below 30% after which it starts decreasing with an increase in RA content. The results concluded that the RA replacement ratio is an important parameter influencing the ultimate shear

load. This can be attributed to the micro- and meso structure feature of RA concrete which can be improved by removing the old attached cement matrix.

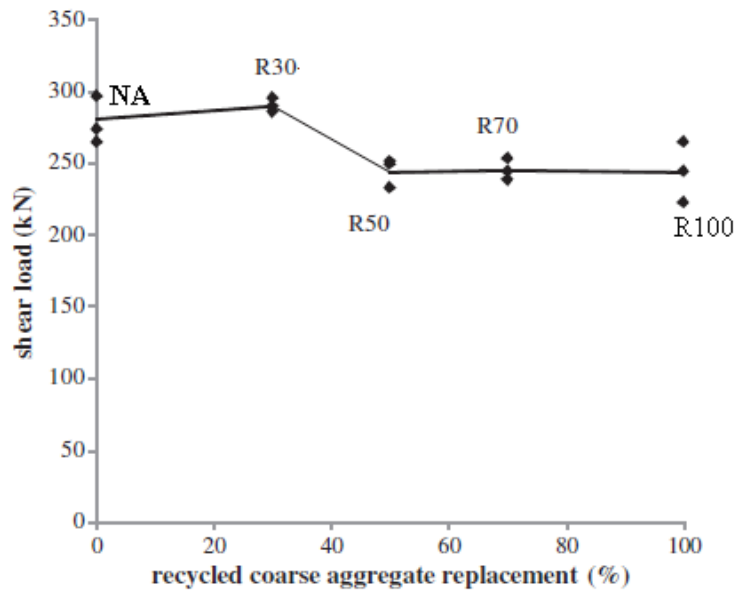


Figure 2.45 Effect of recycled aggregate replacement ratio to shear load [121].

2.7.1 Design methods for shear resistance of reinforced concrete beams

Figure 2.46 illustrates the different contributions to shear resistance of a reinforced concrete beam, including compression contribution (V_{cz}), shear transferred across cracks in the vertical component by interlocked aggregates (V_{av}) and dowel action of the longitudinal reinforcement (V_d). These contributions in general would not be sufficient to prevent shear failure so as to achieve the preferred flexural bending failure mode. Therefore, web or shear reinforcement is required to ensure the full flexural capacity of reinforced concrete beams [124].

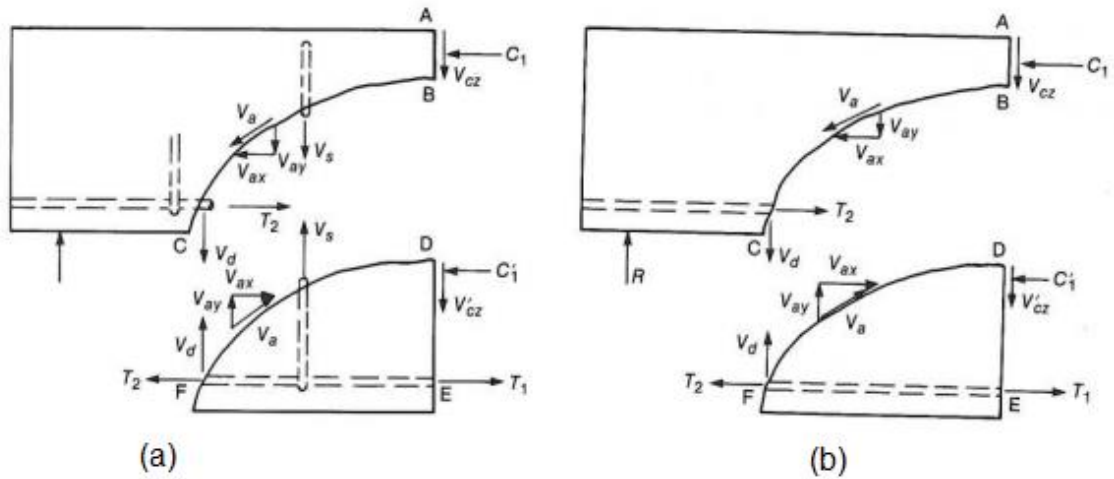
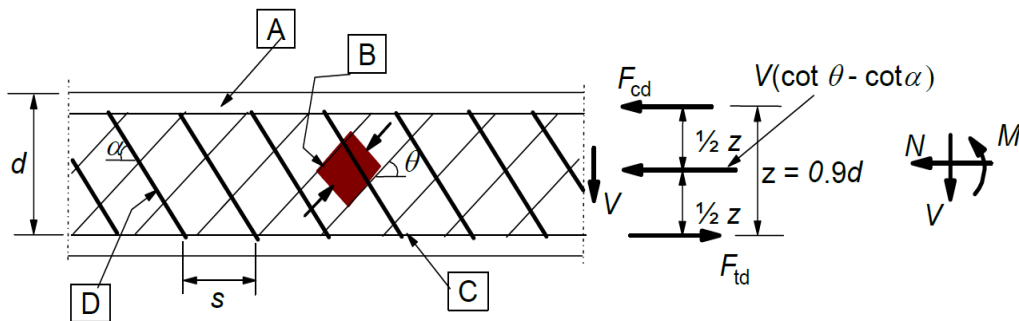


Figure 2.46 Internal forces in a cracked beam section with (a) and without (b) web reinforcements [124]

2.7.2 Eurocode 2 method for shear design

Eurocode 2 adopts a variable strut inclination model to simplify the calculation of shear resistance of reinforced concrete beam sections as shown in Figure 2.47.



[A] - compression chord, [B] - struts, [C] - tensile chord, [D] - shear reinforcement

Figure 2.47 Variable truss inclination model [113]

Where; α = Angle between shear links and axis perpendicular to shear force.

θ = Angle between the concrete compressive strut and beam axis

perpendicular to shear force.

F_{td} = Tensile force in the longitudinal steel bars

F_{cd} = Compressive force in the longitudinal member axis

Z = Lever arm between upper and lower chord members of the truss model

The maximum shear resistance of the compressive strut is given in Equation 2.3:

$$V_{Rd,max} = \frac{0.36b_w d \left(1 - f_{ck}/250\right) f_{ck}}{(\cot\theta + \tan\theta)} \dots\dots\dots 2.3$$

where $V_{Rd,max}$ and f_{ck} are the maximum shear resistance of concrete and characteristic strength of concrete. The range of application for Equation 2.2 for θ is from 22 to 45 degrees.

The EC2 also gives the following empirical expression to calculate the shear resistance of beams without shear reinforcement in Equation 2.4.

$$V_{Rd,c} = \left[0.18k(100\rho f_{ck})^{1/3}\right] b_w d \dots\dots\dots 2.4$$

Where

$$K = \left(1 + \sqrt{\frac{200}{d}}\right) \leq 2.0 \dots\dots\dots 2.5$$

If the shear resistance of a section is lower than the applied shear force, shear links are necessary. Once shear links are required, EC2 assumes that all the shear forces will be resisted by the shear reinforcement without direct contribution of the concrete shear capacity.

The vertical shear reinforcement required to resist an shear force V_{ED} is given in Equation 2.6 from [125].

$$V_{ED} = \frac{A_{sw}}{s} \times 0.78df_{yk} \cot\theta \dots\dots\dots 2.6$$

Where;

V_{ED} = Applied shear force

A_{sw} = Area of shear reinforcement

S = Spacing of shear links.

2.7.3 ACI 318 method for shear design

Usually beams without shear reinforcement fail when inclined cracking occurs hence the shear strength of such beams is taken as the inclined cracking shear. The main parameters affecting the inclined cracking are the shear span to depth ratio (a/d), tensile strength of concrete, longitudinal reinforcement ratio (ρ_w) etc. With the above parameters, different equations were established by different codes to estimate the inclined cracking resistance of reinforced concrete beams without web reinforcements. ACI assumes the shear strength of beams without shear links as the inclined cracking load given in Equation 2.7.

$$V_c = \frac{\sqrt{f_c} b_w d}{6} \dots\dots\dots 2.7$$

The total resistance is obtained from the combination of concrete and that of shear links. The ACI gives the following to calculate the shear resistance from shear reinforcements:

$$V_s = \frac{A_v f_y d}{s} \dots\dots\dots 2.8$$

where

$V_s =$ Resistance from shear reinforcements

A_v and f_y are the area and yield strength of shear reinforcement respectively.

‘S’ is the spacing of the shear reinforcement and ‘d’ is the concrete beam depth.

The total resistance of the section is a combination of the concrete and shear links in ACI unlike the EC2 method where there is no direct contribution of the concrete in resisting shear force. However, shear links are provided when the shear force exceeds half the shear resistance of the concrete.

In summary, the vertical shear links are responsible for resisting the vertical shear force and therefore the low strength recycled concrete used in the tension region of the two-layer beams in our study will not have a serious impact on the shear performance of the proposed beams.

2.8 Interfacial shear stress between concrete layers

If concrete in a reinforced concrete beam is cast at different times, as in the case of this research where two types of concrete are used, it is important that the interface between the two layers of concrete has sufficient strength and stiffness to achieve monolithic behaviour. Monolithic behaviour of a beam under bending in Figure 2.48(a) is where a perfect bond enables the internal forces to be transmitted across the layers and hence the whole beam section deforms as a single member with linear strain distribution as in Figure 2.48(b). If the interface fails and slips occur as shown in Figure 2.48(c), the different beam layers will resist forces independently as shown in Figure 2.48(d) with reduced load carrying capacity [126]. If the horizontal shear force at the interface of two layers exceeds the shear capacity of the interface, then a slip between the two layers occurs.. In design, this scenario is usually avoided by introducing shear ties to resist the shear force at the interface.

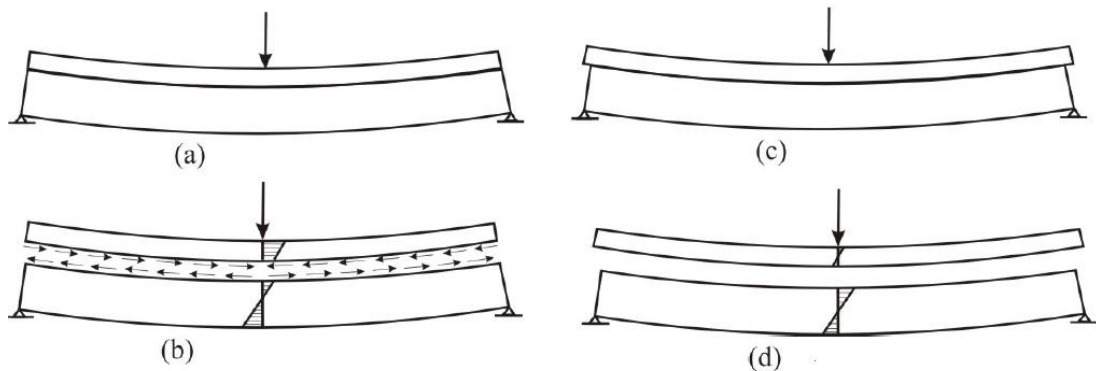


Figure 2.48(a) Composite beam section of two layers (b) Horizontal shear stresses of a composite section (c) Horizontal slip due to interface failure (d) Non composite section under bending due to interface failure [126]

The interfacial shear strength between two layers of concrete is influenced by cohesion, friction and dowel action of rebars crossing the interface [113, 127]. The contribution of cohesion and friction to interfacial bond strength is a function of the nature of the surfaces in terms of their roughness [126, 128-130]. In order to estimate the horizontal

interfacial shear strength of concrete cast at different times, design codes including [125, 127, 131] have recommended design values based on the surface texture of the interfaces [128-130].

[130] was one of the pioneers that proposed a designed expression for horizontal shear strength between concrete layers given in Equation 2.9:

$$V_u = T_u \tan\theta = A_s f_y \tan\theta = \rho f_y \tan\theta = \rho f_y \mu \dots \dots \dots 2.9$$

Equation 2.9 is applicable within the following range: $\rho \leq 0.15\%$; $V_u \leq 5.52 \text{MPa}$;

$$f_c \geq 27.58 \text{Mpa}.$$

f_c = Compressive strength of concrete

where V_u is the maximum shear strength at the interface, f_y is the yield strength of reinforcement, ρ is the reinforcement ratio and $\tan\theta$ or μ is the angle of internal friction or coefficient of friction. The coefficient of friction for monolithic concrete is 1.7; for artificially roughened construction joints, it is taken as 1.4 while it is 0.8 to 1.0 for ordinary construction joints or concrete cast against steel surface.

The method assumes the tensile strength of concrete is zero and as such, the reinforcement crossing the interface resists all the tensile stresses as shown in Figure 2.49. As the concrete layers slide against each other under external force followed by the opening of cracks, the reinforcement will be tensioned, thereby inducing compressive stresses on the concrete interface. This achieves frictional resistance along the interface due to the induced compressive stresses on the concrete

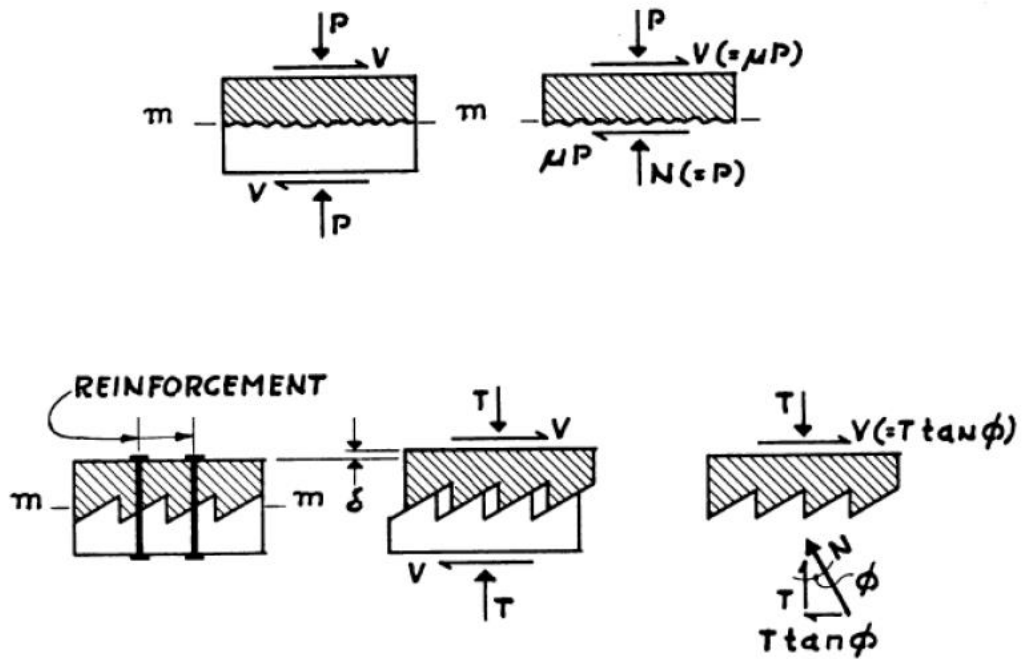


Figure 2.49 Shear friction hypothesis [130]

Eurocode 2 [125]

In Eurocode 2, the interfacial shear strength between two concrete layers of different surface roughness is calculated as follows:

$$V_{Rdi} = C f_{ctd} + \mu \sigma_n + \rho f_{yd} (\mu \sin \alpha + \cos \alpha) \leq 0.5 V f_{cd} \dots \dots \dots 2.10$$

where c and μ are coefficient of cohesion and frictions; σ_n is the external normal stress acting on the interface. f_{ctd} is the design tensile strength of the concrete. ρ and f_{yd} are the ratio and yield strength of the reinforcement crossing the interface. α is the angle between the shear reinforcement and the shear plane of the interface. V and f_{cd} are the strength reduction factor and design compressive strength of concrete. If the applied maximum horizontal shear stress is less than the resistance from mechanical bond (cohesion) of the interface, shear reinforcement is not required.

The proposed [127] expression for calculating the horizontal shear strength of concrete on concrete interface is based on the friction theory of [130]. However, ACI 318 introduces the orientation of shear reinforcement crossing the interface as shown in Figure 2.50. Consequently, the interfacial shear strength is calculated using the following Equation 2.11:

$$V_n = \rho f_{yd} (\mu \sin \alpha + \cos \alpha) \dots \dots \dots 2.11$$

Where μ is the coefficient of friction and ρ is the reinforcement ratio while f_{yd} is the designed yield strength of steel.

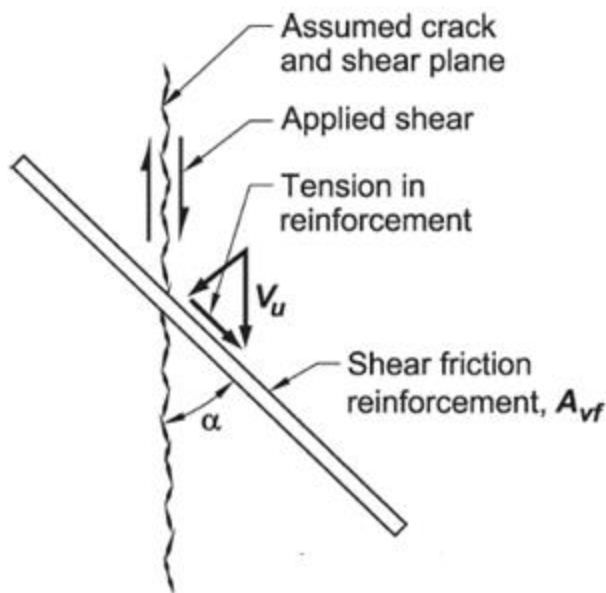


Figure 2.50 Inclined shear friction of reinforcement [127]

2.8.1 Methods of checking horizontal shear stress of two-layer interface.

There are several other methods of estimating horizontal shear stress at the interface of a two-layer section. The most common methods are;

2.8.1.1 Global force equilibrium from compressive and tensile forces.

Here, the horizontal shear stresses are estimated from changes in the compressive or tensile force of any segment of the beam section as shown in Figure 2.51 and this procedure is adopted in [127, 132].

The horizontal interfacial force which is the difference in tensile force is given in Equation 2.12 and the shear stress is obtained by dividing the horizontal force by the interface area in Equation 2.13.

$$V_h = T_1 - T_2 \dots \dots \dots 2.12$$

$$v_h = \frac{T_1 - T_2}{(l \times b_v)} \dots \dots \dots 2.13$$

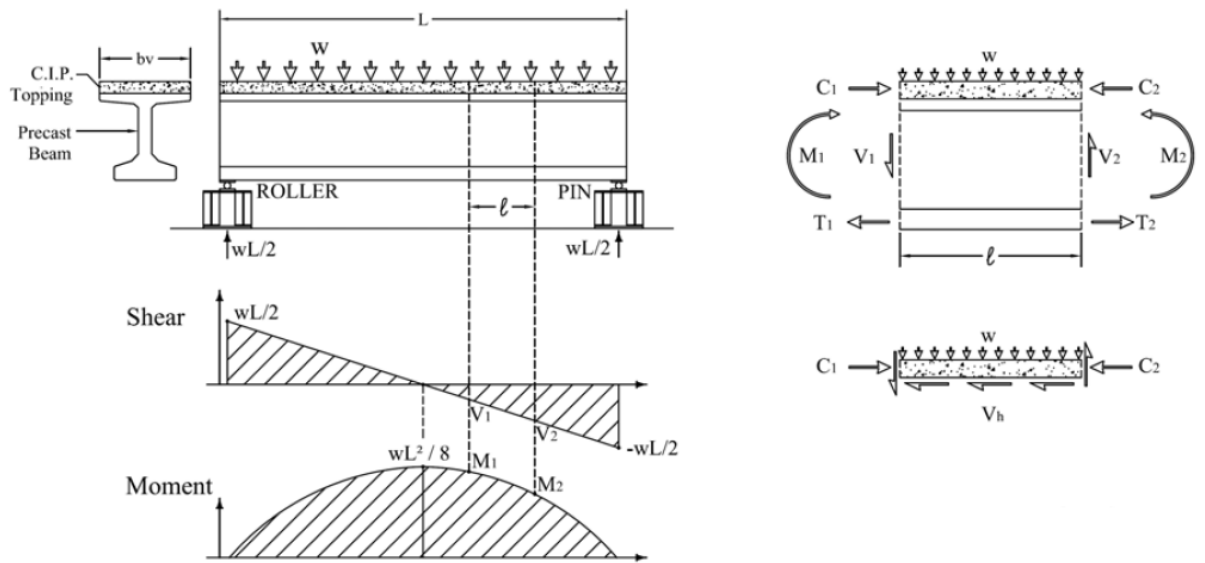


Figure 2.51 Interfacial shear stresses in a simply supported beam under transverse load

V_h = Horizontal shear force in segment 1 – 2 of the beam interface

T_1 = Tensile force at point 1

T_2 = Tensile force at point 2

l = Interface length between point 1 and 2

b_v = Width of the interface between the beam layer

v_h = Horizontal shear stress at interface 1 and 2

This design method assumes that the interfacial shear resistance within the segment can achieve “plastic” behaviour so that the same interfacial shear resistance can be developed along the entire segment length. However, the codes do not specify an appropriate segment length (l above). Also, the results of existing studies on interfacial shear resistance indicate brittle behaviour. Therefore, it may not be safe to assume “plastic” behaviour. Instead, the maximum interfacial shear stress should be checked not to exceed the interfacial shear resistance.

2.8.1.2 Simplified elastic beam behaviour

In this case, the beam section uses the flexural beam theory to equate the horizontal shear force to the vertical shear as shown in Figure 2.52 and Equation 2.14. This method is also adopted by Eurocode 2 and AASTHTO.

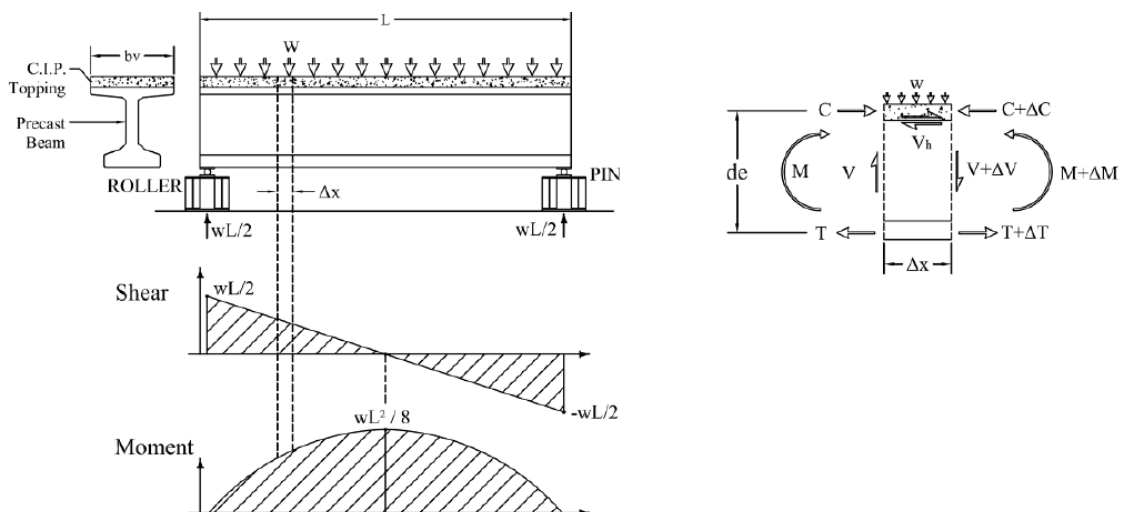


Figure 2.52 Horizontal shear stress based on elastic beam behaviour

From Figure 2.52, for an infinitesimal length ΔX ,

$$\Delta M = V \times \Delta X \quad ; \quad \Delta M = d_e \times \Delta C$$

Where $\Delta C = V_h$

$$V_h(\text{shear force}) = \frac{V \times \Delta X}{d_e}$$

$$v_h(\text{shear stress}) = \frac{V}{b_v \times d_e} \dots \dots \dots 2.14$$

Where;

v_h = Horizontal shear stress

V = Vertical shear force

b_v = Interface width between the section two layers

d_e = Effective depth of the full two layer section

In this research, the interface is between a layer of natural aggregate concrete and a layer of concrete using recycled aggregates with or without rubber. There is no data regarding this type of interface. Therefore, our research will provide some experimental data and use the experimental results to assess whether interfacial shear failure would present an issue in two-layer beams and if so, what the implications are in terms of the increased use of shear reinforcement.

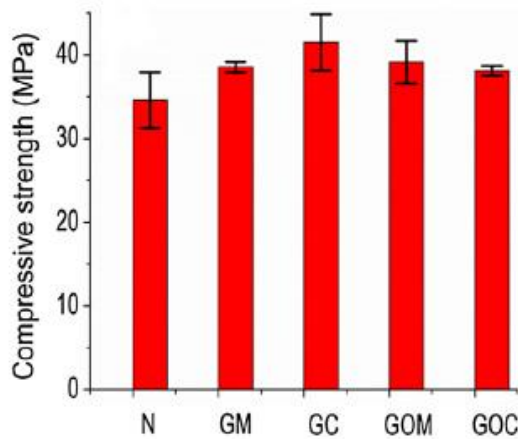
2.9 Influence of graphene on concrete mix

Due to the high demand of concrete, many research studies have focused on increasing concrete material performance. In order to truly remove the issues of concrete (prone to cracking, quasi brittle nature, low toughness etc.) as a composite material, a thorough

research study at the nanoscale needs to be conducted as most of the issues in concrete can be traced to the chemical and mechanical defects in cement structure as the binding material. The unique physical and chemical properties of the nanomaterials render them the most efficient way of enhancing the internal matrix of concrete. Nanomaterials consisting of high surface to volume ratio such as carbon nanotube, nano-silica, titanium oxide etc. are used as additives to enhance the microstructure of cement matrix [133-135]. Despite the issues in its dispersion and cost, the nanoparticles have the potential of producing a stronger and more durable construction material. The most recent discovered nanomaterial is graphene which can also be used as an additive in cementitious materials. Graphene differs from other nanomaterials because of the atom thick-sp² bonded 2D structure. Due to its atomic structure, the graphene nanomaterial exhibits some unique properties such as super high surface area, ultrahigh tensile strength and elastic modulus, excellent thermal, electrical and optical conductivity [136-138].

[46] conducted research into the effect of graphene size and graphene oxides on the performance of cement matrix, using two graphene sizes of 6-8 μ m and 2 μ m thickness classified as GM and GC respectively. Nitric acid was used in this study to convert GM and GC to their respective oxides GOM and GOC respectively. This study used 0.1% weight loading of graphene (as a ratio of the cement weight) as additives. The composition of the reference cement matrix was not reported but Type 1 Portland cement and sand of unknown size was used for this study. Figure 2.53 shows that the compressive strength of concrete is improved by 11.5%, 19.9%, 13.2% and 10.2% for specimens GM, GC, GOM and GOC respectively compared to the concrete without graphene additives. The size of the test sample for compressive strength is not reported in this study. The GC graphene particles with smaller thickness gain twice the strength of the GM with a larger thickness ranging from 6-8 μ m as shown in Figure 2.53. This is attributed to the larger specific surface area of GM compared to GC. Also the increase in the standard deviation of the GC specimens may be attributed to the proper distribution of the graphene particles in the concrete mix. Deterioration tests were also conducted by immersing all specimens into ammonium nitrate solution with 15%

concentration after a 28-day standard curing in order to examine their resistance to chemical attacks. Figure 2.53 shows a decrease in strength with respect to the duration of the chemical attack. The strength decreases in the concretes with GM, GC, GOM and GOC are 26%, 21%, 22% and 21% respectively. The slower rate of strength decrease compared to the normal mix shows that graphene has the potential to decelerate the effect of chemical attack on cementitious material. This finding is consistent with the works of [139]



N*-Natural aggregate concrete without graphene additives.

Figure 2.53 Compressive strength of concrete with graphene and graphene oxides compared to reference concrete [46].

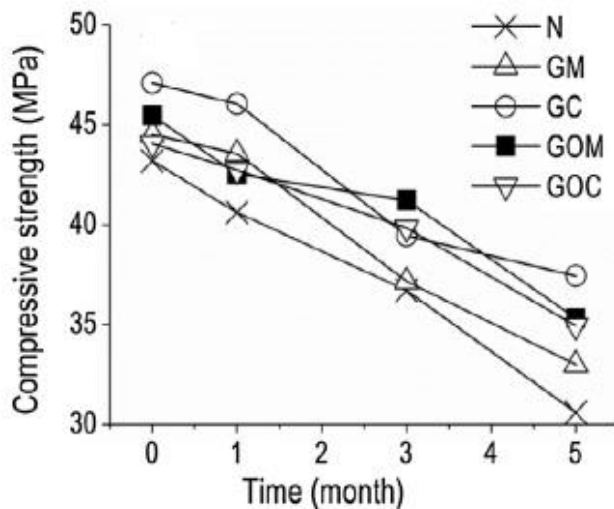


Figure 2.54 Residual strength with respect to the duration of chemical attack [46].

[139] also conducted some tests to investigate the effects of graphene on water penetration depth, chloride diffusion coefficient and chloride migration. 0%, 2.5%, 5% and 7.5% of graphene nanoparticles of cement weight were added into the cement matrix. Ordinary Portland cement and natural sand with density of 2.65 (saturated surface dry) and fineness modulus of 2.95 were used for this study. The mix composition involves different concentration of graphene (GNT) and super plasticizers (SP) of cement weight (1.25GNP+1.25SP, 5.0GNT+2.5SP and 7.5GNT +3.75SP) as presented in Figure 2.55. The GNT and SP prefix stands for the concentration of graphene and super plasticizer of cement weight in the mix. However, the mix composition of the reference cement matrix was not reported. The test results reveal that an addition of 2.5% of graphene in the cement matrix decreased the water penetration depth, chloride diffusion coefficient and chloride migration by 64%, 70% and 31% respectively. The decrease in water penetration and ion ingress can be attributed to a reduction in the critical pore diameter to about 30%. Water penetration decreased with an increasing the amount of graphene in the cement matrix but started to increase when the concentration reached 7.5% as shown in Figure 2.55. This may be attributed to non-uniform dispersion of graphene in the cement matrix when the concentration was high, thereby causing clustering of the graphene and eventually compromising the blocking efficiency of the water ingress.

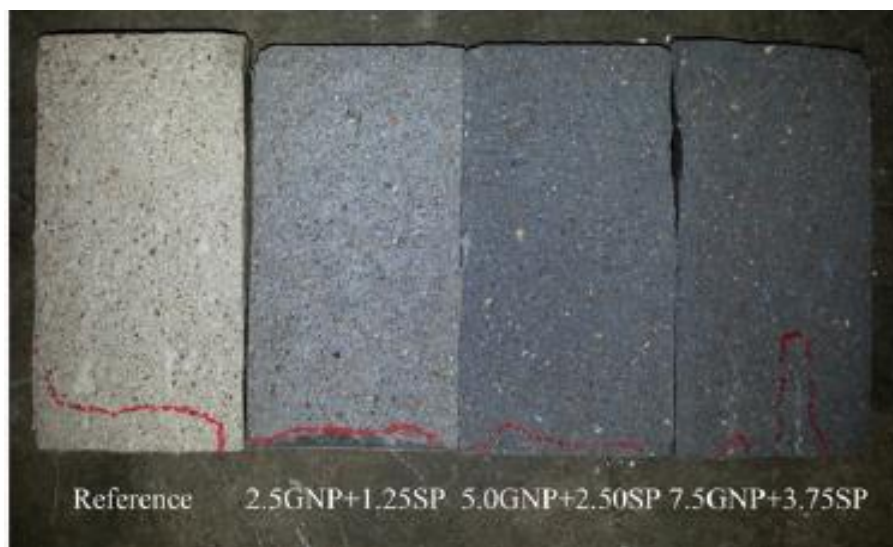


Figure 2.55 Result of water permeability test for cement matrix [139].

A limited amount of work has been conducted on the effects of graphene on concrete [45, 140], unlike with cement matrix which has been extensively researched. [45] conducted tests to investigate the effects of surfactant functionalized graphene (FG), industrial graphene (IG) and ultrathin graphene flakes (UTGs) on concrete. However, the composition of the constituent materials (cement, water, sand and coarse aggregates) of the natural aggregate concrete was not reported in this study. Therefore, only qualitative conclusions can be drawn from these studies. Nevertheless, the review of this section can be used to demonstrate the feasibility of using graphene to enhance the mechanical properties of concrete. Figure 2.56(a) reveals that graphene in concrete increased compressive strength up to 146%. However, the concrete with UTGs had a compressive strength lower than the reference concrete. This is due to the fact that the 24um thickness ultrathin graphene (UTGs) hinders the hydration reaction, thereby preventing the interlocking of cement crystals.

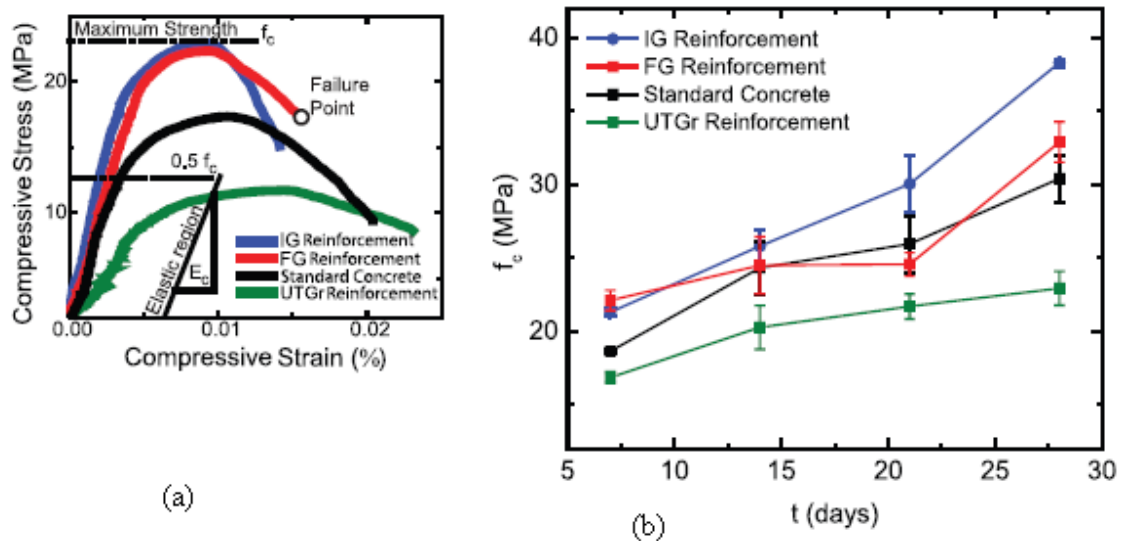


Figure 2.56(a) Stress strain plot of concrete and graphene reinforced concrete (b) strength of concrete over time compared with graphene reinforced concrete.

The compressive strength of graphene reinforced concrete increases with an increase in curing time as shown in Figure 2.56(b). The IG and FG reinforced concretes developed higher strengths than the standard (reference) concrete for 7 and 28 days of curing. The optimal IG concentration in concrete was found to be 0.7g L^{-1} which increased the

elastic modulus and compressive strength by 80.5% and 146% respectively as shown in Figure 2.57. The optimal FG was found to be 0.59g L^{-1} . The significant variations in the mechanical properties of the optimized concentrations are likely due to the non-uniform distribution of graphene in the concrete mix. The reduction in elastic modulus at graphene concentration beyond 0.4g L^{-1} and the sudden increase from 0.6g L^{-1} in Figure 2.57 is unclear but may be a result of the mixing procedure of constituent materials and dispersion of graphene.

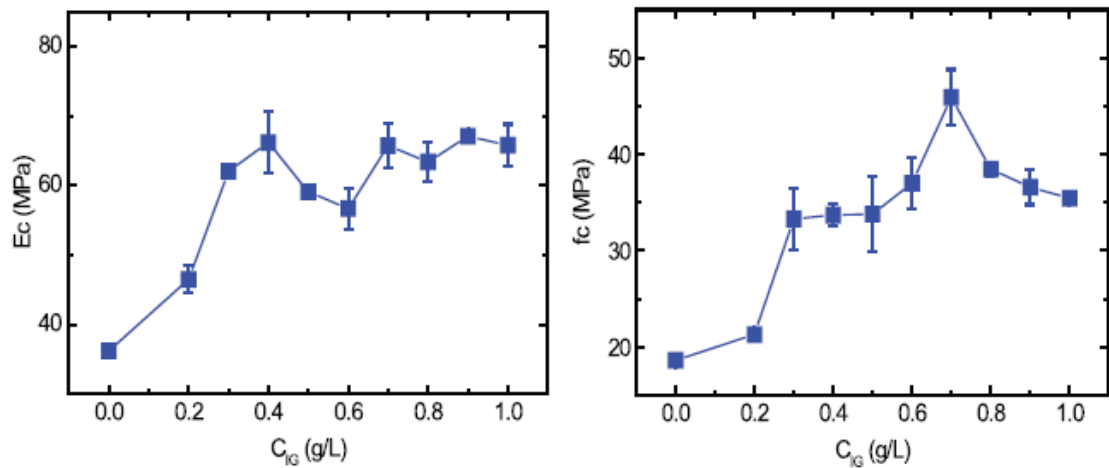


Figure 2.57 Effect of graphene concentration of the strength and elastic modulus of concrete.

It was also recorded that incorporating graphene into concrete to a concentration of 0.8g L^{-1} decreased water penetration by about 400% as shown in Figure 2.58.

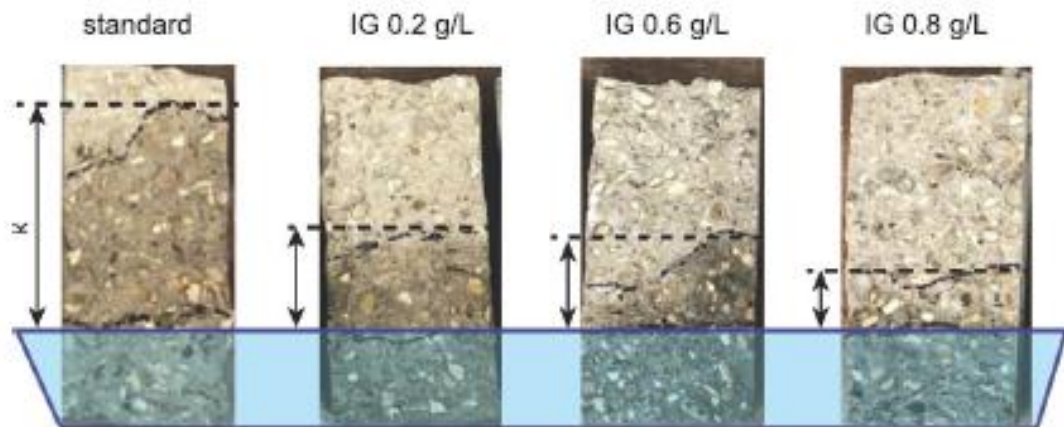


Figure 2.58 Water permeability of graphene reinforced concrete at different concentrations for a 7- day test.

The specimens in Figure 2.58 were cured for seven days and fully dried and immersed in water at an appropriate height. The black dotted lines indicate the level at which water infiltrated the specimen after a seven-day immersion. Figure 2.58 also reveal that the decrease in water infiltration of the graphene reinforced concrete increases with graphene concentration. This reveals that the graphene enhanced the hydration crystal formations and the high surface of graphene formed a denser network of cement interlock, thereby enhancing not just the mechanical properties but also acting as a water infiltration barrier. This behaviour is very beneficial in terms of durability of the concrete over time.

[140] also conducted a study into the effects of including graphene oxide (GO) nanosheets on the mechanical properties of concrete. Figure 2.59 presents a summary of their results, showing the compressive strength of concrete with GO nanosheet contents of 0.00%, 0.02%, 0.03%, 0.04%, 0.06%, and 0.08% by weight of the cement for a water–cement ratio of 0.5. The total water content was 168 kg/m³, which included the mixing water and the GO nanosheet water dispersion solution. The coarse aggregates (CA) used were crushed quartz with a size range from 5 mm to 20 mm. The GO nanosheets had a length to width ratio of 2-10 and a thickness of 1-1.5nm. Figure 2.59 shows the results of the compressive strength tests for the ages of 7, 14, and 28 days.

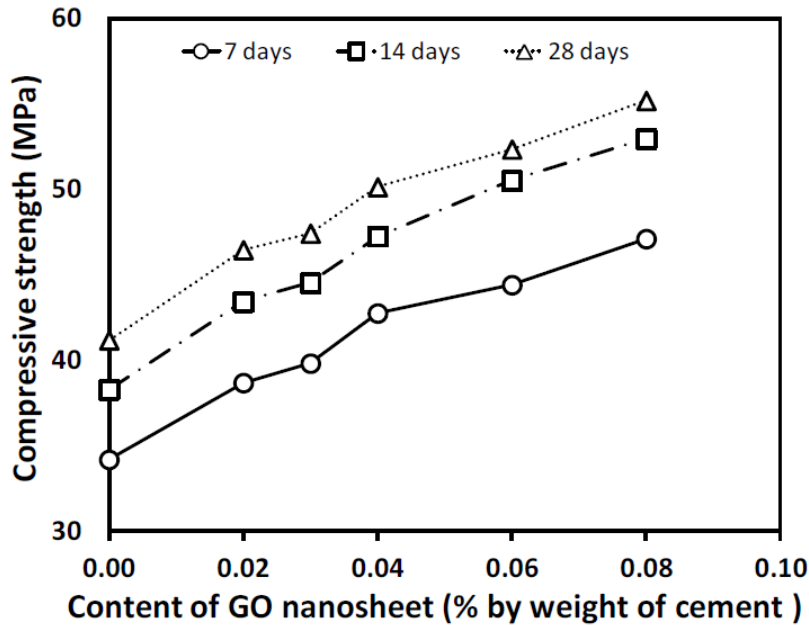


Figure 2.59: Compressive strength of concrete with varying graphene oxide (GO) content at different times of testing [140]

The results indicate that the GO nanosheets enhance the compressive strength of concrete at all the concentration levels considered. When the concentration of GO nanosheets increased from 0.02% to 0.08%, the 28-day compressive strength increased from 46.47 MPa to 55.22 MPa, representing an increase of 12.84% to 34.08% when compared to the reference concrete without GO nanosheets.

In summary, the extents of using graphene to enhance the mechanical properties of concrete differ among the different studies. This is because the mechanical properties of concrete are affected by many factors, such as the water-cement ratio, raw material types, complementary materials and admixtures and the graphene dispersion method adopted. Nevertheless, the review indicates that adding a tiny amount of graphene to concrete can bring about considerable increases in the mechanical properties of concrete with natural aggregates. However, no research has been found to investigate the effects of graphene on recycled aggregate concrete.

2.10 Summary

In summary, the review has presented a comprehensive review of mechanical properties of recycled aggregate concrete, bending and shear behaviour of structural elements using recycled aggregate concrete. The main conclusions are:

- (1) Unless methods of enhancement are employed, the compressive strength, splitting tensile strength and Young's modulus of concrete using recycled aggregate in its crushed condition is lower than that of the concrete using natural aggregates, all other conditions being the same.
- (2) The workability of concrete with recycled aggregates and crumb rubbers decreases but can be enhanced by using super plasticizers and adding extra amounts of water.
- (3) Studies revealed that recycled aggregate concrete would not be an issue for bond strength. Therefore, the same anchorage length for deformed reinforcement bars as in concrete using natural aggregates can be used in recycled aggregate concrete
- (4) It is possible to improve the mechanical properties of recycled aggregate concrete and the current methods include admixtures (super plasticizers), extra amounts of cement, addition of fly ash etc. However, these methods are generally costly and complicate onsite activities.
- (5) As an alternative to the above methods of improving the mechanical properties of recycled aggregate concrete, adding a tiny amount of graphene to concrete has been demonstrated to be effective. However, the existing research studies have focused on concrete with natural aggregates.
- (6) The durability of concrete using recycled aggregates and crumb rubbers suffers loss; however, it can be improved by the use of fly ash as a partial replacement for or addition to cement, removal of the attached cement matrix on recycled aggregates and treatment of crumb rubber with NaOH.
- (7) As expected, if recycled aggregate concrete has the same mechanical properties as concrete using natural aggregates, the structural behaviour of concrete structures using recycled aggregate concrete is the same as that using natural aggregate concrete.
- (8) On the other hand, if recycled aggregate concrete has lower mechanical properties and recycled aggregate concrete replaces the concrete using natural aggregates in its entirety, the structural behaviour will suffer, as exhibited by increased deflections (reduced stiffness), lower flexural bending and shear resistances.

Chapter 3

Mechanical properties of recycled concrete

3.1 Introduction

Extensive work has been conducted on recycled aggregates concrete, rubberized concrete as discussed in Chapter 2 but no work was found incorporating both crumb rubber and recycled aggregates in concrete. Also, no studies are currently found on the use of graphene to improve the mechanical properties of recycled concrete. Hence, this chapter will present the following basic properties of natural aggregate concrete (NAC, for comparison), recycled aggregate concrete (RAC) and rubber recycled aggregate concrete (RRAC) in different mix proportions:

- Workability,
- Mechanical properties

- Bond strength of reinforcement and recycled concrete
- Interfacial shear behaviour between layers of concrete
- Effects of graphene solution (size and concentration) on recycled concrete.

3.2 Specification and preparation of constituent materials.

The mechanical properties of concrete in both wet and hardened are greatly influenced by the constituent materials. The raw materials used in this research are:

- CEM 11/B-V 32.5N Portland cement with fly ash complying with [141].
- Natural aggregates: uncrushed quartzite stones with 14mm maximum size and 10mm medium size.
- Uncrushed river sand
- Tap water
- Crumb rubber of 8mm length with aspect ratio of 4 from worn-out vehicle tyres
- Crushed recycled aggregate (RA1) with the maximum size of 28mm and an average size of 10mm.
- Crushed recycled aggregate (RA2) with the maximum size of 18 mm and an average size of 10mm.

The particle size distribution of natural aggregates, recycled aggregates and fine sand based on [142] is shown in

Figure 3.1. Raw data is shown in Table A1 to A4 of Appendix A.

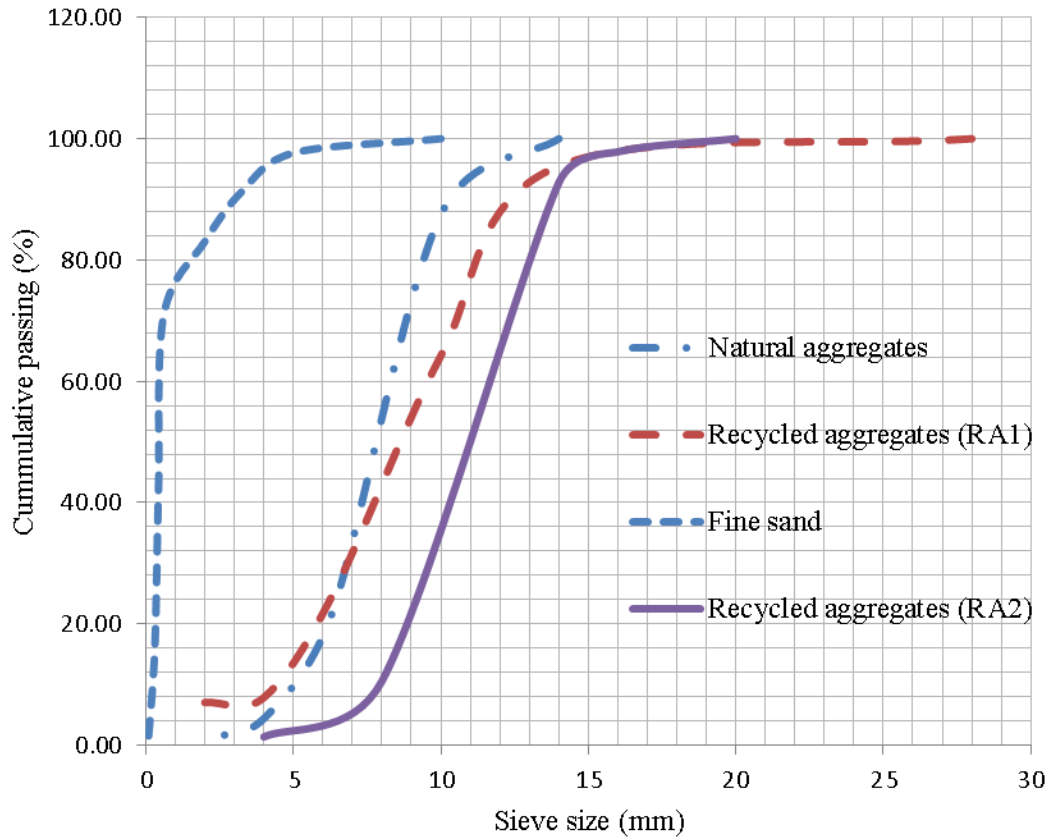


Figure 3.1 Grading of natural aggregates, recycled aggregates and fine sand

The water absorption rates of natural, recycled aggregates RA1 and recycled aggregates RA 2 are shown in Table 3.1. Calculations can be found in Tables A5, A6 and A7 of Appendix A for virgin aggregates, recycled aggregates RA1 and recycled aggregates RA2 respectively.

Table 3.1 Water absorption rate of natural and recycled aggregates

| Type | Apparent particle density | Particle density on oven dry bases | Particle density on saturated and oven dry bases | Water absorption (%) |
|---------------------------|---------------------------|------------------------------------|--|----------------------|
| Natural aggregate | 2.69 | 2.62 | 2.65 | 1.05 |
| Recycled aggregates (RA1) | 2.50 | 2.27 | 2.36 | 4.21 |
| Recycled aggregates (RA2) | 2.61 | 2.27 | 2.40 | 5.77 |

The recycled aggregates used for this research had different impurities as shown in Table 3.2 and were supplied by Offeron Sand and Gravel in Manchester, UK. When building structures are demolished, the reclaiming of recycled aggregates is usually accompanied with tiles, bricks and wooden materials existing on the building. It takes extra efforts to separate recycled aggregates from these impurities, incurring extra cost. The impurities were estimated by randomly taking 1kg weight of three different samples of the recycled aggregates. The samples were initially sieved to measure the weight of dust. The other impurities were carefully separated from the recycled aggregates and weight estimated. The average of the three samples was recorded. It should be noted that high quality recycled aggregates can be obtained in most developed countries without impurities. However, since the purpose of this research is to demonstrate that even the lowest quality of recycled aggregate concrete would not compromise the structural performance of reinforced concrete beams, no attempt was made to obtain high quality and more expensive recycled aggregates.

Table 3.2 Composition of natural and recycled aggregates

| Composition | Proportion |
|-------------------------------|------------|
| Natural aggregates | |
| Quartzite | 79% |
| Sandstone | 6% |
| Basalt | 5% |
| Others | 10% |
| Recycled Aggregates RA1 | |
| Recycled Aggregates | 86.5% |
| Bricks | 8.0% |
| Glass | 3% |
| Others (Dust, rubber strings) | 1% |
| Recycled Aggregates RA2 | |
| Recycled Aggregates | 81% |
| Bricks | 13% |
| Dust | 6% |

The crumb rubber particles used were supplied by SRC Products Ltd, Stockport in the United Kingdom and they were free from wire strings as shown in Figure 3.2. The

crumb rubber particles were not pre-treated before being incorporated into the concrete mix. This was to demonstrate that a lack of elaborate pre-treatment would not adversely affect structural performance. The crumb rubber particles have an average length of 8 mm and 2mm thickness with an aspect ratio of 4.



Figure 3.2 Crumb rubber (8mm length and 2mm thickness) particles from worn-out tyres

3.3 Concrete mixture

An average cylindrical strength of 40MPa concrete was designed as the reference concrete for this research based on the method presented by [143]. The method follows similar principles to those used in Road Note No 4 [144] but not limited to road surfaces. The rationale for the adopted design method is that it covers concrete mixes for workability and strength using Portland cements complying with BS 12 [145] and natural aggregates complying with BS 882 [146]. The mix proportions are also expressed in terms of unit volume of concrete in line with European and American practice. The mix proportion of the reference concrete is shown in Table 3.3. Detailed calculations are presented in Appendix A8. To investigate the mechanical properties of

the recycled concrete (rubber recycled aggregate concrete) in the wet and hardened states, the mix compositions shown in Table 3.4 were adopted. The experimental programme in Table 3.4 allowed the effects of different proportions of recycled aggregates, crumb rubber particles, with water or without super plasticiser, to be systematically investigated.

Table 3.3 Reference concrete composition

| Quantities | Cement(kg) | Water(kg) | W/C ratio | Fine aggregate(kg) | Coarse aggregate(kg) |
|------------|------------|-----------|-----------|--------------------|----------------------|
| Perm3 | 550 | 220 | 0.4 | 626 | 939 |

Table 3.4 Experimental programme

| Specimen Designation | Natural Coarse aggregates (% weight) | Recycled Coarse aggregates (RA1) (% weight) | Crumb rubber (% by RA weight) | Additional water (% weight) | Super plasticizers (1% by cement weight) |
|----------------------|--------------------------------------|---|-------------------------------|-----------------------------|--|
| NAC | 100 | - | - | - | - |
| RAC* | - | 100 | - | - | - |
| RAC | - | 100 | - | 4.21 | - |
| RACSP | - | 100 | - | 4.21 | 1 |
| RRAC5 | - | 95 | 5 | 4.21 | - |
| RRAC10 | - | 90 | 10 | 4.21 | - |
| RRAC15 | - | 85 | 15 | 4.21 | - |
| RRAC20 | - | 80 | 20 | 4.21 | - |
| RRAC5SP | - | 95 | 5 | - | 1 |
| RRAC10SP | - | 90 | 10 | - | 1 |
| RRAC15SP | - | 85 | 15 | - | 1 |
| RRAC20SP | - | 80 | 20 | - | 1 |

NAC- Natural aggregate concrete; RAC- Recycled aggregate concrete with additional water for workability requirement; RAC*- Recycled aggregate concrete without additional water; RACSP- Recycled aggregate concrete with super plasticiser;

RRAC5, RRAC10, RRAC15 and RRAC20- Rubber recycled aggregate concrete with 5, 10, 15 and 20 percent of crumb rubber content respectively of recycled aggregate weight.

RRAC5SP, RRAC10SP, RRAC15SP and RRAC20SP- Rubber recycled aggregate concrete with 5, 10, 15 and 20% respectively of crumb rubber content of recycled aggregate weight. The SP stands for 1% of superplasticizer of cement weight.

The percentages of replacement of recycled aggregates by crumb rubber were carefully selected based on the recommendations made by [24, 30] in order to maintain a substantial proportion of the mechanical properties of the natural aggregate concrete. The two-stage mixing approach recommended by [103] was used in this research. The recycled aggregates and fine sand were incorporated into the concrete mixer and mixed for 60 seconds followed by crumb rubber and 50% of water for another 60 seconds. Cement was then added for another 30 seconds and finally the remaining quantity of water was added in 120 seconds to attain a uniform concrete mix.

All samples were cured for a period of 7, 28 and 100 days in the University of Manchester Concrete Laboratory according to the specifications made by [147]. For each mix, two (2) samples were made for workability tests, three (3) cylinder tests were carried out for compressive strength test, three (3) for tensile strength test, three (3) for reinforcement bond test and three (3) for interfacial shear tests. Further details will be provided in Section 3.5. The fresh mixed concrete was placed in relevant moulds and well compacted by means of a vibration table. After the fresh concrete was properly compacted in moulds, they were left for 24 hours before de-moulding for the curing process to commence.

3.4 Workability of fresh concrete

For each mix, slump tests were carried out and results presented to ascertain the workability of concrete. The workability of all mixes was assessed by means of slump test according to [148]. The concrete was placed in a cone of 300mm in three layers. At each layer, the concrete is compacted with 25 strokes of a tamping rod. After filling and compacting the top layer, the surface of the concrete is struck off by means of sawing and the rolling action of the compacting rod. The mould is then carefully lifted within a

time interval of 2 to 5 seconds. The difference in height between the cone and the highest point of the slumped test in Figure 3.3 is recorded as the slump value (workability) of the concrete in mm. The results in Figure 3.4 and 3.5 show the effects of recycled aggregates and crumb rubber on the workability of concrete.

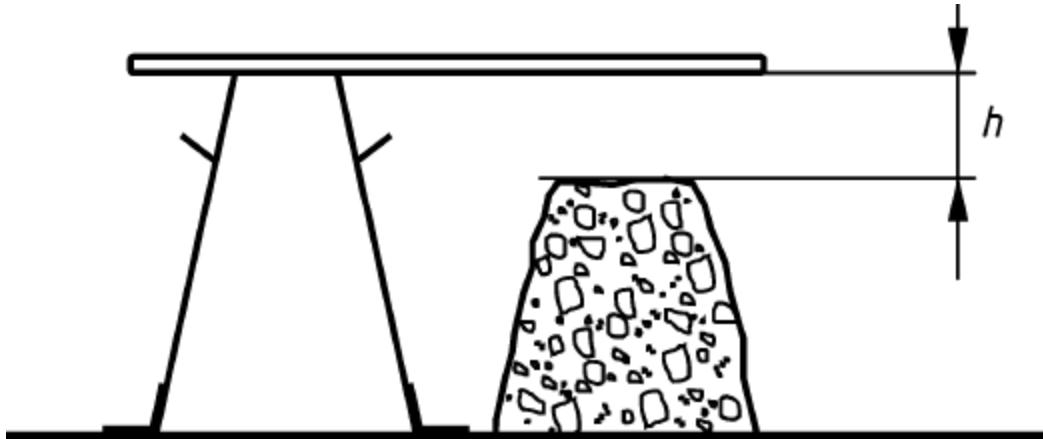
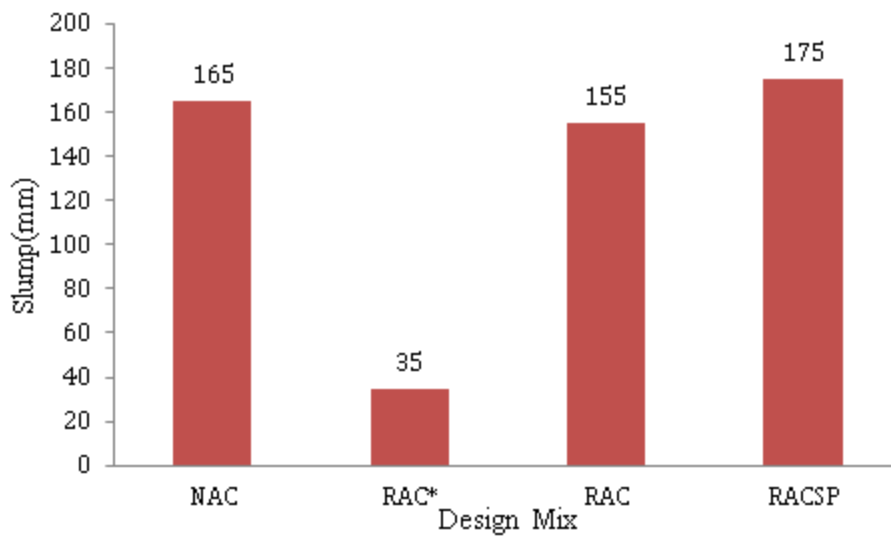
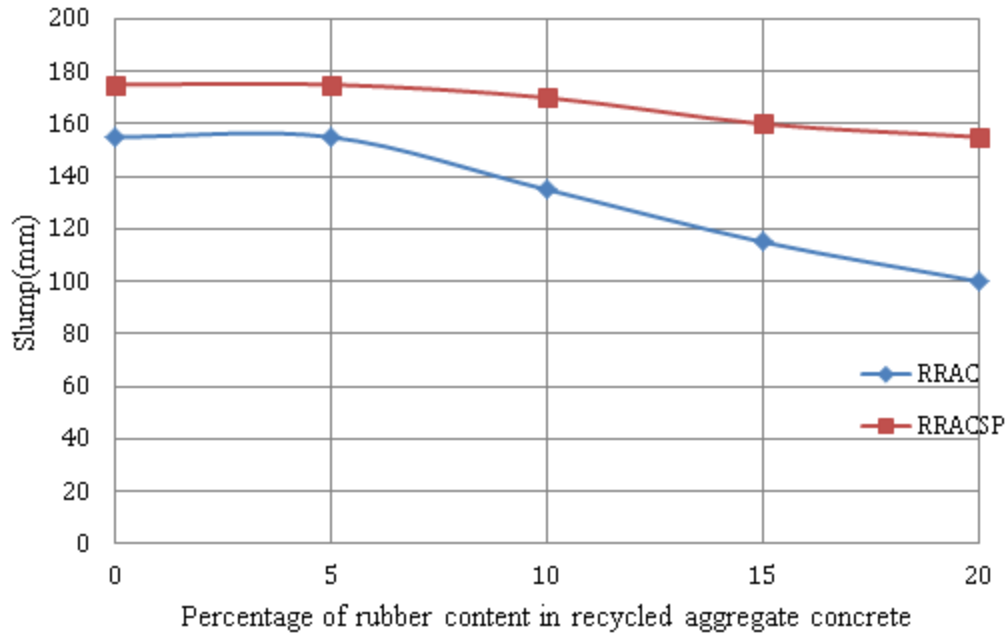


Figure 3.3 Slump measurement [148]



NAC-Natural aggregate concrete mix; RAC*- Recycled aggregate concrete; RAC- Recycled aggregate concrete with extra water; RACSP- Recycled aggregate concrete with super plasticisers

Figure 3.4 Slump of fresh concrete of different mixes.



RRAC-Rubber recycled aggregate concrete with extra water
 RRACSP-Rubber recycled aggregate concrete with super plasticisers

Figure 3.5 Influence of crumb rubber on the workability of recycled aggregate concrete.

Figure 3.4 shows that without additional water or super plasticisers, recycled aggregate concrete (RAC*) suffered a drastic reduction (78.8%) in slump compared to the natural aggregate concrete mix (NAC). This reduction is attributed to the high water absorption rate of coarse recycled aggregates (RA1) which reduced the free water available for lubrication of the concrete constituent materials [8, 40, 59]. The small cracks on the recycled aggregates arising during the crushing process and the attached old cement matrix were the major sources of high rates of water absorption. Figure 3.4 shows that the workability of recycled aggregate concrete was improved to be similar to that of the natural aggregate concrete when extra water or super plasticiser was added to compensate for the water absorbed by the recycled aggregate. The added water was related to the percentage of water absorbed by the recycled aggregates. Unfortunately, the added water caused the concrete strength to decrease as shown in Figure 3.6.

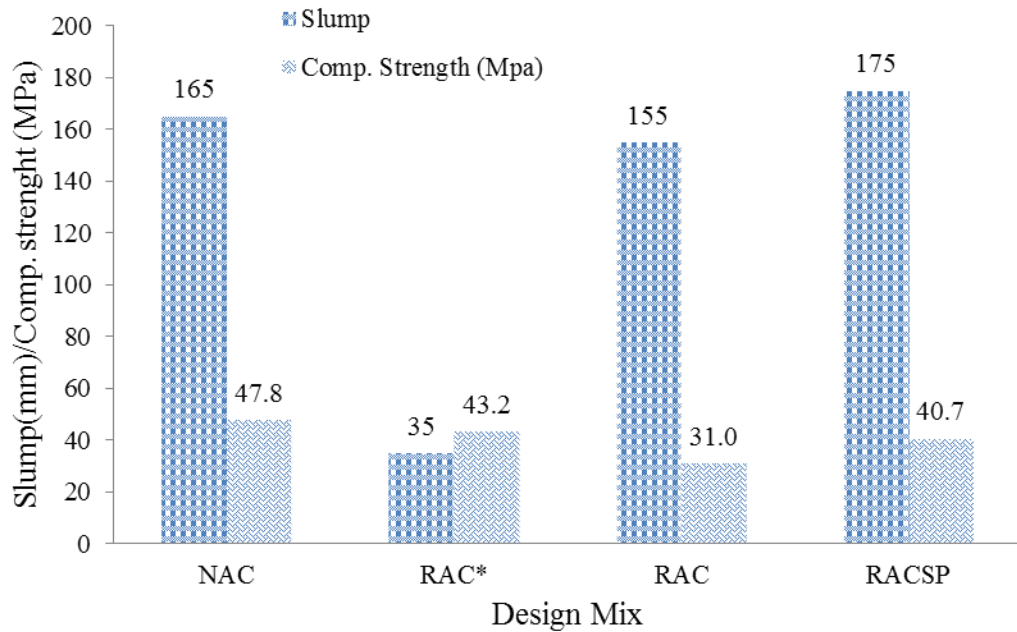


Figure 3.6 Correlation of slump and compressive strength of different mixes.

The strength of recycled aggregate concrete (RAC) with additional free water to enhance workability was 35% lower compared to the natural aggregate concrete. On the other hand, instead of using additional free water to enhance workability, the effects of using super plasticisers to enhance workability on concrete compressive strength were not as severe as that of adding extra water. Figure 3.6 shows that the compressive strength of recycled aggregate concrete mixes with super plasticiser (RACSP) was 31.3% higher than RAC mixes containing extra free water. The results are in line with those of [11].

The results in Figure 3.5 show a reduction in workability of recycled aggregate concrete as the amount of rubber content increases, with and without super plasticisers. This can be attributed to the crumb rubber surface texture and water absorbability of the crumb rubber particles. The observed results are similar to those reported by [30, 36, 52]. There is no significant difference in workability when 5% of the recycled aggregates were replaced with crumb rubber particles in recycled aggregate concrete with and without super plasticisers. A sharp reduction in workability was observed for rubber recycled aggregate without super plasticiser in Figure 3.5 when more than 5% crumb

rubber particles were incorporated into the recycled aggregate concrete, while a more gradual reduction in workability can be observed for recycled aggregate concrete with super plasticiser. This can be attributed to the fact that part of the extra water added to compensate for the high absorption rate of recycled aggregate was taken by the crumb rubber particles, whilst the absorption of super plasticisers by crumb rubber particles were less.

In summary, recycled aggregate concrete with no additional water (RAC*) is not a workable mix because of the low slump value due to the high water absorption rate of recycled aggregates. Adding extra water to compensate for the high rate of recycled aggregate enhances workability, and incorporating crumb rubber reduces workability. On this note, the percentage of crumb rubber in weight should be limited to 15 percent in rubber recycled aggregate concrete (RRAC) to maintain a workable mix. However, this limit could be curtailed by using super plasticisers to enhance workability in place of extra water. Figure 3.5 shows that the rubber recycled aggregate concrete with super plasticisers (RRACSP) maintained a workable mix even with 20 percent of crumb rubber content.

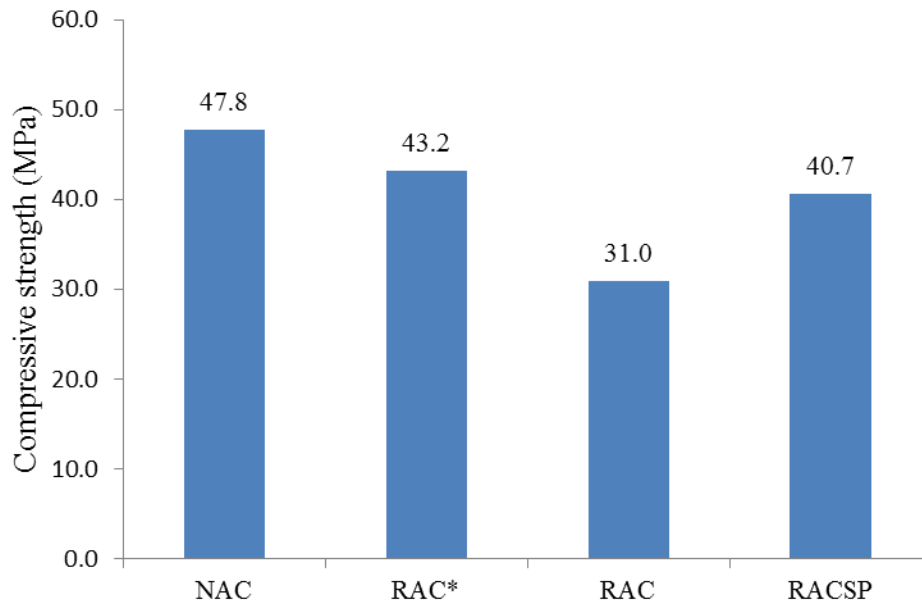
3.5 Properties of hardened concrete

3.5.1 Compressive strength

For each mix, three concrete cubes were tested as per specifications made in [149] and the results presented are the average values for 7, 28 and 90 days of curing. The raw test data are included in Table A9 of Appendix A.

The compressive strength of the concrete made with 100 percent recycled aggregates, but without water or super plasticiser to enhance its workability, was on average 9.6% lower than that of the natural aggregate concrete mix (NAC) as shown in Figure 3.7. Increasing the water- cement ratio of the mix (RAC) to enhance concrete workability resulted in a further reduction in concrete compressive strength of 35%. These results

are similar to those of [9, 69-71]. However, using super plasticisers in the mix (RACSP) instead of extra water, to improve workability, increased the compressive strength of recycled aggregate concrete by 23.8% compared to RAC with extra water, though this was still 14.9% lower than that of the natural aggregate concrete mix (NAC).



NAC-Natural aggregate concrete mix; RAC*- Recycled aggregate concrete; RAC- Recycled aggregate concrete with extra water; RACSP- Recycled aggregate concrete with super plasticisers

Figure 3.7 Comparison of compressive strengths of different concrete mixes

Figures 3.8 and 3.9 show the effects of changing crumb rubber proportion on recycled aggregate concrete at different times for 7 and 28 days of curing. As expected, increasing the percentage of crumb rubber particles reduced the concrete compressive strength. The reduction is more pronounced for recycled aggregate concrete mixes without super plasticisers. Table A10 of Appendix A shows the raw data and the corresponding standard deviations. The variation in results of the 3 samples tested for each specimen in Table A10 of Appendix A may be attributed to differences in the distribution of crumb rubber particles in the concrete samples during casting and vibration of moulds.

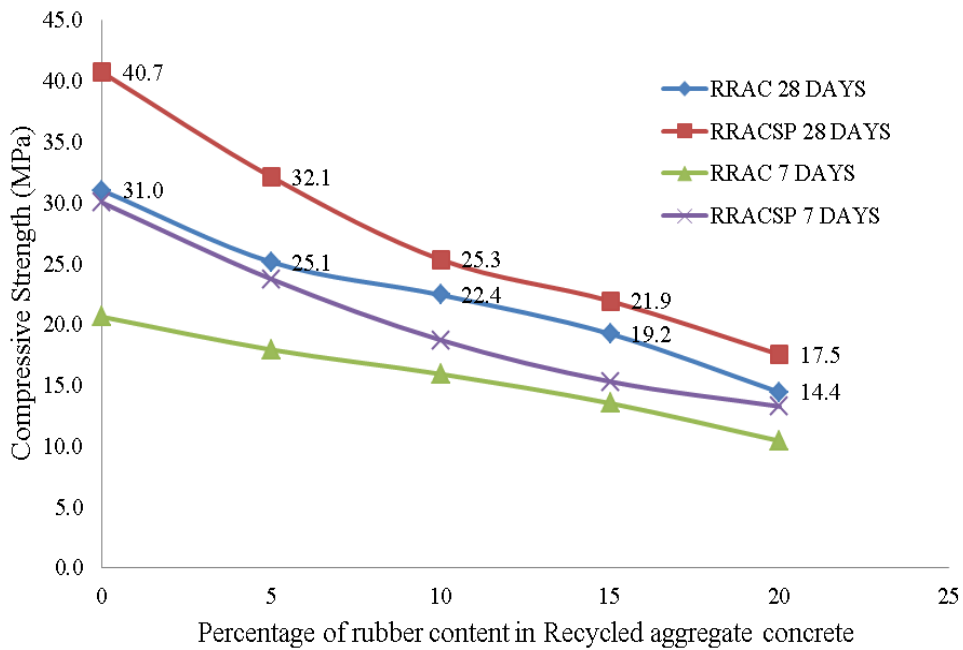


Figure 3.8 Influence of crumb rubber content on the compressive strength of recycled aggregate concrete with and without super plasticisers.

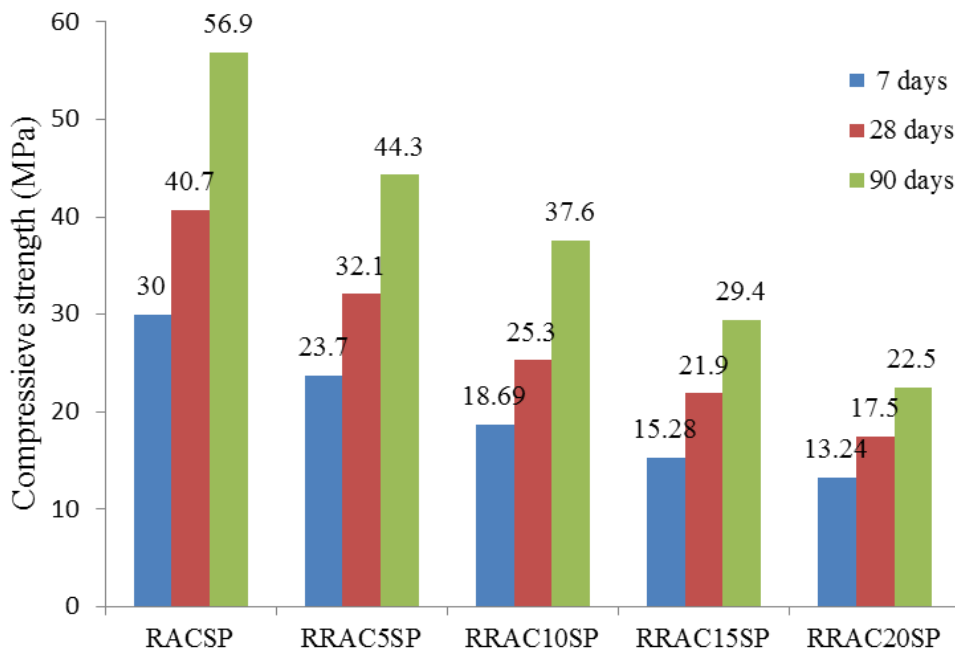


Figure 3.9 Comparison of compressive strengths of rubber recycled aggregate concrete with age.

The same trend of compressive strength increasing as it ages was followed by all concrete mixes.

3.5.2 Splitting tensile strength

Three split tensile strength tests were carried out for each mix based on the specifications in [150] and the average results are presented. Cylindrical specimen with length and a diameter of 200mm and 100mm respectively were used for the splitting test. The splitting tensile strength was estimated using Equation 3.1.

$$f_{ct} = \frac{2 \times F}{\pi \times L \times d} \dots \dots \dots 3.1$$

Where;

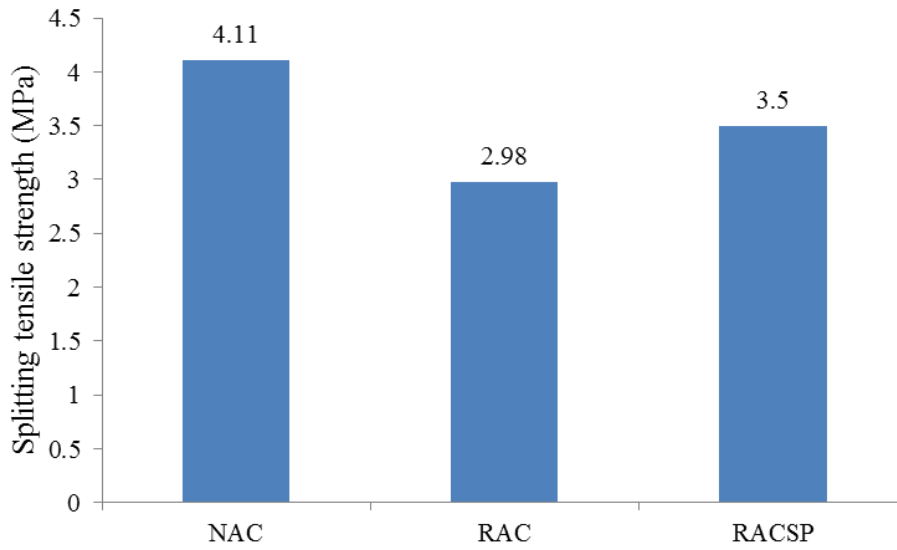
f_{ct} Splitting tensile strength of the concrete specimen

F Applied load

L Length of the test sample

d Diameter of the test sample

Figure 3.10 compares split tensile strengths for different concrete mixes. The split tensile strengths of recycled aggregate concretes with added water or super plasticizers were 27.5% and 14.8% lower than that of the natural aggregate concrete (NAC) respectively. Raw data is presented in Table A11 of Appendix A with the corresponding standard deviations. The variations of results might be attributed to the fact that the constituent materials along the pre-determined failure path of the splitting test of samples may differ. For instance, the number of coarse aggregates with high strength along the pre-determined failure path differs from each sample.



Note: Acronyms are defined in Table 3.4

Figure 3.10 Splitting tensile strength of different design mixes

Figure 3.11 shows how the amount of crumb rubber influenced the splitting tensile strength of rubber recycled aggregate concrete. A linear reduction is the best fit, ranging from 14.3% at 5% crumb rubber to reductions of 21.4%, 35.7% and 45.4% at 10%, 15% and 20% of crumb rubber respectively for rubber recycled aggregate concretes with super plasticiser.

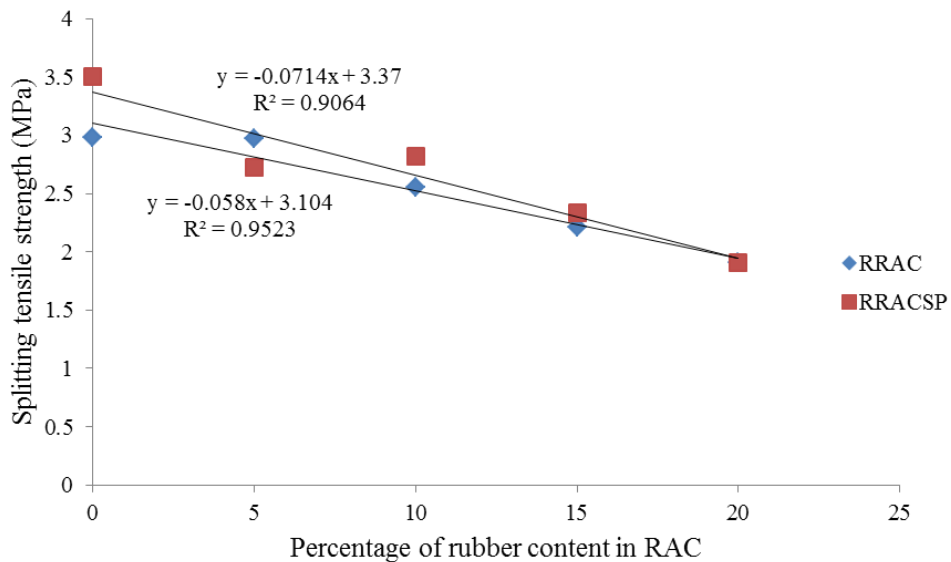


Figure 3.11 Correlation between splitting strength and the percentage of crumb rubber.

Raw data of splitting tensile strength of recycled concrete with and without crumb rubber are presented in Table A12 of Appendix A with the corresponding standard deviation. The variation in results might be attributed to the distribution of crumb rubber particles in the concrete mix.

3.5.3 Elastic Modulus

Figure 3.12 compares elastic modulus of the recycled aggregate concretes with and without super plasticisers with that of the natural aggregate concrete and shows reductions of 4.1% and 24.7% respectively.

Figure 3.13 further shows how increasing crumb rubber content decreases the elastic modulus of the rubber recycled aggregate concrete. At 15% of crumb rubber content, the reductions for mixes with and without super plasticisers were 45.7% and 28.6% respectively.

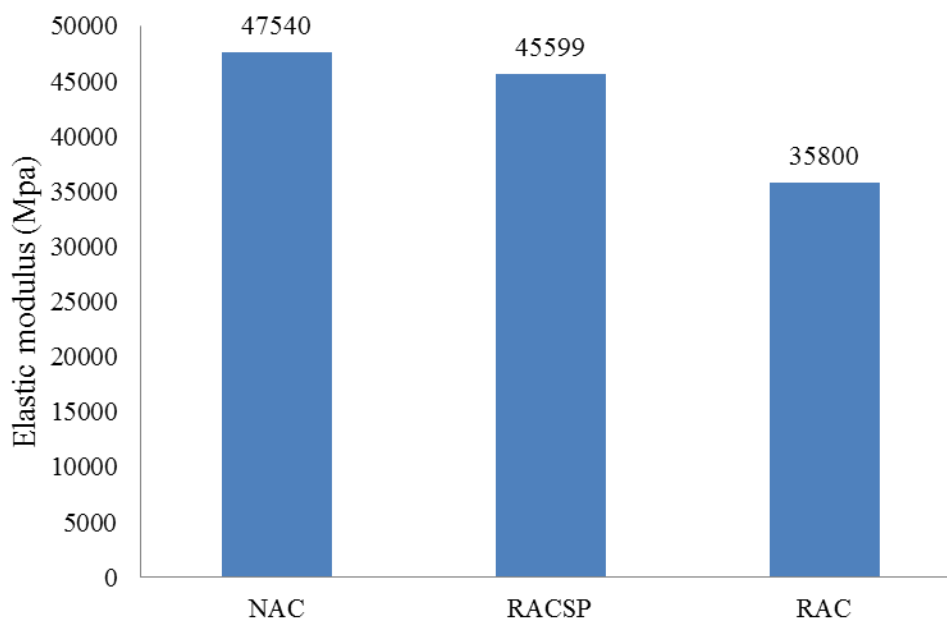


Figure 3.12 Elastic modulus of recycled aggregate concrete with and without super plasticiser compared to the natural aggregate concrete mix (NAC)

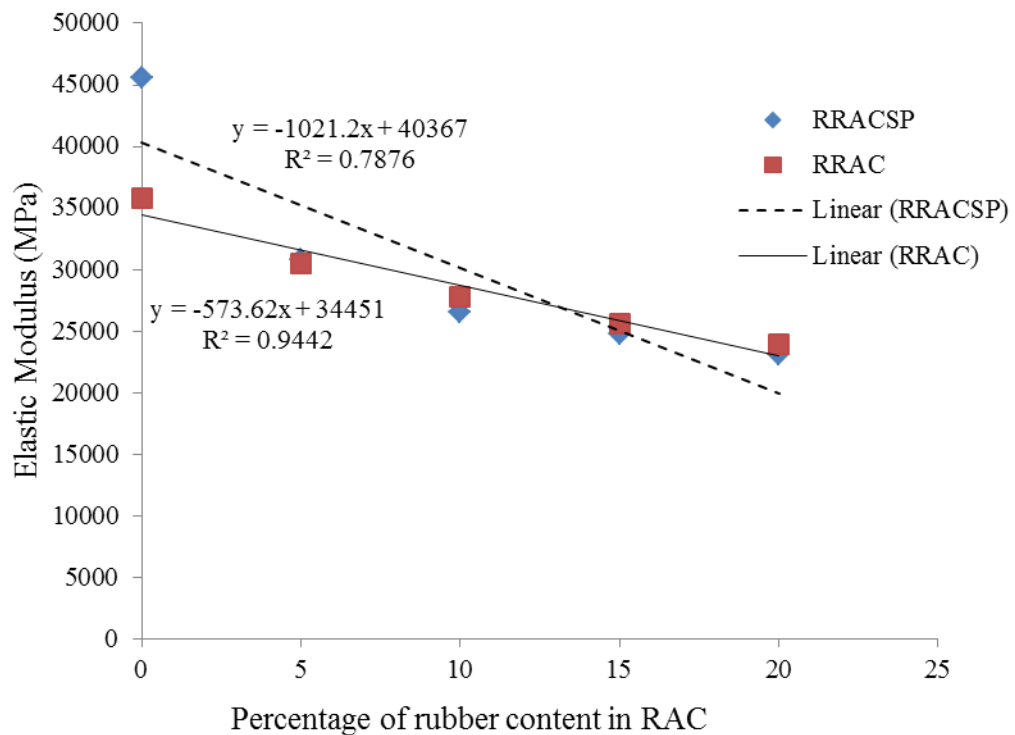


Figure 3.13 Correlation between elastic modulus of recycled aggregate concrete with respect to crumb rubber content

3.5.4 Ultrasonic Pulse Velocity (UPV)

The ultrasonic pulse velocity is often used to ascertain the quality of already cast concrete. It is a non-destructive test that is used to determine the transmission of wave velocity of the concrete specimen. Three tests were done for each concrete mix based on the specifications made in [151] and the presented results are the average values. Table A13 of Appendix A provides the raw data for each of the tested samples.

Figure 3.14 compares UPV values of the recycled aggregate concretes with super plasticisers (RACSP) and with added water but without super plasticisers (RAC). Both suffered a reduction of 6.9% compared to the natural aggregate concrete (NAC). This can be attributed to the micro cracks in recycled aggregates due to the crushing process and also the poor bonding between recycled aggregates and cement paste because of the attached old cement matrix.

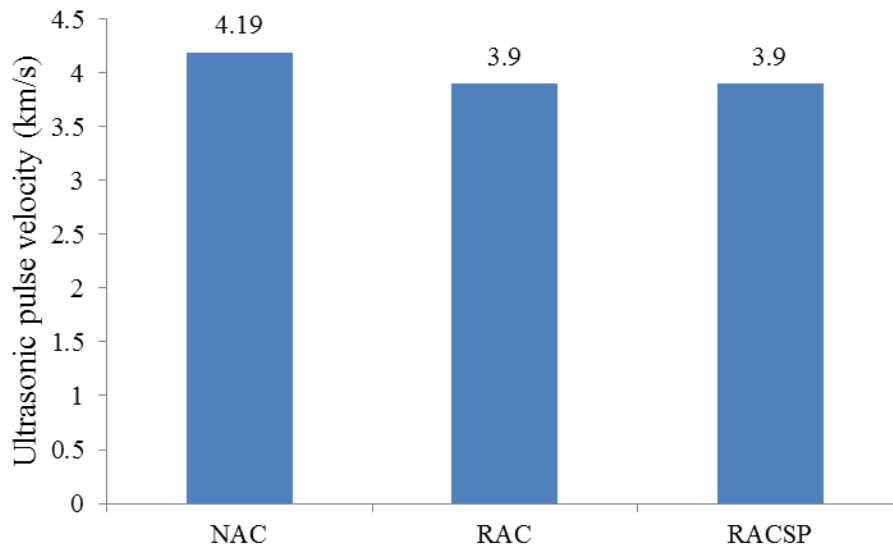


Figure 3.14 UPV of natural aggregate concrete mix and recycled aggregate concrete

The classification of concrete on the basis of ultrasonic pulse velocity is shown in Table 3.5. According to this Table 3.5, the quality of the natural and recycled aggregate concretes can be all considered good quality.

Table 3.5 concrete classification based on ultrasonic pulse velocity (Najim and Hall, 2013b, Mohammed et al., 2011)

| Ultrasonic pulse velocity (m/s) | Concrete classification |
|---------------------------------|-------------------------|
| $V > 4575$ | Excellent |
| $4575 > V > 3660$ | Good |
| $3660 > V > 3050$ | Questionable |
| $3050 > V > 2135$ | Poor |
| $V < 2135$ | Very poor |

However, increasing the amount of rubber particles caused the UPV value to drop significantly, as shown in Figure 3.15. These results are similar to the findings of [30, 41, 152] and are attributed to the entrapped air by the crumb rubber particles, as well as the low ultrasonic wave velocity in crumb rubber [153]. According to the criteria in Table 3.5, the results in Figure 3.14 make rubber recycled aggregate concrete questionable if the rubber content is more than 10%. The raw data of the UPV test results of recycled concrete with and without crumb rubber are presented in Table A14

of Appendix A with the coefficients of variation. The variation in each sample can also be attributed to the distribution of crumb rubbers in concrete mix.

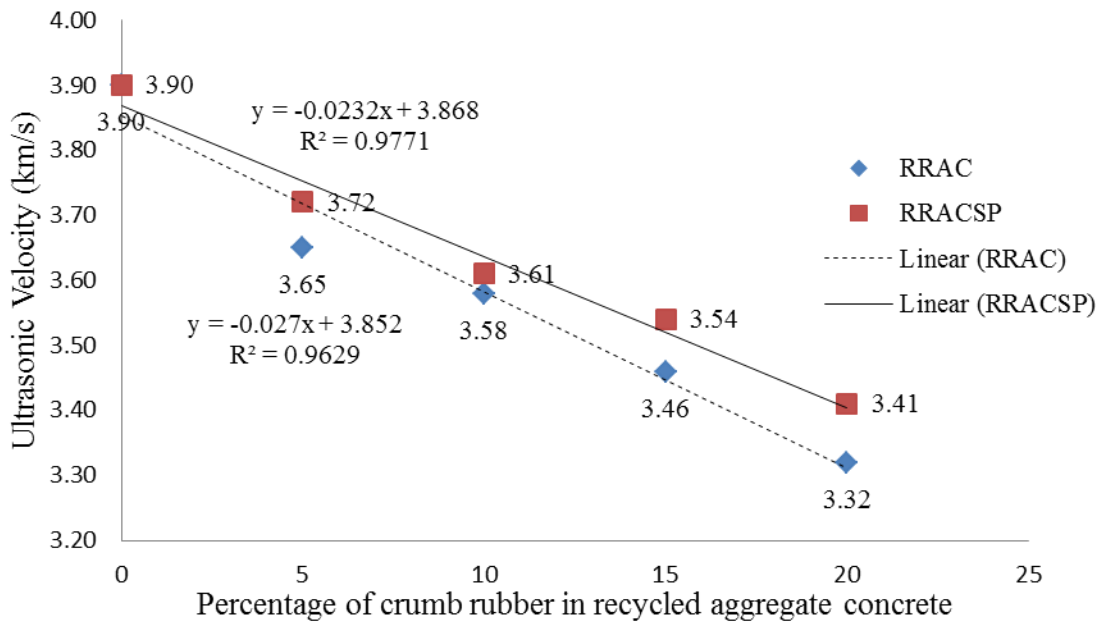
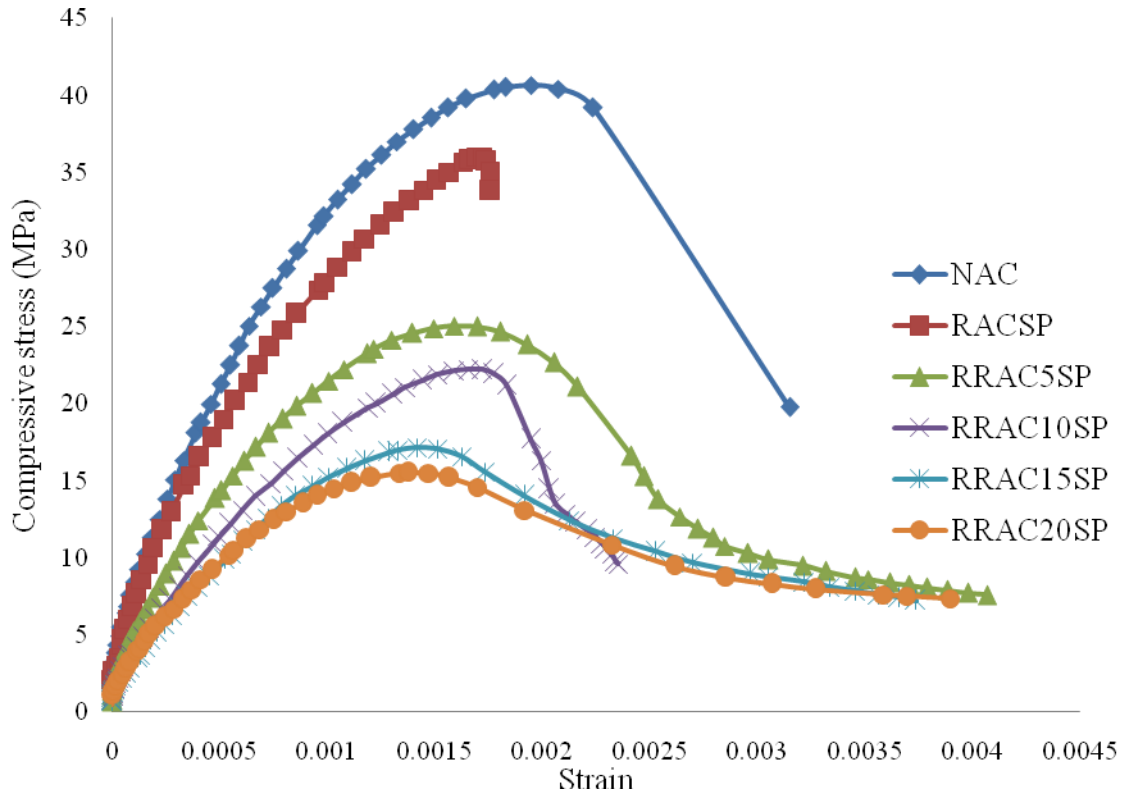


Figure 3.15 Influence of crumb rubber content on the ultrasonic pulse velocity of recycled aggregate concrete.

3.5.5 Stress Strain behaviour

Figure 3.16 compares uniaxial compressive stress-strain curves of the different concrete mixes, at 28 days. It shows that the recycled aggregate concrete without crumb rubber exhibited brittle behaviour compared to the natural aggregate concrete (NAC). However, adding rubber particles made the concrete much more ductile, with a prolonged period of unloading branch. This is owing to the high deformability of crumb rubber particles. This observation agrees with the findings of [33, 78]. The raw data for the stress strain behaviour of natural and recycled aggregate concrete of 2-3 samples each are shown in Figures A1-A6 of Appendix A.



Note: See definitions of acronyms in Table 3.4

Figure 3.16 Compressive stress strain relationships of recycled aggregate concrete with different amounts of rubber particles, all with super plasticiser

3.6 Bond strength of rebar and recycled concrete

Bond is an important parameter of reinforced concrete structures and it entails the cohesion between the reinforcement and the surrounding concrete. Its main responsibility is to transfer axial forces between the elements, thereby providing strain compatibility and composite action between steel and concrete. A few studies have been carried out on bond strength of recycled concrete made with recycled aggregates and rebars [99, 100, 105] as presented in Section 2.5 of Chapter 2 but no study was found for rubber recycled aggregate concrete. Therefore, in order to ensure proper anchorage of the rubber recycled aggregate concrete and deformed rebar, a study of bond strength was conducted for different rubber content in the recycled concrete.

3.6.1 Materials and mix proportions

The same material constituents as in Table 3.4 were used for rebar bond strength investigation. The rebars used for the pull-out test were 12mm ribbed deformed bars and were embedded in the concrete to a length of 60mm.

3.6.2 Pull-out test specimen and test set up

The pull-out test was carried out using cylindrical specimens of 150mm in diameter and 300mm in length with concentric placement of the deformed bar. This test was selected due to its simplicity in terms of fabrication and setup. The embedded steel length was 5 times its diameter in order to avoid rebar yielding during the pull-out test. Figure 3.17 illustrates the pull-out test specimen: showing contact between the rebar and concrete starting at 20mm below the surface to avoid compressive struts. This was achieved by introducing a soft plastic tube at 20mm depth and the space between the rebar and the plastic tube was filled with a clay material which was eventually removed after curing. The specimens were cured for 40 days prior to testing. A total of three samples was cast for each specimen in order to ensure the good reliability of the results.

The pull-out tests were performed using a hydraulic frame rigidly connected to a universal tensile test machine as shown in Figure 3.18. The specimen was fixed against a steel base bolted to the top plate. The top plate was restrained in position by means of bolts and nuts to ensure uniform distribution of the applied load and to minimise friction during loading. The test was performed by pulling the 12mm diameter ribbed bar upwards and the applied load was measured by means of a pressure sensor whose signals are eventually fed into an automatic data acquisition system, as shown in Figure 3.18.

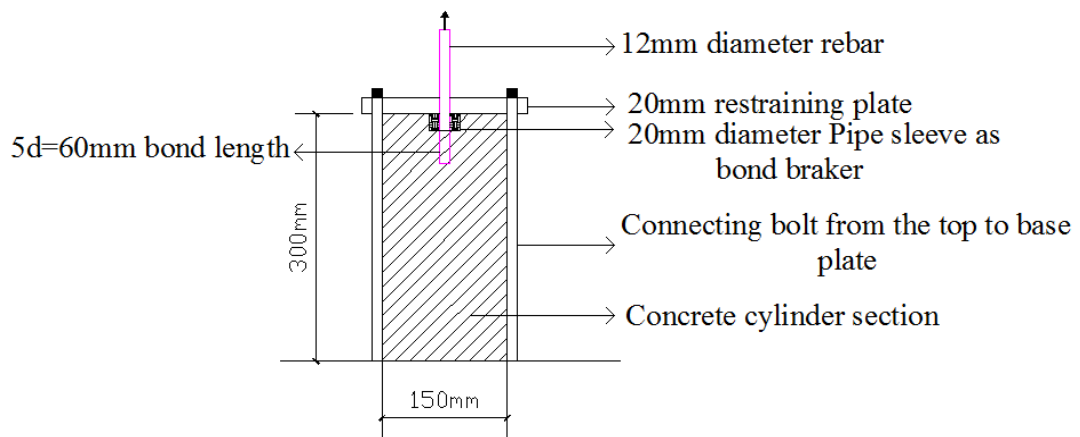


Figure 3.17 Cross sectional view of the pull-out specimen



Figure 3.18 Test set up and instrumentation

The end slip was measured by LVDTs. At the point of maximum load, the specimen was unloaded in order to measure the descending branch of the load slip relationship.

3.6.3 Results and discussion

3.6.3.1 Bond strength

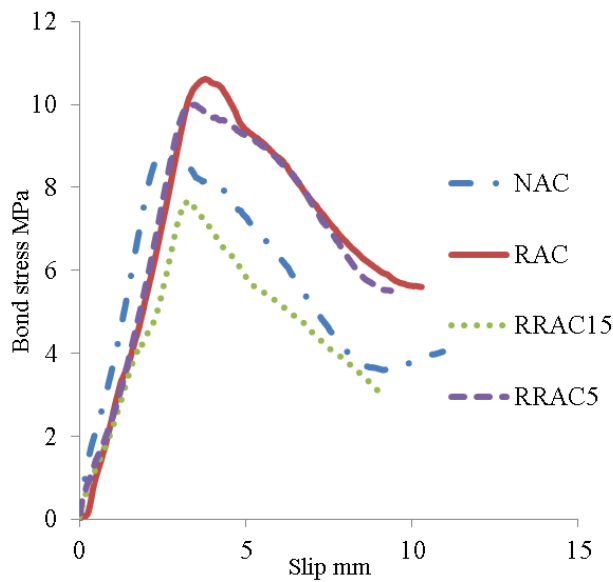
The bond strength was estimated using Equation 3.2, assuming the stress was uniformly distributed over the total embedded rebar length in concrete.

$$\tau_{max} = \frac{P_{max}}{(\pi dl)} \dots\dots\dots 3.2$$

where τ_{max} and P_{max} are the maximum bond stress and peak load between the concrete and rebar while d and l are the diameter (12mm in the test) and the embedded length (60mm in the test) of the rebar. The raw data of all specimens are included in Figure B1 to B4 of Appendix B. Figure 3.19 presents the average bond stress slip relationships. Table 3.6 gives the average values of three samples.

Table 3.6 Experimental results of the pull-out specimens

| Concrete type | f_c (Mpa) | P_{max} (KN) | τ_{max} (Mpa) | $\tau_{max}/(f_c)^{0.5}$ |
|---------------|-------------|----------------|--------------------|--------------------------|
| NAC | 42.1 | 19.7 | 8.7 | 1.34 |
| RAC | 35.06 | 23.5 | 10.4 | 1.75 |
| RRAC5 | 30.2 | 22.4 | 9.9 | 1.8 |
| RRAC15 | 20.3 | 17.4 | 7.7 | 1.71 |



See definition of acronyms in Table 3.4

Figure 3.19 Average bond stress v slip relationships from pull-out tests

The results in Table 3.6 indicate that the bond strength of recycled aggregate concrete without rubber particles was 16.3% higher than the natural aggregate concrete (NAC). This can be attributed to the better interlocking resistance due to the more irregular shapes of recycled aggregates. The results are consistent with the findings of [99, 100] as presented in Section 2.4.6 of Chapter 2. Using crumb rubber particles decreased the rebar pull-out bond strength, due to a lack of resistance of the rubber particles. However, the bond strength of the recycled concrete is still comparable with that of the natural aggregate concrete if the crumb rubber concentration is limited to 5 % (RRAC5) as shown in Figure 3.19. Also, if the rebar bond strength is normalised to the strength of concrete, according to $\tau_{max}/(f_c)^{0.5}$, then incorporating rubber particles has not caused the concrete to suffer in bond strength, as evidenced by the results in Figure 3.20. However this research recommends crumb rubber in recycled concrete to be limited to 10% of the recycled aggregates weight.

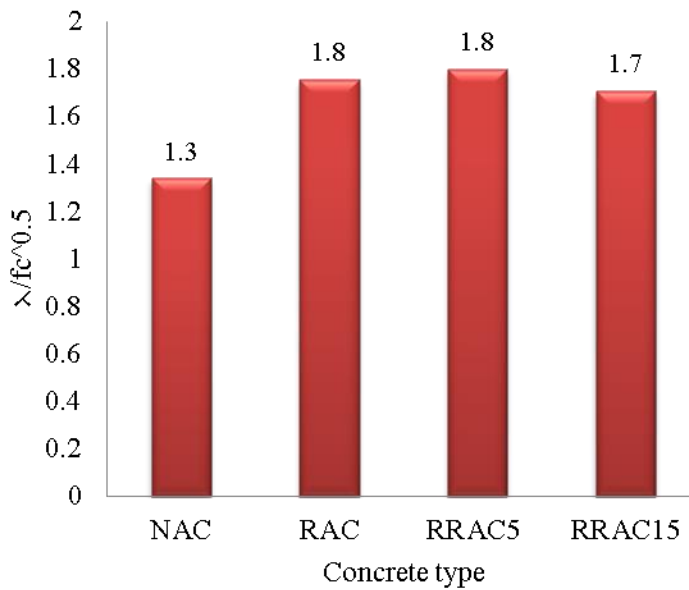


Figure 3.20 Comparison of normalized bond strength to concrete shear strength.

3.7 Interfacial shear strength

In the proposed two-layer beam construction, the two layers of concrete are not cast monolithically. This method of construction is similar to repairing and strengthening of existing concrete structures by adding new layers. It is important to ensure that the concrete interface has sufficient shear strength to prevent interfacial shear failure.

Several codes [113, 115, 154] have presented different methods, as discussed in Chapter Two, to estimate the interfacial shear strength of concrete cast at different times. The methods are based on the shear friction theory proposed by [130]. The interfacial shear resistance consists of three parts: interfacial friction between the layers of concrete, interfacial adhesion (mechanical bonding properties of the interface) and resistance of any shear links or ties crossing the interface.

Of the aforementioned three components of interfacial shear resistance, it is expected that resistance of shear links and ties will be the same, regardless of the concrete used. Friction resistance is also a function of the applied normal stress. In practical applications, the stress normal to the beam length is small; hence the friction resistance at the interface based on normal stress would be negligible. Hence, this study will derive interface resistance from interfacial adhesion (mechanical bonding properties of the interface). Therefore, this research will focus on the interfacial adhesion strength of two-layer concrete without normal stress and without shear links or ties. This component of the interfacial shear strength is dependent on surface preparation (wire brushing, sand brushing, indented, deep groove). Surface preparation will take time in practice. Since this project aims to develop a simple method of using recycled aggregate concrete in beams, any additional time-consuming features cannot be considered.

The interfacial shear behaviour between two different layers of concrete has been investigated before by others [126, 128, 129, 155]; however, their studies were concerned with concrete of the same quality in two layers. The following surfaces were considered in all studies; left as cast, wire brushing, sand brushing and indented surface. The studies considered casting intervals ranging from 28-90 days because they mainly

focused on existing concrete repairs involving the topping of new concrete on existing old concrete. All studies prove that the surface preparation of the existing concrete either by sand brushing, wire brushing or intended, enhances the interfacial shear strength of the two layers of concrete. This was attributed to the better mechanical interlock from the intended or wire brushed surfaces compared to the left as cast surfaces. However, this study focuses on two layers of concrete with different properties, one using natural aggregate concrete and one using recycled aggregate concrete without surface preparation.

3.7.1 Experimental programme

3.7.1.1 Materials, mix design and test parameters

Table 3.7 lists the types of concrete used in the two-layer test specimens. The concrete mixes for the different types are the same as those used in other mechanical property tests, which are listed in Table 3.3 and 3.4. A layer of reference natural aggregate concrete of 40MPa (NAC) was used in every test. The other layer of concrete reflected different possible applications of recycled aggregate concrete.

Table 3.7 Notation and description of test specimen

| Notation | Concrete types | Description |
|----------|-----------------|--|
| T1 | NAC on NAC | Natural aggregate concrete cast on top of natural aggregate concrete with differential stiffness between layers. |
| T2 | NAC on RRAC5SP | Natural aggregate concrete cast on top of recycled aggregate concrete with 5% crumb rubber |
| T3 | NAC on RRAC10SP | Natural aggregate concrete cast on top of recycled aggregate concrete with 10% crumb rubber |

For the proposed beam construction using two layers of concrete, it is envisaged that recycled aggregate concrete will be cast first (the tension layer). A layer of concrete using natural aggregates will be cast after solidification of the first layer, rather than at the same time as the first layer, in order to avoid mixing the ingredients of the two layers of concrete. In this research, two time lags (4 and 24 hours) between casting the

two different layers were investigated. The 4-hour time lag reflected the possible time it would take in practice to cast two layers of concrete on one casting day. The 24-hour time lag represents casting of the two layers of concrete on two different days. Three samples were used for each test. The 4-hour time lag was selected for construction works to be carried out within a day and to make precast beams within the earliest possible time. However, the rapid hardening cement or other admixtures could also be used to achieve the same purpose.

3.7.1.2 Test methods

The slant shear test was used to determine the interfacial shear strength. It is one of the most common methods used by other researchers [129, 155, 156] and is adopted by EU and US codes (EN12615-1999, ASTM C 882-1999). According to a review of the slant test by [129], the test results are sensitive to surface roughness, geometry, size and inclination angle of the test specimen. This research will follow the recommendations of [129]. The push test method was also used in this study along with the results of the slant shear test to estimate pure shear strength based on recommendations made in literature.

Slant shear test description

Figure 3.21 shows the geometry and size of the slant shear test adopted for this study. The prism test specimens were 450mm in height with a square cross section of 150mm by 150mm. The angle of inclination along the shear plane was 30 degrees.

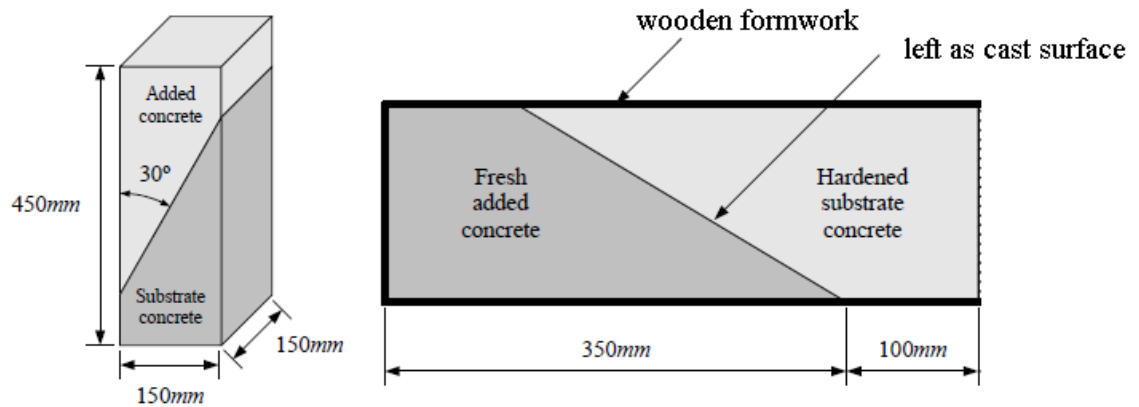


Figure 3.21 Slant shear test specimen configuration

Figure 3.22 shows the wooden mould: it was inclined at an angle of 30 degrees to the horizontal so that the top surface of the first layer of concrete (referred to as substrate concrete in Figure 3.21) was horizontal. After the first layer of concrete was set, the mould was repositioned vertically to receive the added concrete. The specimens were demoulded after 24 hours and cured in a water tank for a period of 35-40 days prior to load testing.



Figure 3.22 Wooden mould for placing the first layer of concrete

The interface of the two layers of concrete in the slant shear test is subjected to a stress state of both compression and shear as shown in Figure 3.23. The load was applied at a

constant rate of 0.02mm/s until failure of the specimen either in compression or interfacial shear.



Figure 3.23 Slant shear test set up and instrumentation

Two failure modes are expected from the slant shear test; Adhesive (interfacial deboning) failure mode where the interface slides against each other, and compressive failure of the prism if the interfacial shear strength is greater. The interfacial shear strength of the slant shear is given in Equation 3.3 [157].

$$\tau = \frac{F \sin \alpha \cos \alpha}{b^2} \dots \dots \dots 3.3$$

Where τ is the interfacial shear strength; F is the applied compressive load at failure; b is the width of the square cross section and α is the angle of inclination between the shear plane and the longitudinal axis of the specimen.

Splitting test

The splitting test is carried out based on the specifications made in [150] but was reported in literature [129] to be less sensitive to surface roughness compared to the slant shear test. The specimen used for this test was 100mm diameter and 200mm length as shown in Figure 3.24. The hardwood parking strip at the lower and upper parts of the test set up were used to uniformly distribute the compressive load on the sample. Tests were carried out after 35-45 days of curing on the same day as the slant shear specimens.

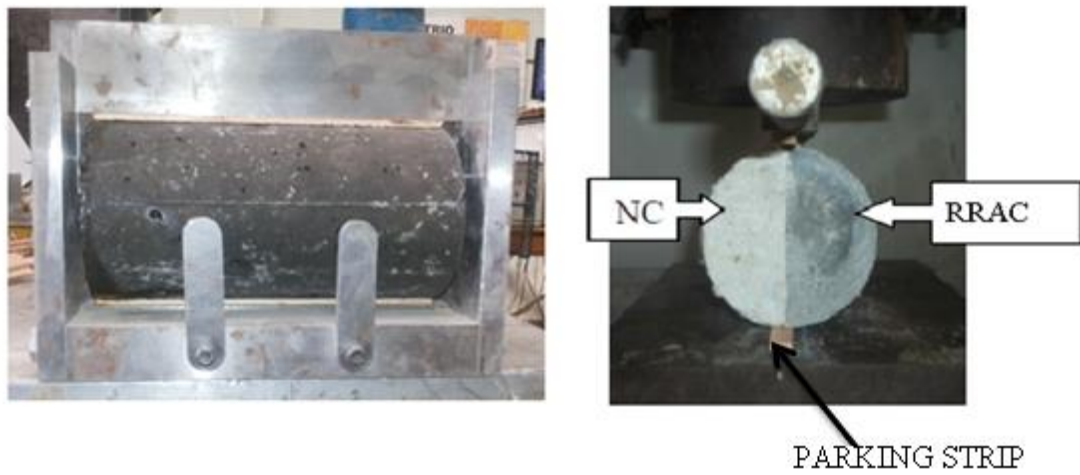


Figure 3.24 Set up for splitting test

The bond strength in tension between the concrete layers is given in Equation 3.4 [157].

$$\sigma = \frac{2 \times F}{\pi \times L \times d} \dots\dots\dots 3.4$$

Where σ is the interfacial bond strength in tension; F is the applied load at failure; L is the length of the cylinder and d is the diameter of the cylinder.

3.7.1.3 Interpretation of results (Mohr-Coulomb Criterion)

The interfacial shear strength calculated using Equation 3.3 from the slant shear test is that under a combined compressive and shear stress. In order to obtain the interfacial shear strength without a compressive stress, the failure envelope of concrete according

to Mohr-Coulomb criteria as shown in Figure 3.25 can be used. The failure envelope at the interface under pure shear stress between the bottom and top layer concrete according to Mohr-coulomb criterion in Figure 3.25 can be estimated using the compressive strength (f_c) obtained from at least three cubes cured and tested on the same day with the slant shear and splitting test. The tensile strength (f_t) of the concrete can be estimated analytically using the EC2. The tensile strength of concrete is influenced by the shape and surface texture of the aggregates and can also be reduced due to environmental effects which may not be reflected using the EC 2 method. However, this study evaluates the tensile strength of all concrete mixes by conducting splitting tensile tests.

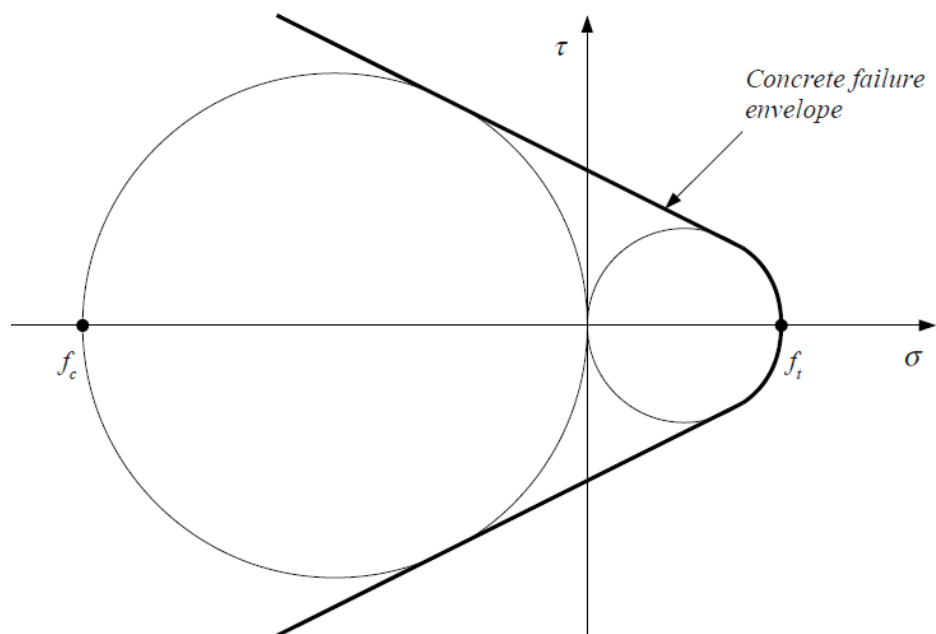


Figure 3.25 Failure envelope of both natural aggregate concrete and recycled concrete.

From Figure 3.26, the pure interfacial shear strength without normal stress can be estimated according to the following procedure:

- Obtain the shear strength (τ) with a combined effect of shear and compressive stress (σ), from the slant shear stress test. This determines point (τ) in Figure 3.26.
- Obtain the shear strength in tensile ($f_{t,i}$) from split tensile strength test. This gives point ($f_{t,i}$) in Figure 3.26.
- Draw a tension circle using ($f_{t,i}$) as diameter.
- Draw a line from point tangent of the interfacial shear strength (τ) from the combined effect of shear and compression to that of the shear strength ($f_{t,i}$) in tension.

At the intercept between this line and the vertical axis, the shear stress gives the pure interfacial shear strength (τ_0) without a normal stress.

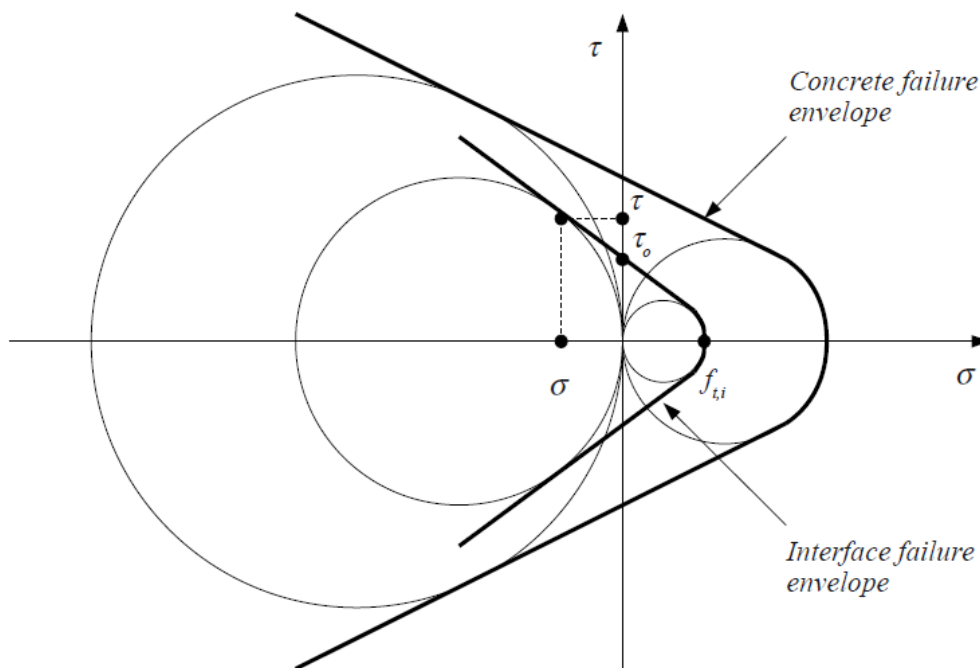


Figure 3.26 Pure shear strength of slant shear test specimens with interfacial failure

3.7.2 Results and discussion

3.7.2.1 Failure mode and differential stiffness

All the specimens failed at the interface (interface de-bonding) except specimens T1 and T2 cast at a time lapse of four hours. Figure 3.27 (a) and (b) show the two different failure modes.

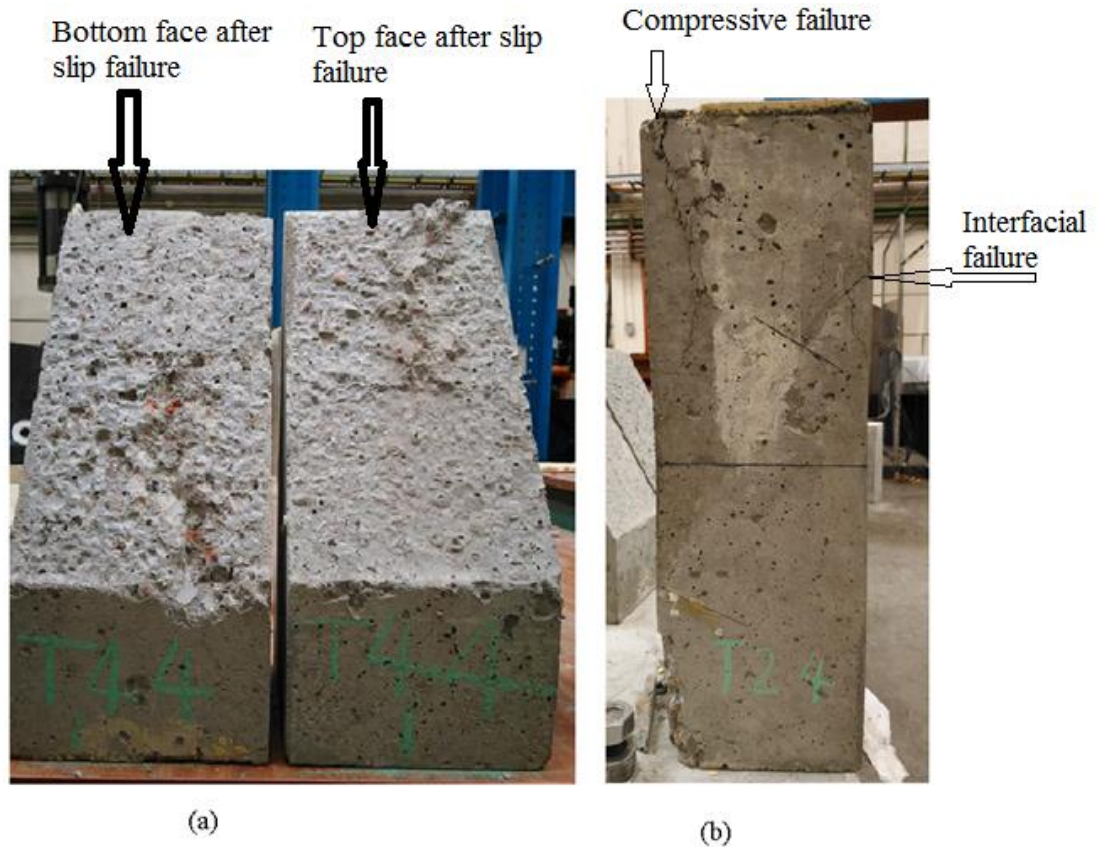


Figure 3.27(a) Interfacial and (b) compressive (monolithic behaviour) failure modes of specimens

The results of all specimens as shown in Table 3.8 revealed that those with a 4-hour cast time interval predominantly exhibits compressive (monolithic behaviour) failure unlike the 24-hour cast time interval that fails at the interface. The failure modes of all specimens are summarized in Table 3.8. Figure 3.27(a) shows that the interfaces between the two layers slide against each other prior to reaching the full capacity of the concrete prism. On the other hand, Figure 3.27 (b) for casting the two concrete layers at a 4-hour interval, exhibits compressive failure. Hence the interface shear strength was sufficient to withstand loads to reach the full capacity of the concrete prism.

3.7.2.2 Slant shear strength results (interfacial shear strength under a combined normal and shear stress)

Each test was repeated three times and the results were similar as shown in Table C1 and C2 of Appendix C. Therefore, only the average values are presented here. Table 3.8 summarises all the test results and Figure 3.28 shows the comparison. The interfacial shear strength suffered marked reductions as the time interval between concrete casting increased from 4 hours to 24 hours. This is expected as the longer interval will make it difficult for the two layers of concrete to adhere well once one layer has become dry. For this reason, the interfacial bond strength is expected to decrease.

This suggests that in practice, the second layer of concrete should be cast as early as possible once the second layer can no longer flow into the first layer.

Table 3.8 Summary of slant shear and splitting tests of all specimens.

| SPECIMEN | | Fc(MPa) | | Splitting Bond strength mpa | Slant shear Bond strength mpa | Test age (days) | Slant shear Failure modes |
|----------|-------|---------|------|-----------------------------|-------------------------------|-----------------|---------------------------|
| | | NAC | RAC | | | | |
| T1 | 4hrs | 37/28 | - | 2.4 | - | 46 | Compressive |
| | 24hrs | 37/28 | - | 2.1 | 4.10 | 43 | Interfacial |
| T2 | 4hrs | 40.8 | 20.7 | 2.30 | - | 46 | Compressive |
| | 24hrs | 38.7 | 20.7 | 1.31 | 6.41 | 43 | Interfacial |
| T3 | 4hrs | 35.7 | 15.5 | 1.48 | 5.89 | 40 | Interfacial |
| | 24hrs | 38.6 | 15.5 | 1.62 | 5.22 | 45 | interfacial |

Note: 37/28 stands for NAC of 37MPa top layer and 28MPa bottom layer.

The bond strength in shear for specimens T1 and T2 at 4 hours of concrete casting interval which exhibited compressive failure mode was estimated using the compressive strength of the lower grade of concrete.

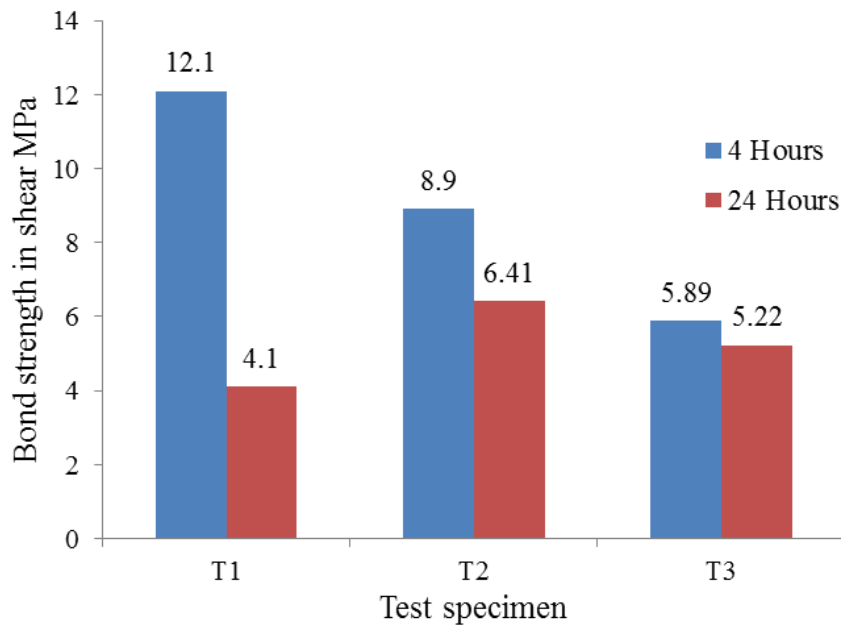


Figure 3.28 Comparison of interfacial shear strength

At a four-hour cast time interval, the specimen T1 at 4 hours behaved monolithically under the applied load. The results for T2 and T3 recycled concrete for a 24 hour cast time interval is higher than that of T1 without recycled materials. This can also be attributed to the high surface roughness of the recycled aggregates originating from the recycled concrete mix compared to the uncrushed quartzite aggregates used for the NAC mix.

3.7.2.3 Bond split tensile strength

The failure mode is either pure interfacial failure or interfacial failure with partial failure of the substrate (recycled concrete) as shown in Figure 3.29. In general, the bond tensile strength in Table 3.6 and Figure 3.30 decreases with the time lap between casting the two concrete layers. However, due to some partial failure of the substrate, as shown in Figure 3.29(b), Test T3 did not follow this trend, although the results for 4-hour and 24-hour time intervals are similar. Failure of T3 specimens did not occur exactly at the interface of the concrete layers but split through the substrate (weak recycled concrete).

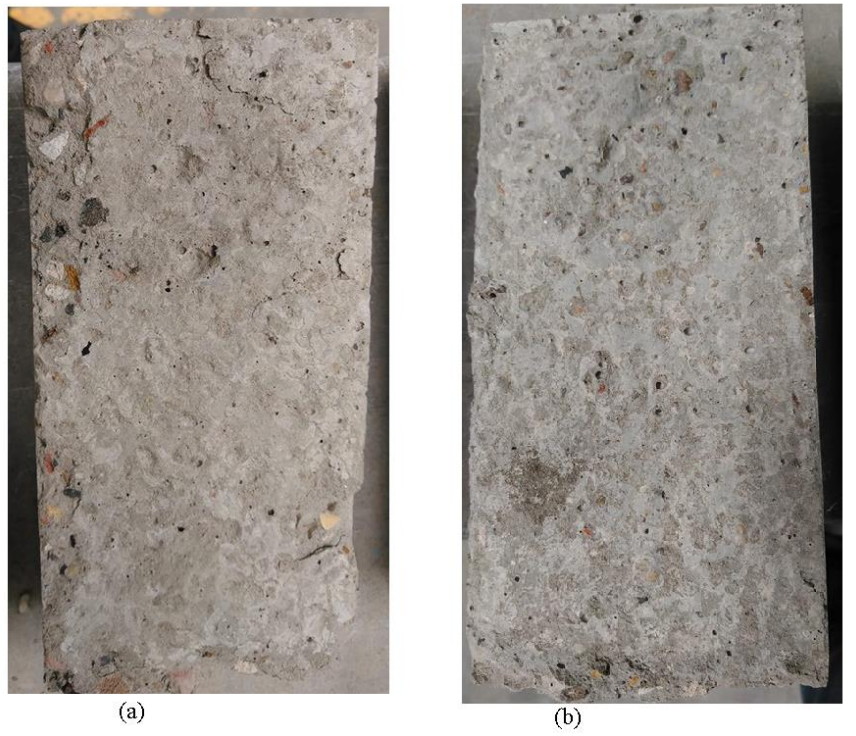


Figure 3.29 Failure modes of specimens (a) Interfacial failure with partial failure of the substrate (recycled concrete) (b) pure shear failure.

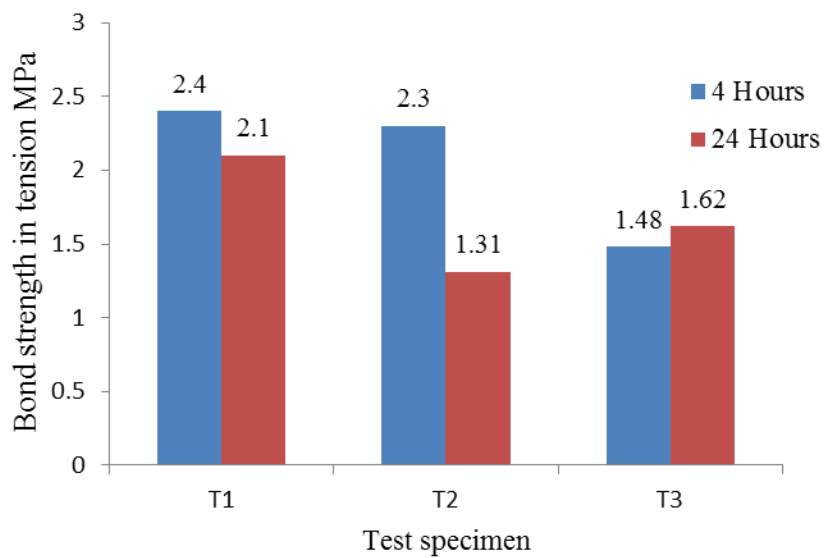


Figure 3.30 Bond strength in tension of test specimen

3.7.2.4 Interfacial shear strength without normal stress

Following the procedure outlined in Section 3.7.1.3, interfacial shear strengths without the application of normal stress were calculated. The results are compared in Figure 3.31.

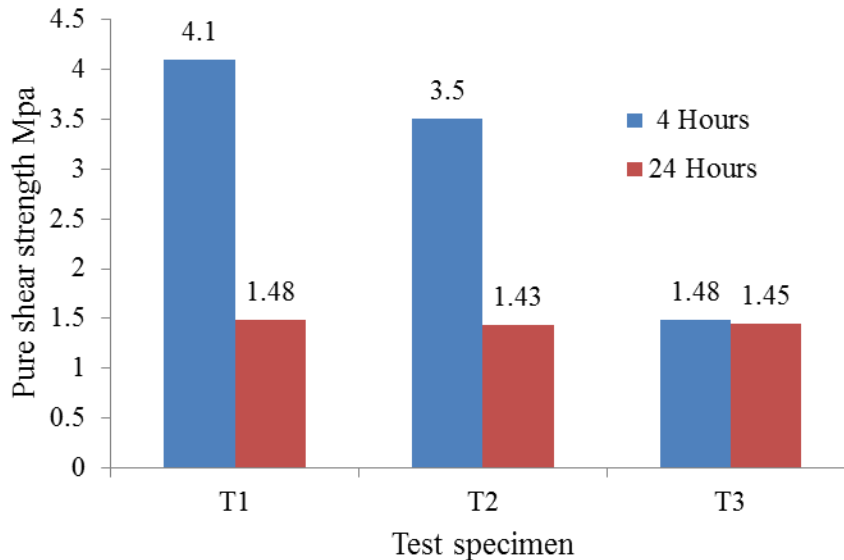


Figure 3.31 Comparison of interfacial shear strength without a normal stress.

Figure 3.31 indicates that if the time interval between casting two layers of concrete is 24 hours, the interfacial shear strength is very similar, giving a value of just under 1.5N/mm^2 . The interfacial shear strength for the four-hour casting interval is higher than that for the 24-hour interval; therefore, the second layer of concrete should be cast as soon as possible after casting the first layer. The interfacial shear strength for the 4-hour casting interval varies with the mix composition, with specimen T2 (NAC on RRAC with 5% rubber crumb) giving the best results compared to T3 (NAC on RRAC with 10% rubber crumb). This is attributed to the better surface roughness of T2 specimens containing 5% of crumb rubber. With crumb rubber content beyond 5%, the interfacial shear strength is reduced due to lower mechanical properties. Nevertheless, due to limited resources, the number of tests done is not sufficient to allow this phenomenon to be investigated more thoroughly.

3.7.3 Summary and Conclusions

This study focused on the effect of different cast times with the same surface roughness (left as cast) on the interfacial shear strength of two layers of concrete. The behaviour of the two layer concrete cast in a 4-hour time interval under stress behaves monolithically while those cast at a 24-hour cast time interval fails at the interface under stress for specimens T1 and T2. Therefore this research recommends a construction of the two layers of concrete within a time limit of 4 hours in order to reduce the cost of construction by avoiding provisions of extra shear links resisting horizontal shear stress of two-layer beams. The impact of the construction technique on the cost of proposed construction (two-layer beams) will be dealt with in Chapter 6 of this report.

3.8 Effects of graphene on recycled aggregate concrete

The concrete with recycled aggregates with or without crumb rubber has inferior performance in the wet and hardened state compared to the natural aggregate concrete using natural aggregates. Although the main emphasis of this thesis is about utilising such recycled aggregate concrete in bending members to achieve comparable structural performance as those made with natural aggregate concrete, there is a continuous search for methods to help make recycled aggregate concrete achieve properties similar to those of natural aggregate concrete (NAC) so that recycled aggregate concrete can replace NAC without limitation. The methods investigated so far include adding an extra amounts of cement in recycled concrete mix [14, 76], use of silica fume, super plasticisers[7, 11], etc. A comprehensive review of improvement methods and the extent of their positive impacts on properties of recycled concrete are presented in Table 2.8 and 2.9 in Chapter Two of this thesis. However, all these methods were considered to be time-consuming and costly. For instance, the production of cement is environmentally damaging and contributes to about 5% of the total global carbon dioxide (CO₂) emission [158]. Hence, producing graphene reinforced concrete that has

the same strength as natural aggregate concrete with less cement will be beneficial to the environment.

This research explores the feasibility of using graphene to improve the mechanical properties of recycled aggregate concrete. Graphene has been shown to greatly enhance the mechanical properties of fresh concrete [45, 140] due to its ability to drastically increase bonding between cement and aggregate. This research will investigate whether graphene can also achieve similar positive effects on the mechanical properties of recycled aggregate concrete.

3.8.1 Experimental programme

3.8.1.1 Materials and concrete mix proportion

The materials used for this test include: CEM 11/B-V 32.5N Portland cement with fly ash, Recycled aggregates (RA2) from Offerton, Stockport, UK, comprising different debris as shown in Table 3.2 and Figure 3.32(a), crumb rubber shown in Figure 3.2. The grading of the recycled aggregates (RA2) is shown in Figure 3.1. The graphene used in this research was supplied by First Graphene in Australia (www.firstgraphene.com) with different nominal flake sizes of 5 μm , 10 μm , 20 μm and 40 μm . For this research, the graphene was dispersed in one litre (1L) liquid by dedicated technicians experienced in making graphene solution. The dispersion procedure is as follows:

- The desired amounts of graphene and super plasticiser were mixed with 50-100ml of water, depending on the weight of the composition.
- The mix composition was then put in a magnetic stirrer for about 30 minutes.
- The mix was poured into the rest of the water to give one litre of graphene solution by using a square-holed mixer head for 30 minutes.
- The entire mix composition was then incorporated into a glass reagent bottle for ultrasound process in order to ensure the uniform dispersion of the graphene.

- The one litre mix was stored in a plastic bottle (Figure 3.32b) ready for use.

For each concrete mix, all the graphene was dispersed in one litre solution (Figure 3.32b). Graphene concentrations of 0.01%, 0.02%, 0.05% and 0.1% of the combined weight of cement and sand were incorporated into concrete. In order to ensure proper dispersion, super plasticiser of half of the weight of graphene was mixed with the graphene solution in the 1 litre bottle. Table 3.9 shows the amount of graphene in the one litre graphene solution for different graphene concentrations. The one litre graphene solution replaced part of the water for casting concrete in order to maintain the required w/c ratio. As an example of designation, G5 0.01 in Table 3.9 stands for graphene size $5\mu\text{m}$ with a loading of 0.01% of the combined cement and sand weight.

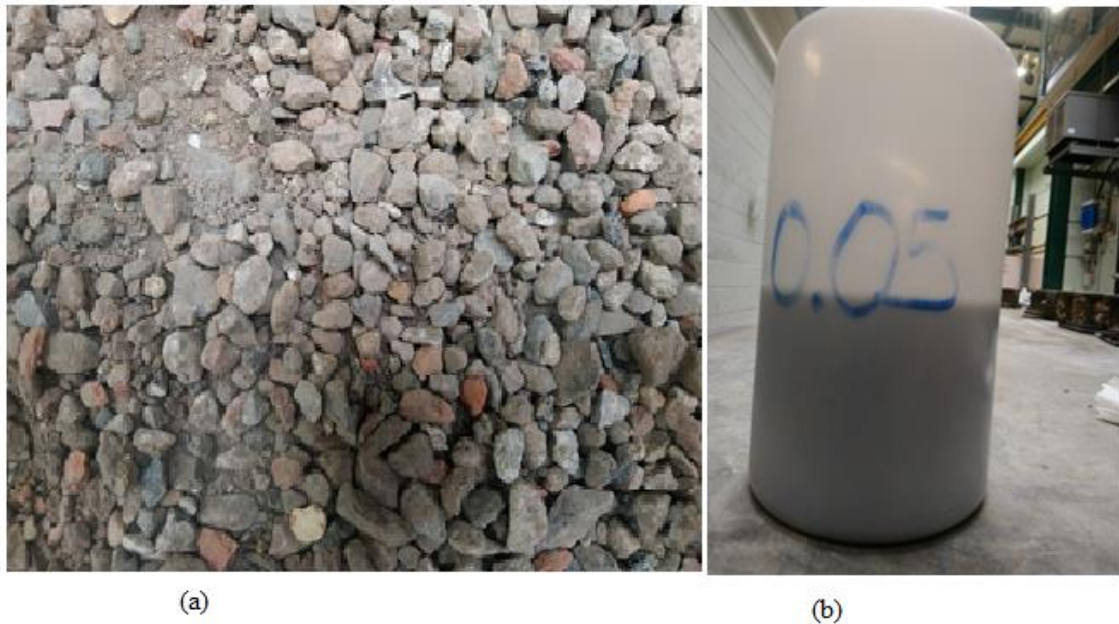


Figure 3.32 (a) Recycled aggregates (RA2) from crushed brick/concrete (<https://www.offertonsandandgravel.co.uk/gravel-aggregate/crushed-brick-concrete-mot>) (b) Graphene solution

Table 3.9 Mix composition of graphene solution

| | | Graphene solution mix design | | |
|-------------|---------|------------------------------|--------------|----------------------|
| | | Mix composition | | |
| Designation | Size um | Water | Graphene (g) | Super plasticiser(g) |
| G5 0.01 | 5 | 1L | 2.2 | 1.1 |
| G5 0.02 | 5 | 1L | 4.4 | 2.2 |
| G5 0.05 | 5 | 1L | 11.0 | 5.5 |
| G5 0.1 | 5 | 1L | 22.0 | 11 |
| G20 0.01 | 20 | 1L | 2.2 | 1.1 |
| G20 0.02 | 20 | 1L | 4.4 | 2.2 |
| G20 0.05 | 20 | 1L | 11.0 | 5.5 |
| G20 0.1 | 20 | 1L | 22.0 | 11 |

All concrete mixes had the same water/cement ratios as shown in Table 3.10, based on C40 concrete, with a water cement ratio of 0.57. Thus, to make concretes with different amounts of graphene, Table 3.11 was followed. If using crumb rubber, 10% by weight of the recycled aggregate was used.

Table 3.10 Reference mix for C40 concrete

| Quantities | Cement(kg) | Water(kg) | Fine aggregate(kg) | Coarse aggregate(kg) |
|--------------------|------------|-----------|--------------------|----------------------|
| Per m ³ | 360 | 206 | 732 | 1011 |

Table 3.11 Detailed mix compositions of recycled aggregate concretes with graphene

| TYPE | Cement (kg) | Water (kg) | Fine Aggregate (kg) | Recycled Aggregate (kg) | Graphene solution (kg) | Crumb rubber (kg) |
|------|-------------|------------|---------------------|-------------------------|------------------------|-------------------|
| RAC | 7.2 | 5.1 | 14.6 | 20.2 | - | - |
| RRAC | 7.2 | 5.1 | 14.6 | 18.2 | - | 2 |

| | | | | | | |
|------------------|-----|-----|------|------|---|---|
| RRAC G5 0.01 | 7.2 | 4.1 | 14.6 | 18.2 | 1 | 2 |
| RRAC G5 0.02 | 7.2 | 4.1 | 14.6 | 18.2 | 1 | 2 |
| RRAC G5 0.05 | 7.2 | 4.1 | 14.6 | 18.2 | 1 | 2 |
| RRAC G5 0.1 | 7.2 | 4.1 | 14.6 | 18.2 | 1 | 2 |
| RRAC G20 0.01 | 7.2 | 4.1 | 14.6 | 18.2 | 1 | 2 |
| RRAC G20 0.02 | 7.2 | 4.1 | 14.6 | 18.2 | 1 | 2 |
| RRAC G20 0.05 | 7.2 | 4.1 | 14.6 | 18.2 | 1 | 2 |
| RRAC G20 0.1 | 7.2 | 4.1 | 14.6 | 18.2 | 1 | 2 |

As will be shown by the test results, adding graphene to the raw recycled aggregates concrete without any processing did not achieve much improvement in the mechanical properties. This was attributed to the inability of graphene to improve bond properties at cement/recycled aggregate interface as a result of an excessive amount of dust in the raw recycled aggregates. Therefore, this study also investigated using washed recycled aggregates. For this part of the investigation, graphene concentrations by weight of 0.01%, 0.02% and 0.05% of sand/cement, and graphene size 10 μm were used, in both natural aggregate concrete and washed recycled aggregate concrete. Table 3.12 presents weights of different components in 1 litre of graphene solution. Washing recycled aggregates was done by agitating recycled aggregates a few cycles in a basket of water as shown in Figure 3.33(a). The process was done by inserting a sieve of 2.36mm size filled with the recycled aggregates in a plastic drum full of water. The sieve was agitated to filter the dust off easily for about a minute. The water after washing was reused. Because the recycled aggregates were of the lowest quality, a large amount dust, about 11.4% of the recycled aggregates, was filtered off. This was done by comparing the weight of the washed samples in Figure 3.33(b) after air drying with that of the unwashed recycled aggregates in Figure 3.32(a).



Figure 3.33(a) Washing set up of recycled aggregates (b) Washed recycled aggregates

Table 3.12 Mix composition of graphene solution

| | | Graphene solution mix design | | |
|-------------|---------|------------------------------|--------------|----------------------|
| | | Mix composition | | |
| Designation | Size um | Water | Graphene (g) | Super plasticiser(g) |
| G10 0.01 | 10 | 1L | 2.2 | 1.1 |
| G10 0.02 | 10 | 1L | 4.4 | 2.2 |
| G10 0.05 | 10 | 1L | 11.0 | 5.5 |

For each concrete mix, three cube samples of 100mm x 100mm x 100mm size were cast and tested after 28 days of curing according to the specifications in [149] and the results presented are average values.

Three splitting tensile tests were carried out for each mix according to the specifications in [150], on cylinders of 100mm diameter x 200mm length after 28 days of curing, and the average results will be presented.

3.8.2 Experimental results

3.8.2.1: Compressive strength of RRAC with and without graphene solution

Figure 3.34 compares the compressive strengths of the different recycled aggregate concretes, with crumb rubber and unwashed recycled aggregates (RRAC), with or without graphene solution. The results show that the three replicate samples of each mix gave consistent results; therefore, the average values can be used. Except for G5 0.02 (graphene size $5\mu\text{m}$, 0.02% by weight), including graphene decreased compressive strength of RRACs, which was attributed to the low bonding strength between the rubber particles and the cement matrix due to excessive amounts of dust, and graphene further decreased this bonding by behaving as another source of dust. G5 0.02 graphene solution increased the compressive strength of recycled concrete strength by 12.2% (from 18.9MPa to 21.2MPa), but this increase is not sufficiently high to upgrade the recycled aggregate concrete so that it can be used to replace concrete with fresh aggregates in load-bearing members.

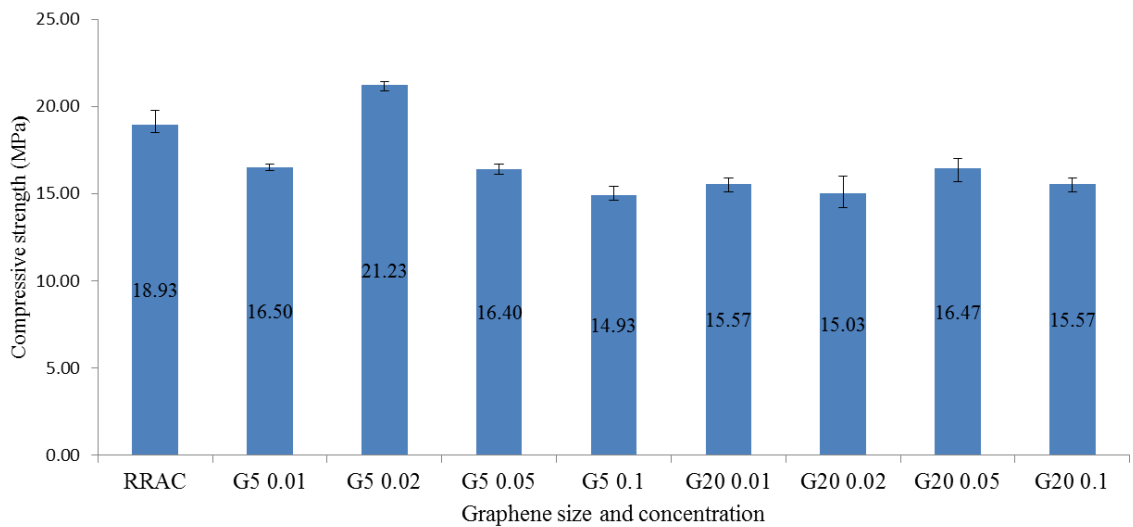
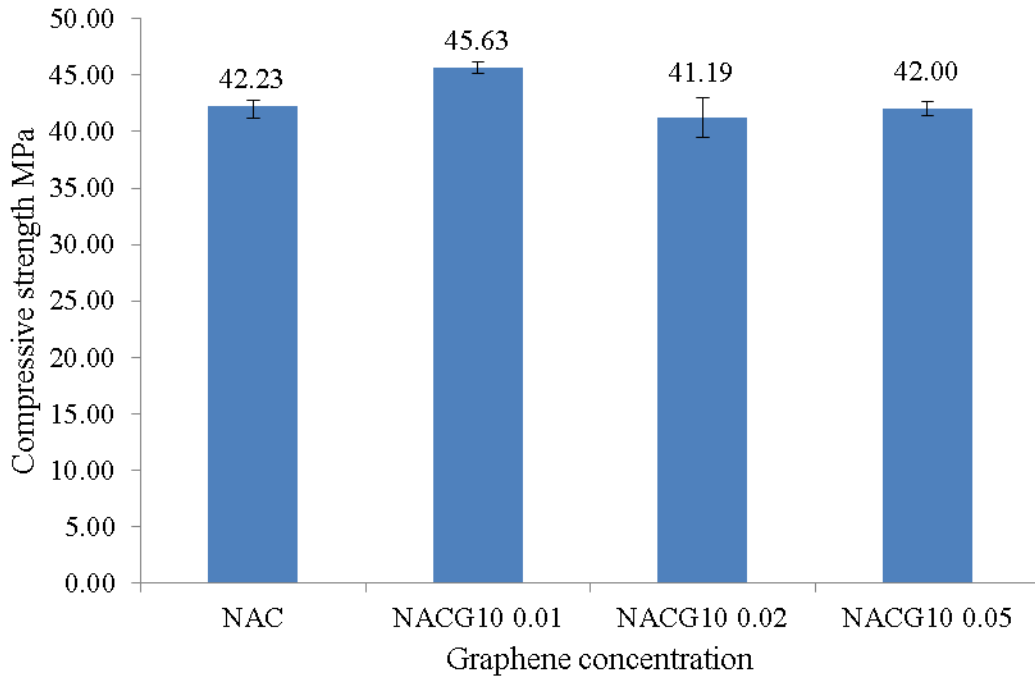


Figure 3.34 Comparison of compressive strengths of recycled aggregate concrete with crumb rubber (RRAC) with different concentrations of graphene solution

3.8.2.2: Compressive strength of RAC/NAC with and without graphene solution

Previous research studies by [45] reported very high increases in compressive strength of concrete of fresh aggregates by using graphene. To check whether this could be achieved using the graphene of this research, a few tests were carried out on C40 natural aggregate concrete with different G10 graphene weight percentages. Figure 3.35

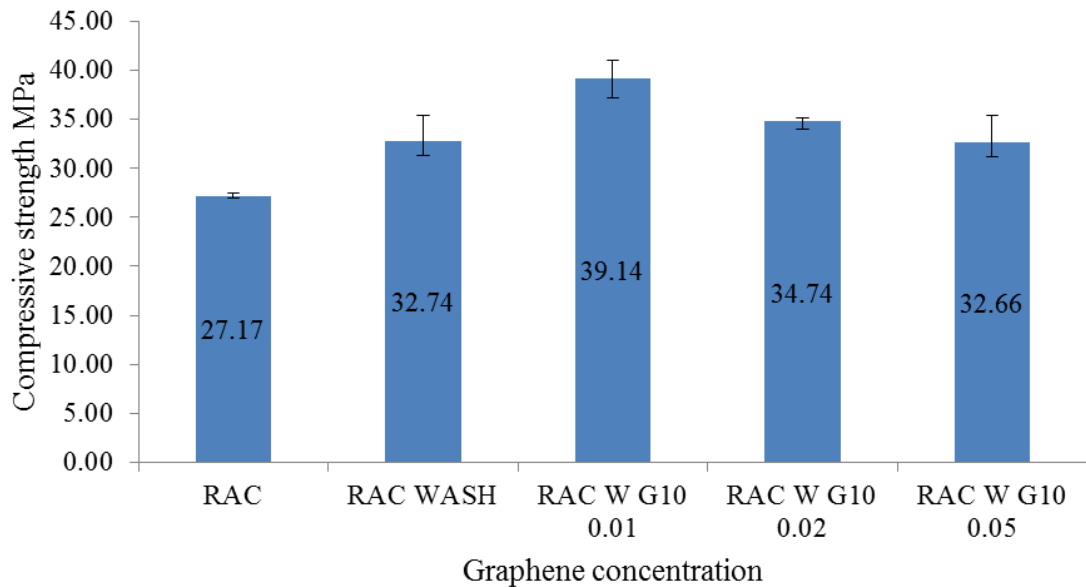
compares the test results. The errors bars in Figure 3.35 indicate very consistent results from the three samples of each mix and adding graphene did not adversely change the consistency. With 0.01% graphene, there was a very small increase (8.1%) in compressive strength of the natural aggregate concrete. However, increasing the amount of graphene in concrete did not yield any further improvement. In fact, the concrete strength was slightly lower than that without graphene.



NACG10 0.01, 0.02 and 0.05*- Natural aggregate concrete with 0.01%, 0.02% and 0.05% of size 10um graphene powder solution

Figure 3.35 Effects of different graphene concentrations on the compressive strength of natural aggregate concrete

As explained earlier, crumb rubber and the excessive amount of dust in recycled aggregates prevented graphene from being of any use in enhancing the mechanical properties of rubber recycled aggregate concrete. Further tests were conducted on recycled aggregate concrete with washed recycled aggregates and without crumb rubber. Figure 3.36 compares the compressive strengths of various recycled aggregate concretes with washed recycled aggregates.



RAC*-Recycled aggregate concrete; RACWASH*-Washed recycled aggregate concrete; RACWG10 0.01, 0.02 and 0.05- Washed recycled aggregate concrete with 0.01%, 0.02% and 0.05% of size 10um graphene concentration.

Figure 3.36 Effects of different graphene concentrations on the compressive strength of recycled aggregate concrete

Without any graphene, the compressive strength (32.74 MPa) of recycled aggregate concrete with washed aggregates was higher than that (27.2 MPa) with unwashed aggregates by 20%. However, this increase is still not sufficient to achieve the target natural aggregate concrete strength of 40 MPa. By adding 0.01% G10 graphene to the washed recycled aggregate concrete, the compressive strength was further enhanced by 20% (from 32.74 to 39.14 MPa). Although the value of 39.14MPa is still slightly lower than that of the natural aggregate concrete (42.2MPa in Figure 3.35), the difference is now very small, demonstrating the potential of adding a very small amount of graphene to enhance the compressive strength of recycled aggregate concrete to the level when it can be used to directly replace concrete using natural aggregates.

Further increasing the amount of graphene (0.02%, 0.05%) did not result in any noticeable improvement in the compressive strength of recycled aggregate concrete. This suggests that there is an optimal graphene dosage. For the type of graphene and concrete used in this research, the optimal level appears to be 0.01% of G10 by weight

of cement/sand. However, the optimal level of graphene may be different for different concrete mixes and graphene type. Therefore, tests will need to be carried out for any new mix design. The results observed in this study regarding the trend of increase in compressive strength are comparable to those of [140] as discussed in Section 2.9 of Chapter 2. Although the increase in compressive strength of recycled aggregate concrete, due to the use of graphene, is modest, this increase allows the recycled aggregate concrete to achieve nearly the same strength as natural aggregate concrete. However, the type and quantity of graphene used should be further studied because the use of graphene may lead to reductions in the mechanical properties of recycled aggregate concrete. The trend of recycled aggregate concrete compressive strength in Figures 3.35 and 3.36 is attributed to the stability of the dispersed graphene used in the concrete mix, and this was also observed in the study of [159] on cement composites using graphene.

Obviously, for practical consideration of adding graphene (which is a very expensive material) to recycled aggregate concrete (which is a very low cost material), the total cost should not exceed the cost of making the same grade of concrete using normal aggregates. The practices introduced in the current research (0.01% by weight of sand/cement, and washing recycled aggregates by agitating them in reused water) are not onerous. However, the main benefit of using recycled aggregates to replace natural aggregates is the massive reduction in environmental damage of making and transporting natural aggregates.

3.8.2.3: Tensile strength of RAC/NAC with and without graphene solution

Tensile tests were carried out only for the natural aggregate concrete and for recycled aggregate concrete with washed recycled aggregates because it was concluded that adding graphene to recycled aggregate concrete with unwashed recycled aggregates could not be pursued further.

Figure 3.37 and 3.38 compare tensile strengths for natural aggregate and recycled aggregate concretes. The results of the three samples are consistent based on the error bars showing the range of values. Figure 3.39 shows the standard deviation of the

splitting tensile strength of natural aggregate concrete of different studies compared to the current experimental results. The results are comparable.

The findings for natural aggregate concrete are similar to those of recycled concrete for compressive strength - adding 0.01% of G10 graphene provided a moderate level of increase, but adding more graphene resulted in a negligible improvement in concrete strength.

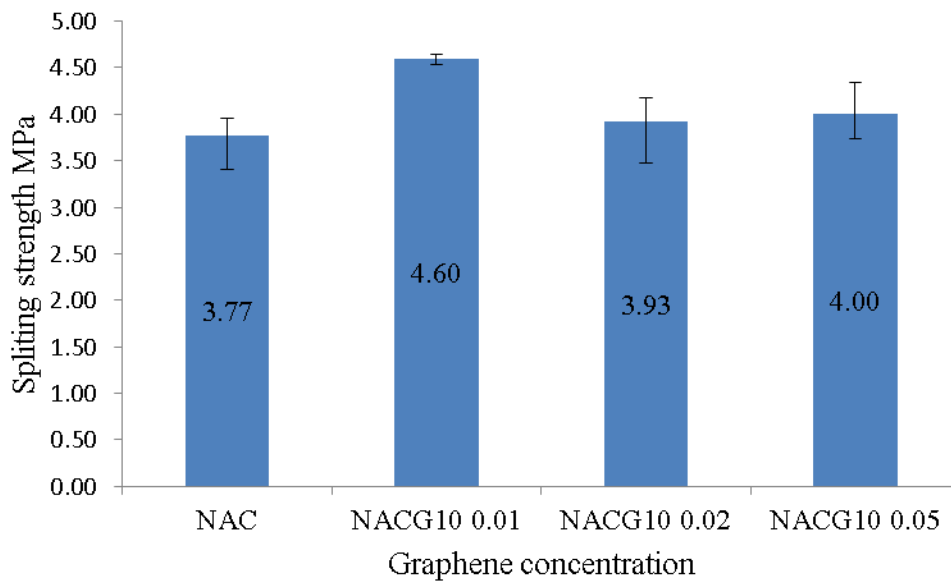


Figure 3.37 Effect of different graphene concentrations on the tensile strength of natural aggregate concrete.

Adding 0.01% G10 graphene to washed recycled aggregate concrete increased the tensile strength by 19.7% (from 3.14 to 3.76 MPa). The enhanced tensile strength is now almost identical to that achieved by the natural aggregate concrete (3.8 MPa in Figure 3.37), indicating that it is now possible to replace the natural aggregate concrete. Adding more graphene did not result in any additional increase in the tensile strength of concrete.

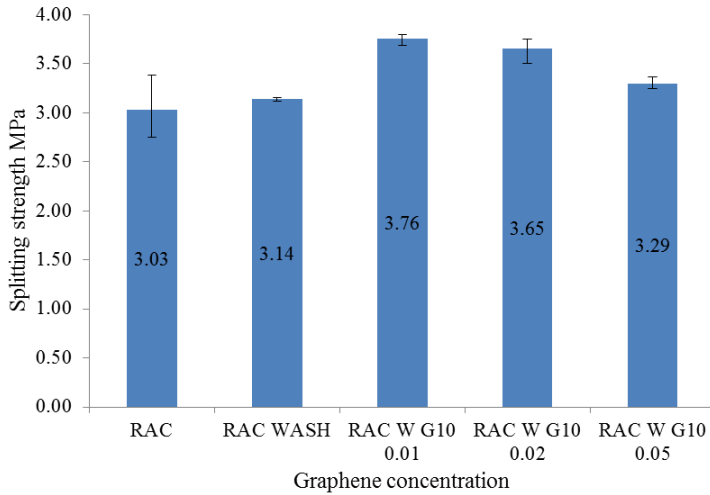
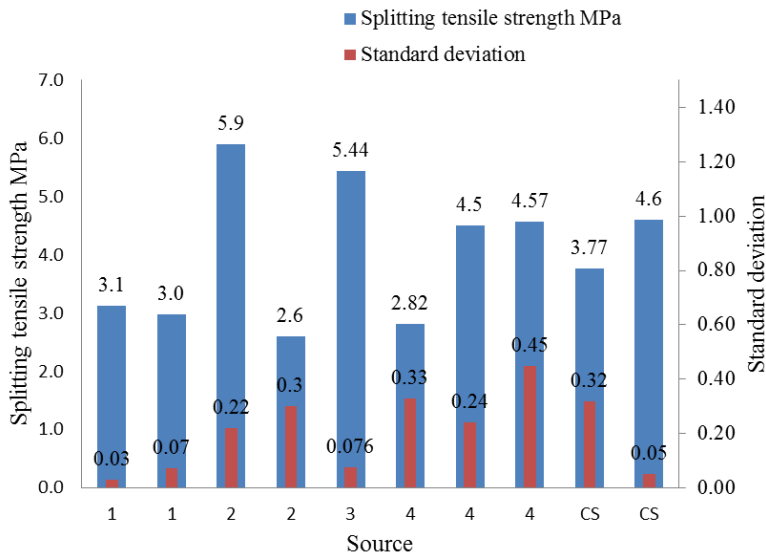


Figure 3.38 Effect of different graphene concentrations on the tensile strength of recycled aggregate concrete.



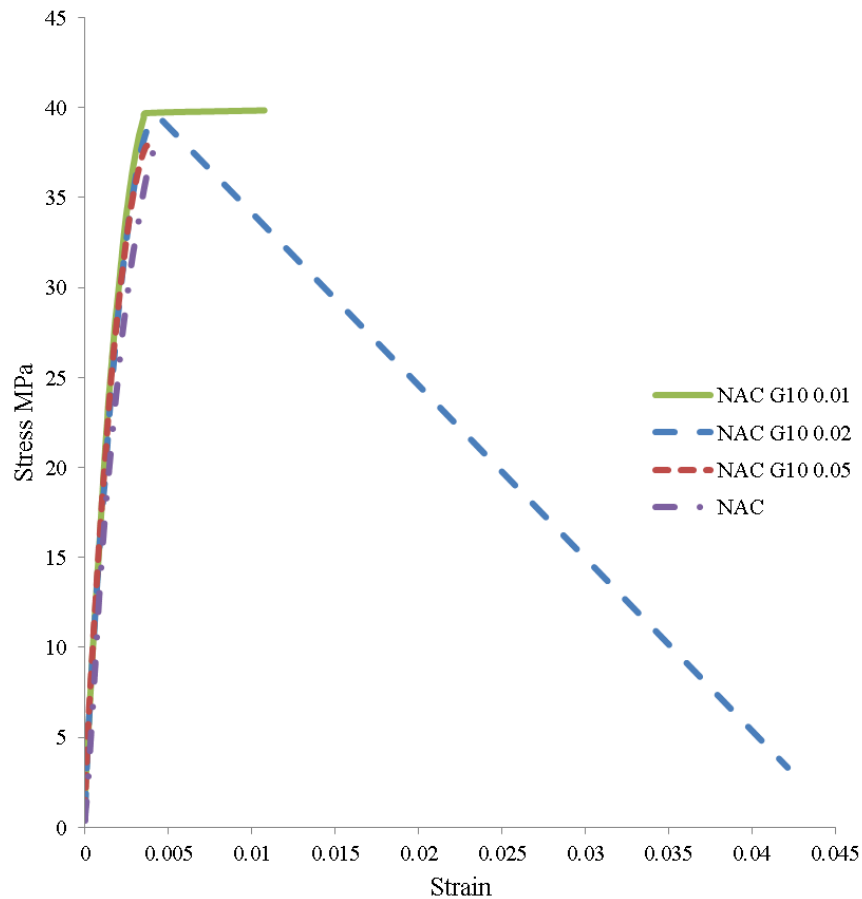
cs*-current studies.

Figure 3.39 Splitting tensile strength and standard deviation of natural aggregate concrete compared to current studies 1[160]; 2[161];3[61];3[162]

3.8.2.4: Stress strain curves

Figures 3.40 and 3.41 compare uniaxial compressive stress-strain curves of the natural aggregate concrete and recycled concrete mixes respectively containing different concentrations of graphene at 28 days. Strain gauges of 85mm gauge length were

attached on both sides of the cylinders. Due to the test setup, it was difficult to obtain the descending part of the stress-strain curve. Once the loaded cylindrical specimen cracks at ultimate strength, the attached strain gauge loses its grip on the specimen, resulting to unrealistic readings. Therefore, only information about initial stiffness is usable.

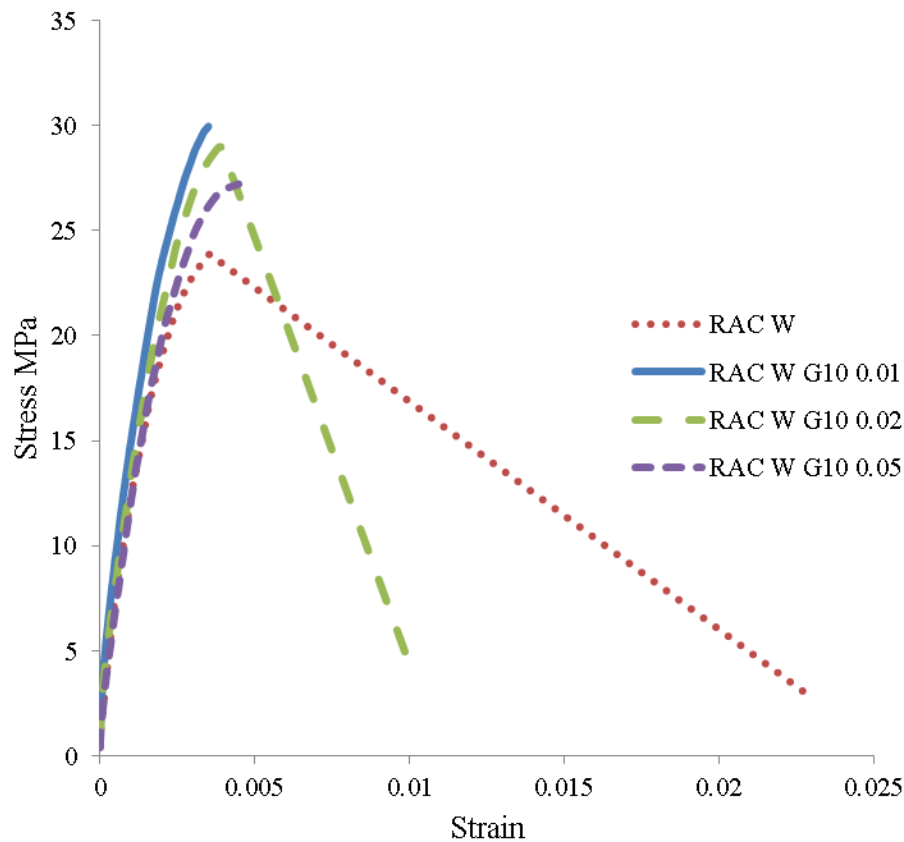


*NAC G10 0.01, NAC G10 0.02 and NAC G10 0.05 are natural aggregate concrete with 0.01, 0.02 and 0.03 graphene concentration of cement/sand weight.

Figure 3.40 Stress strain curves of natural aggregate concrete with different graphene concentrations

For recycled aggregate concretes, adding 0.01% of graphene increased the initial stiffness value by 25.1% compared to the mix without graphene. The stiffness at 40% of

the compressive strength of the washed recycled concrete with 0.01% of graphene is 32.4% more than that of the natural aggregate concrete without graphene.



*RAC W G10 0.01, CC G10 0.02 and CC G10 0.05 are recycled aggregate concrete with 0.01, 0.02 and 0.03 graphene concentration of cement/sand weight.

Figure 3.41 Stress strain curves of washed recycled aggregate concrete with different graphene concentrations

The results of the three samples of each mix for both the natural and recycled aggregate concrete with graphene concentrations are shown in Table D1 to D5 and Figure D1 to D7 of Appendix D .

3.8.3 Cost of implication of graphene in a cubic meter of concrete

For a cubic meter of concrete shown in Table 3.10, the optimal amount of graphene is required to enhance concrete compressive and splitting tensile strength 0.01% of the

total amount of cement and sand. The weight of the graphene required is estimated as follows:

$$\text{Weight of graphene (kg)} = (0.01/100) \times (360+732) = 0.109\text{kg}$$

The cost of graphene having 4-7 layers is currently at £40 per kg. Hence, the cost of graphene required for a cubic metre of concrete is £4.36. The current cost of a 40MPa natural aggregate concrete in the UK is £125.03 [163]. Therefore, the graphene reinforced concrete will add up to £129.39. Apart from the benefit of enhancing strength, graphene also enhances concrete durability [45] as discussed in the review of Chapter 2 but not covered in this study. Also, adding £4.36 worth of graphene to enhance cheap recycled aggregate concrete strength of 27MPa to 39.19MPa for structural applications is beneficial in terms of increasing the use of recycled aggregates for a green environment. With the large scale use of graphene, the cost of graphene recycled aggregate concrete will further decrease

Small amounts of polycarboxylate super plasticisers (SP) are used to disperse graphene before being incorporated into concrete. The amount of SP needed is equivalent to half the weight of graphene. Therefore, a cubic metre of concrete containing 0.109kg of graphene will require 0.055kg of SP for dispersion. The cost of 1kg of polycarboxylate SP (ADVA650) from GCP Applied Technologist (UK)Ltd is £1.98; hence £0.11 SP is required to disperse graphene for a cubic metre of concrete.

3.8.4 Conclusions

The results of this investigation suggest that it is possible to use graphene to enhance the mechanical properties (compressive and tensile strengths) of recycled aggregate concrete. The recycled aggregates should be washed. If the recycled aggregates are not washed, the excessive amount of dust prevents graphene from bonding with the aggregates at their interfaces. This study did not conduct any microscopic analysis of the graphene influence on the concrete matrix; however [46, 164] have proved that graphene reshapes the microstructure of cement matrix and accelerates the hydration reaction to increase its efficiency. The washing of the recycled aggregates could be

easily done and it was not necessary to use clean water. Crumb rubber had a similar effect as dust in preventing graphene from bonding with aggregates, so should not be used if the use of graphene is considered.

The optimal graphene for this research is G10 at 0.01% by weight of cement and sand. Adding more graphene did not achieve any further increase in the mechanical properties of fresh concrete or recycled aggregate concrete.

The highest increases in the mechanical properties of recycled aggregate concrete with washed aggregates and without crumb rubber, due to the washing and addition of graphene, are 30.5% (from 27.2 to 39.14 MPa) and 19.4% (from 3.03 to 3.76 MPa) for compressive strength and tensile strength respectively. The improved properties are very similar to those of natural aggregate concrete (42.2MPa and 3.8 MPa) respectively, indicating that recycled aggregate concrete can be used to replace natural aggregate concrete.

The process of preparing recycled aggregates to achieve the abovementioned high performance is not time-consuming and the additional cost is small, making it economically viable. However, the main benefit is reduction in environmental damage in producing natural aggregates.

Chapter 4

Experimental study of bending and shear behaviour of two-layer beams

4.1 Introduction

This chapter reports the results of bending and shear experiments to demonstrate the effects of placing RRAC in the tension region of reinforced concrete beams on their bending and shear resistance and to provide experimental data for validation of numerical modelling (Chapter 5).

4.2 Specimen design

A total of eight simply supported regular reinforced concrete beams were tested, consisting of six tests for assessment of bending resistance (bending tests) and two tests for assessment of shear resistance (shear tests).

Figure 4.1 shows the overall dimensions of bending test beams. The bending test beams were designed to fail under flexure bending according to EC2 [125]; therefore, they were provided with transverse reinforcement to prevent shear failure. The cross section of all beams is 150mm width and an overall depth of 150mm. The concrete cover to the bottom longitudinal reinforcement for all beams was taken as 10mm. The width and thickness of the support plate is 75mm by 50mm. In the two-layer beams (for both bending and shear tests), the top 50mm of concrete was made of natural aggregate concrete and the bottom 100mm of concrete was of recycled concrete, as shown in Figure 4.1. According to calculations using EC2 [125], the plastic neutral axis is just above the interface of the two different types of concrete, so the recycled concrete is entirely in the tension zone.

A longitudinal reinforcement ratio of 2.03% was used for all beams in bending: consisting of two 16mm diameter ribbed bars at the bottom and two 8mm diameter rebar bars at the top.

Figure 4.2 shows the shear test beam dimensions. The chosen specimen size and reinforcement arrangement were determined to ensure shear failure. The shear span depth ratio was 3.4. Only four shear links were provided as hanger bars located at the support and loading positions. The shear test beams were designed to preclude flexural failure, which was ensured by a longitudinal reinforcement ratio of 2.64% at the bottom. The beam size in Figure 4.2 having a shear span to depth ratio of 3.4 is slender; hence it is expected to fail with an inclined cracking load along the shear span since no web reinforcements are provided.

CHAPTER 4. EXPERIMENTAL STUDY OF BENDING AND SHEAR BEHAVIOUR
OF TWO LAYER BEAMS

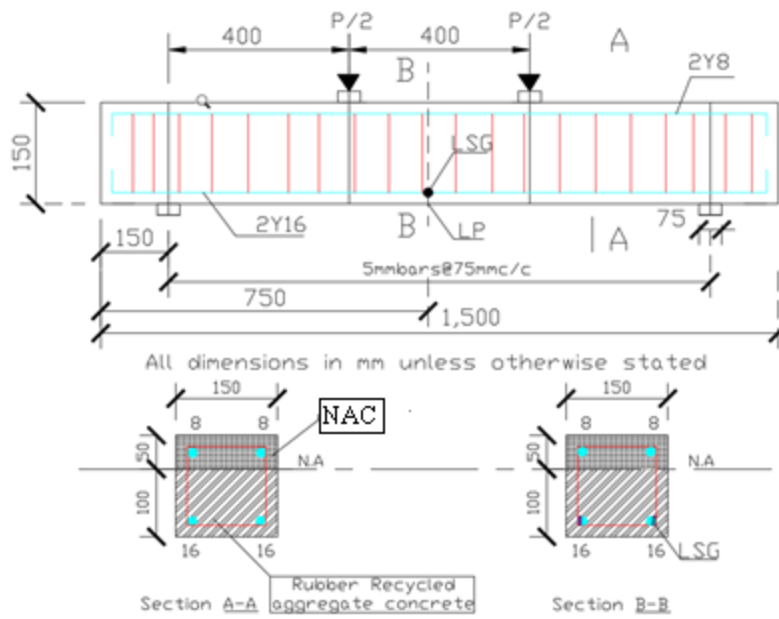


Figure 4.1 Dimensions of two-layer beam for bending tests

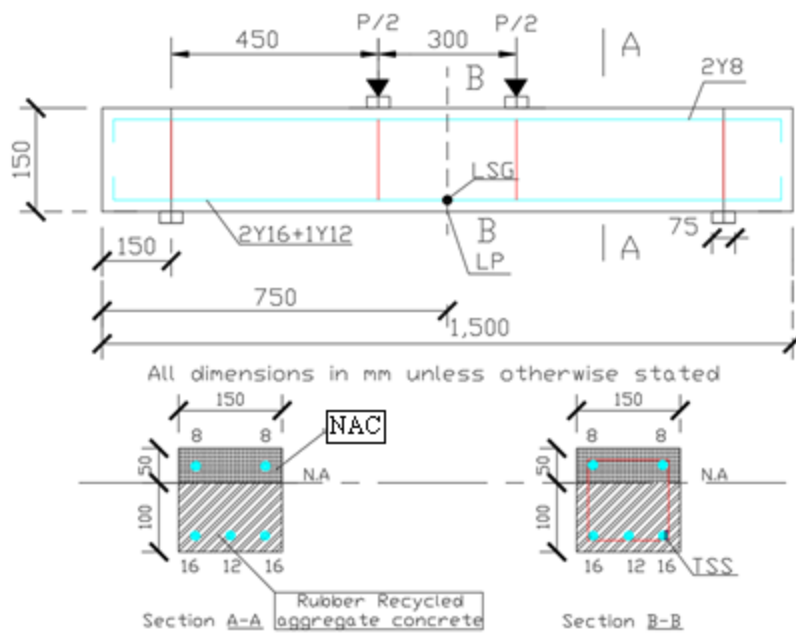


Figure 4.2 Dimensions of two-layer shear test beams

4.3 Concrete mix and properties

The target grade for the natural aggregate concrete was 40MPa compressive cylinder strength. Table 4.1 compares material compositions of the natural aggregate concrete (NAC) and the rubber recycled aggregate concrete with 10% replacement of recycled aggregates by crumb rubbers (RRAC10). The recycled concrete composition for this study was selected based on the results of the different mixes made to meet the workability and mechanical properties for structural applications. Additional water was added to the recycled concrete to compensate for the excessive water absorbed by the recycled aggregates in Table 3.1 of the previous chapter. The added water was carefully measured based on the amount of water absorbed (4.21%) by the recycled aggregates (RA1) in order to maintain the same free water cement ratio with NAC mix. From the series of mix designs made, this research also used super plasticiser (DARACEM 215) of 1% of cement weight to meet the workability requirement of the proposed recycled concrete due to the added crumb rubber. The size of both the recycled aggregates (RA1) and natural aggregate is 10mm from the sieve analysis conducted in Figure 3.1 of Chapter 3. The composition of the recycled aggregates (RA1) is also shown in Table 3.2 of Chapter 3. The natural aggregates are 10mm quartzite stones with a water absorption rate of 1.05%.

Table 4.1 Mix composition of natural aggregate concrete and rubber recycled aggregate concrete with 10% of rubber particles of recycled aggregate weight (RRAC10) per m³

| Specimen designation | Cement (kg) | Water (kg) | | w/c* ratio | Natural aggregates (kg) | Recycled aggregates (kg) | Fine sand (kg) | Crumb rubber (kg) | SP (kg) |
|----------------------|-------------|------------|-------|------------|-------------------------|--------------------------|----------------|-------------------|---------|
| | | free | Added | | | | | | |
| NAC | 550 | 220 | - | 0.4 | 939 | - | 626 | - | - |
| RRAC10 SP | 550 | 220 | 39.5 | 0.4 | - | 845.1 | 626 | 93.9 | 5.5 |

*NAC-Natural aggregate concrete; *RRAC10SP-Rubber recycled aggregate concrete with 10% of recycled aggregate weight as crumb rubber, *SP-Super plasticiser

The crumb rubbers were supplied by SRC products Ltd, Stockport in the United Kingdom. They were free from wire strings with an average length and thickness of 8mm and 2mm respectively as shown in Figure 4.3 (c). They were not pre-treated

CHAPTER 4. EXPERIMENTAL STUDY OF BENDING AND SHEAR BEHAVIOUR
OF TWO LAYER BEAMS

before being incorporated into the concrete mix. The recycled aggregates (RA1) were supplied from the commercial market (Offerton sand and gravel, Manchester) within the UK comprising other debris (bricks, glass, and tiles) in Figure 4.3(a). The 10% of rubber particles of the recycled aggregate weight was carefully selected in order to maintain the basic mechanical properties of the recycled concrete for structural application and the bond strength existing between rebar and recycled concrete in tension as recommended in Chapter 3 of this thesis.

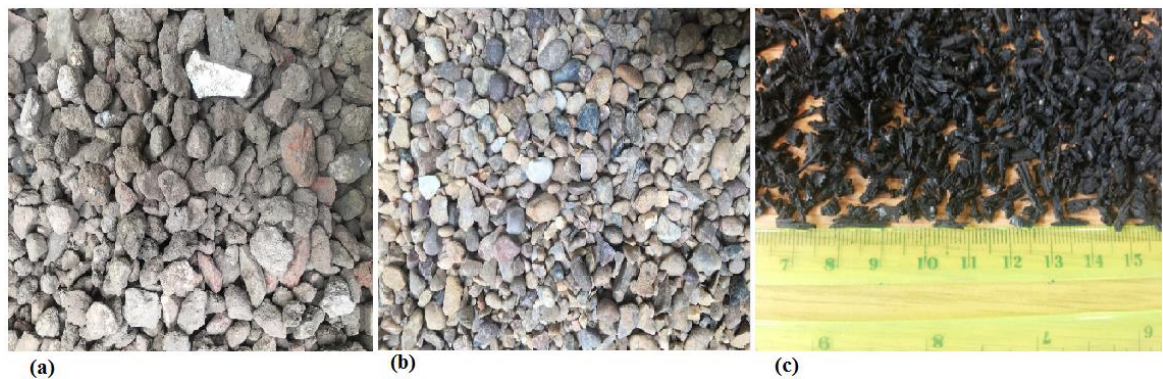


Figure 4.3(a) Recycled aggregates (b) Natural aggregates (c) crumb rubber from worn-out tyres.

Table 4.2 compares the wet and hardened concrete properties between natural aggregate concrete and rubber recycled aggregate concrete for the bending and shear test respectively.

Table 4.2 Properties of fresh and hardened concrete for bending and shear tests

| Mix type | Slump mm | 28 days cylinder strength MPa | Unit wt (kg) | Tensile strength MPa | UPV(km/s) |
|--------------|----------|-------------------------------|--------------|----------------------|-----------|
| Bending test | | | | | |
| NAC | 165 | 40.1 | 2.39 | 4.11 | 4.19 |
| RRAC10SP | 170 | 30.3 | 2.19 | 2.82 | 3.61 |
| Shear test | | | | | |
| CC | 165 | 41.4 | - | 4.15 | - |
| RRAC10SP | 175 | 27.0 | - | 2.6 | - |

Table 4.3 gives details of the longitudinal and shear reinforcement properties from the tensile test used for all the beams.

Table 4.3 Properties of shear and longitudinal reinforcement for all test beams

| Beam type | 16mm rebar MPa | 8mm rebar MPa | 6mm rebar MPa | 5mm rebar MPa |
|--|---------------------|------------------------|-------------------|-------------------|
| Regular concrete beam for bending tests | Y= 551 ULT=643 | Y= 547.02 ULT=666.4 | – | Y= 280 ULT=310 |
| Two layer beam for bending tests | Y= 524.1 ULT=616 | Y= 547.02 ULT=666.4 | Y= 383 ULT=466 | Y= 280 ULT=310 |
| Regular concrete and two-layer beams for shear tests | Y= 551 ULT=643 | Y= 547.02 ULT=666.4 | – | Y= 280 ULT=310 |

*Y- Yield strength; *ULT- Ultimate strength

4.3.1 Test set up and instrumentation

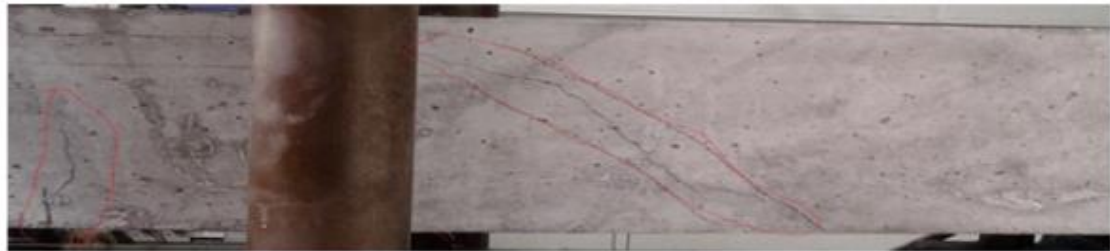
All the beams were simply supported with a span of 1.2m between the supports. The shear span (450mm) to depth (150mm) ratio was maintained at 3 to achieve the intended bending failure for all beams. The beams had an unsupported length of 150mm and the supports were made of cylindrical steel rollers of 50mm in diameter. Two actuators applied loads to create a four-point bending test. Two linear strain gauges (FLA-6-11) with a gauge length and a gauge factor of 6 and 2.13 respectively were attached to the bottom longitudinal bars at the centre of the beam to obtain reinforcement strain data. The deflection of the beam was measured at the bottom of the centre span by means of a linear potentiometer (LP). The test was displacement controlled at a rate of 0.02mm per second until failure. All beams were tested at 28 days after casting.

4.4 Results and discussions

4.4.1 Crack pattern and failure modes for bending test

Figure 4.4 shows the bending test beams after failure. In all cases, the failure mode of regular concrete beams was flexural bending, as indicated by the vertical cracks in the

pure bending region shown in Figure 4.4. The mid span and diagonal cracks on the regular concrete beams indicates combined bending and shear failure of the beam specimen. However, the tensile reinforcement reached yield, as shown in Figure 4.6 for the regular concrete beams and two-layer beams.



Regular concrete beam



Two layer beam

Figure 4.4 Failure modes of beams in bending

4.4.2 Load-deflection curves

Figure 4.5 compares load deflection curves for bending test beams. They show almost identical elastic behaviour. This indicates that the bond strength between the tensile rebars and the recycled concrete of the two-layer beams is not affected as illustrated in Section 3.6 of Chapter 3. The ultimate load carrying capacities of the two-layer beams are slightly lower than those of the regular concrete beams. This is attributed to the lower yield strength of the 16mm diameter longitudinal rebar used for the two-layer beams than those for the regular concrete beams in Table 4.3. The rebars used for the beam specimens were extracted and tested for tensile strength. However, one rebar was tested for each set of beams. The load-deflection curves in Figure 4.5 indicate that the two types of beam have very similar stiffness at a serviceability limit state load of 60%

of the ultimate load carrying capacity. The numerical results in Chapter 5 reveal that with identical materials, the bending resistances of two-layer beams are the same as those of regular concrete beams.

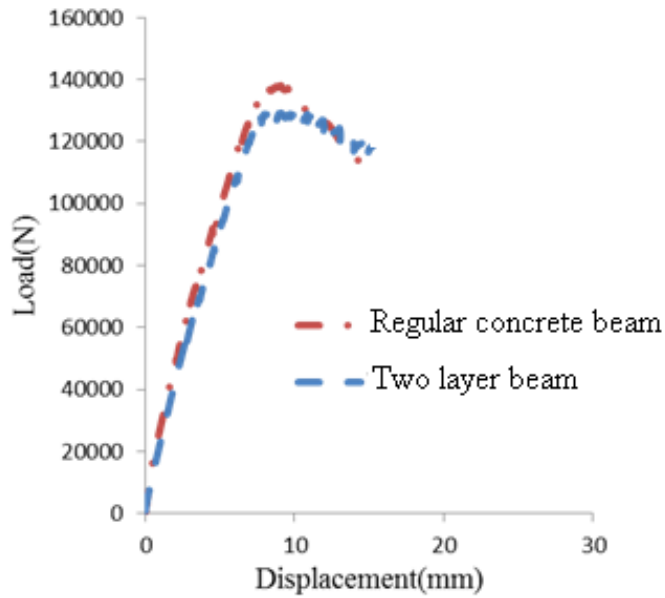


Figure 4.5 Load deflection curves of bending test beams

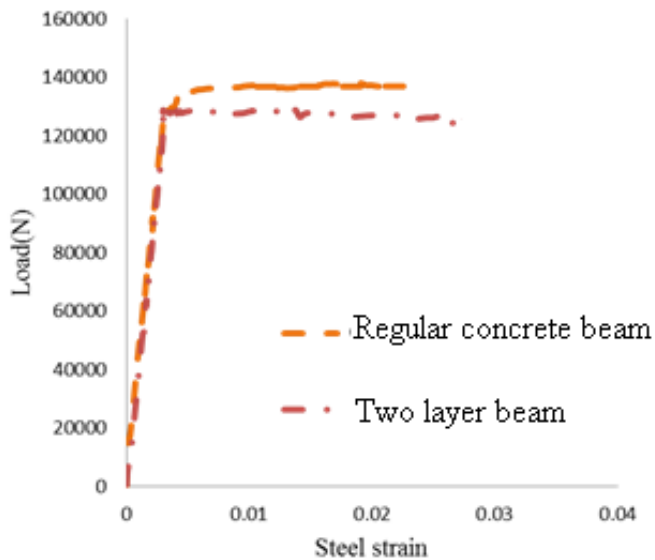


Figure 4.6 Comparison of experimental load-longitudinal reinforcement bar strain curves of bending test tests

4.4.3 Crack pattern and failure modes for shear test

The crack patterns and failure modes of the regular concrete beam and two-layer beams were the same. However, the failure modes of both beams were shear as intended, as clearly indicated by the wide diagonal cracks in the shear span shown in Figure 4.7 (a) and (b). The shear failure mode of both beams is further confirmed by the brittle response of both beams, as shown by their load-deflection curves in Figure 4.8, after peak loads are reached.



Figure 4.7 Failure modes of shear test beams

It was also observed that the interface between the recycled and the natural aggregate concrete did not fail as shown in Figure 4.7(b) for the two-layer beams. This indicates a monolithic behaviour between the concrete layers; hence the interfacial shear strength was sufficient to transfer shear forces from the bottom layer to the top layer natural aggregate concrete without shear reinforcements. It is worth pointing out that the casting of the top layer was carried out within four hours after the bottom layer was cast. As shown in Section 3.7 of Chapter 3, the interface of the concrete on recycled

concrete at a 4-hour cast time interval exhibited monolithic behaviour which is also demonstrated in Figure 4.7 (b) of the two-layer beams.

4.4.4 Load deflection plot for shear test

The ultimate load for the regular concrete beam in Figure 4.8 is 13.6% higher than the two-layer beams. This can be explained by the lower compressive and shear strength of the recycled concrete at the bottom layer of the beam compared to the natural aggregate concrete at the top layer. Once the lower strength (recycled concrete) concrete has failed in shear, it loses its shear resistance and transfers the shear force from the failed lower strength concrete to the natural aggregate concrete.

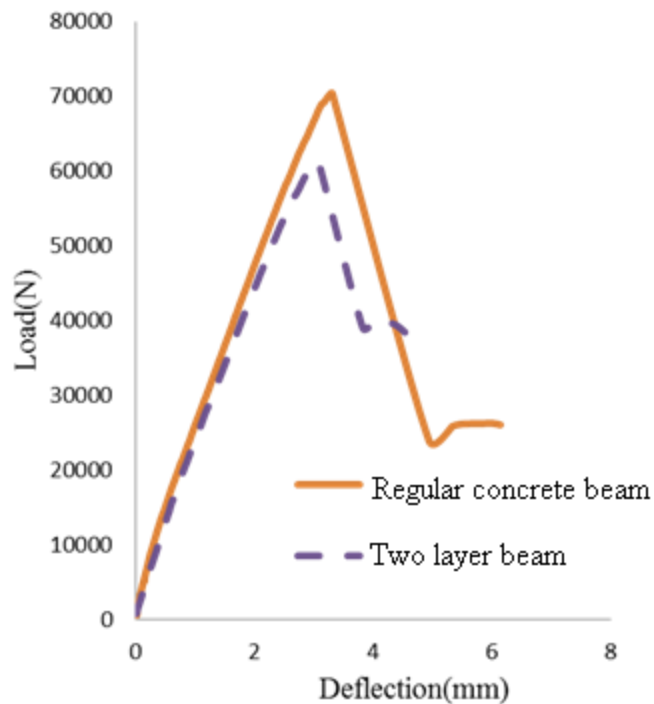


Figure 4.8 Load deflection curves for the regular concrete beams and two-layer beams of the shear test.

However, the normalized shear strength in Table 4.4 indicates identical performance of the two-layer beams compared to the regular concrete beams. The normalized shear strength is calculated using Equation 4.1 [122].

$$v_c = \frac{V}{bd * \sqrt{f_c^1}} \dots\dots\dots 4.1$$

Where v_c the normalized is shear strength and f_c^1 is the compressive strength of concrete. b and d is the width and depth of the concrete beam respectively.

The compressive strength of the recycled concrete in the tension region of the beams is used in calculating the normal shear strength. This is because the top-layer concrete does not contribute to the shear capacity of the two-layer beams. This assertion will be validated in Chapter 5 of this thesis.

Table 4.4 Results of beam tests

| Beam type | Ultimate shear Load KN | Normalized shear strength | Failure mode |
|-----------------------|------------------------|---------------------------|--------------|
| Regular concrete beam | 70.5 | 0.25 | shear |
| Two-layer beam | 60.9 | 0.26 | shear |

In summary, the unzipping effect from the failed recycled concrete at the bottom of the concrete beams constitutes the low shear capacity of the two-layer beams compared to the regular concrete beams. However the normalized shear strength predicts identical performance of both beams as shown in Table 4.4.

An ABAQUS validated model in Chapter 5 is used to run a series of parametric studies on the behaviour of the two-layer beams in bending and shear.

4.5 Summary and Conclusions

The experimental results of the two-layer beams in bending are similar to those of the regular concrete beams; however exhibits lower resistance in shear. The lower shear strength of the two-layer beams was attributed to the unzipping effect of the failed low grade concrete in tension. However, more parametric studies will be conducted in Chapter 5 using a validated model in ABAQUS to enhance the understanding of the two-layer beams in bending and shear.

Chapter 5

Validation of Numerical Modelling and parametric study

5.1 Introduction

This chapter reports the results of numerical modelling of reinforced concrete beams with a layer of RRAC (with or without rubber crumb) in the tension layer. This includes validation of the simulation model by comparison against the experimental results in Chapter 4 and a series of parametric studies to investigate the effects of different parameters (natural and recycled concrete strength, top and bottom layer thickness ratio, reinforcement ratios, shear span to depth ratio) on the bending and shear behaviour of two-layer beams. The results (experiments and numerical) of the two-layer beams are assessed against the EC2 method of design in bending and shear. The chapter also validated a numerical model of RC beam with published experiments [44] as part of the sensitivity study with respect to material models to be used in this study.

5.2 Finite element modelling using ABAQUS

The general finite element software ABAQUS 6.13 was used to carry out numerical simulations to help in explaining the behaviour of the two-layer beam and to extend the scope of the limited experiments.

To validate the ABAQUS model, all the bending and shear tests were simulated. In the ABAQUS model, concrete was modelled with C3D8R SOLID elements comprised of eight nodes with three degrees of freedom at each nodal point as shown in Figure 5.1. This type of element can be used to model linear and nonlinear behaviour involving contacts, plasticity, cracking, crushing and large deformations. For both longitudinal and shear reinforcements, beam elements were used and embedded in solid concrete elements. The beam elements have two nodes with three degrees of freedom at each node as shown in Figure 5.1. The interface between the two concrete layers is modelled as a perfect contact. The perfect contact is assumed based on the results shown in Figure 3.27 (b) and 4.7 (b) of Chapter 3 and 4 respectively. The concrete interface cast at four-hour intervals behaves monolithically in the slant shear tests in Chapter 3 and also replicates the same behaviour in the two-layer beams cast at 4-hour intervals. Therefore a tie constraint in the ABAQUS model is used in connecting the two layers of concrete at the interface.

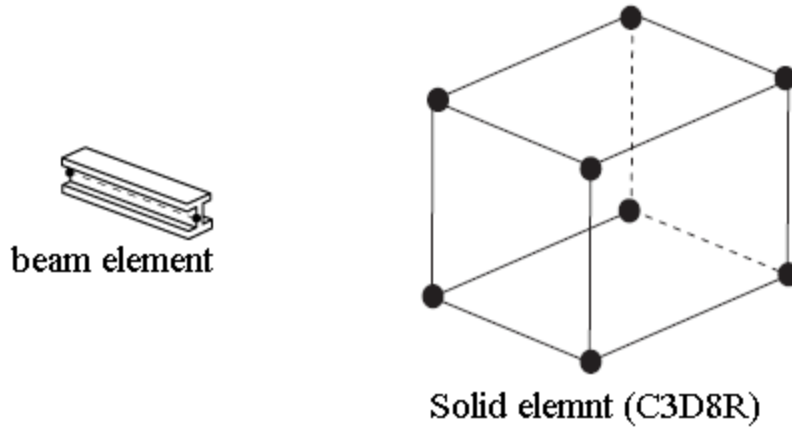


Figure 5.1 Element types for concrete and steel reinforcement [165]

5.3 Material properties and constitutive models

The concrete damage plasticity (CDP) model was used for defining the behaviour of concrete in the inelastic range. The main failure criteria of the concrete damage plasticity model are tensile cracking and compressive crushing of concrete. This model assumes linear uniaxial compressive behaviour up to the initial yield point followed by the plastic range characterizing the stress hardening and strain softening after peak stress. The uniaxial stress strain relationship is converted to true stress and plastic strain using Equations 5.1 and 5.2.

$$\sigma_{true} = \sigma_{engineering} * (1 + \epsilon_{engineering}) \dots \dots \dots 5.1$$

$$\epsilon_{In}^{plastic} = \ln(1 + \epsilon_{engineering}) - \frac{\sigma_{true}}{E} \dots \dots \dots 5.2$$

CHAPTER 5. VALIDATION OF NUMERICAL MODELLING AND
PARAMETRIC STUDY

Where σ_{true} and $\epsilon_{In}^{plastic}$ is the true stress and plastic strain respectively. $\sigma_{engineering}$ is the engineering stress, $\epsilon_{engineering}$ is the engineering strain, E is the modulus of elasticity. $\ln(1 + \epsilon_{engineering})$ represents the total strain and $\frac{\sigma_{true}}{E}$ is the elastic strain (recoverable part of the strain).

This numerical simulation defined the uniaxial compressive stress strain curves of both the natural aggregate concrete and rubber recycled aggregate concrete, based on the experimental test. They were then converted into true stress-plastic strain curves based on Equation 5.1 and 5.2.

After cracking, concrete retains a small amount of tensile strength normal to the direction of crack. This phenomenon is called tensile stiffening. In this study, the tensile stiffening action of concrete is accounted for by defining the stress crack opening curve as specified in [131] as shown in Figure 5.2. The stress crack opening is chosen in this study because it is able to simulate the tensile behaviour of the concrete cracked sections. The bilinear descending branch of the CEB code model in tension simplifies the parabolic behaviour as defined by [166].

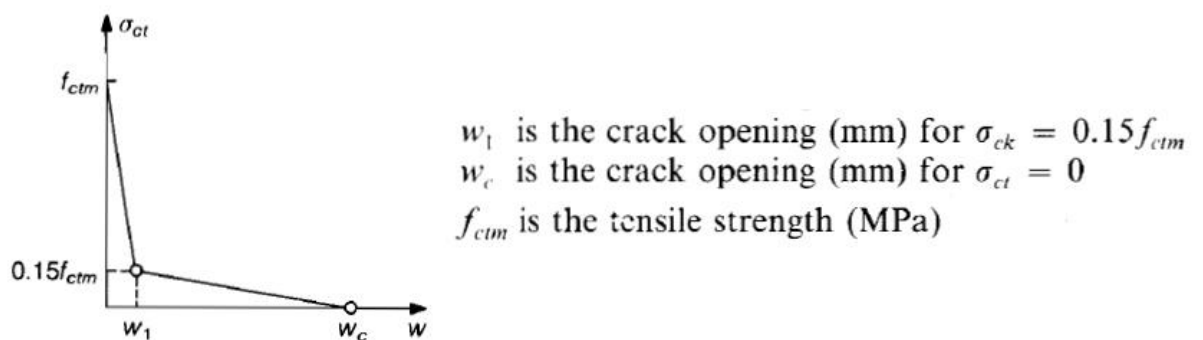


Figure 5.2 Stress crack opening width curve for cracked concrete [131]

The post peak behaviour of the stress crack opening is assumed to be bilinear and fracture energy is required for defining the model parameters. The fracture energy of the concrete was determined based on the provisions made in [115] and is defined as the energy required to propagate a tensile crack per unit area as given in Equation 5.3.

$$G_F = G_{FO} \left(\frac{f_{cm}}{f_{cm0}} \right)^{0.7} \dots\dots\dots 5.3$$

Where f_{cm} is the compressive strength of concrete and f_{cm0} taken as 10MPa. The G_{FO} is the base value of the fractured energy which depends on the maximum size of the aggregate concrete mix. Linear interpolation was adopted to predict the base fracture energy in this study. The detail calculation of the fracture energy is shown in E1 of Appendix E.

The steel reinforcement bars were modelled as elastic perfectly plastic material embedded in concrete for all the validated models.

5.4 Validation of finite element model with published experiment [44]

This simulation model was also validated by comparison against reinforced concrete beams under bending published by others, as shown in Figure 5.3. The longitudinal reinforcement ratio was 0.67% and shear links were used to ensure flexural failure and to avoid shear failure of the beam. After casting, the specimens were cured for 28 days prior to testing.

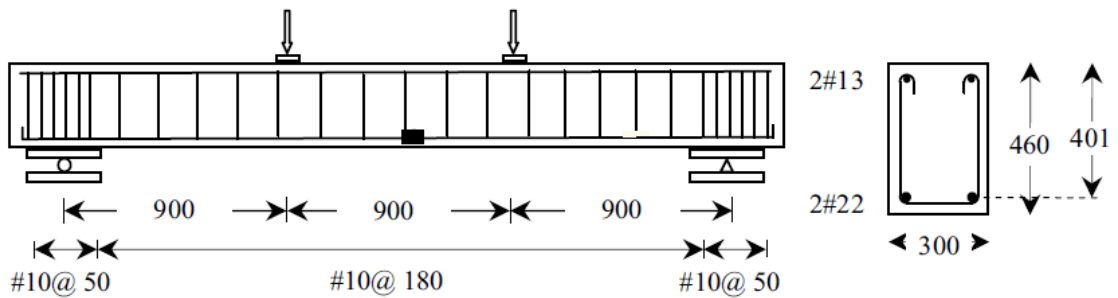


Figure 5.3 Cross section and reinforcement layout of flexural beam test [44]

The material properties of the steel and concrete are presented in Table E1 and E2 of Appendix E. The concrete and steel models used for the numerical model are the same as those explained in Section 5.3. However, the EC2 model [113] was used to define the behaviour of the uniaxial compressive stress strain curve of the concrete because of the unavailability of experimental data.

The mesh density (35mm) of the 3D solid element (concrete) and the embedded beam elements (reinforcement) for the reinforced concrete beam are shown in Figure 5.4

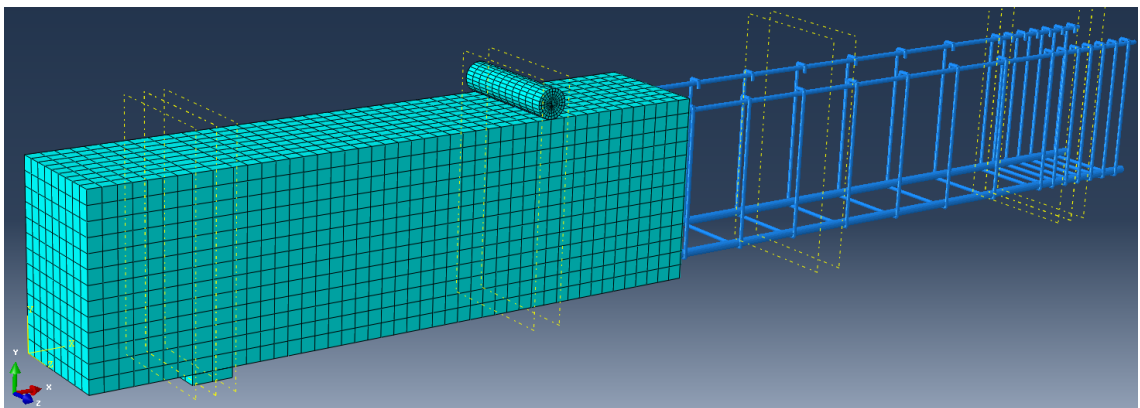


Figure 5.4 Geometry and Mesh density of the test beam [44]

Figure 5.5 shows the load deflection plot at mid span for the experiment and numerical simulation. Figure 5.5 shows good agreement between the numerical and experimental results at the linear range. However, higher stiffness is shown for the numerical results

compared to the experimental results beyond the cracking load. This may be attributed to the assumed perfect bond between concrete and steel bar for the numerical model. Also micro cracks resulting from drying shrinkage and poor handling of the beam could have reduced stiffness of the test beam to some degree which could not be accounted for in the numerical model. Figure 5.6 compares load – reinforcement bar tensile strains at mid span. Again the correlation is good prior to cracking load but more tensile strains in the reinforcement are shown in the experiment beyond the cracking load.

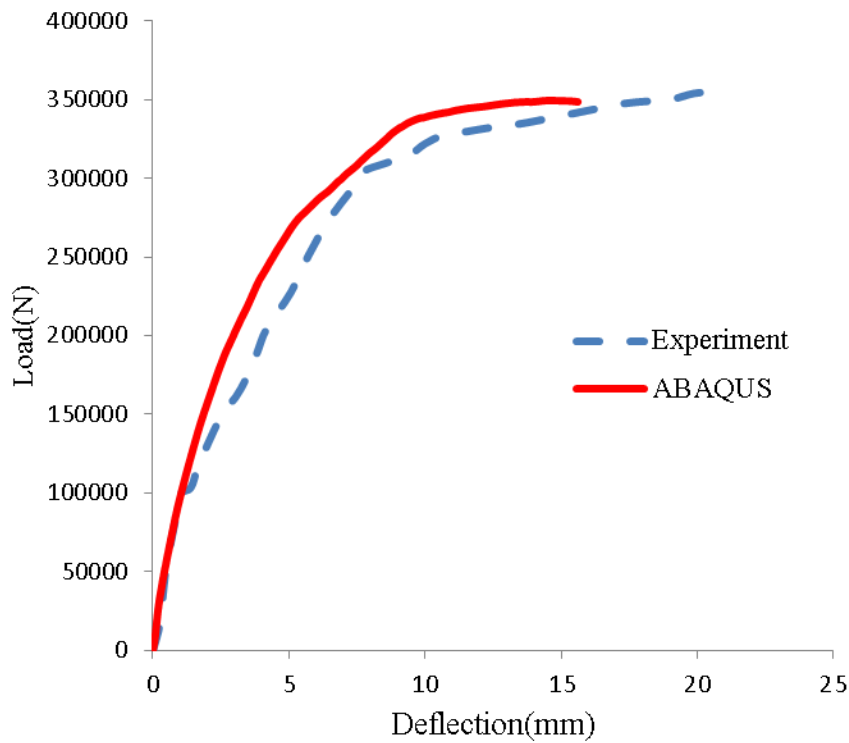


Figure 5.5 Comparison between load deflection plots at mid span between the experiment of [44] and the author's ABAQUS simulation

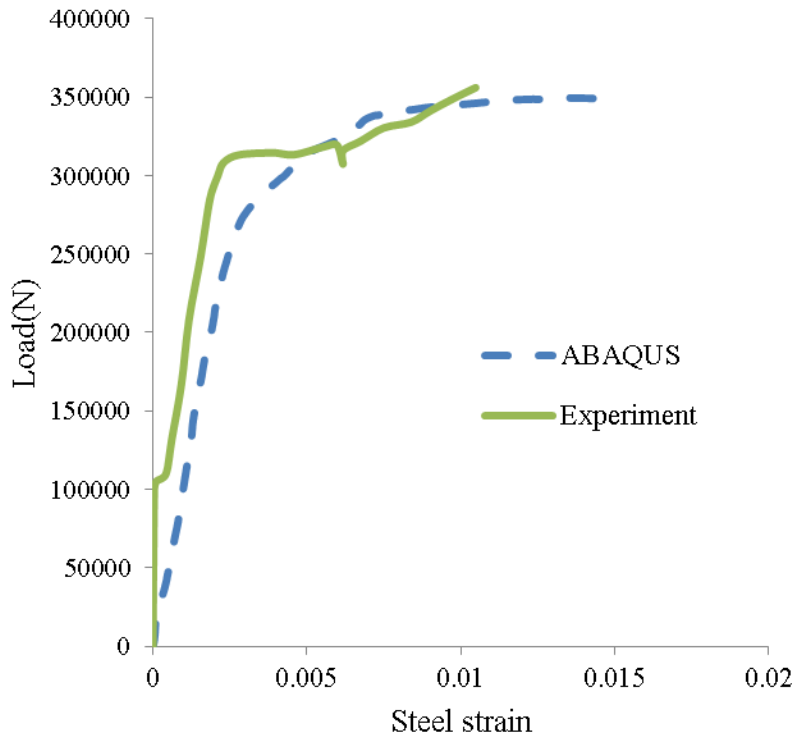


Figure 5.6 Comparison of load tensile strain plots for the main reinforcement bar [44]

5.5 Finite element discretization for this study

A mesh sensitivity test was carried out to determine the most appropriate mesh density for the simulation model. Figure 5.7 compares the mesh sensitivity study results. Accordingly, a mesh size of 15mm was chosen. Mesh sizes 10 to 20mm give the same bending performance based on the load deflection plots. The resulting mesh density is shown in Figure 5.8.

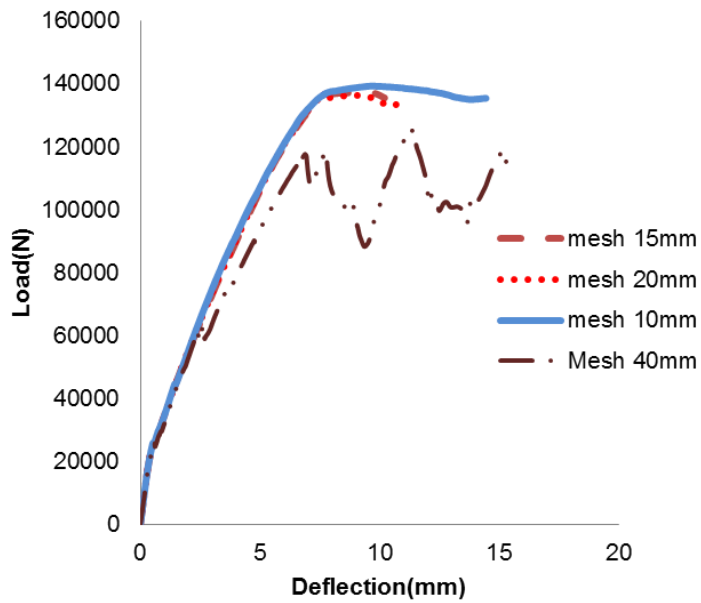


Figure 5.7 Results of mesh sensitivity analysis of regular reinforced concrete beam

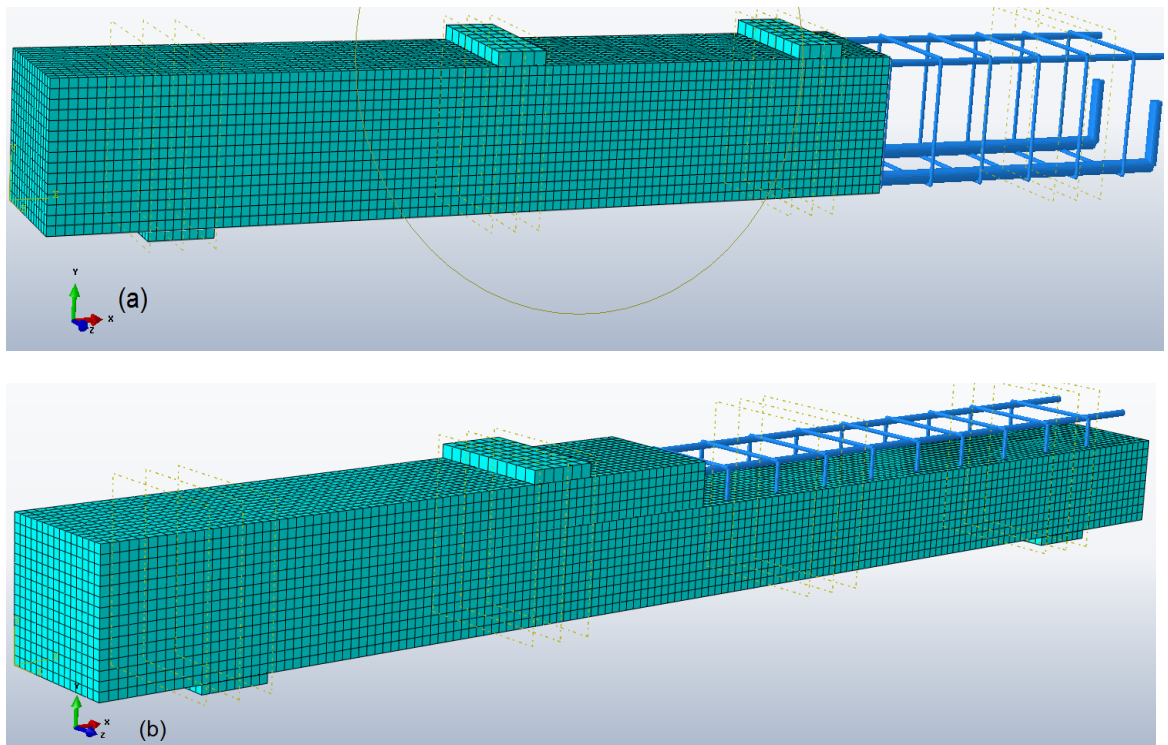


Figure 5.8 Geometry and mesh density of (a) Regular concrete beam (b) Two-layer beam

5.6 Comparison between ABAQUS numerical simulation results with experimental results

5.6.1 Load deflection curves at mid-span

Figure 5.9 and Figure 5.10 compare the experimental and numerical simulation results of the load-deflection curves for both the regular concrete and two-layer beams for the bending and shear test respectively. The simulation results include some post-peak results to ensure that the numerical models reached full capacities of the beams. Agreements between the experiment and simulation results are very good. The results of the regular concrete beams are higher than those of the two-layer beams because of the variability of the yield strength of the steel bars used for the tests and numerical simulations. This is attributed to the fact that an increase in the yield strength of steel decreases the ultimate beams curvature and enhances the moment of resistance [167]. As illustrated in Section 5.6, with identical material properties, the bending capacity of all RC beams is the same.

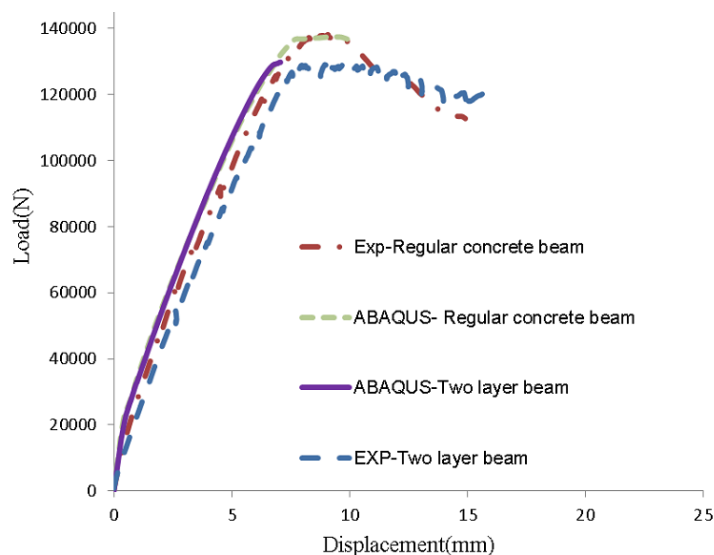


Figure 5.9 Comparison of experimental and numerical load deflection plots for regular concrete beams and two-layer beams in bending

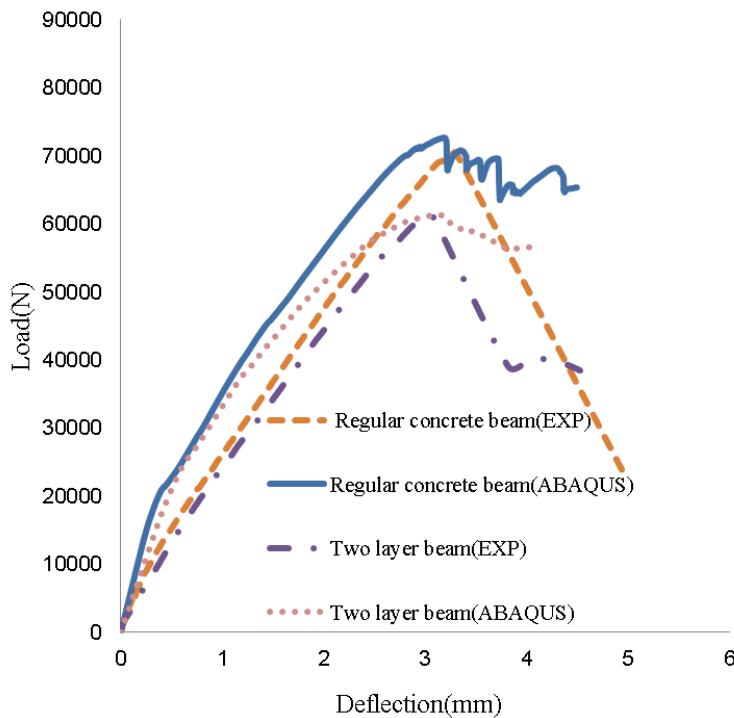


Figure 5.10 Comparison of experimental and numerical load-deflection plots, for regular concrete beams and two-layer beams in shear

5.6.2 Tensile strain in longitudinal reinforcement

Figure 5.11 and Figure 5.12 compares the numerical simulation and experimental results for tensile strain of the bottom reinforcement at the mid-span of beams. There is good correlation for both the regular concrete beams and two-layer beams. The reinforcement for all beams fully reached its yield strain and stayed on the yield plateau to enable the beam to reach full bending resistance prior to failure. The strain gauges were designed to obtain reliable results up to a strain of 0.03. The ribbed longitudinal rebars were carefully smoothed before attachment of strain gauges in order to avoid induced stresses as a result of rough surfaces. The strain gauges were wrapped with three layers of water-resisting agents before being embedded into the concrete. The steel rebars are modelled as elastic perfectly plastic material embedded into the concrete. The

logarithm strain (LE) was plotted as the numerical output for strain due to large deformations. The results correlate well with those of the experiments.

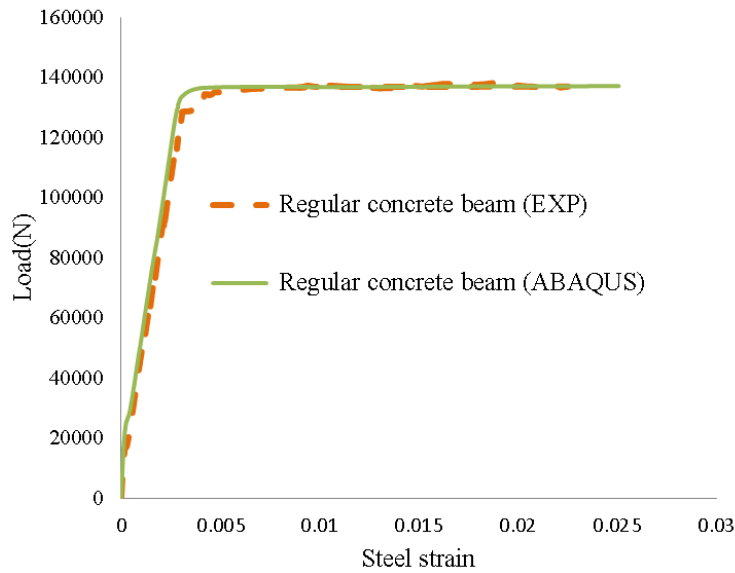


Figure 5.11 Comparison of experimental and numerical simulation results for load-longitudinal tensile steel strain curves for regular concrete beams

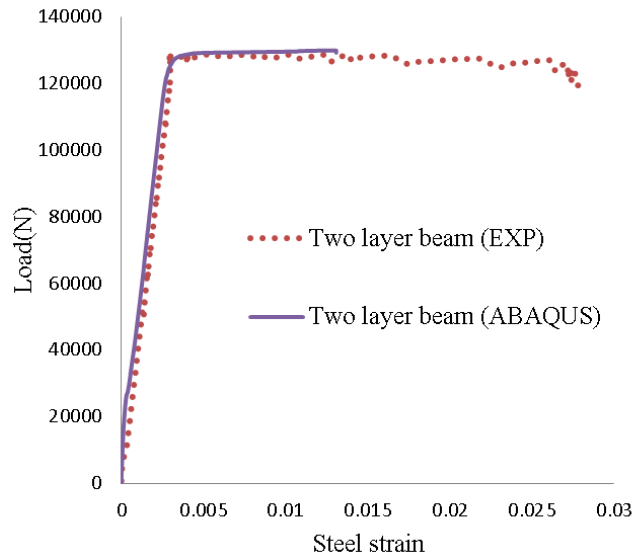


Figure 5.12 Comparison of experimental and numerical simulation results for load-longitudinal tensile steel strain curves for two-layer beams

The concrete stresses across the depth of the beams for identical materials are plotted in Section 5.6.1

5.6.2 Crack pattern and failure mode

Figure 5.13 and Figure 5.14 show the simulated failure patterns of the regular concrete beams and two-layer beams. The PEEQ and PEMAG contour plots in Figure 5.13 and Figure 5.14 indicate the magnitude of the plastic strain at failure. They correspond well with the test observations. Vertical cracks in the bending region were fully developed for beams under bending, indicating flexural failure mode. Figure 5.13 indicates that the beams under shear failed by inclined cracking load run from the support to the point of applied load. This is due to the fact that the beams are slender with a shear span depth ratio of 3.4. The result correlates well with the test results presented in Chapter 4.

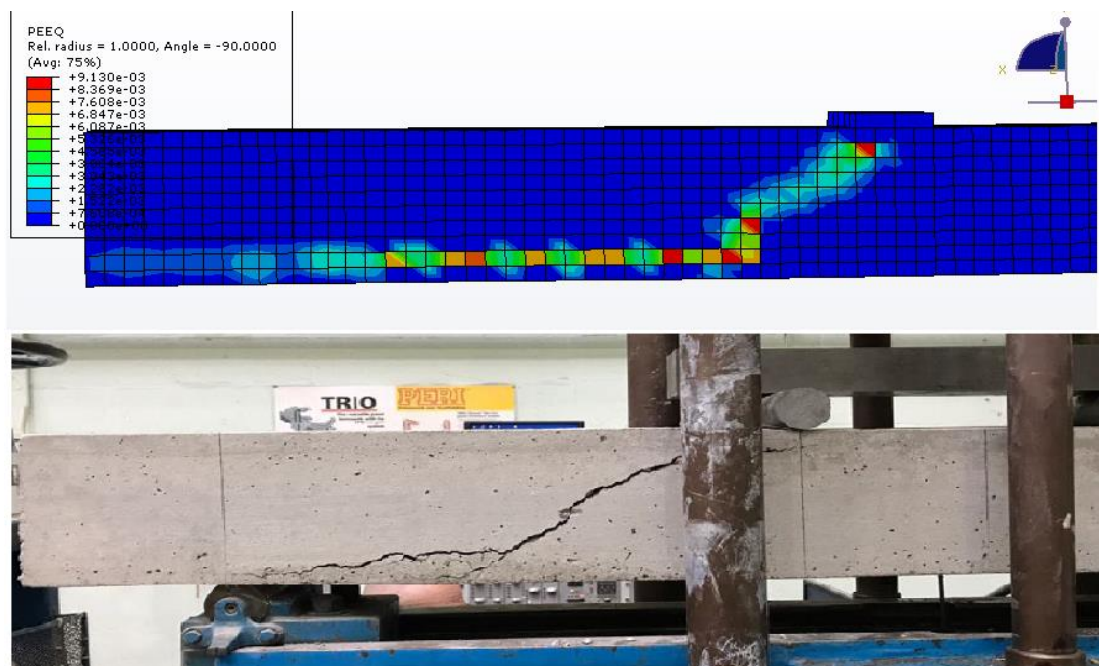


Figure 5.13 Numerical simulation results of crack pattern and failure mode of shear beams

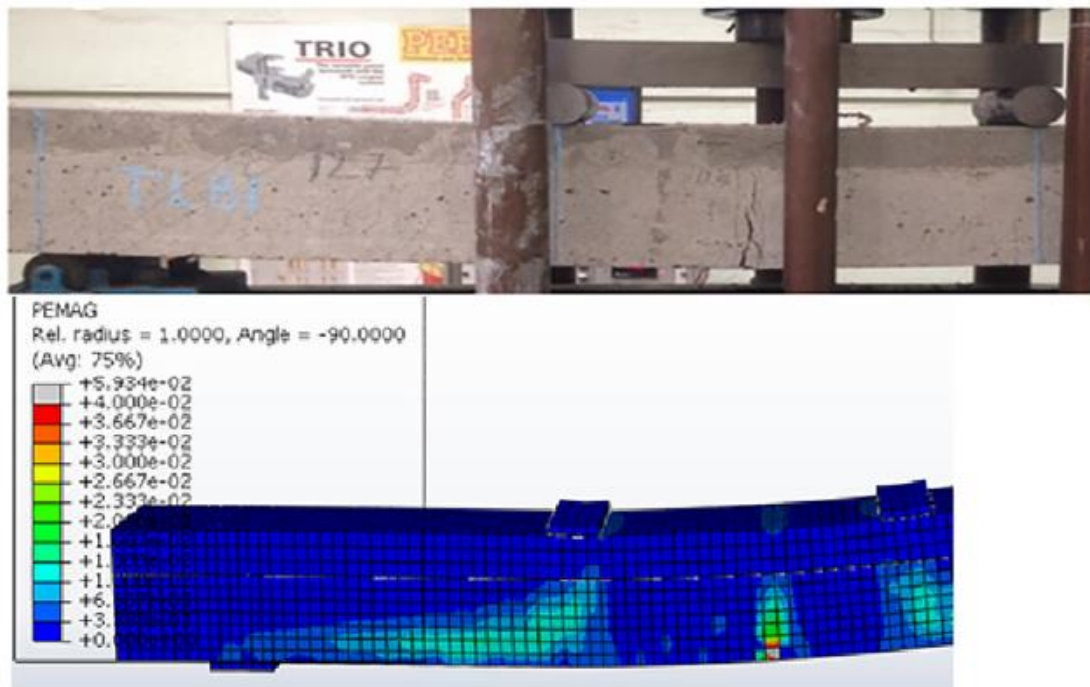


Figure 5.14 Numerical simulation results of crack pattern and failure mode of flexural beams

5.7 Numerical parametric study results

The validated ABAQUS model was used to investigate the effects of changing a number of design parameters, such as grade of recycled concrete, depth of recycled concrete layer and shear span to depth ratio. Effects of reinforcement ratios are shown in Figure E1 to E2 of Appendix E based on ABAQUS results.

5.7.1 Effects of recycled concrete grade on bending performance of two-layer beam

In order to re-affirm the hypothesis that a concrete grade in the tension zone plays no role in determining bending resistance, two different grades of recycled concrete (22MPa, 30MPa) were used while maintaining the natural aggregate concrete mix of

40MPa at the top. Figure 5.15 confirms that all beams achieve the same bending resistance. Figure 5.16 shows that the longitudinal reinforcement in all beams reaches its yield strain and maintains a long plateau.

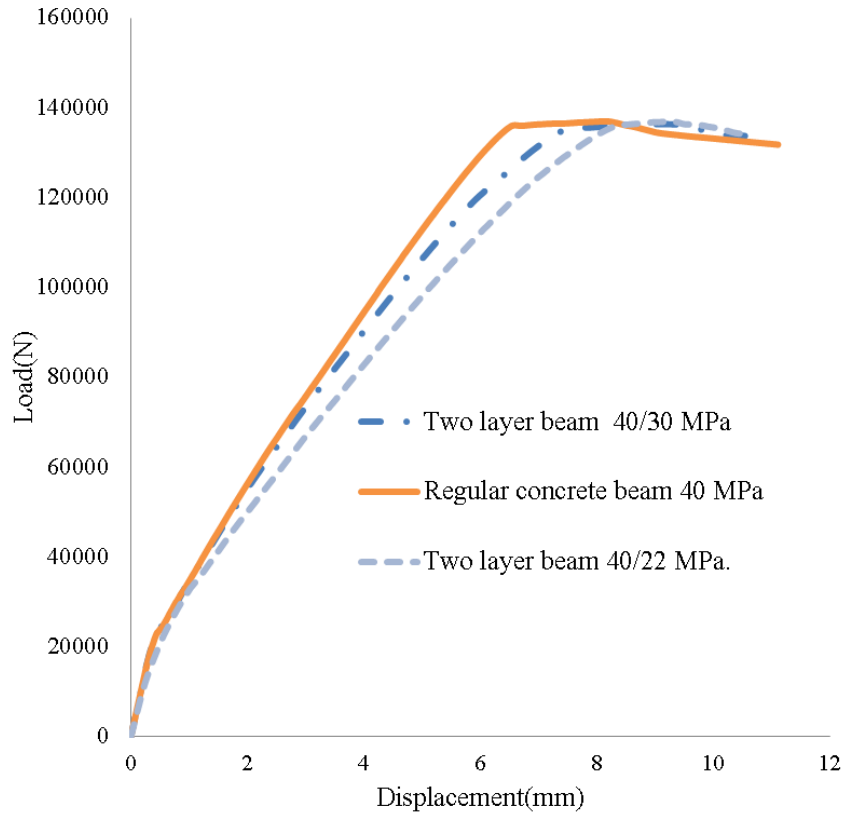


Figure 5.15 Comparison of numerical results of load-deflection at mid-span of two-layer beams of different recycled concrete grades with regular concrete beam

The distribution of stresses at mid-span along the depth of the section of the regular concrete beams and two-layer beams of identical steel properties is shown in Figure 5.17. The stresses in compression are slightly higher than the input 40MPa due to the inevitable difficulty of modelling strain values exactly. The concrete in the tension region fails at very low stresses due to the low tensile strength of concrete. However, it

is not possible to compare the concrete stresses against the experimental results because they were not measured.

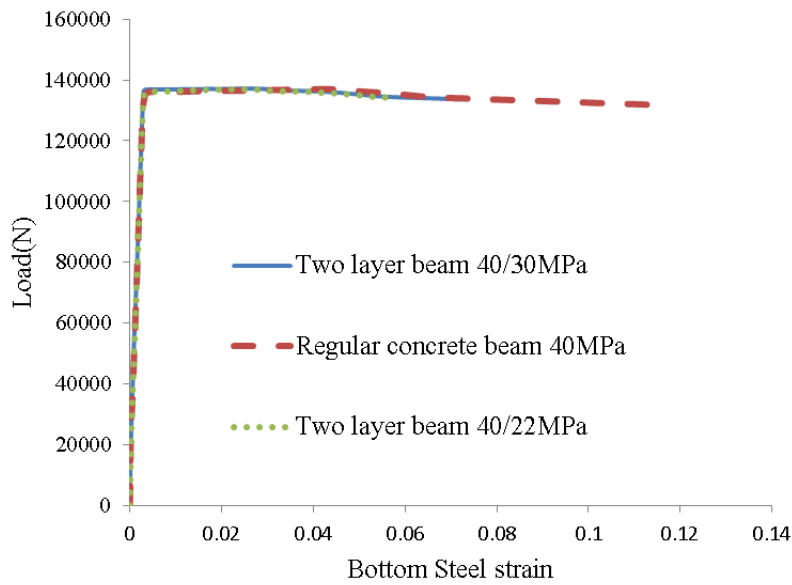


Figure 5.16 Comparison of numerical results of strain in longitudinal reinforcement of two-layer beams of different recycled concrete grades with regular concrete beam at mid-span.

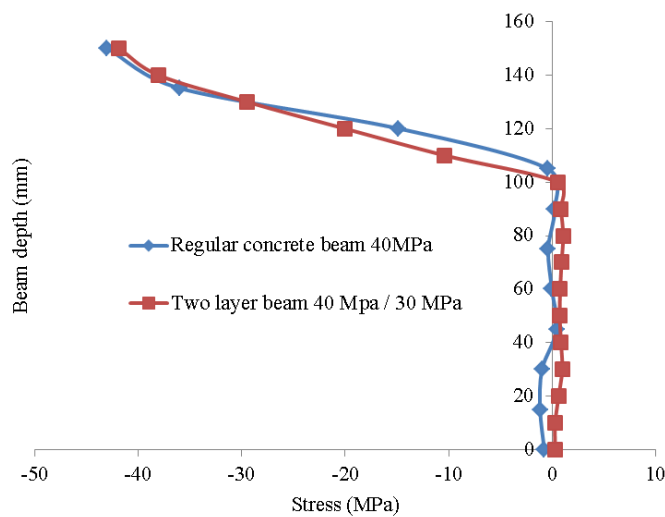


Figure 5.17 Concrete stress distribution diagram along beam depth at mid-span.

5.7.2 Concrete shear resistance mechanism: effects of top layer/bottom layer concrete depth ratio and top layer NAC mix on shear capacity of two-layer beams

From the two shear test validated model, the ratio of natural aggregate concrete depth to recycled concrete depth was changed (ratio = 0.5, 1, 2) to develop understanding of shear resistance mechanism of two-layer beams. Figure 5.18 compares the simulation results of the load-deflection curve. It suggests that the shear resistances of these beams are almost identical. Also the influence of the top layer NAC was investigated to aid understanding of the shear failure mechanism of the two-layer beams. Figure 5.19 shows that the beam made entirely of recycled aggregate concrete has identical shear resistance as the two-layer beams. This was attributed to the unzipping effect: once the lower strength (recycled concrete) concrete has failed in shear, it loses its shear resistance and transfers the shear force from the failed lower strength concrete to the NAC.

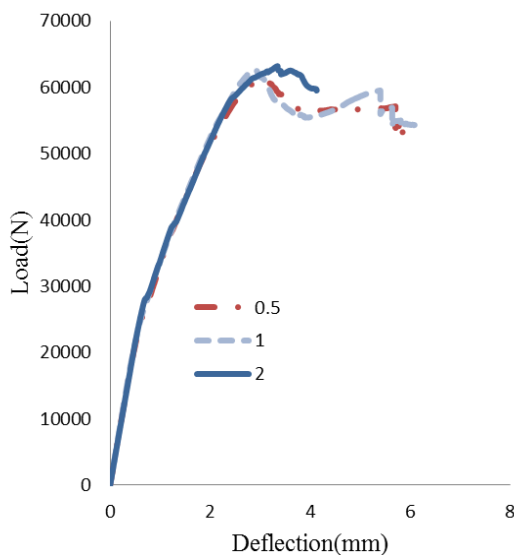


Figure 5.18 Influence of ratio of top layer thickness to bottom layer thickness on shear resistance of two-layer beam.

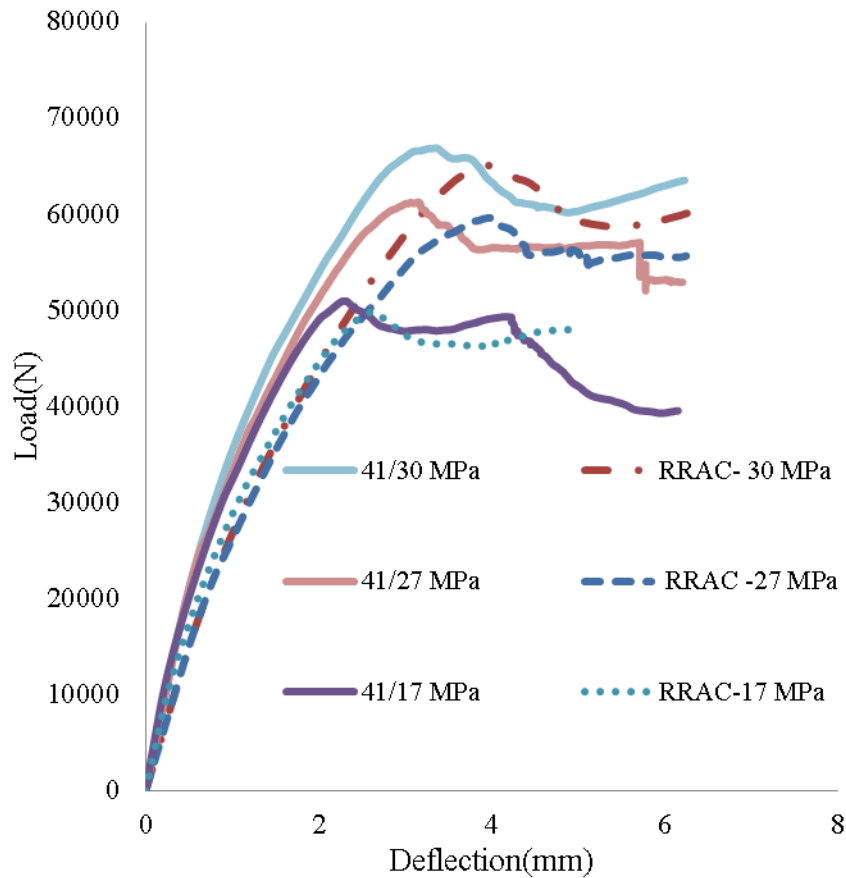


Figure 5.19 Influence of top layer NAC mix on shear resistance of two-layer beam.

The validated model was also used to further explore the performance of the two-layer beams for different shear span to depth ratios (2.6, 3.4 and 3.9). The results in Figure 5.20 show that the two-layer beams for different shear span to depth ratios have lower shear capacities compared to the regular concrete beams. This reaffirms the finding that the natural aggregate concrete in the compressive zone plays no role in enhancing the shear resistance of two-layer beams.

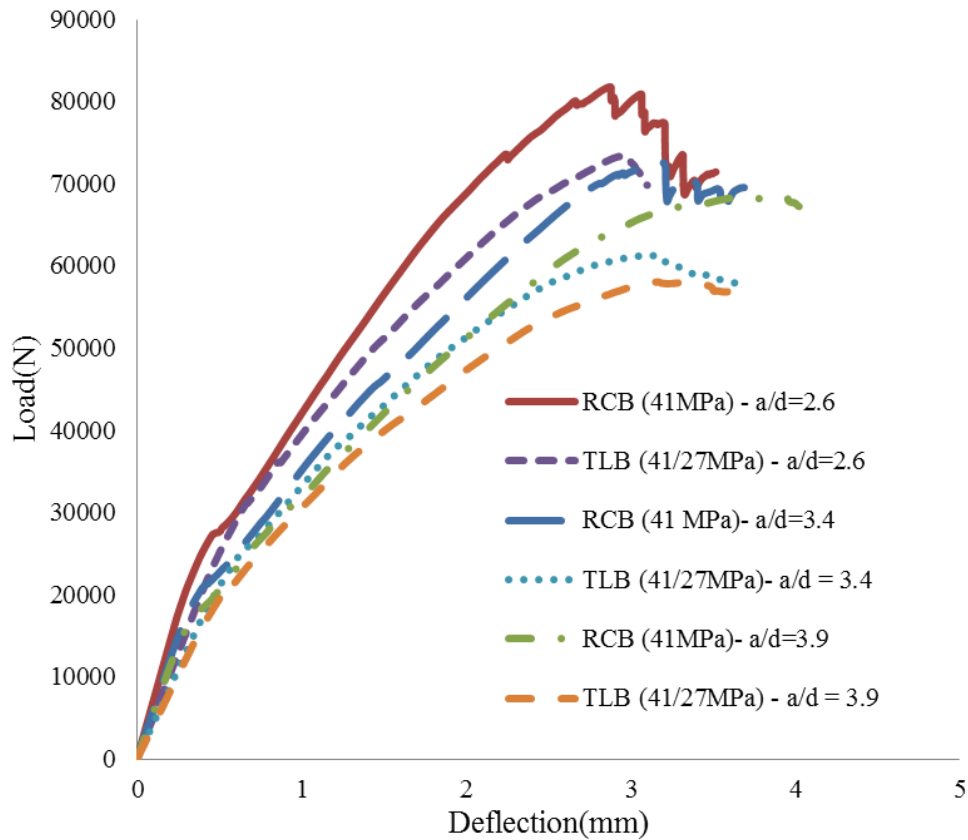


Figure 5.20 Comparison of shear resistance of two-layer beams for different shear span to depth ratios (2.6, 3.4 and 3.9).

5.8 Assessment of design methods

5.8.1 Bending resistance

The experimental and numerical simulation results have confirmed that two-layer beams reach the same bending resistance as regular concrete beams. Table 5.1 compares the design calculation results using EC2 with all the test and simulation results of bending resistance. This study omitted the material safety factors when using the EC2 method. See calculation details in E2 of Appendix E.

**CHAPTER 5. VALIDATION OF NUMERICAL MODELLING AND
PARAMETRIC STUDY**

Table 5.1 Comparison of bending resistance for all beams to EC2

| Beam type | Concrete strength MPa | Reinforcement yield strength MPa | Test Bending resistance KN-m | EC2 result/test or simulation result |
|-----------------------|-----------------------|----------------------------------|------------------------------|--------------------------------------|
| Regular concrete beam | 40.0 | D16= 551 D8=547.02 | 27.4 | 0.977 |
| Two layer beam | 40.0/30.0 | D16= 551 D8=547.02 | 27.3 | 0.980 |
| Two layer beam | 40.0/22.0 | D16= 551 D8=547.02 | 27.3 | 0.980 |

As expected, Table 5.1 reveals that the two-layer beams attain the same bending resistance as the regular concrete beams. EC2 calculation results are accurate and on the safe side. Therefore, this research concludes that the EC 2 method of calculating regular reinforced concrete beam bending resistance can be used, without modification, for the two-layer beams.

5.8.2 Shear resistance

According to the shear resistance mechanism as discussed earlier, due to unzipping effect, the shear resistance of two-layer concrete beams is the same, regardless of the depth and grade of the top layer concrete. Therefore, the shear resistance of a two-layer beam can be calculated in the same way as a beam made entirely of recycled concrete. To check this, the shear resistances for all the test and simulation beams were checked against EC2 and ACI 318. The code methods of predicting the shear capacity of reinforced concrete beams are summarized in Table 5.2.

**CHAPTER 5. VALIDATION OF NUMERICAL MODELLING AND
PARAMETRIC STUDY**

Table 5.2 Code methods of the shear strength of beams without stirrups

| CODES | MODEL |
|---|--|
| <p style="text-align: center;"> $V_c = \frac{\sqrt{f_{ck}^1}}{6} * bd$ </p> <p>ACI (2014)</p> <p>f_{ck}^1 is the compressive strength MPa, ρ is the reinforcement ratio. b and d is the width and depth of beams.</p> | |
| <p>EC2</p> | $V_c = \left[0.18K(100\rho f_{ck}^1)^{1/3} \right] b * d$ $K = \text{Size effect factor} \left(K = 1 + \sqrt{\frac{200}{d}} \right) \leq 2.0$ |

The ratio of the predicted (EC2 and ACI (318)) to tests or simulations are shown in Table 5.3.

Table 5.3 Comparison of shear resistance for all test and numerical simulation beams

| Codes/test or simulations | RCB 41 | TLB 41/27 | RRC 27 | TLB 41/30 | RRC 30 | TLB 41/22 | RRC 22 | TLB 41/17 | RRC 17 |
|---------------------------|--------|-----------|--------|-----------|--------|-----------|--------|-----------|--------|
| EC2/test | 0.898 | 0.891 | - | - | - | - | - | - | - |
| EC2/Simulation | 0.868 | 0.891 | 0.918 | 0.849 | 0.869 | 0.933 | 0.962 | 0.940 | 0.948 |
| ACI/test | 0.567 | 0.525 | - | - | - | - | - | - | - |
| ACI/Simulation | 0.537 | 0.525 | 0.541 | 0.508 | 0.521 | 0.531 | 0.547 | 0.511 | 0.515 |

*RCB 41- Regular concrete beam with $f_c=41\text{Mpa}$; *TLB 41/27- Two-layer beam with NAC $f_c=41\text{MPa}$ and recycled concrete $f_c=21\text{MPa}$; *RRC- Regular recycled concrete

**CHAPTER 5. VALIDATION OF NUMERICAL MODELLING AND
PARAMETRIC STUDY**

Table 5.3 reveals that the codes (EC 2 and ACI (318)) underestimated the shear strength of the two-layer beams using the compressive strength of the recycled concrete in the tension region. However, EC2 gives the most conservative results compared to the ACI method. This is due to the fact that the ACI overestimate the shear capacity for low reinforcement ratio (0-0.01) and underestimate it for high reinforcement ratio (0.01-0.04). Moreover, the effect of shear span to depth ratio greater than 2 on the shear capacity of concrete beams is neglected in the ACI method [127]. The Table 5.3 also unveils identical shear capacity for the two-layer beams and recycled concrete beams signifying little or no contribution of the top layer.

Also the shear capacity of the two-layer beams were evaluated and compared to existing models [168, 169] presented in Table 5.4. All the models considered include concrete strength f_{ck} , span to effective depth ratio (a/d) and reinforcement ratio as the main parameters(ρ). Details of the calculations are given in E3 and E4 of Appendix E.

Table 5.4 Prediction of shear strength of concrete beams with existing equations

| Proposed Model | Ultimate shear strength |
|----------------|--|
| [168] | $v_c = 2.1746 \left(f_{ck} * \rho * \frac{d}{a} \right)^{1/3} [Mpa] \quad \text{for } \frac{a}{d} \geq 2.5$ $v_c = \left(2.5 \frac{d}{a} \right) * 2.1746 \left(f_{ck} * \rho * \frac{d}{a} \right)^{1/3} [Mpa] \quad \text{for } \frac{a}{d} \leq 2.5$ |
| [169] | $v_c = \frac{0.831 \sqrt[3]{\rho}}{\sqrt{1 + \left(\frac{d}{25} * d_0 \right)}} * \left(\sqrt{f_{ck}} + 249 \sqrt{\frac{\rho}{\left(\frac{a}{d} \right)^5}} \right) [Mpa]$ |

[169] considers the maximum size of aggregates d_0 in the Table 5.4.

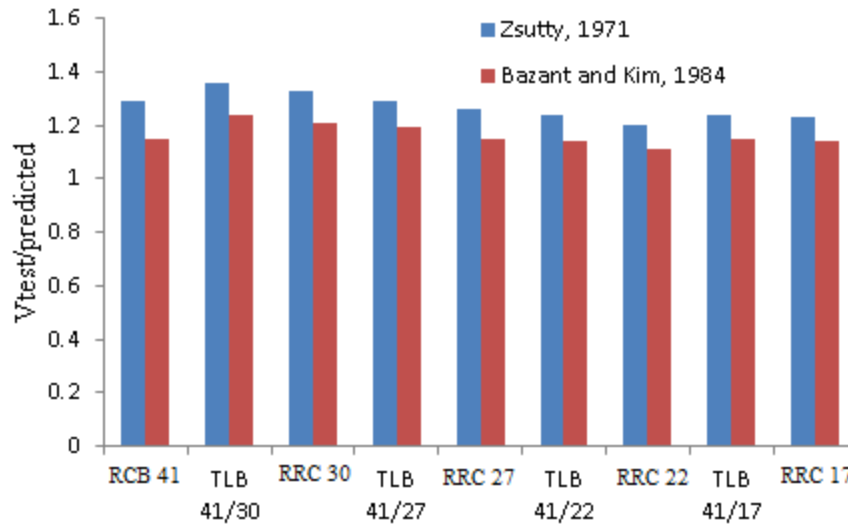


Figure 5.21 Ratio of tests or simulation results to predict shear strength of two-layer beams by existing models for a reinforcement ratio of 2.64% and shear span to depth ratio 3.4.

The models predict the shear capacity of the two-layer beams conservatively using the assumed recycled concrete strength as shown in Figure 5.21. However, the estimated results using [168] are more conservative in all cases of the two-layer beams. Therefore, the assumption made in this research using the recycled concrete strength for estimated shear strength is conservative based on the above codes and predicted methods.

5.9 Conclusions

Based on the simulations and results of the parametric studies, the following conclusions can be drawn:

CHAPTER 5. VALIDATION OF NUMERICAL MODELLING AND PARAMETRIC STUDY

- The simulation results of this study confirm that the grade of recycled concrete in the tension zone has no influence on bending resistance of reinforced concrete beams. Consequently, the EC 2 method of calculating beam bending resistance can be used, without modification, to the proposed two-layer beam construction.
- Using weak, recycled aggregate concrete with rubber crumb in the tension zone slightly reduces the beam stiffness.

- Under shear failure mode, the proposed two-layer beam demonstrates unzipping effect: once the lower strength concrete has failed in shear, it loses its shear resistance and transfers the shear force from the failed lower strength concrete to the natural aggregate concrete. Consequently, when calculating the shear resistance of plain concrete of the proposed two-layer beam, the EC2 and predicted calculation method can still be used, but the beam should be considered as a one-layer beam with the lower shear strength of the weaker concrete.

Chapter 6

Practical implications of two-layer beams

6.1 Introduction

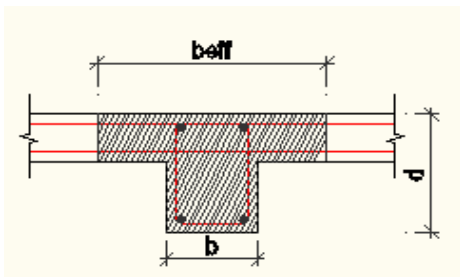
The results in Chapter 5 of this thesis have demonstrated that with identical materials, the flexural bending resistance of the two-layer beam is the same as the regular concrete beam. However, the results in Chapter 4 and Chapter 5 of this thesis also indicate that the two-layer beam will have lower concrete vertical shear resistance and may also suffer horizontal interfacial shear failure. Should the concrete vertical and horizontal interfacial shear resistances be lower than the applied loads, it would be necessary to provide steel rebars and the amount of shear rebars may be more than that required for the regular concrete beam. This of course would incur extra cost. This chapter will use an example to illustrate the amount of possible additional shear reinforcement. The assessment is made for a simply supported beam of 7.2m in span, carrying a UDL of 64.37kN/m on a 350mm by 350mm square column. Uniformly distributed load was considered to simulate beams supporting floor slabs. A value of 64.37kN/m was

obtained based on characteristic permanent and variable loads of 31.68kN/m and 14.4kN/m respectively, and the partial safety factors were 1.35 and 1.5 respectively. The characteristic permanent and variable loads represent typical practical values of 8.3kN/m² and 4kN/m² on floor slabs.

6.2 Bending reinforcements based on [113]

Required area of reinforcement for the beam in bending at midspan.

$$\text{Maximum bending moment} = \frac{WL^2}{8} = \frac{64.37 * 7.2^2}{8} = 417.12\text{KNm}$$



$$l_0 = 0.85 \times \text{span} = 6120 \text{ mm}$$

$$b_{\text{eff}} = 0.2b_f + 0.1 \times l_0 \leq 0.2l_0$$

$$= 0.2 \times (3600 - 350) + 0.1 \times 6120$$

$$= 1262 \text{ mm} > 1224 \text{ mm}$$

$$b_{\text{eff}} = (2 * 1224) + 250 = 2,698\text{mm}$$

$$\text{Effective depth} = 500 - 30 - (0.5 * 20) - 10 = 450 \text{ mm}$$

$$K = M / b d^2 f_{ck} = (417.12 * 10^6) / (2698 * 450^2 * 40) = 0.019$$

$K \leq 0.167$ for singly reinforced beams. Therefore, no compressive reinforcement is required.

$$Z = d \left[0.5 + \left(0.25 - \frac{0.019}{1.133} \right)^{0.5} \right] \leq 0.95d$$

$$Z = 450 \left[0.5 + \left(0.25 - \frac{0.019}{1.133} \right)^{0.5} \right] = 441 \leq 0.95 * 450 = 427.5 \text{ mm}$$

$$Z = 427.5 \text{ mm}$$

$$s = 2(d - z) = 2(450 - 427.5) = 45 \text{ mm}$$

Stress block lies within the flange, Hence design as rectangular section

$$f_{yd} = \frac{f_{yk}}{\gamma_s} = \frac{500}{1.15} = 434.8 \text{ MPa}$$

$$A_s(\text{Midspan}) = \frac{M}{f_{yd} Z} = \frac{420.23 * 10^6}{434.8 * 589} = 2261 \text{ mm}^2$$

$$\text{Area of 28mm diameter bar} = 615.8 \text{ mm}^2$$

$$\text{Area of 25mm diameter bar} = 490.9 \text{ mm}^2$$

Use 3, 25mm diameter bars+1, 18mm diameter bars (Area= 2338.4mm²)

Maximum and minimum reinforcement areas according to [113]

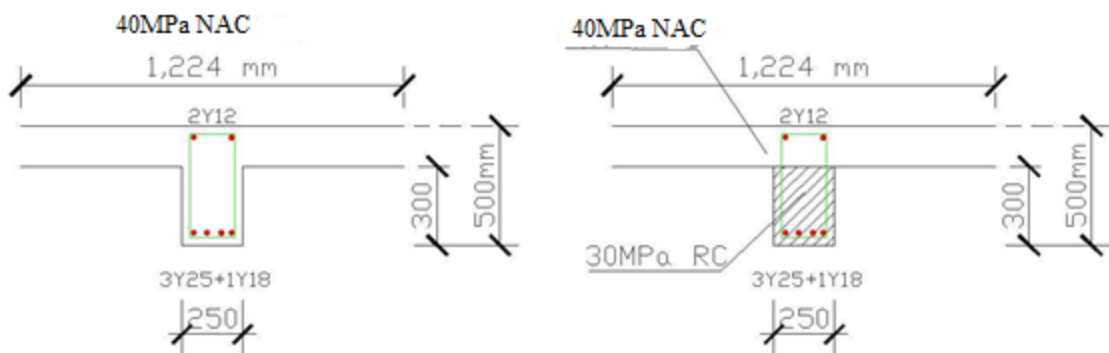
$$A_{s,min} = 0.26 \frac{f_{ctm}}{f_{yk}} bd \text{ but not less than } 0.0013bd = 0.0013 * 250 * 450$$

$$= 146.3mm^2$$

$$A_{s,min} = 0.26 * \frac{3.5}{434.8} * 250 * 450 = 235.5 mm^2$$

$$A_{s,max} = 0.04A_c = 0.04 * 250 * 450 = 4500mm^2$$

$$A_{s,min} = 235.5mm^2 \leq 2338.4mm^2 \leq 4500mm^2 \text{ OK}$$



RC*-Recycled concrete, NAC*- Natural aggregate concrete

Figure 6.1 Detailed section of RC Beam (a) Regular concrete beam section (b) two-layer beam section

6.3 Assessment for additional vertical shear reinforcement

The design resistance calculations were according to [113]

6.3.1 Vertical shear links for the regular concrete beams

The vertical shear links required for the regular concrete beams is 5Y10mm @ 275mm c/c required at each end of the beam. The designed calculations for the vertical shear links are presented in F1 of Appendix F.

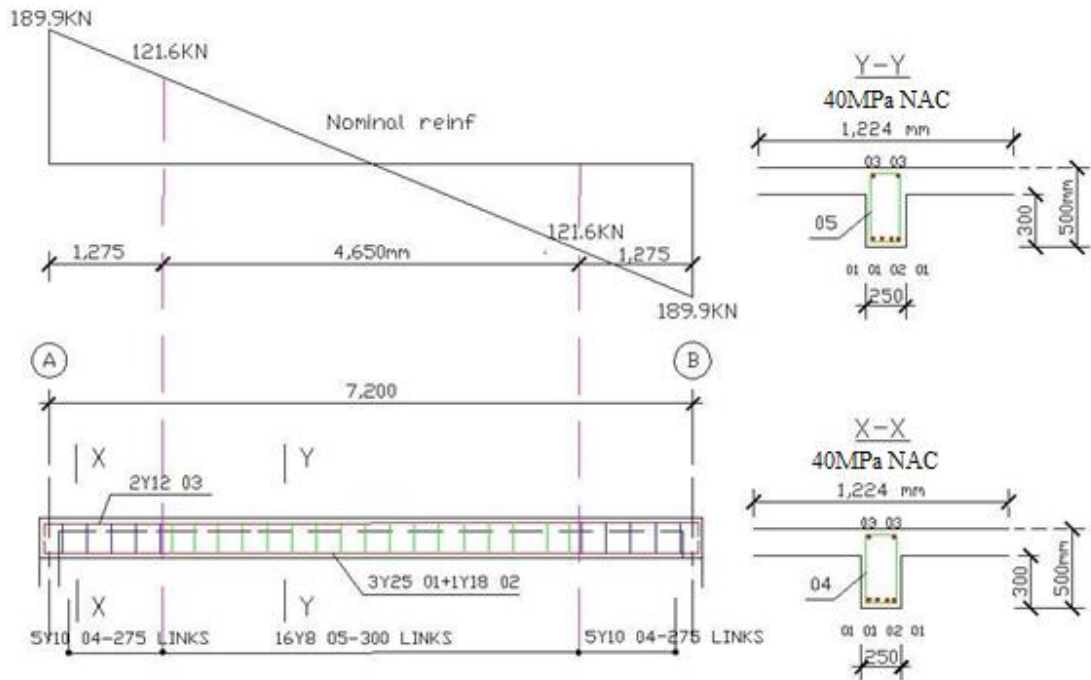


Figure 6.2 and Table 1 show the vertical shear reinforcement and bar bending schedule.

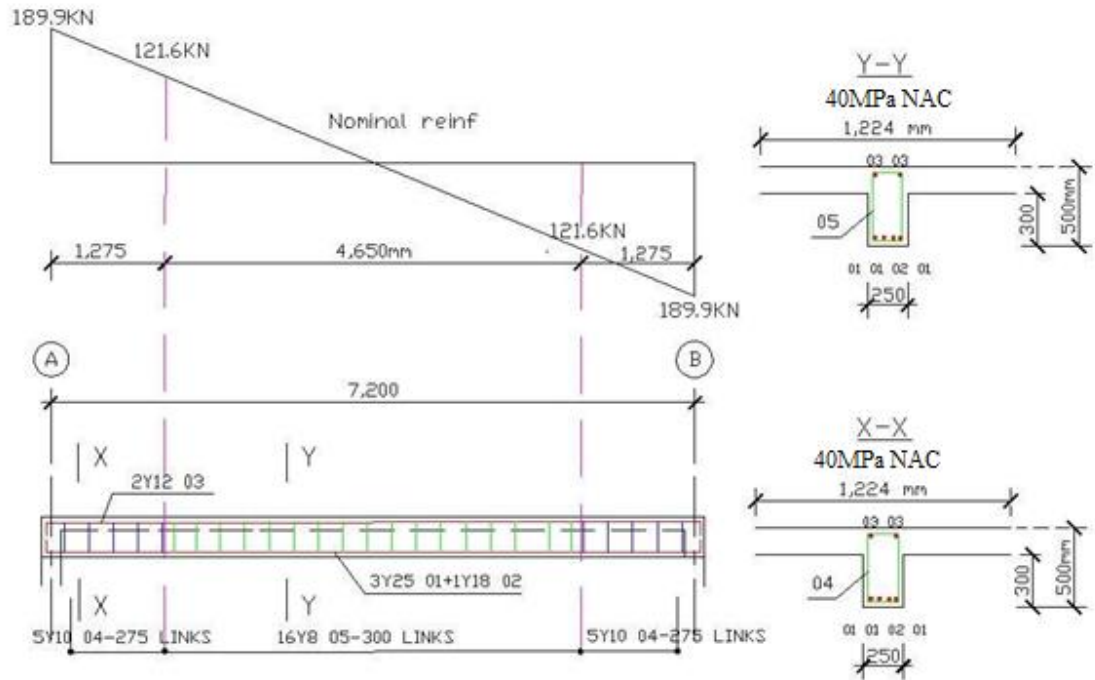

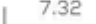


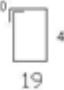


Figure 6.2 Structural detailing of the regular concrete beam

Table 6.1 Bar bending schedule for flexural and vertical shear links for the regular concrete beam

| REGULAR CONCRETE BEAM BAR SCHEDULE | | | | | | | |
|------------------------------------|----------|------|----------------|-------------|----------------|------------------|---|
| LOCATION | BAR MARK | SIZE | NO. OF MEMBERS | NO. IN EACH | BAR LENGTH (m) | TOTAL LENGTH (m) | SHAPE (m, cm) |
| BTM REBAR | 01 | Y25 | 1 | 3 | 7.82 | 23.46 |  |
| BTM REBAR | 02 | Y18 | 1 | 1 | 7.82 | 7.82 |  |
| TOP REBAR | 03 | Y12 | 1 | 2 | 7.32 | 14.64 |  |
| V. LINKS | 04 | Y10 | 1 | 5+5 | 1.42 | 14.2 |  |
| V. LINKS | 05 | Y8 | 1 | 16 | 1.42 | 22.72 |  |

Note: V. LINKS are vertical links resisting vertical shear force

6.3.2 Vertical shear links for the two-layer beam

Since the number of vertical shear links is independent of the shear resistance of concrete, the same shear links as for the regular concrete beam are provided for the two-layer beam between the support face and the location of starting nominal (minimum) shear reinforcement.

a) Minimum shear links

$$\frac{A_{sw,min}}{s} = \frac{0.08 f_{ck}^{0.5} b_w}{f_{yk}} = \frac{0.08 * 30^{0.5} * 250}{420} = 0.261$$

Provide Y8mm@ 380mm/c $\frac{A_{sw,min}}{s} = 0.265$

$$V_{min} = 0.78 \frac{A_{sw}}{s} d f_{yk} \cot \theta = 0.78 * 0.265 * 450 * 420 * 2.5 = 97.7KN$$

b) Extent of shear links

Shear links are required from the face of the support at both ends of the beam to a point where the design shear force is $V_{min} = 218.9KN$.

From the face of the support, distance x is given by

$$\frac{V_{ED} - V_{min}}{W_u} = \frac{218.9 - 97.7}{64.37} = 1.9metres$$

Therefore, the number of Y10mm @ 275mm c/c required at each end of the beam is

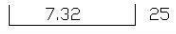


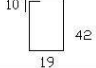
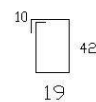
$$1 + \frac{1900}{275} = 8$$

Spaced at a distance of

$$(8 - 1) * 275 = 1,925mm$$

In summary, even though the two-layer concrete beam has lower concrete shear resistance than the regular concrete beam, because the required vertical shear links are independent of concrete shear resistance, the only possible source of additional shear links in the two-layer beam is the increased beam length requiring vertical shear links. However, as has been demonstrated in this example, the additional length is very small, no greater than the spacing of vertical shear links. Therefore, at most, one additional vertical shear link is required as shown in the bar bending schedule in Table 6.2.

Table 6.2 Bar bending schedule for flexural and vertical shear links for the two-layer beam.

| TWO LAYER BEAM BAR SCHEDULE | | | | | | | |
|-----------------------------|----------|------|----------------|-------------|----------------|------------------|---|
| LOCATION | BAR MARK | SIZE | NO. OF MEMBERS | NO. IN EACH | BAR LENGTH (m) | TOTAL LENGTH (m) | SHAPE (m, cm) |
| BTM REBAR | 01 | Y25 | 1 | 3 | 7.82 | 23.46 |  |
| BTM REBAR | 02 | Y18 | 1 | 1 | 7.82 | 7.82 |  |
| TOP REBAR | 03 | Y12 | 1 | 2 | 7.32 | 14.64 |  |
| V. LINKS | 04 | Y10 | 1 | 8+8 | 1.42 | 22.72 |  |
| V. LINKS | 05 | Y8 | 1 | 8 | 1.42 | 11.36 |  |

6.4 Assessment for additional horizontal shear links

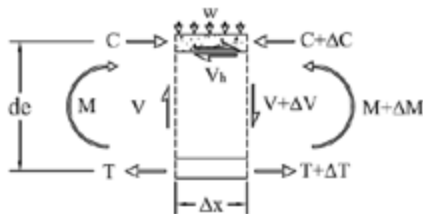
For the two-layer beam with the two layers of concrete cast within 4 hours, as has been demonstrated in Chapter 3, the interface would behave monolithically as the regular concrete beam and no interfacial shear failure would occur. Therefore, there would be no need for horizontal shear links.

Therefore, additional horizontal shear links are required only if the delay between casting the two concrete layers is long. In this study, it is assumed that the delay is 24

hours. For this situation, it is assumed that the interfacial shear resistance is 1.45MPa, based on the test results of Chapter 3 of this thesis.

The design calculations for the additional horizontal shear links are according to [170]. This standard involves checking the maximum horizontal shear stress at the interface. If the maximum horizontal shear stress does not exceed the concrete interfacial shear resistance, no horizontal shear link is needed. Otherwise, horizontal shear links are needed in the regions where the horizontal shear stress is greater than the interfacial shear resistance.

The relationship between the horizontal shear stress and the vertical shear force is as follows:



$$\Delta T = b * \mu * \Delta X \frac{\Delta T}{\Delta X} = b * \mu$$

$$\Delta T = \frac{\Delta M}{Z} \frac{\Delta M}{Z} = b * \mu * \Delta X$$

$$\frac{\Delta M}{\Delta X} = V\mu = \frac{V}{b * Z}$$

So the interfacial shear stress is calculated as:

$$v_h(\text{shear stress}) = \frac{V}{b_v \times d_s} \dots \dots \dots 6.1$$

Where;

v_h = Horizontal shear stress

V = Vertical shear force

b_v = Interface width between the section two layers

d_s = Effective depth of the full two layer section defined as the distance from the top of the compressive fibre for the entire composite section to the centroid of the longitudinal tension reinforcements.

(a) Amount of vertical ties

The maximum horizontal shear force that can be transferred by the interface without shear reinforcements is:

$$V = v_h * b_v d_s$$

The interfacial shear strength for concrete on recycled concrete for a 24-hour cast time interval obtained in Chapter 3 is 1.45MPa

$$V = 1.45 * 250 * 450 = 163.13KN$$

Therefore provision of interfacial shear links is required as 163.13KN is less than the maximum shear force 218.9KN at the face of the support.

[170] recommends Equation 6.2 for the provision of interfacial shear links of concrete interfaces with an amplitude of 6.35mm.

$$V_R = (1.8 + 0.6\rho f_y) b_v d \dots\dots\dots 6.2$$

$$218.9 * 1000 = (1.8 + 0.6\rho * 420)250 * 450$$

$$\rho = 0.00058$$

Assume the ties are 2 legs stirrups of 6mm diameter spaced at a distance S mm c/c.

$$\rho = \frac{A_s}{b_v * s} = \frac{2 * 28.28}{250 * S} = 0.00058$$

$$S=390\text{mm}$$

Therefore, provide 6mm diameter rebars at a spacing of 390mm c/c from the face of the support to a distance where the shear force is less than or equal to 163.13KN.

b) Extend of vertical ties along the beam

At shear stress of 1.45MPa, there will be no need to provide vertical ties across the interface. The vertical shear force that will result in 1.45MPa interface shear stress is

$$V_{Min} = 1.45 * 250 * 450 = 163.13\text{KN}$$

From the face of the support, distance x is given by

$$\frac{V_{ED} - V_{min}}{W_u} = \frac{218.9 - 163.13}{64.37} = 0.9\text{metres}$$

Therefore, the number of Y6mm @ 390mm c/c required from the face of the support at both ends to a distance of 900mm is as follows:

$$1 + \frac{900}{390} = 4$$

Figure 6.3 shows the vertical tie arrangement. Table 6.3 summarises the total reinforcement schedule.

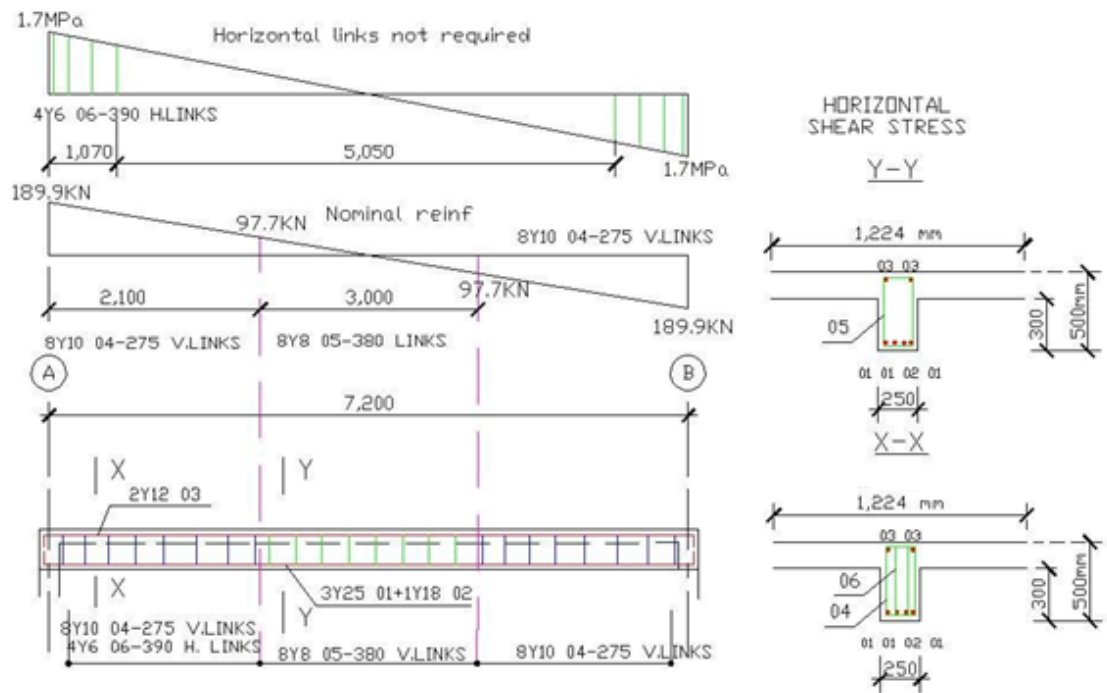



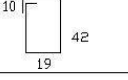
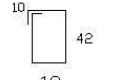
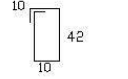


Figure 6.3 Structural detailing for the two-layer beam.

Table 6.3 Reinforcement schedule for two-layer beam

| TWO LAYER BEAM BAR SCHEDULE | | | | | | | |
|-----------------------------|----------|------|----------------|-------------|----------------|------------------|---|
| LOCATION | BAR MARK | SIZE | NO. OF MEMBERS | NO. IN EACH | BAR LENGTH (m) | TOTAL LENGTH (m) | SHAPE (m, cm) |
| BTM REBAR | 01 | Y25 | 1 | 3 | 7.82 | 23.46 |  |
| BTM REBAR | 02 | Y18 | 1 | 1 | 7.82 | 7.82 |  |
| TOP REBAR | 03 | Y12 | 1 | 2 | 7.32 | 14.64 |  |
| V. LINKS | 04 | Y10 | 1 | 8+8 | 1.42 | 22.72 |  |
| V. LINKS | 05 | Y8 | 1 | 8 | 1.42 | 11.36 |  |
| H. LINKS | 06 | Y8 | 1 | 8 | 1.24 | 9.92 |  |

Note: V. LINKS are vertical links resisting vertical shear force while H.LINKS are links resisting horizontal shear stress.

6.5 Comparison of shear rebars

Table 6.4 compares vertical shear links and vertical ties between the regular concrete beam and the two-layer beams (TLB) cast at 4 and 24 hours between the two layers.

Table 6.4 Weight of rebars used to resist vertical and horizontal shear for all beams

| Beam type | Rebars for vertical shear force (Kg) | Rebars for horizontal shear stress (Kg) | Total weight (Kg) |
|-----------------------|--------------------------------------|---|-------------------|
| Regular concrete beam | 17.78 | - | 17.78 |
| TLB 4HRS | 18.57 | - | 18.57 |
| TLB 24HRS | 18.57 | 2.2 | 20.77 |

Regarding the two-layer beam where the two layers of concrete are cast within 4 hours, there is no need for additional steel rebar. As for the two-layer beam where the interval between casting the two layers of concrete is 24 hours, Table 6.4 reveals that the additional steel rebar is substantial compared to the regular concrete beam. However, taking into account the total reinforcement for the beam, this increase is very small. The

total weight of flexural reinforcement in the beam is 106.04Kg. The additional vertical ties are 2.1% of the flexural reinforcement.

Also, in view of the additional cost of fixing extra shear links, a cost analysis based on the specifications of Spons Civil Engineering and Highway Works [163] was conducted and results presented in Table 6.5. The extra cost for shear links incurred for the two-layer beams (TLB) cast at 4 and 24-hour time intervals is approximately 4.3% and 15.4% higher than the regular concrete beams. However, the shear link cost for the regular concrete beam is only about 2.79% of the total cost of the beam in Table F 1 of Appendix F. Therefore, the additional costs for the two-layer beams for 4-hour and 24-hour cast time intervals are only 2.91% and 3.3% of the total beam cost. However, one should recognise that the two-layer concept encourages the increased use of recycled aggregates in new construction works.

Table 6.5 Cost analysis of vertical and horizontal shear links of the two-layer beams compared to the regular concrete beams

| ITEM | DESCRIPTION | QTY | UNIT | RATE(£) | AMOUNT(£) |
|--|--|----------|-------|----------|--------------|
| A. Regular concrete beams vertical shear links | | | | | |
| 1.00 | Deformed high yield steel bars to BS 4449 | | | | |
| 1.01 | 10mm nominal size | 0.008804 | tonne | 1,704.74 | 15.01 |
| 1.02 | 8mm nominal size | 0.008974 | tonne | 1,704.74 | 15.30 |
| | Total cost | | | | 30.31 |
| B. TLB vertical shear links for 4-hr cast time intervals | | | | | |
| 2.00 | Deformed high yield steel bars to BS 4449 | | | | |
| 2.01 | 10mm nominal size | 0.014086 | tonne | 1,704.74 | 24.01 |
| 2.02 | 8mm nominal size | 0.004487 | tonne | 1,704.74 | 7.65 |
| | Total cost | | | | 31.66 |
| C. TLB vertical shear links for 24-hr cast time intervals | | | | | |
| 3.00 | Deformed high yield steel bars to BS 4449 | | | | |
| 3.01 | 12mm nominal size | 0.014086 | tonne | 1,704.74 | 24.01 |

| | | | | | |
|------|-------------------|----------|-------|----------|--------------|
| 3.02 | 8mm nominal size | 0.004487 | tonne | 1,704.74 | 7.65 |
| 3.03 | 6mm nominal size | 0.002202 | tonne | 1,902.43 | 4.19 |
| | Total cost | | | | 35.85 |

6.6 Conclusion.

Chapter 6 has used an example to illustrate the cost implication of adopting two-layer beams. It was revealed that casting of the two-layer beams within an interval of 4 hours does not need extra ties. However, extra 2.1% of the flexural reinforcement is needed for vertical ties to resist the horizontal shear stress for two-layer beams cast at 24-hour time intervals. Additional cost is also incurred for the two-layer beams with respect to the increased shear links and fixing time when compared to the regular concrete beams.

Chapter 7

Conclusions and recommendation for future research studies

7.1 Summary of research and achievements

7.1.1 General

This research investigates the means of enabling recycled aggregates and crumb rubber from waste tyres to be used in structural engineering applications without limitations resulting from its low strength compared to natural aggregates. The research was carried out in two strands: to find the means of increasing the mechanical properties of recycled aggregate concrete to achieve those of concrete with natural aggregates, and to investigate a particular type of structure where the low strength of recycled aggregate

concrete would have a negligible effect on structural behaviour. Adding a small amount of graphene was investigated in order to improve the mechanical properties of recycled aggregate concrete. Placing recycled concrete of low strength in the tension zone of reinforced concrete beams was considered feasible based on the design assumption that concrete in the tensile zone has zero mechanical strength. This study included the following main parts:

7.1.2 Mechanical properties of wet and hardened rubber recycled aggregate concrete

The mechanical properties of rubber recycled aggregate concrete in both the wet and hardened state with different concentrations (5%, 10%, 15% and 20%) of crumb rubber of recycled aggregate weight was experimentally investigated. The main findings are:

1. Without additional water or super plasticizers, recycled aggregate concrete (RAC*) suffered a drastic reduction (78.8%) in slump compared to the natural aggregate concrete (NAC). This reduction was attributed to the high water absorption rate of coarse recycled aggregates which reduced the free water available for lubrication of the concrete constituent materials. However, the workability of RAC was improved to that of the NAC when extra water 4.21% of the weight of the recycled aggregate obtained from the absorption test or super plasticiser of 1% of cement weight was added to compensate for the water absorbed by the recycled aggregate.
2. The workability of recycled aggregate concrete decreased as the amount of rubber content increased, with and without super plasticizers. The percentage of crumb rubber in weight should therefore be limited to 15 percent in rubber recycled aggregate concrete (RRAC) to maintain a workable mix. However, this limit could be loosened to 20% of crumb rubber, by using super plasticisers to enhance workability in place of extra water.
3. The compressive strength of concrete made with 100 percent recycled aggregates, but without water or super plasticiser to enhance its workability, was

on average 9.6% lower than that of the NAC. Increasing the water cement ratio of the RAC to enhance concrete workability resulted in a further reduction in concrete compressive strength to 35%. However, using super plasticisers in the RAC mix instead of extra water, to improve workability, increased the compressive strength of recycled aggregate concrete by 23.8% compared to RAC with extra water, although this was still 14.9% lower than that of the NAC. As expected, increasing the percentage of crumb rubber particles further reduced the concrete compressive strength.

4. The amount of crumb rubber also influenced the splitting tensile strength of rubber recycled aggregate concrete. For rubber recycled aggregate concretes with super plasticiser, the reduction in split tensile strength as a function of crumb rubber weight, was almost linear, ranging from 14.3% at 5% crumb rubber to reductions of 21.4%, 35.7% and 45.4% at 10%, 15% and 20% of crumb rubber respectively.

7.1.3 Influence of graphene on the mechanical properties of recycled aggregate concrete

This research explores the feasibility of using graphene to improve the mechanical properties of recycled aggregate concrete and rubber recycled aggregate concrete with 10% of crumb rubber content. The following conclusions were drawn:

1. Except for G5 0.02% (graphene size 5 μ m, 0.02% by weight), including graphene decreased compressive strength of rubber recycled aggregate concrete, this was attributed to the low bonding strength between the rubber particles and the cement matrix due to excessive amount of dust. G5 0.02% graphene solution increased the compressive strength of recycled concrete strength by 12.2% (from 18.9MPa to 21.2MPa) with minimum error, but this increase is not sufficiently high to upgrade the recycled aggregate concrete so that it can be used in loadbearing members.

2. With 0.01% graphene, there was a very small increase (7.5%) in compressive strength of the NAC. However, increasing the amount of graphene in concrete did not produce any further improvement; in fact, the concrete strength was slightly lower than without graphene. Likewise, adding 0.01% of G10 graphene provided a moderate level of increase of up to 18% of splitting tensile strength compared to NAC without graphene, but adding more graphene resulted in negligible improvement in concrete tensile strength.
3. Without any graphene, the compressive strength (32.74 MPa) of recycled aggregate concrete with washed aggregates was higher than that (27.2 MPa) with unwashed aggregates by 20%. By adding 0.01% G10 graphene to the washed recycled aggregate concrete, the compressive strength was further enhanced by 20% (from 32.74 to 39.14 MPa) which is equivalent to the 40MPa of the target NAC. The results demonstrate the potential of adding a very small amount of graphene to enhance the compressive strength of recycled aggregate concrete to the level when it can be used to replace concrete using natural aggregates.
4. Adding 0.01% G10 graphene to washed recycled aggregate concrete increased the tensile strength by 19.7% (from 3.14 to 3.76 MPa). The enhanced tensile strength is now almost identical to that achieved by the NAC (3.8 MPa), indicating that it is now possible to replace the NAC with RAC. Adding more graphene did not result in any additional increase in the tensile strength of concrete.
5. For recycled aggregate concretes, adding 0.01% of graphene increased the initial stiffness value by 25.1% compared to the mix without graphene. The stiffness of the washed recycled concrete with 0.01% of graphene is 32.4% more than that of the NAC without graphene.

7.1.4 Bond strength of recycled concrete and embedded reinforcement bars.

In order to ensure proper anchorage of the rubber recycled aggregate concrete and deformed rebars, a study of bond strength was conducted for different rubber contents in recycled concrete. The main conclusions are:

1. The bond strength of recycled aggregate concrete without rubber particles was 16.3% higher than the NAC. This is consistent with the research findings of others and can be attributed to the better interlocking resistance due to the more irregular shapes of recycled aggregates.
2. Using crumb rubber particles decreased the rebar pull-out bond strength, due to a lack of resistance of the rubber particles. However, if the rebar bond strength is normalised to the compressive strength of concrete, according to $\tau_{max}/(f_c)^{0.5}$, then incorporating rubber particles would not adversely affect the normalised bond strength of recycled aggregate concrete.
3. It is recommended the amount of crumb rubber in recycled concrete should be limited to 10% of the recycled aggregate weight in order to ensure proper anchorage of the rubber recycled aggregate concrete and deformed rebars.

7.1.5 Interfacial bond strength between two-layers of concrete of different grades.

In the proposed two-layer beam construction, the two layers of concrete are not cast monolithically. It is important that that the concrete interface has sufficient shear strength to prevent interfacial shear failure. The slant shear test was used to determine the interfacial shear strength. The main conclusions are:

1. The two-layer concrete cast in 4-hour time intervals behaved monolithically while those cast at 24 hour cast time intervals failed at the interface with an interfacial strength of about 1.5MPa for all tests.
2. The interfacial shear strength for 4-hour casting intervals varied with the mix composition, with specimen T2 (NAC on RRAC with 5% rubber crumb) giving the best results compared to T3 (NAC on RRAC with 10% rubber crumb).
3. It is recommended to cast the two-layers of concrete within a time limit of 4 hours in order to reduce the cost of construction by avoiding provisions of extra shear links that may be necessary for preventing interfacial shear failure between the two layers of concrete.

7.1.6 Experiments, numerical modelling (ABAQUS), validation, parametric study and design assessment of bending behaviour of two-layer beams.

The main conclusions are:

1. The two-layer beams attain the same bending resistance as the regular concrete beams. Therefore, conventional design methods for reinforced concrete beams, such as Eurocode 2, can be directly used without modification to calculate bending resistance of simply supported reinforced concrete beams using recycled aggregate concrete with or without rubber.
2. Using recycled aggregate concrete with or without rubber crumb in the tension zone slightly decreased the beam stiffness, but the reduction is small.

7.1.7 Experiments, numerical modelling (ABAQUS), validation, parametric study and design assessment of shear behaviour of two-layer beams.

The shear tests were carried out on beams without shear reinforcement in the shear span length and with a shear span/depth ratio of 3.4. The main conclusions are:

1. The two layers of concrete were cast within 4 hours and the interface between the recycled and the natural aggregate concrete did not fail.
2. The ultimate load for the regular concrete beam was higher than the two-layer beams. This was attributed to the lower compressive strength of the recycled concrete at the bottom layer of the beam compared to the top layer NAC. Under shear, once the lower strength (recycled concrete) concrete fails, it loses its shear resistance and transfer the shear force from the failed lower strength concrete to the NAC. This was termed unzipping.
3. The unzipping effect was investigated numerically by comparing the shear behaviour of two-layer beams with that of the beam made entirely of recycled aggregate concrete. They were found to have identical shear resistance. This was attributed to the unzipping effect.
4. Consequently, this study recommends that when calculating the concrete shear resistance of two-layer beams, the beam should be considered as a one-layer beam with the lower shear strength of the weaker concrete. Conventional design methods, such as Eurocode 2, can be used without modification.

7.1.8 Practical implication of two-layer beams

Due to two-layer beams having lower vertical shear resistance compared to regular concrete beam, they may also suffer interfacial shear failure hence, additional vertical shear and horizontal shear links may be necessary. A practical illustration was used to examine the possible amount of additional shear reinforcement. The main conclusions are:

1. It was revealed that casting of the two-layer beams within an interval of 4h ours does not need extra ties. However, an extra 2.1% of the flexural reinforcement is needed for vertical ties to resist the horizontal shear stress for two-layer beams cast at 24-hour time intervals. Additional cost is also incurred for the two-layer beams with respect to increased shear links and fixing time when compared to the regular concrete beams.

7.2 Recommendations for future research

The aim of this study was to investigate the possibility of using recycled concrete in mainstream structural applications such as the reinforced concrete beams. This research has demonstrated feasibility of the proposed approaches of either using a tiny amount of graphene to improve the mechanical properties of recycled aggregate concrete, or the innovative approach of placing low strength recycled aggregate concrete in the tension zone of bending members. However, there was not enough time and resources in this PhD project to completely solve all problems. More research studies are needed to help achieve the full potential of the proposed methods of this project. The following further research studies may be considered:

1. The durability of recycled concrete, in particular, rubber recycled aggregate concrete, should be investigated. Previous researchers have reported the use of fly ash as partial replacement for cement to enhance durability [9]; there

were also reports using air entrainment and polypropylene fibres in recycled concrete to achieve the same freeze and thaw durability [107]. [108] demonstrated acceptable durability performance of recycled concrete by removing the attached cement matrix on the recycled aggregates. These studies indicate the available means to ensure durability of recycled aggregate concrete. These studies were for recycled aggregate concrete without crumb rubber. Further studies should be conducted on rubber RAC.

2. The recycled aggregates from the commercial market are of varying qualities and composition. The results of this research indicate they can have major influences on the properties of recycled aggregate concrete. It would be necessary to conduct further research to classify recycled aggregates based on quality and their influences on properties of RAC.
3. Incorporation of graphene in recycled concrete has demonstrated the potential to directly replace concrete with natural aggregates by using graphene modified RAC. Further research studies are necessary to show consistence of this approach for different types and sizes of graphene, different graphene dispersion methods and different concrete mixes.
4. This study has focused on simply supported two-layer beams. However, the behaviour of continuous two-layer beams needs further study.
5. More tests for the two layer beams especially with respect to shear performance may be required to account for different size effects.
6. The elevated temperature properties of recycled aggregate concrete, with and without graphene, with and without crumb rubber, should be investigated.

Appendix A

Mix design and raw data collated from experiments of recycled and NAC with coefficient of variations

APPENDIX A. MIX DESIGN AND RAW DATA COLLATED FROM EXPERIMENTS OF
RECYCLED AND NAC WITH COEFFICIENT OF VARIATIONS

Table A.1 Sieve analysis of virgin aggregates

| Sieve aperture size(mm) | Mass of material retained(Kg) | | | percentage of material retained | Cumulative % retained | Cumulative % passing |
|---|----------------------------------|-------|--------|---------------------------------------|--------------------------|-------------------------|
| | 1 | 2 | Mean | | | |
| 14 | 0 | 0 | 0 | 0 | 0.00 | 100.00 |
| 10 | 0.098 | 0.151 | 0.1245 | 12.45 | 12.45 | 87.55 |
| 6.3 | 0.655 | 0.663 | 0.659 | 65.9 | 78.35 | 21.65 |
| 4 | 0.189 | 0.155 | 0.172 | 17.2 | 95.55 | 4.45 |
| 2 | 0.043 | 0.024 | 0.0335 | 3.35 | 98.90 | 1.10 |
| material in pan P | 0.001 | 0.001 | 0.001 | 0.1 | 99.00 | 1.00 |
| Percentage of fines passing 0.063mm sieve= | | | | | 1.05 | |

Total dry mass M1= 1 kg
 Dry mass after washing
 M2= 0.9905 kg
 Dry mass of fines removed after washing
 M1-M2= 0.0095 kg

Table A.2 Sieve analysis of recycled aggregates (RA1)

| Sieve aperture size(mm) | Mass of material retained(Kg) | | | percentage of material retained | Cumulative % retained | Cumulative % passing |
|---|----------------------------------|----------|----------|--|--------------------------|-------------------------|
| | 1 | 2 | Mean | | | |
| 28 | 0 | 0 | 0 | 0 | 0.00 | 100 |
| 14 | 0.052 | 0.038 | 0.045 | 4.5 | 4.50 | 95.5 |
| 10 | 0.34 | 0.285 | 0.3125 | 31.25 | 35.75 | 64.25 |
| 6.3 | 0.391 | 0.403 | 0.397 | 39.7 | 75.45 | 24.55 |
| 4 | 0.144 | 0.189 | 0.1665 | 16.65 | 92.10 | 7.9 |
| 2 | 0.014 | 0.02 | 0.017 | 0.85 | 92.95 | 7.05 |
| material in pan P | 0.001 | 0.002 | 0.0015 | 0.15 | 93.10 | 6.9 |
| Percentage of fines passing 0.063mm sieve= | | | | | 6.15 | |

APPENDIX A. MIX DESIGN AND RAW DATA COLLATED FROM EXPERIMENTS OF
RECYCLED AND NAC WITH COEFFICIENT OF VARIATIONS

Total dry mass M1= 1 kg
 Dry mass after washing M2= 0.94 kg
 Dry mass of fines removed after washing M1-M2= 0.06 kg

Table A.3 Sieve analysis of recycled aggregates (RA2)

| Sieve aperture size(mm) | Mass of material retained (Kg) | | | percentage of material retained | Cumulative % retained | Cumulative % passing |
|--|--------------------------------|-------|--------|---------------------------------|-----------------------|----------------------|
| | 1 | 2 | Avg | | | |
| 20 | 0 | 0 | 0 | 0 | 0.00 | 100 |
| 16 | 0.034 | 0.009 | 0.0215 | 2.15 | 2.15 | 97.85 |
| 14 | 0.062 | 0.039 | 0.0505 | 5.05 | 7.20 | 92.8 |
| 8 | 0.809 | 0.835 | 0.822 | 82.2 | 89.40 | 10.6 |
| 4 | 0.081 | 0.103 | 0.092 | 9.2 | 98.60 | 1.4 |
| material in pan P | 0.016 | 0.012 | 0.014 | 1.4 | 100.00 | 0 |
| Percentage of fines passing 0.063mm sieve= | | | | | 17.40 | |

Total dry mass M1= 1 kg
 Dry mass after washing M2= 0.84 kg
 Dry mass of fines removed after washing M1-M2= 0.16 kg

Table A.4 Sieve analysis of fine sand

| Sieve aperture size(mm) | Mass of material retained(Kg) | | | percentage of material retained | Cumulative % retained | Cumulative % passing |
|-------------------------|-------------------------------|-------|--------|---------------------------------|-----------------------|----------------------|
| | 1 | 2 | Mean | | | |
| 10 | 0 | 0 | 0 | 0 | 0.00 | 100.00 |
| 5 | 0.024 | 0.023 | 0.0235 | 2.35 | 2.35 | 97.65 |
| 3.25 | 0.06 | 0.067 | 0.0635 | 6.35 | 8.70 | 91.30 |
| 2 | 0.085 | 0.079 | 0.082 | 8.2 | 16.90 | 83.10 |
| 0.6 | 0.122 | 0.122 | 0.122 | 12.2 | 29.10 | 70.90 |
| 0.425 | 0.312 | 0.258 | 0.285 | 28.5 | 57.60 | 42.40 |
| 0.3 | 0.242 | 0.279 | 0.2605 | 26.05 | 83.65 | 16.35 |
| 0.075 | 0.148 | 0.169 | 0.1585 | 15.85 | 99.50 | 0.50 |
| material in pan P | 0.002 | 0.003 | 0.0025 | 0.25 | 99.75 | 0.25 |

APPENDIX A. MIX DESIGN AND RAW DATA COLLATED FROM EXPERIMENTS OF
RECYCLED AND NAC WITH COEFFICIENT OF VARIATIONS

| | |
|---|------|
| Percentage of fines passing 0.063mm sieve= | 0.25 |
|---|------|

Total dry mass M1= 1 kg

Table A.5 Water absorption test of virgin aggregates

| | DESCRIPTION | SAMPLE(g) | | |
|---|---|-----------|--------|--------|
| | | 1 | 2 | Avg |
| 1 | Weight of sample | 1000 | 1000 | 1000 |
| 2 | Weight of vessel+ Sample + Water (M2) g | 4353 | 4283 | 4318 |
| 3 | Weight of vessel + water (M3) g | 3733 | 3648 | 3690.5 |
| 4 | Weight of saturated and surface dry sample (M1) g | 1003 | 1014 | 1008.5 |
| 5 | Weight of oven dry sample (M4) g | 993 | 1003 | 998 |
| | | | | |
| | Apparent particle density (pa)= | 2.657 | 2.7206 | 2.689 |
| | Particle density on oven dry bases (prd) | 2.593 | 2.6464 | 2.6196 |
| | Particle density on saturated and oven dry bases(pssd) | 2.619 | 2.6755 | 2.6471 |
| | Water absorption(%)after 24hrs immersion in water | 1.007 | 1.0967 | 1.0519 |

Table A.6 Water absorption test of recycled aggregates (RA1)

| | DESCRIPTION | SAMPLE(g) | | |
|---|--|-----------|--------|--------|
| | | 1 | 2 | Avg |
| 1 | Weight of sample | 1000 | 1000 | 1000 |
| 2 | Weight of vessel+ Sample + Water (M2) g | 4282 | 4286 | 4284 |
| 3 | Weight of vessel + water (M3) g | 3692 | 3691 | 3691.5 |
| 4 | Weight of saturated and surface dry sample (M1) g | 1029 | 1025 | 1027 |
| 5 | Weight of oven dry sample (M4) g | 988 | 983 | 985.5 |
| | | | | |
| | Apparent particle density (pa)= | 2.478 | 2.5289 | 2.5034 |
| | Particle density on oven dry bases (prd) | 2.251 | 2.286 | 2.2683 |
| | Particle density on saturated and oven dry bases(pssd) | 2.344 | 2.3837 | 2.3638 |
| | Water absorption(%) after 24hrs immersion in water | 4.15 | 4.2726 | 4.2112 |

APPENDIX A. MIX DESIGN AND RAW DATA COLLATED FROM EXPERIMENTS OF
RECYCLED AND NAC WITH COEFFICIENT OF VARIATIONS

Table A.7 Water absorption test of recycled aggregates (RA2)

| | DESCRIPTION | SAMPLE(g) | | |
|---|--|-----------|--------|--------|
| | | 1 | 2 | Avg |
| 1 | Weight of sample | 1000 | 1000 | 1000 |
| 2 | Weight of vessel+ Sample + Water (M2) g | 2993 | 2991 | 2992 |
| 3 | Weight of vessel + water (M3) g | 2439 | 2432 | 2435.5 |
| 4 | Weight of saturated and surface dry sample (M1) g | 946 | 961 | 953.5 |
| 5 | Weight of oven dry sample (M4) g | 894 | 909 | 901.5 |
| | Apparent particle density (pa)= | 2.625 | 2.5925 | 2.6086 |
| | Particle density on oven dry bases (prd) | 2.281 | 2.2612 | 2.2709 |
| | Particle density on saturated and oven dry bases(pssd) | 2.413 | 2.3905 | 2.4019 |
| | Water absorption(%) after 24hrs immersion in water | 5.817 | 5.7206 | 5.7686 |

Table A.8 Mix design of natural aggregate concrete

| Stage | Item | Values |
|-------|-----------------------------|---|
| 1 | 1.1 Characteristic Strength | Compressive 40N/mm ² at 28 days Proportions defective say 5 percent |
| | 1.2 Standard deviation | Say 8N/mm ² |
| | 1.3 Margin | 1.64 X 8 = 13N/mm ² |
| | 1.4 Target mean strength | 40+13 = 53 |
| | 1.5 Cement Type | Ordinary Portland cement |
| | 1.6 Aggregate type: Coarse | Unrushed Aggregates |
| | Aggregate type: Fine sand | Uncrushed |
| | 1.7 Free-water/cement ratio | 0.4 |
| 2 | 2.1 Slump or V.B | Slump 60-180mm or V.B 0-3 secs |

APPENDIX A. MIX DESIGN AND RAW DATA COLLATED FROM EXPERIMENTS OF
RECYCLED AND NAC WITH COEFFICIENT OF VARIATIONS

| | | |
|---|----------------------------------|--------------------------------------|
| | 2.2 Maximum aggregate specified | 10mm |
| | 2.3 Free water content | 220 kg/m ³ |
| 3 | 3.1 Cement content | 220/0.40 = 550 kg/m ³ |
| 4 | 4.1 Relative density of concrete | 2.6 Assumed for uncrushed stones |
| | 4.2 Concrete density | 2325 kg/m ³ |
| | 4.3 Total aggregate content | 2340-550-225= 1565 kg/m ³ |
| 5 | 5.1 Grading of fine aggregates | Zone 3 as specified in BS 882 |
| | 5.2 Proportion fine aggregates | 40 percent |
| | 5.3 Fine aggregate content | 1565 X 0.4 = 626 kg/m ³ |
| | 5.4 Coarse aggregate content | 1565- 626 = 939 kg/m ³ |

Table A.9 Compressive strength of 3 samples of different recycled concrete mix without crumb rubber

| Concrete type | Compressive strength MPa | | | | | |
|---------------|--------------------------|-------|-------|---------|------|------|
| | 1 | 2 | 3 | Average | SD | CV% |
| NAC | 46.50 | 48.00 | 48.90 | 47.80 | 1.21 | 2.54 |
| RAC* | 40.00 | 44.10 | 45.50 | 43.20 | 2.86 | 6.62 |
| RAC | 32.10 | 30.50 | 30.40 | 31.00 | 0.95 | 3.08 |
| RACSP | 42.50 | 40.10 | 39.50 | 40.70 | 1.59 | 3.90 |

SD*- Standard deviation;

CV%- Coefficient of variation

NAC- Natural aggregate concrete

RAC*-Recycled aggregate concrete with no extra water or superplasticizer

RAC- Recycled aggregate concrete with extra water

RACSP- Recycled aggregate with superplasticizer

APPENDIX A. MIX DESIGN AND RAW DATA COLLATED FROM EXPERIMENTS OF
RECYCLED AND NAC WITH COEFFICIENT OF VARIATIONS

Table A.10 Compressive strength of 3 samples of different recycled concrete mix with and without crumb rubber

| Concrete type | Compressive strength MPa | | | | | |
|---------------|--------------------------|-------|-------|---------|------|------|
| | 1 | 2 | 3 | Average | SD | CV% |
| RAC 0% | 29.40 | 30.90 | 32.70 | 31.00 | 1.65 | 5.33 |
| RRAC 5% | 25.00 | 24.50 | 25.80 | 25.10 | 0.66 | 2.61 |
| RRAC 10% | 21.80 | 22.30 | 23.10 | 22.40 | 0.66 | 2.93 |
| RRAC 15% | 19.00 | 19.50 | 19.10 | 19.20 | 0.26 | 1.38 |
| RRAC 20% | 14.70 | 13.90 | 14.60 | 14.40 | 0.44 | 3.03 |
| RAC SP 0% | 42.50 | 40.10 | 39.50 | 40.70 | 1.59 | 3.90 |
| RRAC SP5% | 30.50 | 32.90 | 32.90 | 32.10 | 1.39 | 4.32 |
| RRAC SP10% | 24.50 | 25.60 | 25.80 | 25.30 | 0.70 | 2.77 |
| RRAC SP15% | 20.90 | 21.20 | 23.60 | 21.90 | 1.48 | 6.76 |
| RRAC SP20% | 17.30 | 18.00 | 17.20 | 17.50 | 0.44 | 2.49 |

Table A.11 Tensile strength of 3 samples of natural aggregate concrete and recycled aggregate concrete

| Concrete type | Tensile strength MPa | | | | | |
|---------------|----------------------|------|------|---------|------|------|
| | 1 | 2 | 3 | Average | SD | CV% |
| NAC | 3.98 | 4.20 | 4.15 | 4.11 | 0.12 | 2.81 |
| RAC | 2.79 | 3.00 | 3.15 | 2.98 | 0.18 | 6.07 |
| RACSP | 3.60 | 3.35 | 3.55 | 3.50 | 0.13 | 3.78 |

Table A.12 Tensile strength of 3 samples of different recycled concrete mixes with and without crumb rubber

| Concrete type | Tensile strength MPa | | | | | |
|---------------|----------------------|------|------|---------|------|------|
| | 1 | 2 | 3 | Average | SD | CV% |
| RAC 0% | 2.74 | 3.01 | 3.19 | 2.98 | 0.23 | 7.60 |
| RRAC 5% | 2.90 | 2.78 | 3.23 | 2.97 | 0.23 | 7.85 |
| RRAC 10% | 2.44 | 2.60 | 2.61 | 2.55 | 0.10 | 3.74 |
| RRAC 15% | 2.00 | 2.40 | 2.23 | 2.21 | 0.20 | 9.08 |
| RRAC 20% | 1.80 | 2.00 | 1.93 | 1.91 | 0.10 | 5.31 |

APPENDIX A. MIX DESIGN AND RAW DATA COLLATED FROM EXPERIMENTS OF
RECYCLED AND NAC WITH COEFFICIENT OF VARIATIONS

| | | | | | | |
|------------|------|------|------|------|------|------|
| RAC SP 0% | 3.60 | 3.35 | 3.55 | 3.50 | 0.13 | 3.78 |
| RRAC SP5% | 2.82 | 2.77 | 2.57 | 2.72 | 0.13 | 4.86 |
| RRAC SP10% | 2.78 | 2.86 | 2.82 | 2.82 | 0.04 | 1.42 |
| RRAC SP15% | 2.20 | 2.26 | 2.53 | 2.33 | 0.18 | 7.54 |
| RRAC SP20% | 1.90 | 1.78 | 2.05 | 1.91 | 0.14 | 7.08 |

Table A.13 Ultrasonic pulse velocity (UPV) of recycled and natural aggregate concrete

| Concrete type | UPV MPa | | | | | |
|---------------|---------|------|------|---------|------|------|
| | 1 | 2 | 3 | Average | SD | CV% |
| NAC | 4 | 4.5 | 4.07 | 4.19 | 0.27 | 6.46 |
| RAC | 3.65 | 3.95 | 4.1 | 3.90 | 0.23 | 5.88 |
| RACSP | 4.11 | 3.8 | 3.79 | 3.90 | 0.18 | 4.66 |

Table A.14 Ultrasonic pulse velocity (UPV) of recycled concrete with different crumb rubber content

| Concrete type | Tensile strength MPa | | | | | |
|---------------|----------------------|------|------|---------|------|------|
| | 1 | 2 | 3 | Average | SD | CV% |
| RAC 0% | 3.65 | 3.95 | 4.10 | 3.90 | 0.23 | 5.88 |
| RRAC 5% | 3.50 | 3.70 | 3.75 | 3.65 | 0.13 | 3.62 |
| RRAC 10% | 3.70 | 3.55 | 3.49 | 3.58 | 0.11 | 3.02 |
| RRAC 15% | 3.33 | 3.45 | 3.60 | 3.46 | 0.14 | 3.91 |
| RRAC 20% | 3.25 | 3.43 | 3.28 | 3.32 | 0.10 | 2.90 |
| RAC SP 0% | 4.11 | 3.80 | 3.79 | 3.90 | 0.18 | 4.66 |
| RRAC SP5% | 3.75 | 3.65 | 3.76 | 3.72 | 0.06 | 1.64 |
| RRAC SP10% | 3.59 | 3.63 | 3.61 | 3.61 | 0.02 | 0.55 |
| RRAC SP15% | 3.40 | 3.60 | 3.62 | 3.54 | 0.12 | 3.44 |
| RRAC SP20% | 3.45 | 3.30 | 3.48 | 3.41 | 0.10 | 2.83 |

APPENDIX A. MIX DESIGN AND RAW DATA COLLATED FROM EXPERIMENTS OF
RECYCLED AND NAC WITH COEFFICIENT OF VARIATIONS

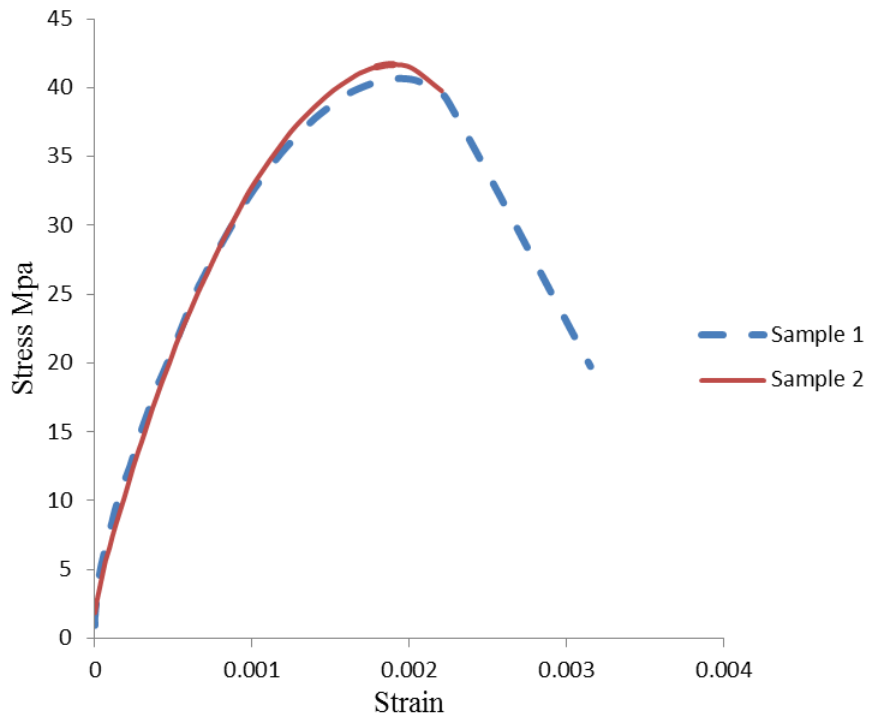


Figure A.1 Compressive stress strain curves of natural aggregate concrete samples

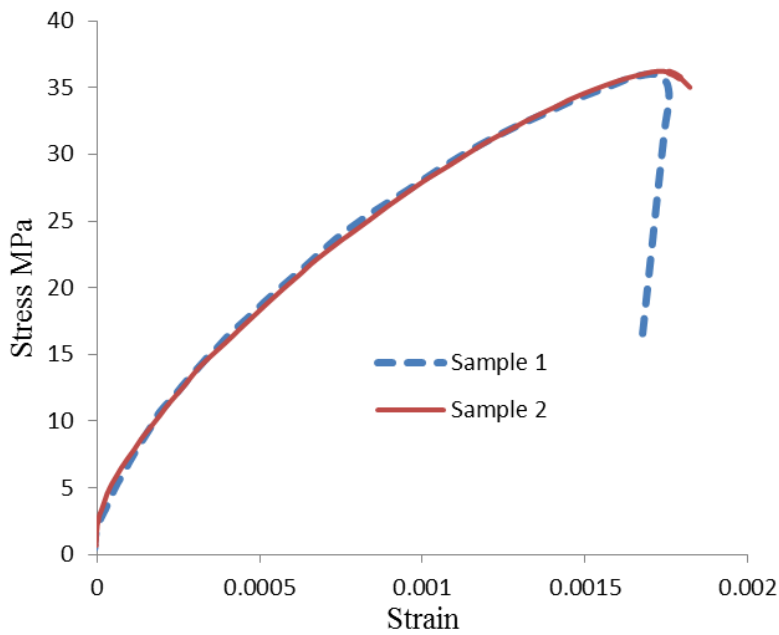


Figure A.2 Compressive stress strain curves for recycled aggregate concrete without crumb rubber

APPENDIX A. MIX DESIGN AND RAW DATA COLLATED FROM EXPERIMENTS OF
RECYCLED AND NAC WITH COEFFICIENT OF VARIATIONS

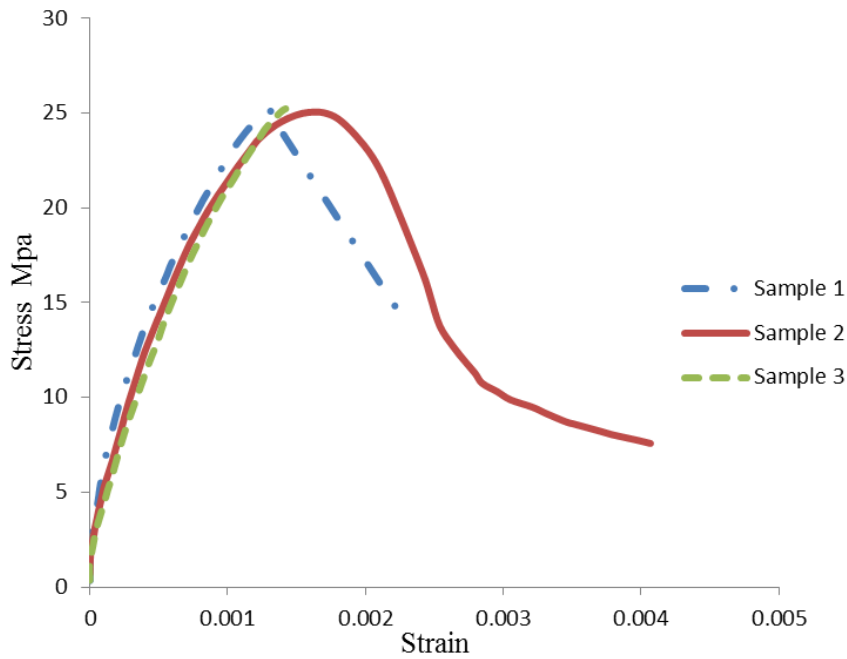


Figure A.3 Compressive stress strain curves for recycled aggregate concrete with 5% crumb rubber content (RRACSP 5%)

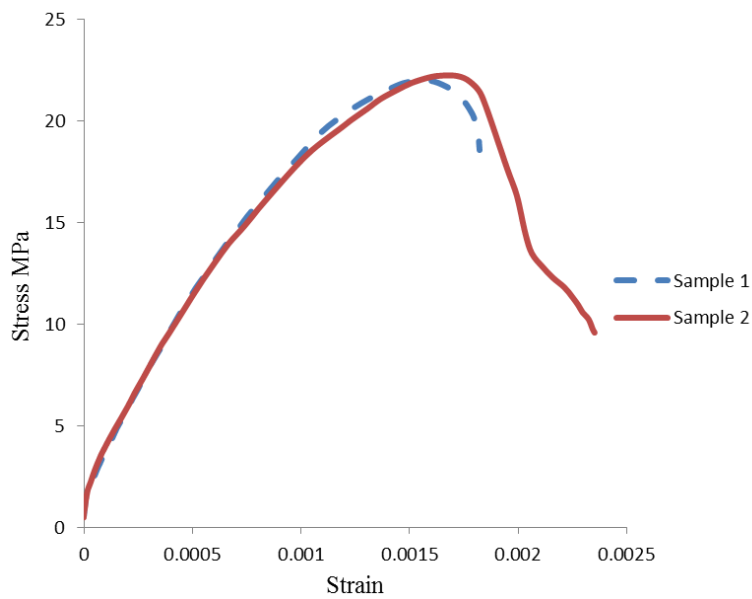


Figure A.4 Compressive stress strain curves for recycled aggregate concrete with 10% crumb rubber content (RRACSP 10%)

APPENDIX A. MIX DESIGN AND RAW DATA COLLATED FROM EXPERIMENTS OF
RECYCLED AND NAC WITH COEFFICIENT OF VARIATIONS

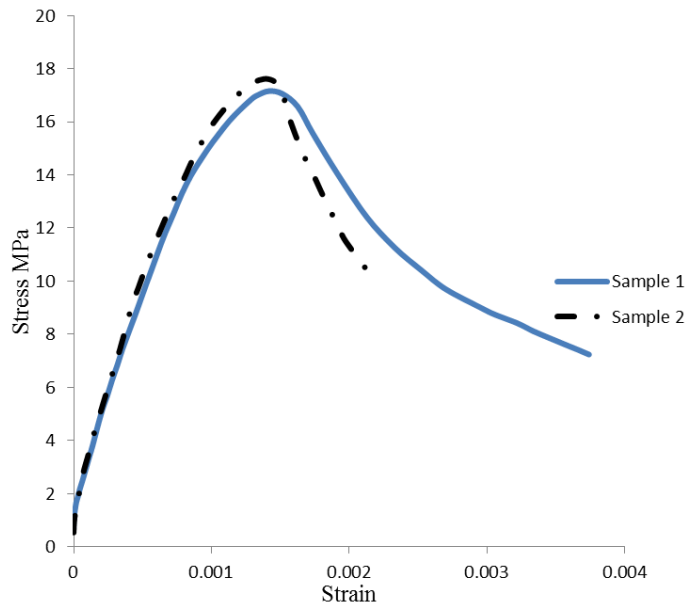


Figure A.5 Compressive stress strain curves for recycled aggregate concrete with 15% crumb rubber content (RRACSP 15%)

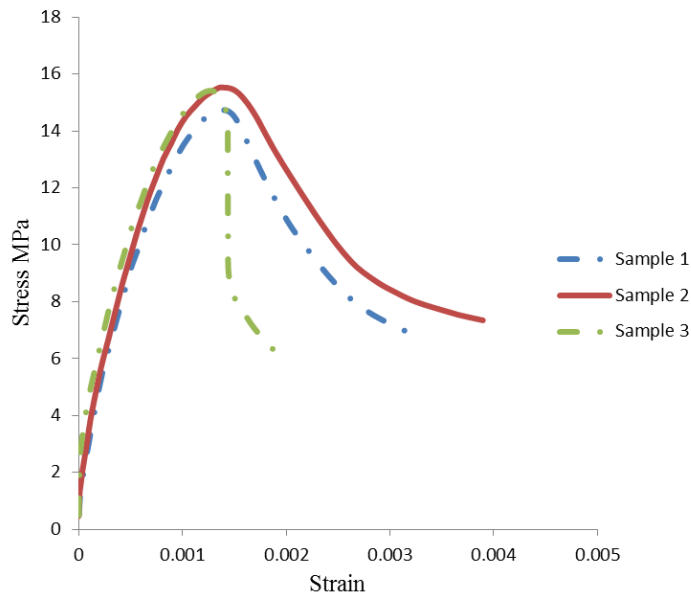


Figure A.6 Compressive stress strain curves for recycled aggregate concrete with 15% crumb rubber content (RRACSP 20%)

Appendix B

**Raw data collated from
experiments of bond stress slip
relationships for all samples.**

APPENDIX B. RAW DATA COLLATED FROM EXPERIMENTS OF BOND
STRESS SLIP RELATIONSHIPS FOR ALL SAMPLES

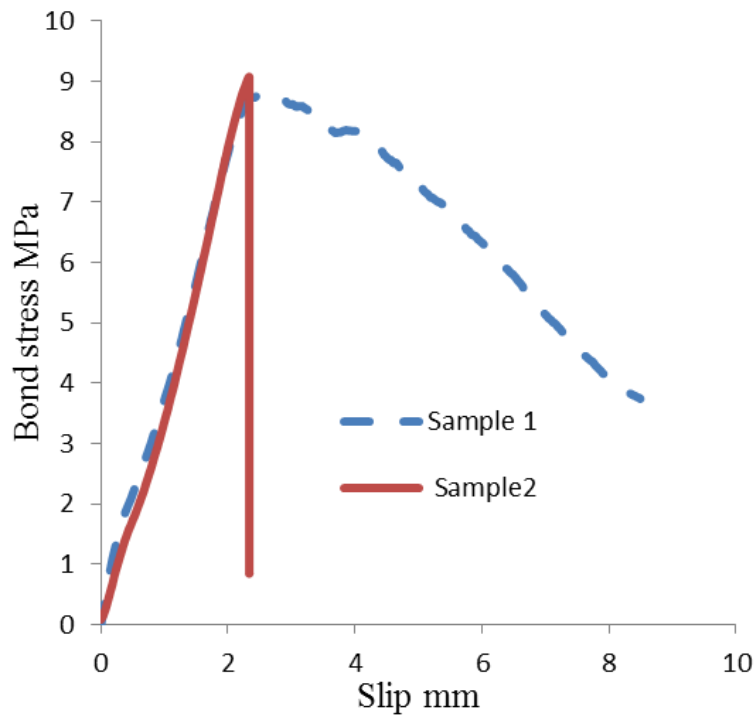


Figure B.1 Average bond stress slip relationship of pull-out test of natural aggregate concrete and rebars for all samples.

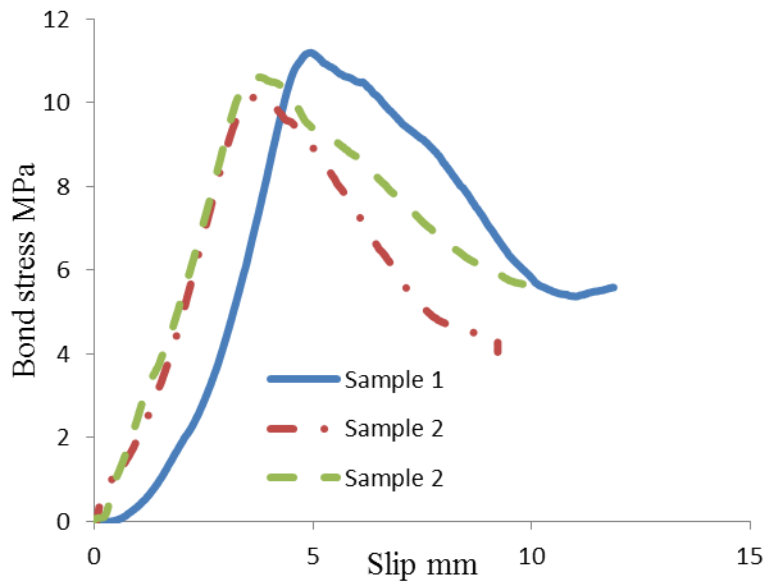


Figure B.2 Average bond stress slip relationship of pull-out test of recycled aggregate concrete (RAC) and rebars for all samples.

APPENDIX B. RAW DATA COLLATED FROM EXPERIMENTS OF BOND
STRESS SLIP RELATIONSHIPS FOR ALL SAMPLES

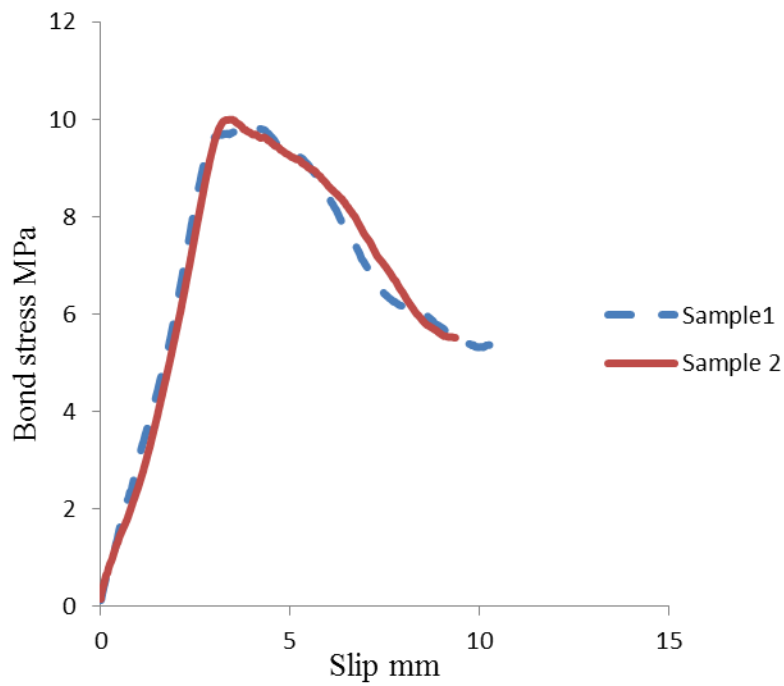


Figure B.3 Average bond stress slip relationship of pull-out test of recycled aggregate concrete with 5% crumb rubber (RRAC 5%) and rebars for all samples.

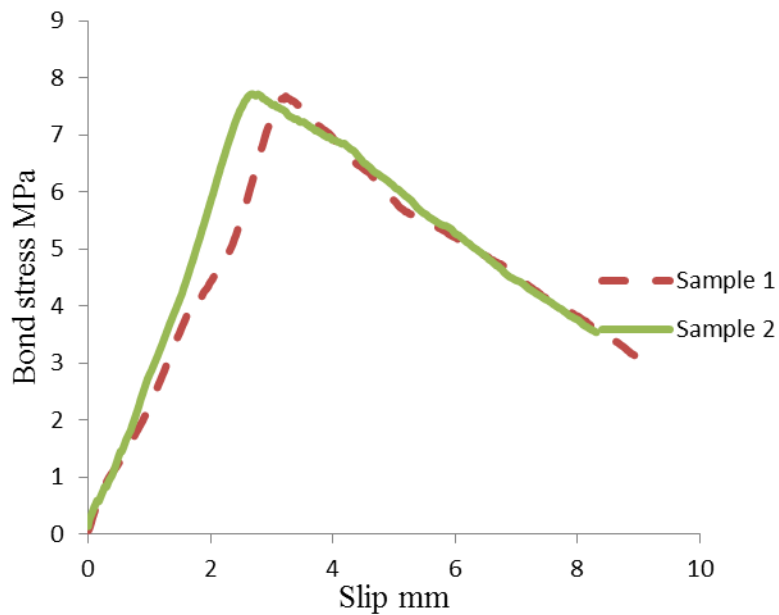


Figure B.4 Average bond stress slip relationship of pull-out test of recycled aggregate concrete with 15% crumb rubber (RRAC 15%) and rebars for all samples.

Appendix C

**Raw data collated from
experiments of interfacial shear
strength tests for all samples.**

APPENDIX C. RAW DATA COLLATED FROM EXPERIMENTS OF BOND
STRESS SLIP RELATIONSHIPS FOR ALL SAMPLES

Table C.1 Slant shear test results of 3 samples of all specimens

| Specimen | Cast time interval | Samples | | | Average | SD | CV% |
|----------|--------------------|---------|-------|-------|---------|------|-------|
| | | 1 | 2 | 3 | | | |
| T1 | 4 hrs | 11.80 | 12.40 | 12.10 | 12.10 | 0.30 | 2.48 |
| | 24hrs | 3.90 | 4.40 | 4.00 | 4.10 | 0.26 | 6.45 |
| T2 | 4 hrs | 9.00 | 8.50 | 9.20 | 8.90 | 0.36 | 4.05 |
| | 24hrs | 6.00 | 6.70 | 6.53 | 6.41 | 0.37 | 5.70 |
| T3 | 4 hrs | 6.00 | 5.00 | 6.67 | 5.89 | 0.84 | 14.27 |
| | 24hrs | 4.99 | 5.50 | 5.17 | 5.22 | 0.26 | 4.95 |

Table C.2 Splitting shear test results of 3 samples of all specimens

| Specimen | Cast time interval | Samples | | | Average | SD | CV% |
|----------|--------------------|---------|------|------|---------|------|-------|
| | | 1 | 2 | 3 | | | |
| T1 | 4 hrs | 2.20 | 2.55 | 2.45 | 2.40 | 0.18 | 7.51 |
| | 24hrs | 1.95 | 2.30 | 2.05 | 2.10 | 0.18 | 8.58 |
| T2 | 4 hrs | 2.50 | 2.20 | 2.20 | 2.30 | 0.17 | 7.53 |
| | 24hrs | 1.45 | 1.10 | 1.38 | 1.31 | 0.19 | 14.14 |
| T3 | 4 hrs | 1.60 | 1.30 | 1.54 | 1.48 | 0.16 | 10.73 |
| | 24hrs | 1.25 | 1.55 | 2.06 | 1.62 | 0.41 | 25.28 |

Table C.3 Notation and description of specimen types

| Notation | Concrete types | Description |
|----------|-----------------|--|
| T1 | NAC on NAC | Natural aggregate concrete cast on top of natural aggregate concrete with differential stiffness between layers. |
| T2 | NAC on RRAC5SP | Natural aggregate concrete cast on top of recycled aggregate concrete with 5% crumb rubber |
| T3 | NAC on RRAC10SP | Natural aggregate concrete cast on top of recycled aggregate concrete with 10% crumb rubber |

Appendix D

**Raw data collated from
experiments of graphene recycled
concrete for all samples.**

APPENDIX D. RAW DATA COLLATED FROM EXPERIMENTS OF GRAPHENE
RECYCLED CONCRETE FOR ALL SAMPLES

Table D.1 Influence of graphene concentration on the strength of recycled concrete with 10% crumb rubber

| Concrete type | Compressive strength MPa | | | | | |
|---------------|--------------------------|-------|-------|---------|------|------|
| | 1 | 2 | 3 | Average | SD | CV% |
| RRAC | 19.80 | 18.50 | 18.50 | 18.93 | 0.75 | 3.96 |
| G5 0.01 | 16.30 | 16.50 | 16.70 | 16.50 | 0.20 | 1.21 |
| G5 0.02 | 20.90 | 21.40 | 21.40 | 21.23 | 0.29 | 1.36 |
| G5 0.05 | 16.10 | 16.40 | 16.70 | 16.40 | 0.30 | 1.83 |
| G5 0.1 | 15.40 | 14.60 | 14.80 | 14.93 | 0.42 | 2.79 |
| G20 0.01 | 15.90 | 15.70 | 15.10 | 15.57 | 0.42 | 2.67 |
| G20 0.02 | 14.20 | 14.90 | 16.00 | 15.03 | 0.91 | 6.04 |
| G20 0.05 | 15.70 | 16.70 | 17.00 | 16.47 | 0.68 | 4.13 |
| G20 0.1 | 15.90 | 15.70 | 15.10 | 15.57 | 0.42 | 2.67 |

Table D.2 Influence of graphene concentration on the compressive strength of natural aggregate concrete.

| Concrete type | Compressive strength MPa | | | | | |
|---------------|--------------------------|-------|-------|---------|------|------|
| | 1 | 2 | 3 | Average | SD | CV% |
| NAC | 42.70 | 42.80 | 41.20 | 42.23 | 0.90 | 2.12 |
| NACG10 0.01 | 45.60 | 45.10 | 46.20 | 45.63 | 0.55 | 1.21 |
| NACG10 0.02 | 39.50 | 41.06 | 43.00 | 41.19 | 1.75 | 4.26 |
| NACG10 0.05 | 41.40 | 42.70 | 41.90 | 42.00 | 0.66 | 1.56 |

Table D.3 Influence of graphene concentration on the tensile strength of natural aggregate concrete.

| Concrete type | Tensile strength Mpa | | | | | |
|---------------|----------------------|------|------|---------|------|------|
| | 1 | 2 | 3 | Average | SD | CV% |
| NAC | 3.96 | 3.95 | 3.40 | 3.77 | 0.32 | 8.50 |
| NACG10 0.01 | 4.54 | 4.61 | 4.64 | 4.60 | 0.05 | 1.12 |
| NACG10 0.02 | 4.18 | 3.48 | 4.12 | 3.93 | 0.39 | 9.88 |

APPENDIX D. RAW DATA COLLATED FROM EXPERIMENTS OF GRAPHENE
RECYCLED CONCRETE FOR ALL SAMPLES

| | | | | | | |
|-------------|------|------|------|------|------|------|
| NACG10 0.05 | 3.93 | 4.34 | 3.74 | 4.00 | 0.31 | 7.66 |
|-------------|------|------|------|------|------|------|

Table D.4 Influence of graphene concentration on the compressive strength of washed and unwashed recycled aggregate concrete without crumb rubber

| Concrete type | Compressive strength MPa | | | | | |
|-------------------|--------------------------|-------|-------|---------|------|------|
| | 1 | 2 | 3 | Average | SD | CV% |
| RAC | 27.40 | 26.90 | 27.21 | 27.17 | 0.25 | 0.93 |
| RAC WASH | 35.39 | 31.50 | 31.33 | 32.74 | 2.30 | 7.01 |
| RAC W G10 0.01 | 39.17 | 37.20 | 41.05 | 39.14 | 1.93 | 4.92 |
| RAC W G10 0.02 | 35.15 | 35.11 | 33.95 | 34.74 | 0.68 | 1.96 |
| RAC W G10 0.05 | 31.47 | 35.35 | 31.17 | 32.66 | 2.33 | 7.14 |

Table D.5 Influence of graphene concentration on the tensile strength of washed and unwashed recycled aggregate concrete without crumb rubber

| Concrete type | Tensile strength MPa | | | | | |
|-------------------|----------------------|------|------|---------|------|-------|
| | 1 | 2 | 3 | Average | SD | CV% |
| RAC | 2.75 | 2.96 | 3.38 | 3.03 | 0.32 | 10.59 |
| RAC WASH | 3.15 | 3.14 | 3.12 | 3.14 | 0.02 | 0.49 |
| RAC W G10 0.01 | 3.80 | 3.69 | 3.78 | 3.76 | 0.06 | 1.56 |
| RAC W G10 0.02 | 3.50 | 3.71 | 3.75 | 3.65 | 0.13 | 3.68 |
| RAC W G10 0.05 | 3.26 | 3.37 | 3.25 | 3.29 | 0.07 | 2.02 |

APPENDIX D. RAW DATA COLLATED FROM EXPERIMENTS OF GRAPHENE
RECYCLED CONCRETE FOR ALL SAMPLES

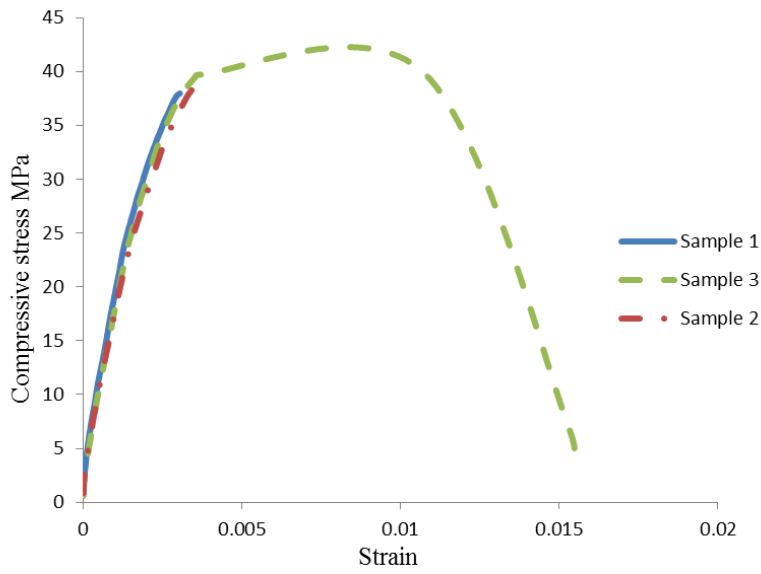


Figure D.1 Compressive stress strain of natural aggregate concrete with 0.01% graphene concentration.

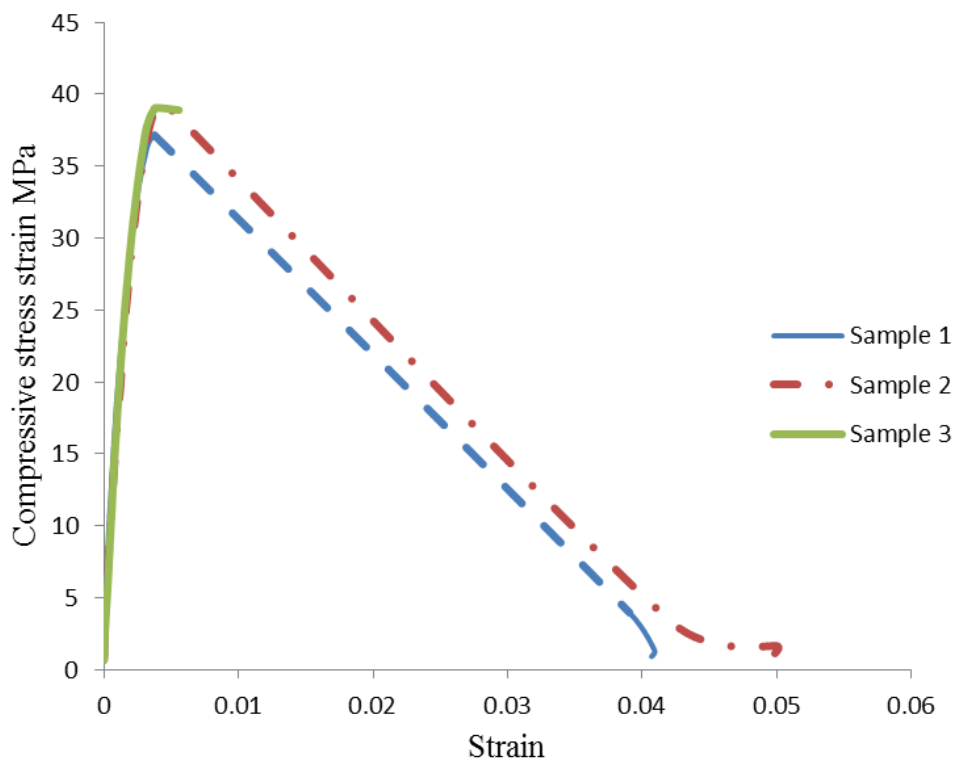


Figure D.2 Compressive stress strain of natural aggregate concrete with 0.02% graphene concentration

APPENDIX D. RAW DATA COLLATED FROM EXPERIMENTS OF GRAPHENE
RECYCLED CONCRETE FOR ALL SAMPLES

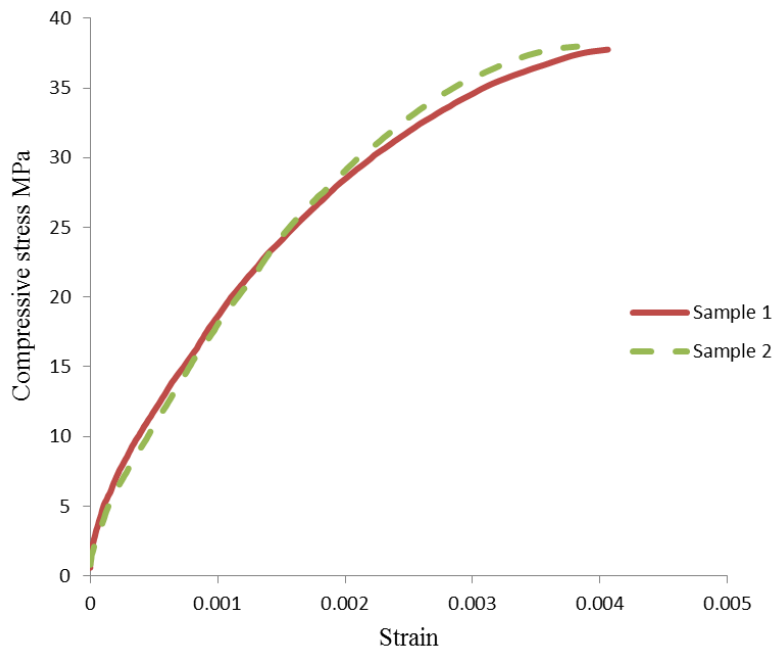


Figure D.3 Compressive stress strain of natural aggregate concrete with 0.05% graphene concentration

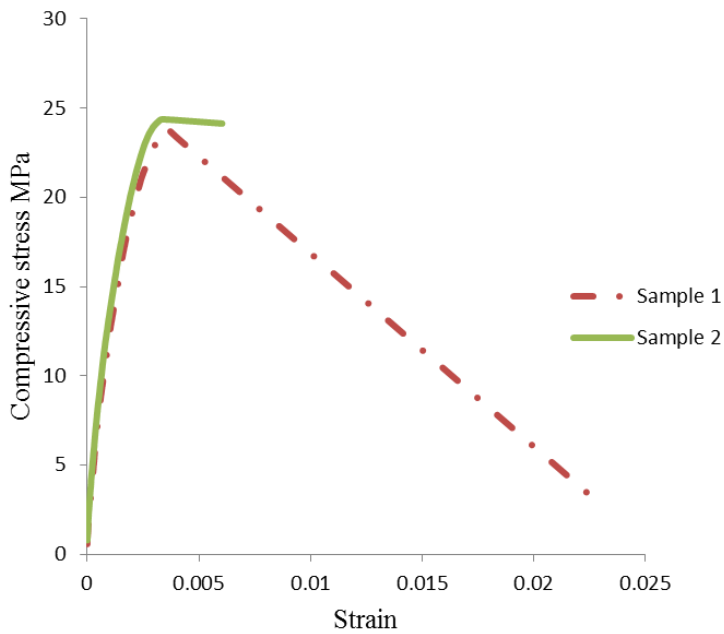


Figure D.4 Compressive stress strain of washed recycled aggregate concrete without graphene solution

APPENDIX D. RAW DATA COLLATED FROM EXPERIMENTS OF GRAPHENE
RECYCLED CONCRETE FOR ALL SAMPLES

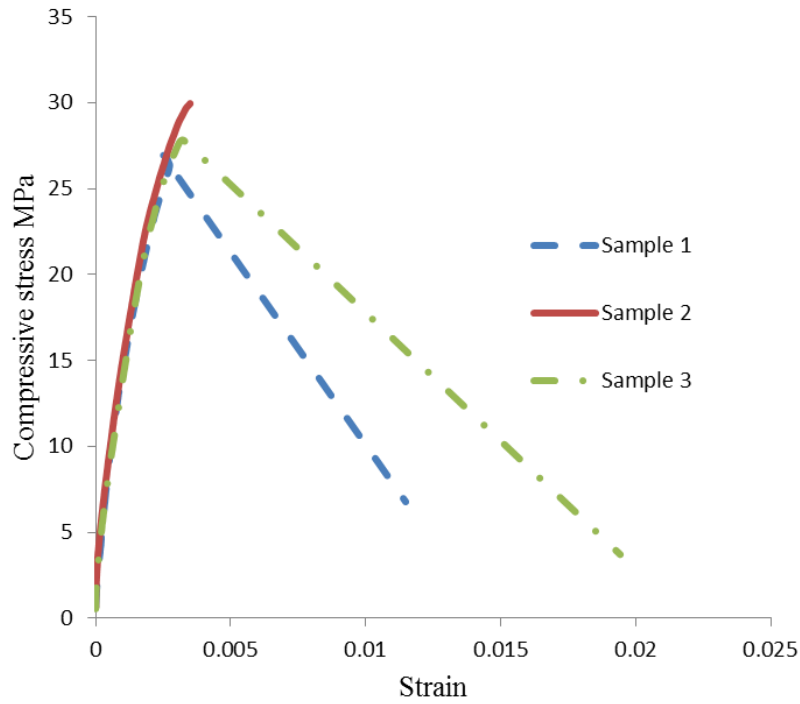


Figure D.5 Compressive stress strain of washed recycled aggregate concrete with 0.01% graphene concentration

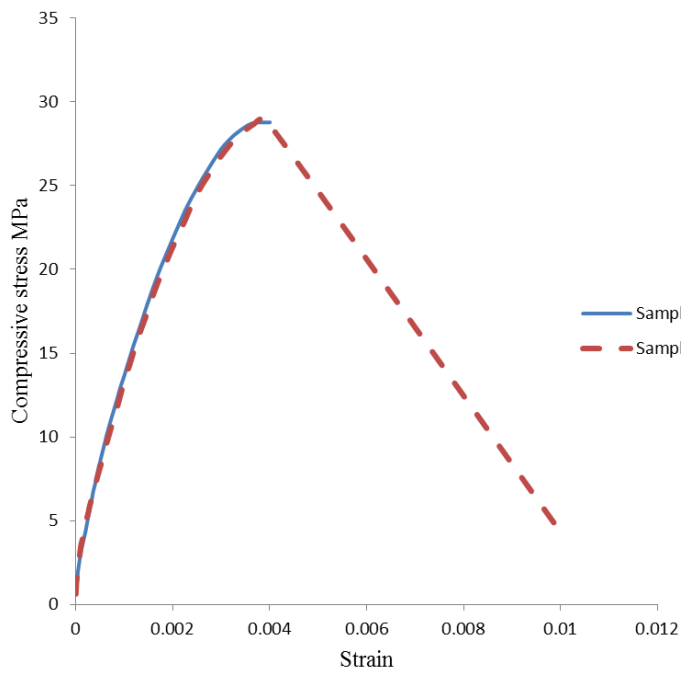


Figure D.6 Compressive stress strain of washed recycled aggregate concrete with 0.02% graphene concentration

APPENDIX D. RAW DATA COLLATED FROM EXPERIMENTS OF GRAPHENE
RECYCLED CONCRETE FOR ALL SAMPLES

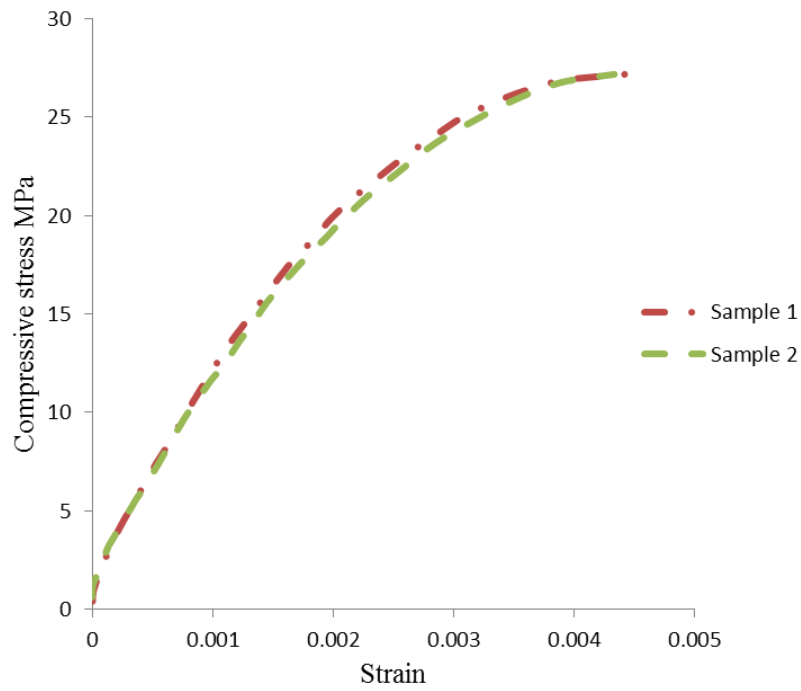


Figure D.7 Compressive stress strain of washed recycled aggregate concrete with 0.05% graphene concentration

Appendix E

Bending moment and shear capacity calculations of the RC section in Fig4.2 & 4.3 to EC2 and predicted methods. Effects of reinforcement ratio and shear span depth ratio on two-layer beams (ABAQUS).

APPENDIX E. BENDING MOMENT AND SHEAR CAPACITY CALCULATIONS
OF THE REINFORCED CONCRETE SECTION IN FIGURE 4.2 AND 4.3 TO EC2
AND PREDICTED METHODS

Table E.1: Mechanical properties of steel reinforcement for flexure [44]

| Bar size (mm). | Yield stress (MPa) | Ultimate stress (MPa) | Elastic Modulus (MPa) |
|----------------|--------------------|-----------------------|-----------------------|
| 10 | 494 | 746 | 206,890 |
| 19 | 568 | 811 | 196,570 |
| 22 | 517 | 791 | 193,140 |

Table E.2: Summary of concrete material properties [44]

| Designation | Compressive Strength (MPa) | Splitting tensile strength (MPa) | Elastic modulus (MPa) | Poissons ratio |
|--------------|----------------------------|----------------------------------|-----------------------|----------------|
| Bending test | 37.2 | 3.48 | 34614 | 0.2 |

E.1: Details of fractured energy calculations

The fractured energy (G_F) of concrete is the energy required to propagate a tensile crack of unit area.

$$G_F = G_{FO} \left(\frac{f_{cm}}{f_{cm0}} \right)^{0.7}$$

Where $f_{cm0} = 10$ MPa

G_{FO} is the base fractured energy which depends on the size of the aggregates

$$G_{FO} = 0.0275 Nmm/mm^2 \text{ For aggregate size } 10mm$$

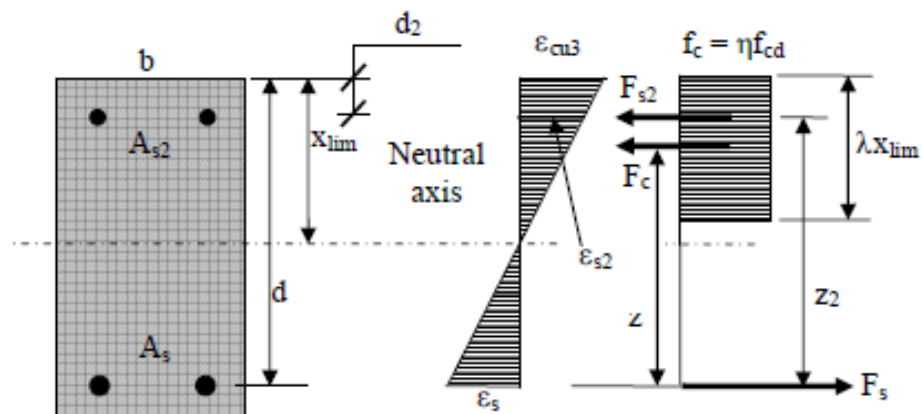
f_{cm} : Axial tensile strength assumed as 0.9 of splitting test strength

APPENDIX E. BENDING MOMENT AND SHEAR CAPACITY CALCULATIONS
 OF THE REINFORCED CONCRETE SECTION IN FIGURE 4.2 AND 4.3 TO EC2
 AND PREDICTED METHODS

$$f_{cm} = 0.9 * 4.11 = 3.699 \text{ MPa}$$

$$G_F = G_{FO} \left(\frac{f_{cm}}{f_{cm0}} \right)^{0.7} = 0.0275 \left(\frac{3.699}{10} \right)^{0.7} = 0.0137 \text{ Nmm/mm}^2$$

E.2: Bending RC beams calculations to EC2



For equilibrium of the above section

$$F_{st} = F_{cc} + F_{sc}$$

$$z_{bal} = d - \frac{s_{bal}}{2} = d - \frac{0.8x_{bal}}{2}$$

The depth of the neutral axis

$$A_s f_y = (0.8 * 40 * 150 * s) + (A_{s2} f_y)$$

$$402.18 = (0.8 * 40 * 150 * s) + (100.54 * 547.2)$$

APPENDIX E. BENDING MOMENT AND SHEAR CAPACITY CALCULATIONS
OF THE REINFORCED CONCRETE SECTION IN FIGURE 4.2 AND 4.3 TO EC2
AND PREDICTED METHODS

$$s = 34.7mm$$

$$z_{bal} = 132 - \frac{34.7}{2} = 114.65mm$$

Taking moment about the centroid of the tension steel

$$M = F_{cc} * z_{bal} + F_{sc}(d - d')$$

$$M = (0.8 * 40 * 150 * 34.7) * 114.65 + (100.54 * 547.2 * 120) = 26KNm$$

E.3: Shear capacity of RC beams calculations to EC2

Shear capacity of concrete beams without links is given by:

$$V_c = \left[0.18K(100\rho f_{ck}^1)^{1/3} \right] b * d$$

$$K = \text{Size effect factor} \left(K = 1 + \sqrt{\frac{200}{d}} \right) \leq 2.0$$

$$K = 1 + \sqrt{\frac{200}{132}} = 2.33$$

Therefore, $K = 2$

$$\rho = \frac{A_s}{b_w d} \leq 0.02$$

APPENDIX E. BENDING MOMENT AND SHEAR CAPACITY CALCULATIONS
OF THE REINFORCED CONCRETE SECTION IN FIGURE 4.2 AND 4.3 TO EC2
AND PREDICTED METHODS

$$\rho = \frac{402.18}{150 * 132} = 0.02$$

$$V_c = \left[0.18 * 2 * (100 * 0.02 * 41)^{1/3} \right] * 150 * 132$$

$$V_c = 1.5617 * 150 * 132 = 30.92KN$$

E.4: Shear capacity of RC beams calculations to Zsutty, 1971)

$$v_c = 2.1746 \left(f_{ck} * \rho * \frac{d}{a} \right)^{1/3} [Mpa] \quad \text{for } \frac{a}{d} \geq 2.5$$

$$\frac{a}{d} = \frac{450}{132} = 3.4$$

$$\frac{d}{a} = 0.293$$

$$v_c = 2.1746 \left(41 * 0.0203 * \frac{132}{450} \right)^{1/3} = 1.366MPa$$

$$V_c = 1.366 * 132 * 150 = 27.04KN$$

APPENDIX E. BENDING MOMENT AND SHEAR CAPACITY CALCULATIONS
OF THE REINFORCED CONCRETE SECTION IN FIGURE 4.2 AND 4.3 TO EC2
AND PREDICTED METHODS

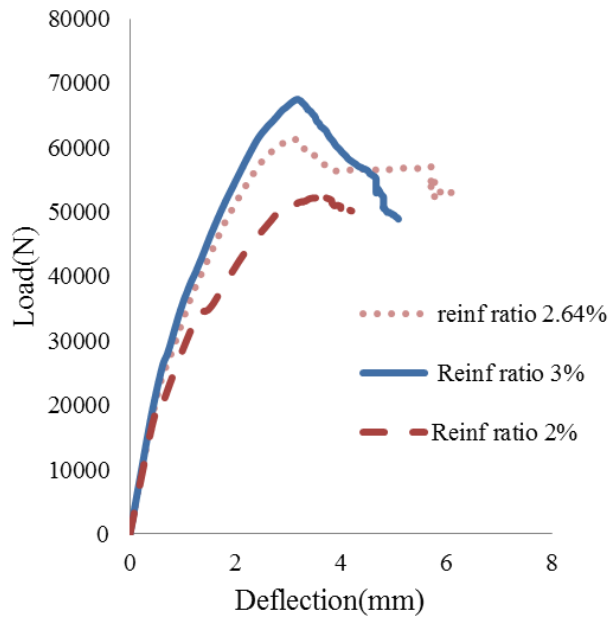


Figure E.1 Effect of reinforcement ratio on the shear capacity of two-layer beams

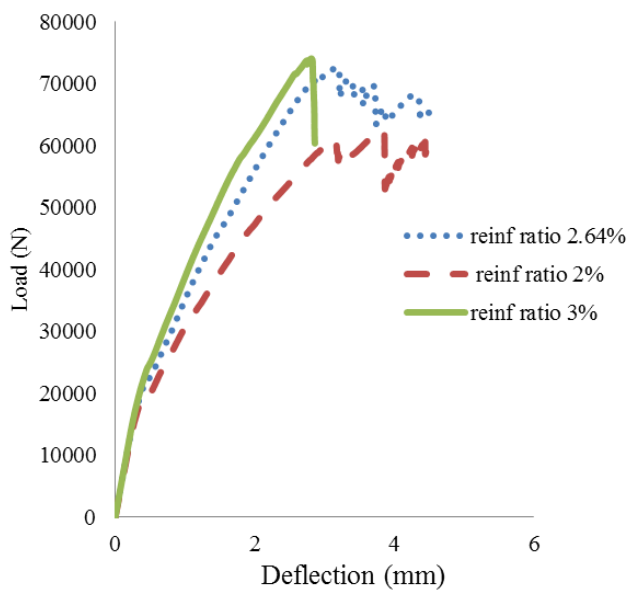


Figure E.2 Effect of reinforcement ratio on the shear capacity of regular concrete beams

Appendix F

Detailed calculations of vertical shear links required for beams

F.1: Vertical shear links for the regular concrete beams

(a) Check the maximum shear force at the face of support

$$\text{Maximum shear force} = \frac{WL}{2}$$

$$V_{ED} = \frac{64.37 * 7.2}{2} = 231.73KN$$

Design shear force at the face of the support

$$V_{ED} = 231.73 - (64.37 * 0.2) = 218.9KN$$

Crushing strength of diagonal strut, assuming angle $\theta = 22^\circ$

$$V_{Rd,max} = 0.124b_w d \left(1 - \frac{f_{ck}}{250}\right) f_{ck} = 0.124 * 250 * 450 \left(1 - \frac{40}{250}\right) * 40 * 10^{-3}$$

$$V_{Rd,max} = 468.7KN > V_{ED} = 218.9KN$$

Therefore, angle $\theta = 22^\circ$ and $\cot \theta = 2.5$ is assumed

b) Shear links

At distance d from the face of the support, the design shear force is

$$V_{ED} = 218.9 - (64.37 * 0.45) = 189.9KN$$

APPENDIX F. VERTICAL SHEAR LINKS REQUIRED FOR TWO LAYER BEAMS
WITH SHEAR SPAN DEPTH RATIO OF 10.6

$$V_{ED} = V_{wd} = f_{ywd} A_{sw} = \frac{f_{yk} A_{sw}}{1.15} = 0.87 f_{yk} A_{sw}$$

If links are spaced at 's' apart, the force in each link is given by

$$V_{wd} \frac{s}{z \cot \theta} = 0.87 f_{yk} A_{sw}$$

$$V_{wd} = 0.87 \frac{A_{sw}}{s} z f_{yk} \cot \theta = 0.87 \frac{A_{sw}}{s} 0.9 d f_{yk} \cot \theta$$

There is no direct contribution of concrete in the shear resistance of the RC beams based on EC2; however, it is necessary to resist the crushing of the concrete diagonal members.

$$\frac{A_{sw}}{s} = \frac{V_{ED}}{0.78 d f_{yk} \cot \theta} = \frac{189.9 * 1000}{0.78 * 450 * 420 * 2.5} = 0.52$$

The cross sectional area of 10mm bar is 78.55mm² Thus for 2 legs of the shear link and a spacing of 250mm

$$\frac{A_{sw}}{s} = \frac{2 * 78.55}{275} = 0.57$$

Therefore provide 10mm @ 275mm c/c

The shear resistance of the links is given by

$$V_{Rds} = 0.78 \frac{A_{sw}}{s} d f_{yk} \cot \theta = 0.78 * 0.57 * 450 * 420 * 2.5 * 10^{-3} = 210KN$$

APPENDIX F. VERTICAL SHEAR LINKS REQUIRED FOR TWO LAYER BEAMS
WITH SHEAR SPAN DEPTH RATIO OF 10.6

210KN > 189.9KN. So it's OK.

Therefore 10mm@275mm c/c is sufficient to resist the 189.9KN shear force at distance 1 d from the face of support.

c) Minimum shear links

$$\frac{A_{sw,min}}{s} = \frac{0.08 f_{ck}^{0.5} b_w}{f_{yk}} = \frac{0.08 * 40^{0.5} * 250}{420} = 0.3$$

Provide Y8mm@ 300mm/c $\frac{A_{sw,min}}{s} = 0.33$

$$V_{min} = 0.87 \frac{A_{sw}}{s} d f_{yk} \cot \theta = 0.78 * 0.33 * 450 * 420 * 2.5 = 121.6KN$$

d) Extent of shear links

Shear links are required from the face of the support at both ends of the beam to a point where the design shear force is $V_{min} = 189.9KN$.

From the face of the support, distance 'x' is given by

$$\frac{V_{ED} - V_{min}}{W_u} = \frac{189.9 - 121.6}{64.37} = 1.1metres$$

Therefore, the number of Y10mm @ 275mm c/c required at each end of the beam is

$$1 + \frac{1100}{275} = 5$$

APPENDIX F. VERTICAL SHEAR LINKS REQUIRED FOR TWO LAYER BEAMS
WITH SHEAR SPAN DEPTH RATIO OF 10.6

Table F 1: Cost estimate of the regular concrete beam

| ITEM | DESCRIPTION | QTY | UNIT | RATE(£) | AMOUNT(£) |
|-------------|---|----------|----------------|----------|-----------------|
| | Regular concrete beams | | | | |
| 1.00 | Concrete C40 MPa | | | | |
| 1.01 | In-situ concrete for grade C40 for beam | 0.900000 | m ³ | 191.42 | 172.28 |
| | | | | | |
| 2.00 | Formwork; fair finish | | | | |
| 2.01 | Form work for beams with a constant cross section of 250mm X 500mm deep | 8.280000 | m ² | 98.48 | 815.41 |
| | | | | | |
| 3.00 | Deformed high yield steel bars to BS 4449 | | | | |
| 3.01 | 25mm nominal size | 0.023460 | tonne | 1,343.87 | 31.53 |
| 3.02 | 18mm nominal size | 0.007820 | tonne | 1,612.18 | 12.61 |
| 3.03 | 12mm nominal size | 0.014460 | tonne | 1,704.74 | 24.65 |
| 3.04 | 10mm nominal size | 0.008804 | tonne | 1,704.74 | 15.01 |
| 3.05 | 8mm nominal size | 0.008974 | tonne | 1,704.74 | 15.30 |
| | | | | | |
| | Total cost | | | | 1,086.78 |

References

1. Fisher, K. and L. Holmes, *UK Statistics on Waste, Department for Environment Food and Rural Affairs*. 2019.
2. Mansikkasalo, A., R. Lundmark, and P. Söderholm, *Market behavior and policy in the recycled paper industry: A critical survey of price elasticity research*. *Forest Policy and Economics*, 2014. **38**: p. 17-29.
3. Oyedele, L.O., S.O. Ajayi, and K.O. Kadiri, *Use of recycled products in UK construction industry: An empirical investigation into critical impediments and strategies for improvement*. *Resources, Conservation and Recycling*, 2014. **93**: p. 23-31.
4. Mehta, P. and H. Meryman, *Tools for reducing carbon emissions due to cement consumption*. *Struct Mag*, 2009: p. 11–5.
5. Oikonomou, N.D., *Recycled concrete aggregates*. *Cement and Concrete Composites*, 2005. **27**(2): p. 315-318.
6. Wang, J., et al., *Mechanical properties of recycled concrete in marine environment*. *ScientificWorldJournal*, 2013. **2013**: p. 728357.
7. Dilbas, H., M. Şimşek, and Ö. Çakır, *An investigation on mechanical and physical properties of recycled aggregate concrete (RAC) with and without silica fume*. *Construction and Building Materials*, 2014. **61**: p. 50-59.
8. García-González, J., et al., *Pre-Saturation Technique of the Recycled Aggregates: Solution to the Water Absorption Drawback in the Recycled Concrete Manufacture*. *Materials*, 2014. **7**(9): p. 6224-6236.
9. Kou, S.C. and C.S. Poon, *Enhancing the durability properties of concrete prepared with coarse recycled aggregate*. *Construction and Building Materials*, 2012. **35**: p. 69-76.

-
10. Limbachiya, M., M.S. Meddah, and Y. Ouchagour, *Use of recycled concrete aggregate in fly-ash concrete*. Construction and Building Materials, 2011.
 11. Barbudo, A., et al., *Influence of water-reducing admixtures on the mechanical performance of recycled concrete*. Journal of Cleaner Production, 2013. **59**: p. 93-98.
 12. Beltran, M.G., et al., *Effect of cement addition on the properties of recycled concretes to reach control concretes strengths*. Journal of Cleaner Production, 2014. **79**: p. 124-133.
 13. Sato R, et al., *Flexural behaviour of reinforced recycled concrete beams*. Journal of Advance Concrete Technology, 2007. **5**, **No. 1**: p. 43-61.
 14. Ignjatović, I.S., et al., *Flexural behavior of reinforced recycled aggregate concrete beams under short-term loading*. Materials and Structures, 2012. **46**(6): p. 1045-1059.
 15. Behera, M., et al., *Recycled aggregate from C&D waste & its use in concrete – A breakthrough towards sustainability in construction sector: A review*. Construction and Building Materials, 2014. **68**: p. 501-516.
 16. Li, X., *Recycling and reuse of waste concrete in China*. Resources, Conservation and Recycling, 2008. **53**(1-2): p. 36-44.
 17. Matias, D., et al., *Mechanical properties of concrete produced with recycled coarse aggregates – Influence of the use of superplasticizers*. Construction and Building Materials, 2013. **44**: p. 101-109.
 18. Etxeberria, M., et al., *Influence of amount of recycled coarse aggregates and production process on properties of recycled aggregate concrete*. Cement and Concrete Research, 2007. **37**(5): p. 735-742.
 19. Tam, V.W.Y., C.M. Tam, and K.N. Le, *Removal of cement mortar remains from recycled aggregate using pre-soaking approaches*. Resources, Conservation and Recycling, 2007. **50**(1): p. 82-101.
 20. Akbarnezhad, A., et al., *Microwave-assisted beneficiation of recycled concrete aggregates*. Construction and Building Materials, 2011. **25**(8): p. 3469-3479.
 21. Katz, A., *Properties of concrete made with recycled aggregate from partially hydrated old concrete*. Cement and Concrete Research, 2003. **33**(5): p. 703-711.
 22. ETRMA, *European Tyre Recycling Association (ETRA)*. 2014.
 23. Torretta, V., et al., *Treatment and disposal of tyres: Two EU approaches. A review*. Waste Manag, 2015. **45**: p. 152-160.
-

-
24. Ling, T.C., H.M. Nor, and S.K. Lim, *Using recycled waste tyres in concrete paving blocks*. Proceedings of the ICE - Waste and Resource Management, 2010. **163**(1): p. 37-45.
 25. Zheng, L., X. Sharon Huo, and Y. Yuan, *Experimental investigation on dynamic properties of rubberized concrete*. Construction and Building Materials, 2008. **22**(5): p. 939-947.
 26. Toutanji, H.A., *The Use of Rubber Tire Particles in Concrete to replace mineral aggregates*. Cement & Concrete Composites, 1995. **18**: p. 135-139.
 27. Hernández-Olivares, F., et al., *Static and dynamic behaviour of recycled tyre rubber-filled concrete*. Cement and Concrete Research, 2002. **32**: p. 1587–1596.
 28. Najim, K.B. and M.R. Hall, *Crumb rubber aggregate coatings/pre-treatments and their effects on interfacial bonding, air entrapment and fracture toughness in self-compacting rubberised concrete (SCRC)*. Materials and Structures, 2013. **46**(12): p. 2029-2043.
 29. Wang, L. and Y.H. Huang, *Study on Rubber Particles Modified Concrete*. Applied Mechanics and Materials, 2013. **477-478**: p. 953-958.
 30. Khaloo, A.R., M. Dehestani, and P. Rahmatabadi, *Mechanical properties of concrete containing a high volume of tire-rubber particles*. Waste Manag, 2008. **28**(12): p. 2472-82.
 31. Atahan, A.O. and A.Ö. Yücel, *Crumb rubber in concrete: Static and dynamic evaluation*. Construction and Building Materials, 2012. **36**: p. 617-622.
 32. Long, G., et al., *Efficiency of waste tire rubber aggregate on the rheological properties and compressive strength of cementitious materials*. Journal of Sustainable Cement-Based Materials, 2014. **3**(3-4): p. 201-211.
 33. Moustafa, A. and M.A. ElGawady, *Mechanical properties of high strength concrete with scrap tire rubber*. Construction and Building Materials, 2015. **93**: p. 249-256.
 34. Holmes, N., A. Browne, and C. Montague, *Acoustic properties of concrete panels with crumb rubber as a fine aggregate replacement*. Construction and Building Materials, 2014. **73**: p. 195-204.
 35. Ganjian, E., M. Khorami, and A.A. Maghsoudi, *Scrap-tyre-rubber replacement for aggregate and filler in concrete*. Construction and Building Materials, 2009. **23**(5): p. 1828-1836.
 36. Aiello, M.A. and F. Leuzzi, *Waste tyre rubberized concrete: properties at fresh and hardened state*. Waste Manag, 2010. **30**(8-9): p. 1696-704.
-

-
37. Eldin, N.N. and A.B. Senouci, *Measurement and Prediction of the Strength of Rubberized Concrete*. Cement & Concrete Composites, 1994. **16 (1994) 287-298**.
 38. Topçu, İ.B., *THE PROPERTIES OF RUBBERIZED CONCRETES*. Cement and Concrete Research, 1995. **Vol. 25, No. 2**; p. 304-310.
 39. Guo, Y.-c., et al., *Compressive behaviour of concrete structures incorporating recycled concrete aggregates, rubber crumb and reinforced with steel fibre, subjected to elevated temperatures*. Journal of Cleaner Production, 2014. **72**: p. 193-203.
 40. Mefteh, H., et al., *Influence of moisture conditioning of recycled aggregates on the properties of fresh and hardened concrete*. Journal of Cleaner Production, 2013. **54**: p. 282-288.
 41. Najim, K.B. and M.R. Hall, *Workability and mechanical properties of crumb-rubber concrete*. Proceedings of the ICE - Construction Materials, 2013. **166(1)**: p. 7-17.
 42. Gupta, T., S. Chaudhary, and R.K. Sharma, *Assessment of mechanical and durability properties of concrete containing waste rubber tire as fine aggregate*. Construction and Building Materials, 2014. **73**: p. 562-574.
 43. Malešev, M., V. Radonjanin, and S. Marinković, *Recycled Concrete as Aggregate for Structural Concrete Production*. Sustainability, 2010. **2(5)**: p. 1204-1225.
 44. Arezoumandi, M., et al., *An experimental study on flexural strength of reinforced concrete beams with 100% recycled concrete aggregate*. Engineering Structures, 2015. **88**: p. 154-162.
 45. Dimov, D., et al., *Ultrahigh Performance Nanoengineered Graphene-Concrete Composites for Multifunctional Applications*. Advanced Functional Materials, 2018. **28(23)**: p. 1705183.
 46. Tong, T., et al., *Investigation of the effects of graphene and graphene oxide nanoplatelets on the micro- and macro-properties of cementitious materials*. Construction and Building Materials, 2016. **106**: p. 102-114.
 47. M. C. Limbachiya, T. Leelawat, and R.K. Dhir, *Use of recycled concrete aggregate in high-strength concrete*. Materials and Structures/Matériaux et Constructions, 2000. **Vol. 33**: p. 574-580.
 48. McNeil, K. and T.H.K. Kang, *Recycled Concrete Aggregates: A Review*. International Journal of Concrete Structures and Materials, 2013. **7(1)**: p. 61-69.
-

-
49. AB-Malek, K. and Stevenson, *The effects of 42 years immersion in sea water on natural rubber*. Journal of Materials Science, 1986. **Vol. 21**: p. 147-154.
 50. Edeskär, T., *Use of Tyre Shreds in Civil Engineering Applications*. 2006.
 51. Evans, A.R., *The Composition of a Tyre: Typical Components* The Waste & Resources Action Programme 2006.
 52. Sara Sgobba, et al., *Use of Rubber Particles from Recycled Tires as Concrete Aggregate for Engineering Applications.pdf*>. Coventry University and The University of Wisconsin Milwaukee Centre for by-products Utilization, 2013.
 53. Najim, K.B. and M.R. Hall, *Mechanical and dynamic properties of self-compacting crumb rubber modified concrete*. Construction and Building Materials, 2012. **27**(1): p. 521-530.
 54. Moo-Young, H., et al., *Physical and Chemical Properties of Recycled Tire Shreds for Use in Construction*. JOURNAL OF ENVIRONMENTAL ENGINEERING © ASCE, 2003.
 55. Baranowski, P., J. Janiszewski, and J. Małachowski, *Tire rubber testing procedure over a wide range of strain rates*. Journal of Theoretical and Applied Mechanics, 2017: p. 727.
 56. BARANOWSKI*, P., et al., *Assessment of mechanical properties of off road vehicle tire: coupons testing and FE model development*. acta mechanica et automatica, 2012. **vol.6 no.2**.
 57. Bhowmick, A.K. and J.R. White, *Thermal, UV- and sunlight ageing of thermoplastic elastomeric natural rubber-polyethylene blends*. Journal of Materials Science, 2002. **Vol. 37**: p. 5141-5151.
 58. Neville, A.M. and J.J. Brooks, *Concrete Technology, second ed.*, Pearson Harlow, United Kingdom. 2010.
 59. Poon, C.S., et al., *Influence of moisture states of natural and recycled aggregates on the slump and compressive strength of concrete*. Cement and Concrete Research, 2004. **34**(1): p. 31-36.
 60. Pepe, M., et al., *Alternative processing procedures for recycled aggregates in structural concrete*. Construction and Building Materials, 2014. **69**: p. 124-132.
 61. Brand, A.S., J.R. Roesler, and A. Salas, *Initial moisture and mixing effects on higher quality recycled coarse aggregate concrete*. Construction and Building Materials, 2015. **79**: p. 83-89.

-
62. Tam, V.W.Y. and C.M. Tam, *Diversifying two-stage mixing approach (TSMA) for recycled aggregate concrete: TSMA_s and TSMA_{sc}*. Construction and Building Materials, 2008. **22**(10): p. 2068-2077.
 63. Dhir, R.K., M.C. Limbachiya, and T. Leelawat, *Suitability of recycled concrete aggregate for use in BS 5328 designated mixes*. Proc. Instn Civ. Engrs Structs & Bldgs, 1999: p. 257 ± 274.
 64. Long, G., et al., *Self-Compacting Concrete Reinforced by Waste Tyre Rubber Particle and Emulsified Asphalt.pdf*>. SUSTAINABLE CONSTRUCTION MATERIALS, 2012.
 65. Bignozzi, M.C. and F. Sandrolini, *Tyre rubber waste recycling in self-compacting concrete*. Cement and Concrete Research, 2006. **36**(4): p. 735-739.
 66. Mohammadi, I., H. Khabbaz, and K. Vessalas, *In-depth assessment of Crumb Rubber Concrete (CRC) prepared by water-soaking treatment method for rigid pavements*. Construction and Building Materials, 2014. **71**: p. 456-471.
 67. Su, H., et al., *Properties of concrete prepared with waste tyre rubber particles of uniform and varying sizes*. Journal of Cleaner Production, 2015. **91**: p. 288-296.
 68. Duan, Z.H. and C.S. Poon, *Properties of recycled aggregate concrete made with recycled aggregates with different amounts of old adhered mortars*. Materials & Design, 2014. **58**: p. 19-29.
 69. Manzi, S., C. Mazzotti, and M.C. Bignozzi, *Short and long-term behavior of structural concrete with recycled concrete aggregate*. Cement and Concrete Composites, 2013. **37**: p. 312-318.
 70. Kwan, W.H., et al., *Influence of the amount of recycled coarse aggregate in concrete design and durability properties*. Construction and Building Materials, 2011.
 71. González-Fonteboa, B., et al., *Effect of recycled coarse aggregate on damage of recycled concrete*. Materials and Structures, 2011. **44**(10): p. 1759-1771.
 72. Thomas, C., et al., *Durability of recycled aggregate concrete*. Construction and Building Materials, 2013. **40**: p. 1054-1065.
 73. Crentsil, K.K.S.-., T. Brown, and A.H. Taylor, *performance of concrete made with commercially produced coarse recycled concrete aggregates*. Cement and Concrete Research, 2001. **31**: p. 707-712.
 74. Bolouri Bazaz, J. and M. Khayati, *Properties and Performance of Concrete Made with Recycled Low-Quality Crushed Brick*. Journal of Materials in Civil Engineering, 2012. **24**(4): p. 330-338.

-
75. de Juan, M.S. and P.A. Gutiérrez, *Study on the influence of attached mortar content on the properties of recycled concrete aggregate*. Construction and Building Materials, 2009. **23**(2): p. 872-877.
 76. Beltrán, M.G., et al., *Effect of cement addition on the properties of recycled concretes to reach control concretes strengths*. Journal of Cleaner Production, 2014. **79**: p. 124-133.
 77. Hernández-Olivares, F., et al., *Static and dynamic behaviour of recycled tyre rubber-filled concrete*. Cement and Concrete Research, 2002. **30**: p. 1587–1596.
 78. SKRIPKIŪNAS, G., A. GRINYS, and B. ČERNIUS, *Deformation Properties of Concrete with Rubber Waste Additives*. MATERIALS SCIENCE (MEDŽIAGOTYRA). 2007. **Vol. 13, No. 3**.
 79. Rao, K.J. and M.A. Mujeeb, *A STUDY ON PROPERTIES OF CRUMB RUBBER CONCRETE BY DESTRUCTIVE AND NON-DESTRUCTIVE TESTING*. ASIAN JOURNAL OF CIVIL ENGINEERING, 2015. **VOL. 16, NO. 7**: p. 933-941.
 80. Grinys, A., H. Sivilevičius, and M. Daukšys, *Tyre Rubber Additive Effect on Concrete Mixture Strength*. Journal of Civil Engineering and Management, 2012. **18**(3): p. 393-401.
 81. Ozbay, E., M. Lachemi, and U.K. Sevim, *Compressive strength, abrasion resistance and energy absorption capacity of rubberized concretes with and without slag*. Materials and Structures, 2010. **44**(7): p. 1297-1307.
 82. Fiore, A., et al., *On the Fresh/Hardened Properties of Cement Composites Incorporating Rubber Particles from Recycled Tires*. Advances in Civil Engineering, 2014. **2014**: p. 1-12.
 83. Bravo, M. and J. de Brito, *Concrete made with used tyre aggregate: durability-related performance*. Journal of Cleaner Production, 2012. **25**: p. 42-50.
 84. Shah, S.F.A., et al., *Evaluation of Thermal and Structural Behavior of Concrete Containing Rubber Aggregate*. Arabian Journal for Science and Engineering, 2014. **39**(10): p. 6919-6926.
 85. Gesoğlu, M. and E. Güneyisi, *Strength development and chloride penetration in rubberized concretes with and without silica fume*. Materials and Structures, 2007. **40**(9): p. 953-964.
 86. Onuaguluchi, O. and D.K. Panesar, *Hardened properties of concrete mixtures containing pre-coated crumb rubber and silica fume*. Journal of Cleaner Production, 2014. **82**: p. 125-131.
-

-
87. Yilmaz, A. and N. Degirmenci, *Possibility of using waste tire rubber and fly ash with Portland cement as construction materials*. Waste Manag, 2009. **29**(5): p. 1541-6.
88. Ma, Q.W. and J.C. Yue, *Effect on Mechanical Properties of Rubberized Concrete due to Pretreatment of Waste Tire Rubber with NaOH*. Applied Mechanics and Materials, 2013. **357-360**: p. 897-904.
89. Ajdukiewicz, A. and A. Kliszczewicz, *Influence of recycled aggregates on mechanical properties of HSHPC*. Cement & Concrete Composites, 2002. **24**: p. 269–279.
90. Rahal, K., *Mechanical properties of concrete with recycled coarse aggregate*. Building and Environment, 2007. **42**(1): p. 407-415.
91. Eguchi, K., et al., *Application of recycled coarse aggregate by mixture to concrete construction*. Construction and Building Materials, 2007. **21**(7): p. 1542-1551.
92. Fonseca, N., J. de Brito, and L. Evangelista, *The influence of curing conditions on the mechanical performance of concrete made with recycled concrete waste*. Cement and Concrete Composites, 2011. **33**(6): p. 637-643.
93. Casuccio, M., et al., *Failure mechanism of recycled aggregate concrete*. Construction and Building Materials, 2008. **22**(7): p. 1500-1506.
94. Xiao, J., J. Li, and C. Zhang, *Mechanical properties of recycled aggregate concrete under uniaxial loading*. Cement and Concrete Research, 2005. **35**(6): p. 1187-1194.
95. Carneiro, J.A., et al., *Compressive stress–strain behavior of steel fiber reinforced-recycled aggregate concrete*. Cement and Concrete Composites, 2014. **46**: p. 65-72.
96. Ismail, M.K. and A.A.A. Hassan, *An experimental study on flexural behaviour of large-scale concrete beams incorporating crumb rubber and steel fibres*. Engineering Structures, 2017.
97. Chakradhara Rao, M., S.K. Bhattacharyya, and S.V. Barai, *Influence of field recycled coarse aggregate on properties of concrete*. Materials and Structures, 2010. **44**(1): p. 205-220.
98. Topçu, İ.B. and S. Şengel, *Properties of concretes produced with waste concrete aggregate*. Cement and Concrete Research, 2004. **34**(8): p. 1307-1312.
99. Xiao, J. and H. Falkner, *Bond behaviour between recycled aggregate concrete and steel rebars*. Construction and Building Materials, 2007. **21**(2): p. 395-401.
-

-
100. Prince, M.J.R. and B. Singh, *Bond behaviour between recycled aggregate concrete and deformed steel bars*. Materials and Structures, 2013. **47**(3): p. 503-516.
 101. Turatsinze, A., S. Bonnet, and J.L. Granju, *Mechanical characterisation of cement-based mortar incorporating rubber aggregates from recycled worn tyres*. Building and Environment, 2005. **40**(2): p. 221-226.
 102. Li, L.J., et al., *Experimental study of recycled rubber-filled high-strength concrete*. Magazine of Concrete Research, 2009. **61**(7): p. 549-556.
 103. Tam, V.W.Y., X.F. Gao, and C.M. Tam, *Microstructural analysis of recycled aggregate concrete produced from two-stage mixing approach*. Cement and Concrete Research, 2005. **35**(6): p. 1195-1203.
 104. Ahmad, S., et al., *Bond–slip behaviour of steel bars in low-strength concrete*. Proceedings of the Institution of Civil Engineers, 2015.
 105. Butler, L., J.S. West, and S.L. Tighe, *The effect of recycled concrete aggregate properties on the bond strength between RCA concrete and steel reinforcement*. Cement and Concrete Research, 2011. **41**(10): p. 1037-1049.
 106. Prince, M.J.R. and B. Singh, *Bond strength of deformed steel bars in high-strength recycled aggregate concrete*. Materials and Structures, 2014. **48**(12): p. 3913-3928.
 107. Richardson, A., K. Coventry, and J. Bacon, *Freeze/thaw durability of concrete with recycled demolition aggregate compared to virgin aggregate concrete*. Journal of Cleaner Production, 2011. **19**(2-3): p. 272-277.
 108. Yadav, S. and S. Pathak, *Durability Aspects of Recycled Aggregate Concrete: An Experimental Study*. International Journal of Civil and Environmental Engineering, 2018. **Vol:12, No:3, 2018**.
 109. Hwang, J.P., et al., *Enhancing the durability properties of concrete containing recycled aggregate by the use of pozzolanic materials*. KSCE Journal of Civil Engineering, 2013. **17**(1): p. 155-163.
 110. Tam, V.W.Y. and C.M. Tam, *Assessment of durability of recycled aggregate concrete produced by two-stage mixing approach*. Journal of Materials Science, 2007. **42**(10): p. 3592-3602.
 111. ASTM:C1202, *Standard Test Method for Electrical Indication of Concrete's Ability to Resist Chloride ion Penetration*. 1997.
 112. Si, R., S. Guo, and Q. Dai, *Durability performance of rubberized mortar and concrete with NaOH-Solution treated rubber particles*. Construction and Building Materials, 2017. **153**: p. 496-505.

-
113. BS-EN1992, *Eurocode 2: Design of concrete structures — Part 1-1: General rules and rules for buildings*. British standard of publication, 2004.
 114. Mattock, A.H., L.B. Kriz, and E. Hognestad, *Rectangular Concrete Stress Distribution in Ultimate Strength Design*. ACI Journal, proceedings, 1961. **Vol. 57, No. 8**: p. pp.875-926.
 115. CEP-FIP, *Model code 1990*. Thomas Telford services Ltd., London., 1990: p. 437pp.
 116. González-Fonteboa, *Shear strength of recycled concrete beams*. Construction and Building Materials, 2007. **21**(4): p. 887-893.
 117. Arezoumandi, M., et al., *An experimental study on shear strength of reinforced concrete beams with 100% recycled concrete aggregate*. Construction and Building Materials, 2014. **53**: p. 612-620.
 118. Yang, H., et al., *Shear behavior of recycled aggregate concrete after exposure to high temperatures*. Construction and Building Materials, 2016. **106**: p. 374-381.
 119. Choi, H.B., et al., *Experimental study on the shear strength of recycled aggregate concrete beams*. Magazine of Concrete Research, 2010. **62**(2): p. 103-114.
 120. Wang, W.-l., S.-c. Kou, and F. Xing, *Deformation properties and direct shear of medium strength concrete prepared with 100% recycled coarse aggregates*. Construction and Building Materials, 2013. **48**: p. 187-193.
 121. Xiao, J., H. Xie, and Z. Yang, *Shear transfer across a crack in recycled aggregate concrete*. Cement and Concrete Research, 2012. **42**(5): p. 700-709.
 122. Ismail, M.K., A.A.A. Hassan, and A.A. Hussein, *Structural behaviour of reinforced concrete beams containing crumb rubber and steel fibres*. Magazine of Concrete Research, 2017. **69**(18): p. 939-953.
 123. Ismail, M.K. and A.A.A. Hassan, *Shear behaviour of large-scale rubberized concrete beams reinforced with steel fibres*. Construction and Building Materials, 2017. **140**: p. 43-57.
 124. MacGregor, J.G. and J.K. Wight, *Reinforced Concrete Mechanics and Design. Fourth Edition*. Prentice-Hall, Inc, Singapore., 2005.
 125. BS-EN1992-1-1, *Eurocode2: Design of concrete structures*. 2004.
 126. Kovach, J.D., *Horizontal Shear Capacity of Composite Concrete Beams without Interface Ties*. ATLSS REPORT NO. 08-05, 2008.

-
127. ACI318-08, C.A., *Building Code Requirements for Structural Concrete (ACI 318R-14)*. 2014.
 128. Mohamad, M.E., et al., *Friction and cohesion coefficients of composite concrete-to-concrete bond*. *Cement and Concrete Composites*, 2015. **56**: p. 1-14.
 129. Santos, P.M.D.d., *Assessment of the Shear Strength between Concrete Layers*. 2009.
 130. PHILIP W. BIRKELAND and H.W. BIRKELAND, *Connections in Precast Concrete Construction*. *JOURNAL OF THE AMERICAN CONCRETE INSTITUTE*, 1966.
 131. CEB-FIP, *Model Code for concrete structures*. 1990.
 132. AASHTO-LRFD, *American Association of State Highway and Transportation Officials. Bridge Design Specifications. Washington DC, 2007*
 133. Hassan, M.M., et al., *Evaluation of the durability of titanium dioxide photocatalyst coating for concrete pavement*. *Construction and Building Materials*, 2010. **24**(8): p. 1456-1461.
 134. Said, A.M., et al., *Properties of concrete incorporating nano-silica*. *Construction and Building Materials*, 2012. **36**: p. 838-844.
 135. Li, H., M.-h. Zhang, and J.-p. Ou, *Abrasion resistance of concrete containing nano-particles for pavement*. *Wear*, 2006. **260**(11-12): p. 1262-1266.
 136. Kuila, T., et al., *Preparation of functionalized graphene/linear low density polyethylene composites by a solution mixing method*. *Carbon*, 2011. **49**(3): p. 1033-1037.
 137. Soldano, C., A. Mahmood, and E. Dujardin, *Production, properties and potential of graphene*. *Carbon*, 2010. **48**(8): p. 2127-2150.
 138. Kuilla, T., et al., *Recent advances in graphene based polymer composites*. *Progress in Polymer Science*, 2010. **35**(11): p. 1350-1375.
 139. Du, H. and S.D. Pang, *Enhancement of barrier properties of cement mortar with graphene nanoplatelet*. *Cement and Concrete Research*, 2015. **76**: p. 10-19.
 140. Wu, Y.Y., et al., *Physical Properties of Concrete Containing Graphene Oxide Nanosheets*. *Materials (Basel)*, 2019. **12**(10).
 141. BS-EN197-1, *Composition, specifications and conformity criteria for common cements*. BSI Standards Publication, 2011.
-

-
142. BS-EN933-1, *Tests for geometrical properties of aggregates - Part 1: Determination of particle size distribution - Sieving method*. BSI Standards Publication, 2012.
 143. Teychenne, D.C., R.E. Franklin, and H.C. Erntroy, *Design of normal concrete mixes*. 1975.
 144. Road_Research_Laboratory, *Design of concrete mixes. Road Note No 4, 2nd Edition*. London, HMSO. 1950.
 145. BS12-1991, *Specification for portland cement*. 1991.
 146. BS882-1992, *Specification for aggregates from natural sources for concrete*. 1992.
 147. BS-EN12390-2, *Testing hardened concrete Part 2: Making and curing specimens for strength tests*. BRITISH STANDARD, 2009.
 148. BS-EN12350-2, *Testing fresh concrete - Part 2: Slump-test*. BRITISH STANDARD PUBLICATIONS, 2009.
 149. BS-EN12390-3-2009, *Testing hardened concrete - Part 3: Compressive strength of test specimens*. BRITISH STANDARD PUBLICATIONS.
 150. BS-EN12390-6, *Testing hardened concrete — Part 6: Tensile splitting strength of test specimens*. BRITISH STANDARD PUBLICATIONS, 2000
 151. BS1881-203:1986, *Testing concrete —Part 203: Recommendations for measurement of velocity of ultrasonic pulses in concrete*. BRITISH STANDARD PUBLICATIONS.
 152. Mohammed, B.S., N.J. Azmi, and M. Abdullahi, *Evaluation of rubbercrete based on ultrasonic pulse velocity and rebound hammer tests*. Construction and Building Materials, 2011. **25**(3): p. 1388-1397.
 153. Benazzouk, A., et al., *Physico-mechanical properties and water absorption of cement composite containing shredded rubber wastes*. Cement and Concrete Composites, 2007. **29**(10): p. 732-740.
 154. ACI318-08., *Building Code Requirements for Structural Concrete and Commentary*. American Concrete Institute, 2008.
 155. Diab, A.M., A.E.M. Abd Elmoaty, and M.R. Tag Eldin, *Slant shear bond strength between self compacting concrete and old concrete*. Construction and Building Materials, 2017. **130**: p. 73-82.

-
156. Tayeh, B.A., et al., *Evaluation of Bond Strength between Normal Concrete Substrate and Ultra High Performance Fiber Concrete as a Repair Material*. Procedia Engineering, 2013. **54**: p. 554-563.
 157. EN12615, *Products and systems for the protection and repair of concrete structures. Test methods. Determination of slant shear strength*, European Committee for standardization, 1999
 158. Pournourmohammadi, S., et al., *Study on the oxidative stress status among cement plant workers*. Human & Experimental Toxicology, 2008: p. 27: 463–469.
 159. Du, H. and S.D. Pang, *Dispersion and stability of graphene nanoplatelet in water and its influence on cement composites*. Construction and Building Materials, 2018. **167**: p. 403-413.
 160. Dashrath, K.B., et al., *Compression and Split Tensile Strength of Concrete Containing Different Aggregates*. International Journal of Engineering Research & Technology, 2014. **Vol. 3**(Issue 3).
 161. Malárics, V. and H.S. Müller, *Evaluation of the splitting tension test for concrete from a fracture mechanical point of view*. Fracture Mechanics of Concrete and Concrete Structures - Assessment, Durability, Monitoring and Retrofitting of Concrete Structures, 2010.
 162. Boulekbache, B., et al., *Failure mechanism of fibre reinforced concrete under splitting test using digital image correlation*. Materials and Structures, 2014. **48**(8): p. 2713-2726.
 163. AECOM, *Civil Engineering and highway works price book. Thirty-second edition*. 2018.
 164. Cao, M.-l., H.-x. Zhang, and C. Zhang, *Effect of graphene on mechanical properties of cement mortars*. Journal of Central South University, 2016. **23**(4): p. 919-925.
 165. ABAQUS-6.14, *Abaqus 6.14 Documentation collection*. Dassault Systèmes Simulia Corp., Providence, RI, USA., 2014.
 166. Hordijk, D.A., *Local approach to fatigue of concrete*. Thesis Technische Universiteit Delft, 1991.
 167. Charif, A., S.M. Mourad, and M.I. Khan, *Flexural Behavior of Beams Reinforced with Steel Bars Exceeding the Nominal Yield Strength*. Latin American Journal of Solids and Structures, 2016. **13**(5): p. 945-963.

-
168. Zsutty, T.C., *Shear Strength Predictions for Separate Categories of Simple Beam Tests*. ACI Journal, Proceedings, 1971: p. 68 (2), 138-143. .
 169. Bazant, Z. and J. Kim, *Size effect in shear failure of longitudinally reinforced beams*. Proceedings of ACI Journal, 1984. **81(5)**: p. 456–468.
 170. ACI318-14, *Building Code Requirements for Structural Concrete. Commentary on Building Code Requirements for Structural Concrete (ACI 318R-14)*. 2014.